Technical University of Civil Engineering of Bucharest

Reinforced Concrete Department

STRUCTURAL RELIABILITY AND RISK ANALYSIS

Lecture notes

Radu VĂCĂREANU

Alexandru ALDEA

Dan LUNGU

2007

Foreword

The lectures on *Structural Reliability and Risk Analysis* at the Technical University of Civil Engineering of Bucharest commenced in early 1970's as an elective course taught by late Professor Dan Ghiocel and by Professor Dan Lungu in the Buildings Department. After 1990 the course became a compulsory one in the Reinforced Concrete Department and it is taught both in the Faculty of Civil, Industrial and Agricultural Buildings and in the Faculty of Engineering in Foreign Languages of Technical University of Civil Engineering of Bucharest. The course is envisaged as to provide the background knowledge for the understanding and implementation of the new generation of Romanian structural codes that follow the structural *Eurocodes* concepts and formats. Also, the lectures on *Structural Reliability and Risk Analysis* provide the required information to understand and apply the concepts and approaches of the performance based design of buildings and structures.

Uncertainties are omnipresent in structural engineering. Civil engineering structures are to be designed for loads due to environmental actions like earthquakes, snow and wind. These actions are exceptionally uncertain in their manifestations and their occurrence and magnitude cannot be treated deterministically. Materials used in civil engineering constructions also display wide scatter in their mechanical properties. Structural engineering activities, on one hand, lead to increase in societal wealth, and, on the other hand, these activities also make society vulnerable to risks. A structural engineer is accountable for the decisions that he takes. A hallmark of professionalism is to quantify the risks and benefits involved. The subject of structural reliability offers a rational framework to quantify uncertainties mathematically. The subject combines statistics, theory of probability, random variables and random processes with principles of structural mechanics and forms the basis on which modern structural design codes are developed.

Structural reliability has become a discipline of international interest, as it is shown by the significant number of books and journals, seminars, symposiums and conferences addressing solely this issue. The present lecture notes textbook provides an insight into the concepts, methods and procedures of structural reliability and risk analysis considering the presence of random uncertainties. The course is addressed to undergraduate students from Faculty of Engineering in Foreign Languages instructed in English language as well as postgraduate students in structural engineering. The objectives of the courses are:

- to provide a review of mathematical tools for quantifying uncertainties using theories of probability, random variables and random processes
- to develop the theory of methods of structural reliability based on concept of reliability indices. This includes discussions on First Order Reliability Methods
- to explain the basics of code calibration
- to evaluate actions on buildings and structures due to natural hazards
- to provide the basics of risk analysis
- to provide the necessary background to carry out reliability based design and risk-based decision making and to apply the concepts and methods of performance-based engineering
- to prepare the ground for students to undertake research in this field.

The content of the Structural Reliability and Risk Analysis textbook is:

- Introduction to probability and random variables; distributions of probability

- Formulation of reliability concepts for structural components; exact solutions, first-order reliability methods; reliability indices; basis for probabilistic design codes
- Seismic hazard analysis
- Seismic vulnerability and seismic risk analysis
- Introduction to the topic of time-variant reliability and random processes; properties of random processes
- Dynamic stochastic response of single degree of freedom systems – applications to wind and earthquake engineering.

The developments and the results of the *Structural Reliability and Risk Analysis Group* of the *Reinforced Concrete Department* at the *Technical University of Civil Engineering of Bucharest* are included in important national structural codes, such as:

- P100-1/2006 - *Cod de proiectare seismică - Partea I - Prevederi de proiectare pentru clădiri*, 2007 (Code for Earthquake Resistant Design of New Buildings)
- CR0-2005 - *Cod de proiectare. Bazele proiectarii structurilor in constructii*, 2005 (Design Code. Basis of Structural Design)
- CR1-1-3-2005 - *Cod de proiectare. Evaluarea actiunii zapezii asupra constructiilor*, 2005 (Design Code. Snow Loads on Buildings and Structures)
- NP 082-04 - *Cod de proiectare. Bazele proiectării şi acţiuni asupra construcţiilor. Acţiunea vântului*, 2005 (Design Code. Basis of Design and Loads on Buildings and Structures. Wind Loads)

The *UTCB Structural Reliability and Risk Analysis Group* embarked in the national efforts towards seismic risk mitigation through the implementation of national and international projects in this field as well as through the organization of international conferences devoted to this aim.

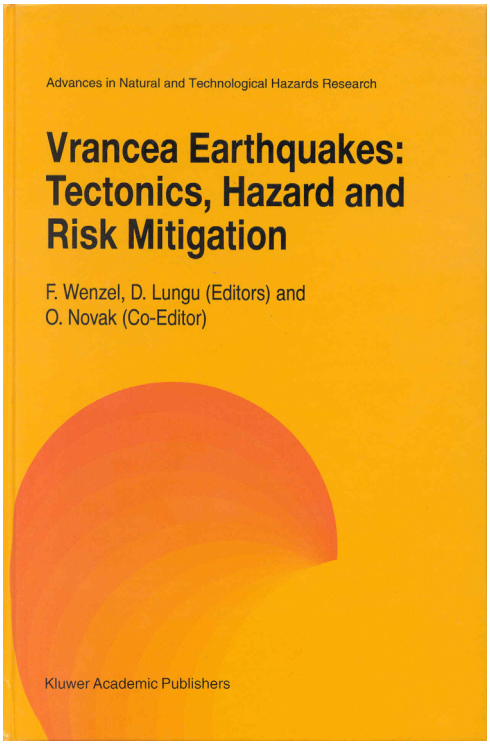

First International Workshop on Vrancea Earthquakes, Bucharest, Nov. 1-4, 1997

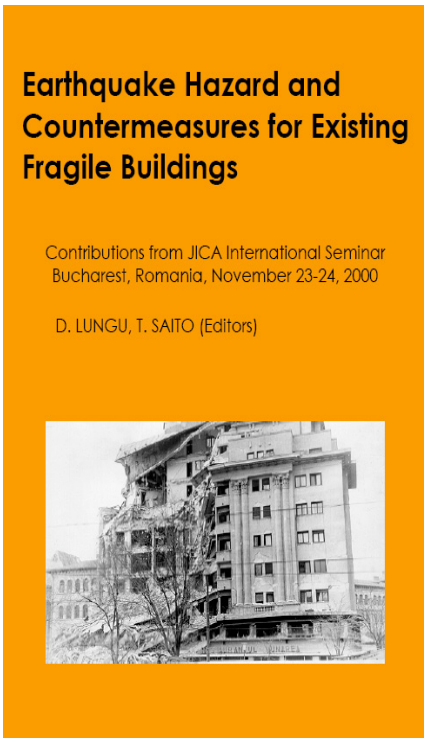

JICA International Seminar, Bucharest, Nov. 23-24, 2000

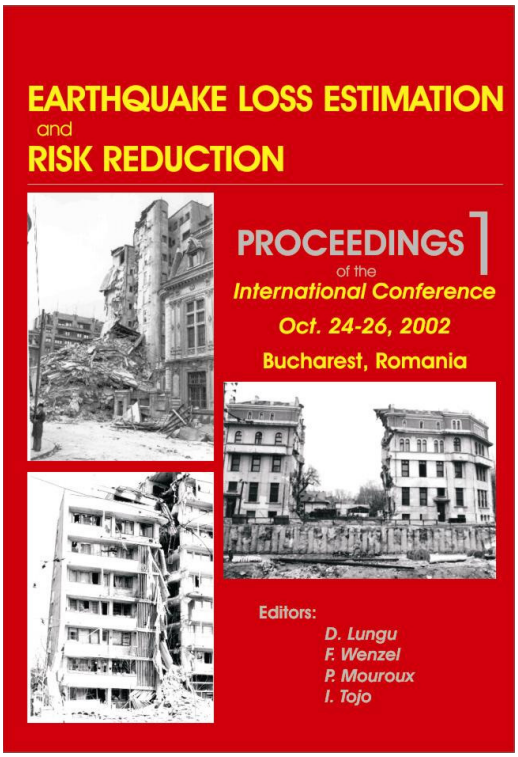

International Conference on Earthquake Loss Estimation and Risk Reduction, Bucharest, Oct. 24-26, 2002

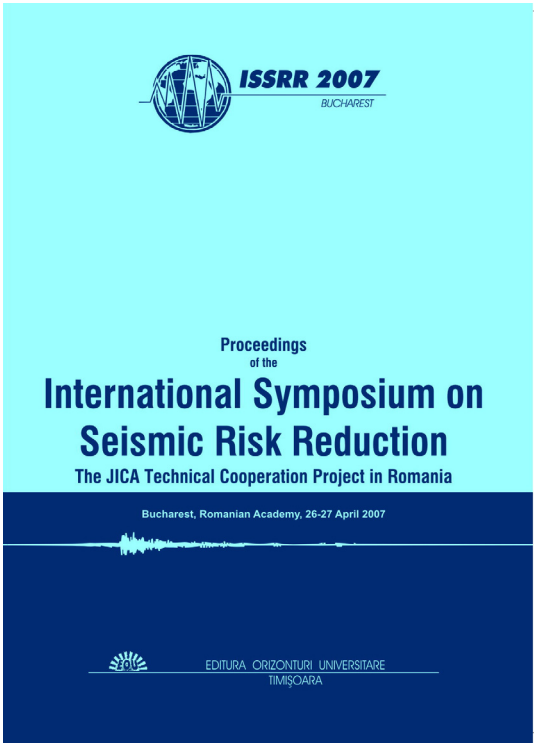

International Symposium on Seismic Risk Reduction – The JICA Technical Cooperation Project, Bucharest, April 26-27, 2007

The international conferences above mentioned consisted in milestones in the development and implementation of the international projects for seismic risk reduction in which *Structural Reliability and Risk Analysis Group* of the *Technical University of Civil Engineering of Bucharest* was involved:

- Collaborative Research Center SFB 461 - *Strong Earthquakes: A Challenge for Geosciences and Civil Engineering*, Karlsruhe University, Germany - 1996-2007
- *RISK-UE An advanced approach to earthquake risk scenarios with applications to different European towns*, EVK4-CT-2000-00014, European Commission, 5th Framework - 2001-2004
- *IAEA CRP on Safety Significance of Near Field Earthquake*, International Atomic Energy Agency (IAEA) - 2002-2005
- *Numerical simulations and engineering methods for the evaluation of expected seismic performance*, European Commission, Directorate General JRC Joint Research Centre, Institute for the Protection and the Security of the Citizen, Italy, C. 20303 F1 EI ISP RO - 2002-2005
- *NEMISREF New Methods of Mitigation of Seismic Risk on Existing Foundations* - GIRD-CT-2002-00702, European Commission, 5th Framework - 2002-2005
- *JICA (Japan International Cooperation Agency) Technical Cooperation Project for Seismic Risk Reduction of Buildings and Structures in Romania* - 2002-2008
- *PROHITECH - Earthquake Protection of Historical Buildings by Reversible Mixed Technologies*, 6th Framework – 2004-2007.

Assoc. Prof., Ph.D. Radu Văcăreanu

Assoc. Prof., Ph.D. Alexandru Aldea

Prof., Ph.D. Dan Lungu

Table of Contents

1. INTRODUCTION TO RANDOM VARIABLES THEORY

1.1. Nature and purpose of mathematical statistics

In engineering statistics one is concerned with methods for designing and evaluating experiments to obtain information about practical problems, for example, the inspection of quality of materials and products. The reason for the differences in the quality of products is the *variation* due to numerous factors (in the material, workmanship) whose influence cannot be predicted, so that the variation must be regarded as a *random variation*.
In most cases the inspection of each item of the production is prohibitively expensive and time-consuming. Hence instead of inspecting all the items just a few of them (a *sample*) are inspected and from this inspection conclusions can be drawn about the totality (the *population*).
The steps leading from the formulation of the statistical problem to the solution of the problem are as follows (Kreyszig, 1979):

1.*Formulation of the problem*. It is important to formulate the problem in a precise fashion and to limit the investigation. This step must also include the creation of a mathematical model based on clear concepts.

2.*Design of experiment*. This step includes the choice of the statistical methods to be used in the last step, the sample size *n* and the physical methods and techniques to be used in the experiment.

3.*Experimentation and collection of data*. This step should adhere to strict rules.

4.*Tabulation*. The experimental data are arranged in a clear and simple tabular form and are represented graphically by bar charts.

5.*Statistical inference*. One uses the sample and applies a suitable statistical method for drawing conclusions about the unknown properties of the population.

1.2. Tabular and graphical representation of samples

In the course of a statistical experiment one usually obtain a sequence of observations that are written down in the order they occur. A typical example is shown in Table 1.1. These data were obtained by making standard tests for concrete compressive strength. We thus have a sample consisting of 30 sample values, so that the size of the sample is n=30.

Table 1.1. Sample of 30 values of the compressive strength of concrete, daN/cm^2

320	380	340
350	340	350
370	390	370
320	350	360
380	360	350
420	400	350
360	330	360
360	370	350
370	400	360
340	360	390

To see what information is contained in Table 1.1, one shall order the data. One writes the values in Table 1.2 (320,330 and so on). The number of occurring numbers from Table 1.1 is

listed in the second column of Table 1.2. It indicates how often the corresponding value x occurs in the sample and is called *absolute frequency* of that value x in the sample. Dividing it by the size n of the sample one obtains the *relative frequency* in the third column of Table 1.2. If for a certain x one sums all the absolute frequencies corresponding to corresponding to the sample values which are smaller than or equal to that x, one obtains the *cumulative frequency* corresponding to that x. This yields column 4 in Table 1.2. Division by the size n of the sample yields the *cumulative relative frequency* in column 5.

Table 1.2. Frequencies of values of random variable

Compressive strength	Absolute frequency	Relative frequency	Cumulative frequency	Cumulative relative frequency
320	2	0.067	2	0.067
330	1	0.033	3	0.100
340	3	0.100	6	0.200
350	6	0.200	12	0.400
360	7	0.233	19	0.633
370	4	0.133	23	0.767
380	2	0.067	25	0.833
390	2	0.067	27	0.900
400	2	0.067	29	0.967
410	0	0.000	29	0.967
420	1	0.033	30	1.000

The graphical representation of the samples is given by histograms of relative frequencies and/or cumulative relative frequencies (Figure 1.1 and Figure 1.2).

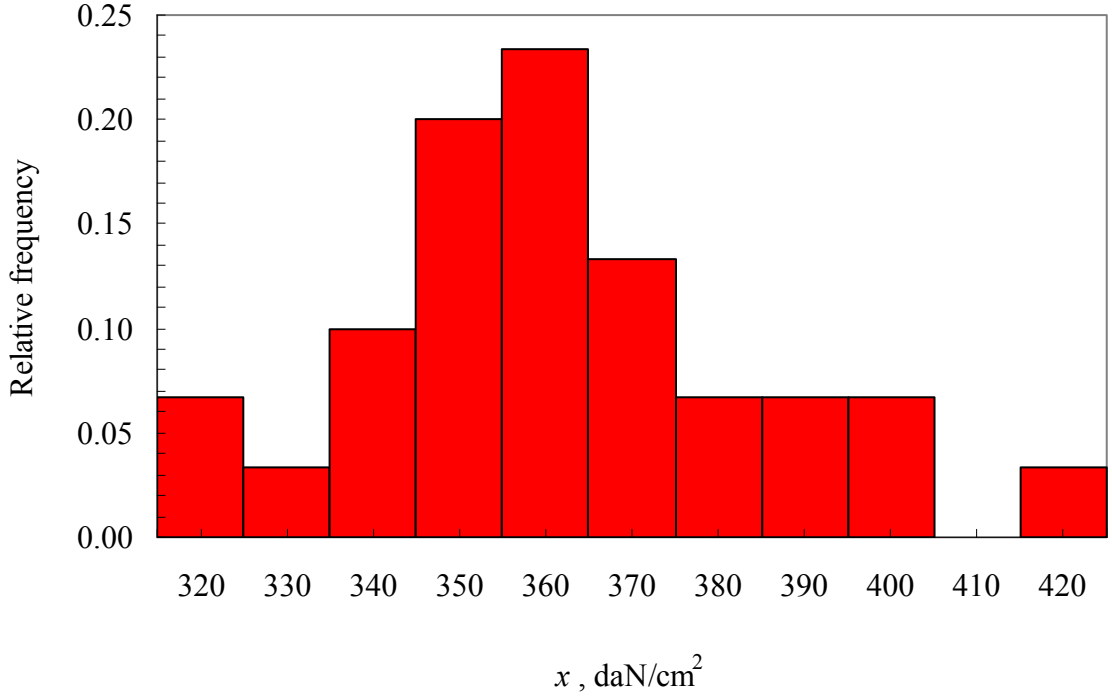

Figure 1.1. Histogram of relative frequencies

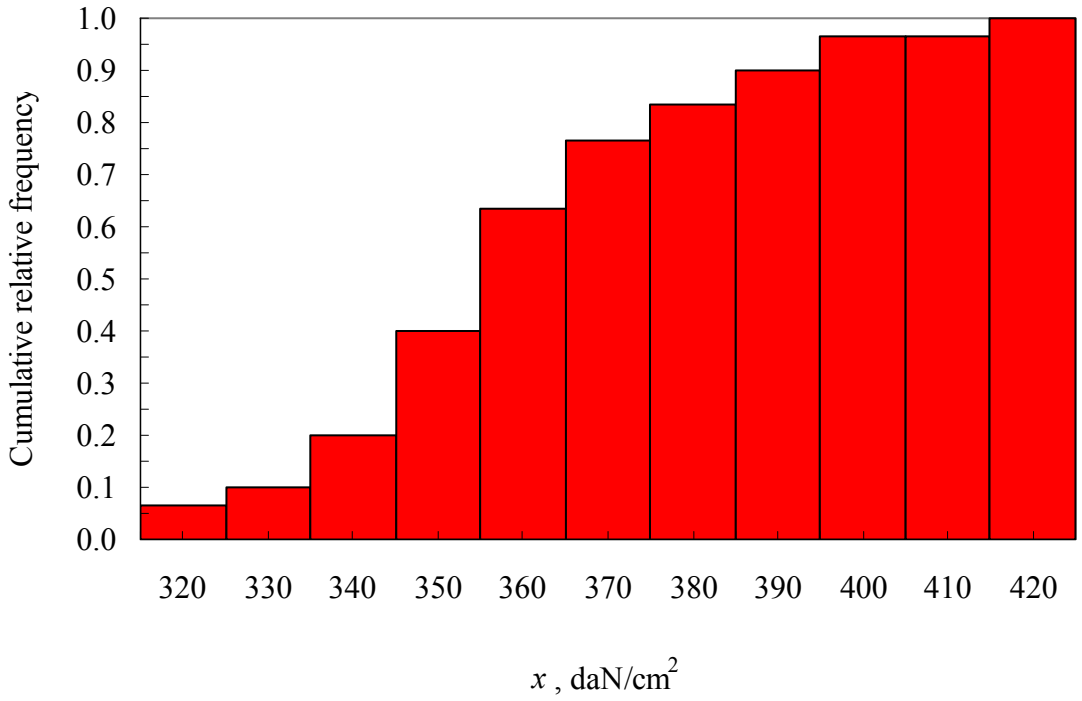

Figure 1.2. Histogram of cumulative relative frequencies

If a certain numerical value does not occur in the sample, its frequency is 0. If all the n values of the sample are numerically equal, then this number has the frequency n and the relative frequency is 1. Since these are the two extreme possible cases, one has:

Theorem 1. The relative frequency is at least equal to 0 and at most equal to 1.

Theorem 2. The sum of all relative frequencies in a sample equals 1.

One may introduce the *frequency function* of the sample that determines the frequency distribution of the sample:

$$\tilde{f}(x) = \begin{cases} \tilde{f}_j, x = x_j \\ 0, x \neq x_j \end{cases} \qquad (1.1)$$

The *cumulative frequency function* of the sample is $\tilde{F}(x)$ = sum of the relative frequencies of all the values that are smaller than or equal to x.

The relation between $\tilde{f}(x)$ and $\tilde{F}(x)$ is:

$$\tilde{F}(x) = \sum_{t \leq x} \tilde{f}(t)$$

If a sample consists of too many numerically different sample values, the process of *grouping* may simplify the tabular and graphical representations, as follows.

A sample being given, one chooses an interval I that contains all the sample values. One subdivides I into subintervals, which are called *class intervals*. The midpoints of these intervals are called *class midpoints*. The sample values in each such interval are said to form a *class*. Their number is called the corresponding *class frequency*. Division by the sample size n gives the *relative class frequency*. This frequency is called the *frequency function of the grouped sample*, and the corresponding cumulative relative class frequency is called the *distribution function of the grouped sample*.

The fewer classes one chooses, the simpler the distribution of the grouped sample becomes but the more information we loose, because the original sample values no longer appear

explicitly. Grouping should be done so that only unessential data are eliminated. Unnecessary complications in the later use of a grouped sample are avoided by obeying the following rules:

1.All the class intervals should have the same length.

2.The class intervals should be chosen so that the class midpoints correspond to simple numbers.

3.If a sample value x_j coincides with the common point of two class intervals, one takes it into the class interval that extends from x_j to the right.

1.3. Sample mean and sample variance

For the frequency function one may compute measures for certain properties of the sample, such as the average size of the sample values, the spread, etc.

The *mean value of a sample* $x_1, x_2, \ldots, x_n$ or, briefly, *sample mean*, is denoted by $\bar{x}$ and is defined by the formula

$$\bar{x} = \frac{1}{n}\sum_{j=1}^{n} x_j \tag{1.2}$$

It is the sum of all the sample values divided by the size n of the ample. Obviously, it measures the average size of the sample values, and sometimes the term *average* is used for $\bar{x}$.

The *variance of a sample* $x_1, x_2, \ldots, x_n$ or, briefly, *sample variance*, is denoted by s^2 and is defined by the formula

$$s^2 = \frac{1}{n-1}\sum_{j=1}^{n} (x_j - \bar{x})^2 \tag{1.3}$$

It is the sum of the squares of the deviations of the sample values from the mean $\bar{x}$, divide by *n-1*. It measures the spread or dispersion of the sample values and is positive. The positive square root of the sample variance s^2 is called the *standard deviation* of the sample and is denoted by *s*.

The *coefficient of variation of a sample* $x_1, x_2, \ldots, x_n$ is denoted by *COV* and is defined as the ratio of the standard deviation of the sample to the sample mean

$$V = \frac{s}{\bar{x}} \tag{1.4}$$

1.4. Random Experiments, Outcomes, Events

A *random experiment* or *random observation*, briefly *experiment* or *observation*, is a process that has the following properties, (Kreyszig, 1979):

1.It is performed according to a set of rules that determines the performance completely.

2.It can be repeated arbitrarily often.

3.The result of each performance depends on “chance” (that is, on influences which we cannot control) and can therefore not be uniquely predicted.

The result of a single performance of the experiment is called the *outcome* of that trial.

The set of all possible outcomes of an experiment is called the *sample space* of the experiment and will be denoted by *S*. Each outcome is called an *element* or *point* of *S*.

In most practical problems one is not so much interested in the individual outcomes but in whether an outcome belongs (or does not belong) to a certain set of outcomes. Clearly, each such set *A* is a subset of the sample set *S*. It is called an *event*.

Since an outcome is a subset of S, it is an event, but a rather special one, sometimes called an *elementary event*. Similarly, the entire space S is another special event.
A sample space S and the events of an experiment can be represented graphically by a *Venn diagram*, as follows. Suppose that the set of points inside the rectangle in Fig. 1.3 represents S. Then the interior of a closed curve inside the rectangle represents an event denoted by E. The set of all the elements (outcomes) not in E is called the *complement of E in S* and is denoted by E^c.

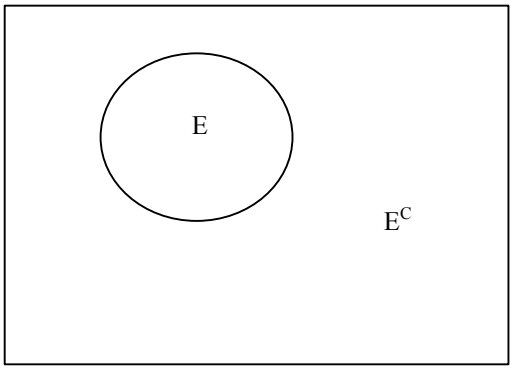

Figure 1.3. Venn diagram representing a sample space S and the events E and E^c

An event containing no element is called the *impossible event* and is denoted by Φ.
Let A and B be any two events in an experiment. Then the event consisting of all the elements of the sample space S contained in A or B, or both, is called the *union* of A and B and is denoted by $A \cup B$.
The event consisting of all the elements in S contained in both A and B is called the *intersection* of A and B and is denoted by $A \cap B$.
Figure 1.4 illustrates how to represent these two events by a Venn diagram. If A and B have no element in common, then $A \cap B = \Phi$, and A and B are called *mutually exclusive events*.

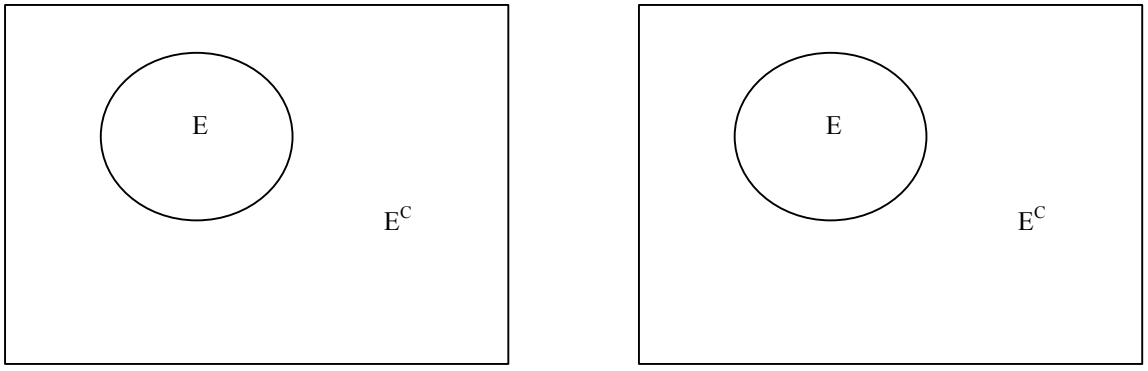

Union $A \cup B$ Intersection $A \cap B$

Figure 1.4. Venn diagrams representing the union (shaded) and intersection (shaded) of two events A and B in a sample space S

If all elements of an event A are also contained in an event B, then A is called a *subevent* of B, and we write
$A \subset B$ or $B \supset A$.
Suppose that one performs a random experiment n times and one obtains a sample consisting of n values. Let A and B be events whose relative frequencies in those n trials are $\tilde{f}(A)$ and $\tilde{f}(B)$, respectively. Then the event $A \cup B$ has the relative frequency

$$\tilde{f}(A \cup B) = \tilde{f}(A) + \tilde{f}(B) - \tilde{f}(A \cap B) \tag{1.5}$$

If A and B are mutually exclusive, then $\tilde{f}(A \cap B) = 0$, and

$$\tilde{f}(A \cup B) = \tilde{f}(A) + \tilde{f}(B) \tag{1.6}$$

These formulas are rather obvious from the Venn diagram in Fig. 1.4.

1.5. Probability

Experience shows that most random experiments exhibit *statistical regularity* or *stability of relative frequencies*; that is, in several long sequences of such an experiment the corresponding relative frequencies of an event are almost equal. Since most random experiments exhibit statistical regularity, one may assert that for any event E in such an experiment there is a number $P(E)$ such that the relative frequency of E in a great number of performances of the experiment is approximately equal to $P(E)$.
For this reason one postulates the existence of a number $P(E)$ which is called *probability of an event E in that random experiment*. Note that this number is not an absolute property of E but refers to a certain sample space S, that is, to a certain random experiment.
The probability thus introduced is the counterpart of the empirical relative frequency. It is therefore natural to require that it should have certain properties which the relative frequency has. These properties may be formulated as so-called *axioms of mathematical probability*, (Kreyszig, 1979).

Axiom 1. If E is any event in a sample space S, then

$$0 \le P(E) \le 1. \tag{1.7}$$

Axiom 2. To the entire sample space S there corresponds

$$P(S) = 1. \tag{1.8}$$

Axiom 3. If A and B are mutually exclusive events, then

$$P(A \cup B) = P(A) + P(B). \tag{1.9}$$

If the sample space is infinite, one must replace Axiom 3 by
Axiom 3. If $E_1, E_2, \ldots$ are mutually exclusive events, then*

$$P(E_1 \cup E_2 \cup \ldots) = P(E_1) + P(E_2) + \ldots \tag{1.10}$$

From axiom 3 one obtains by induction the following

Theorem 1 – Addition rule for mutually exclusive events
If $E_1, E_2, \ldots E_m$ are mutually exclusive events, then

$$P(E_1 \cup E_2 \cup \ldots \cup E_m) = P(E_1) + P(E_2) + \ldots + P(E_m) \tag{1.11}$$

Theorem 2 – Addition rule for arbitrary events
If A and B are any events in a sample space S, then

$$P(A \cup B) = P(A) + P(B) - P(A \cap B). \tag{1.12}$$

Furthermore, an event E and its complement E^c are mutually exclusive, and $E \cup E^c = S$. Using Axioms 3 and 2, one thus has

$$P(E \cup E^c) = P(E) + P(E^c) = 1. \tag{1.13}$$

This yields
Theorem 3 – Complementation rule
The probabilities of an event E and its complement E^c in a sample space S are related by the formula

$$P(E) = 1 - P(E^c) \tag{1.14}$$

Often it is required to find the probability of an event B if it is known that an event A has occurred. This probability is called the *conditional probability of B given A* and it is denoted by $P(B \mid A)$. In this case A serves as a new (reduced) sample space, and that probability is the fraction of $P(A)$ which corresponds to $A \cap B$. Thus

$$P(B \mid A) = \frac{P(A \cap B)}{P(A)} \tag{1.15}$$

Similarly, the *conditional probability of A given B* is

$$P(A \mid B) = \frac{P(A \cap B)}{P(B)} \tag{1.16}$$

Solving equations (1.15) and (1.16) for $P(A \cap B)$, one obtains

Theorem 4 – Multiplication rule
If A and B are events in a sample space S and $P(A) \neq 0$, $P(B) \neq 0$, then

$$P(A \cap B) = P(A)P(B|A) = P(B)P(A|B). \tag{1.17}$$

If the events A and B are such that

$$P(A \cap B) = P(A)P(B), \tag{1.17'}$$

they are called *independent events*. Assuming $P(A) \neq 0$, $P(B) \neq 0$, one notices from (1.15)-(1.17) that in this case

$$P(A|B) = P(A), \qquad P(B|A) = P(B), \tag{1.18}$$

which means that the probability of A does not depend on the occurrence or nonoccurrence of B, and conversely.
Similarly, m events $A_1, \ldots, A_m$, are said to be *independent* if for any k events $A_{j1}, A_{j2}, \ldots, A_{jk}$ (where $1 \leq j_1 < j_2 < \ldots < j_k \leq m$ and $k = 2, 3, \ldots, m$)

$$P(A_{j1} \cap A_{j2} \cap \ldots \cap A_{jk}) = P(A_{j1})\, P(A_{j2}) \ldots P(A_{jk}). \tag{1.19}$$

For a set of events $B_1, B_2, \ldots, B_m$, which are mutually exclusive ($B_1 \cap B_j = \Phi$ for all $i \neq j$ but collectively exhaustive ($B_1 \cup B_2 \cup \ldots \cup B_m = S$), like that shown in the Venn diagram of Fig. 1.5, the probability of another event A can be expressed as

$$P(A) = P(A \cap B_1) + P(A \cap B_2) + \ldots + P(A \cap B_m) \tag{1.20}$$

Using Theorem 4 (Multiplication rule) yields the

Theorem 5 – Total probability theorem

$$P(A) = P(A \mid B_1)P(B_1) + P(A \mid B_2)P(B_2)) + \ldots + P(A \mid B_m)P(B_m) = \sum_{i=1}^{m} P(A \mid B_i)P(B_i) \tag{1.21}$$

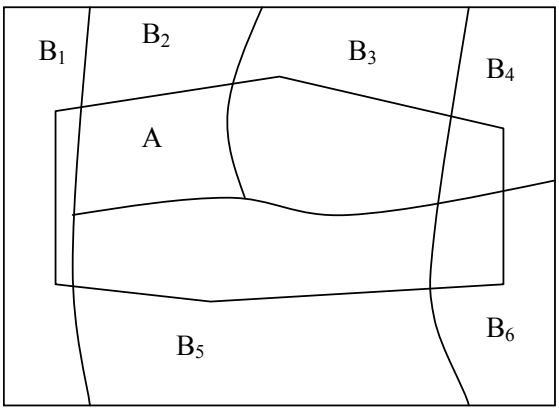

Figure 1.5. Intersection of event A with mutually exclusive but collectively exhaustive events B_I

1.6. Random variables. Discrete and continuos distributions

Roughly speaking, a *random variable X* (also called *stochastic variable* or *variate*) is a function whose values are real numbers and depend on *chance*; more precisely, it is a function *X* which has the following properties, (Kreyszig, 1979):

1.X is defined on the sample space S of the experiment, and its values are real numbers.

2.Let a be any real number, and let I be any interval. Then the set of all outcomes in S for which X=a has a well defined probability, and the same is true for the set of all outcomes in S for which the values of X are in I. These probabilities are in agreement with the axioms in Section 1.5.

If one performs a random experiment and the event corresponding to a number *a* occurs, then we say that in this trial the random variable *X* corresponding to that experiment has *assumed* the value *a*. Instead of "the event corresponding to a number *a*", one says, more briefly, "the event *X=a*". The corresponding probability is denoted by *P(X=a)*. Similarly, the probability of the event

X assumes any value in the interval a<X<b

is denoted by *P(a<X<b)*. The probability of the event

X≤c (X assumes any value smaller than c or equal to c)

is denoted by *P(X≤c)*, and the probability of the event

X>c (X assumes any value greater than c)

is denoted by *P(X>c).*

The last two events are mutually exclusive. From Axiom 3 in Section 5 one obtains

$$P(X \le c) + P(X > c) = P(-\infty < X < \infty). \tag{1.22}$$

From Axiom 2 one notices that the right hand side equals 1, because $-\infty < X < \infty$ corresponds to the whole sample space. This yields the important formula

$$P(X > c) = 1 - P(X \le c). \tag{1.23}$$

In most practical cases the random variables are either *discrete* or *continuos*.

A random variable *X* and the corresponding distribution are said to be *discrete*, if *X* has the following properties:

1.The number of values for which *X* has a probability different from 0 is finite or at most countably infinite.

*2.*If a interval $a < X \le b$ does not contain such a value, then $P(a < X \le b) = 0$.

Let

$$x_1, x_2, x_3, \ldots$$

be the values for which *X* has a positive probability, and let

$$p_1, p_2, p_3, \ldots$$

be the corresponding probabilities. Then $P(X=x_1)=p_1$, etc. One introduces the function:

$$f(x) = \begin{cases} p_j \text{ when } x = x_j \ (j = 1,2,\ldots) \\ 0 \qquad\qquad \text{otherwise} \end{cases} \tag{1.24}$$

f(x) is called the *probability density function of X*, *PDF.*

Since *P(S) = 1* (cf. Axiom 2 in Section 1.5), one must has

$$\sum_{j=1}^{\infty} f(x_j) = 1 \tag{1.25}$$

If one knows the probability function of a discrete random variable *X*, then one may readily compute the probability $P(a < X \le b)$ corresponding to any interval $a < X \le b$. In fact,

$$P(a < X \le b) = \sum_{a < x_j \le b} f(x_j) = \sum_{a < x_j \le b} p_j \tag{1.26}$$

The *probability function* determines the *probability distribution of the random variable X* in a unique fashion.

If X is any random variable, not necessarily discrete, then for any real number x there exists the probability $P(X \leq x)$ corresponding to

$X \leq x$ *(X assumes any value smaller than x or equal to x)*

is a function of x, which is called the *cumulative distribution function of X*, *CDF* and is denoted by $F(x)$. Thus

$$F(x) = P(X \leq x). \tag{1.27}$$

Since for any a and $b > a$ one has

$$P(a < X \leq b) = P(X \leq b) - P(X \leq a) \tag{1.28}$$

it follows that

$$P(a < X \leq b) = F(b) - F(a). \tag{1.29}$$

Suppose that X is a discrete random variable. Than one may represent the distribution function $F(x)$ in terms of probability function $f(x)$ by inserting $a = -\infty$ and $b = x$

$$F(x) = \sum_{x_j \leq x} f(x_j) \tag{1.30}$$

where the right-hand side is the sum of all those $f(x_j)$ for which $x_j \leq x$.

$F(x)$ is a *step function* (piecewise constant function) which has an upward jump of magnitude $p_j = P(X = x_j)$ at $x = x_j$ and is constant between two subsequent possible values. Figure 1.6 is an illustrative example.

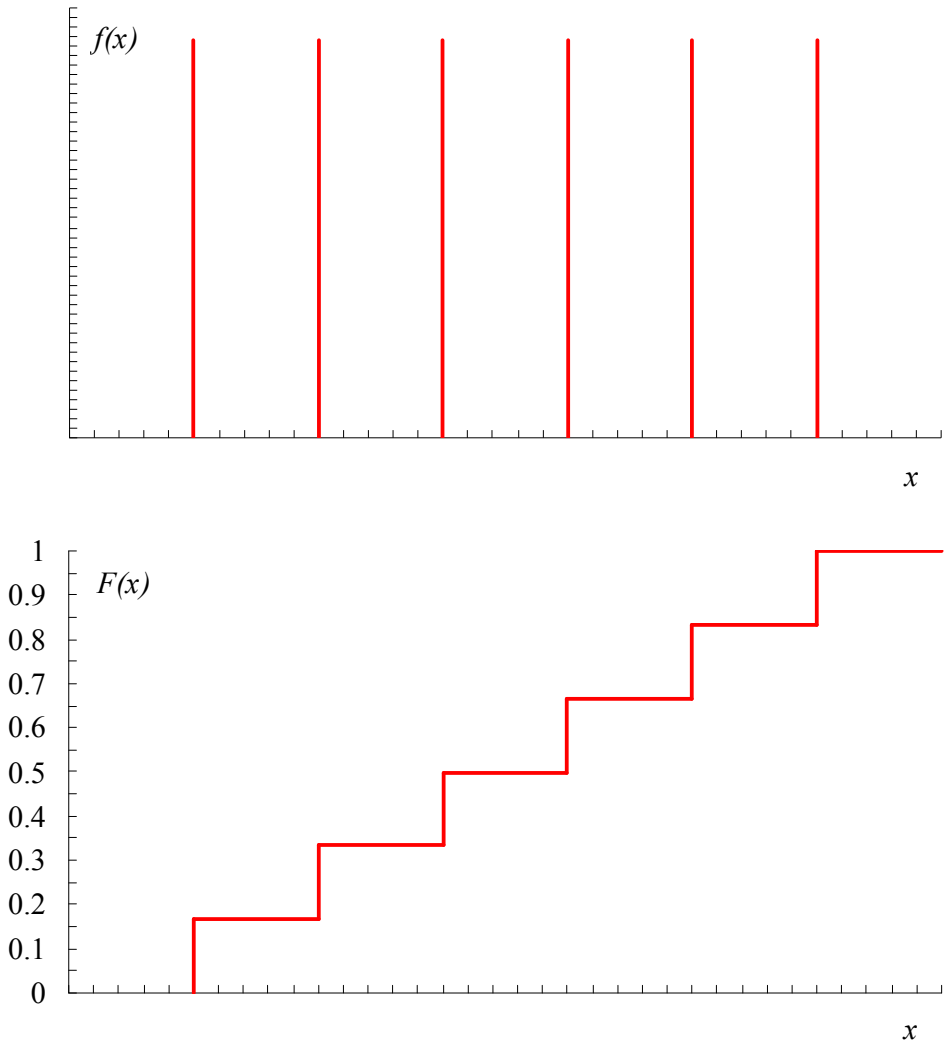

Figure 1.6. Probability function $f(x)$ and distribution function $F(x)$ of the random variable X

One shall now define and consider continuos random variables. A random variable X and the corresponding distribution are said to be of *continuos type* or, briefly, *continuos* if the corresponding distribution function $F(x) = P(X \leq x)$ can be represented by an integral in the form

$$F(x) = \int_{-\infty}^{x} f(u)du \tag{1.31}$$

where the integrand is continuos and is nonnegative. The integrand f is called the *probability density* or, briefly, the *density* of the distribution. Differentiating one notices that

$$F'(x) = f(x) \tag{1.32}$$

In this sense *the density is the derivative of the distribution function.*
From Axiom 2, Section 1.6, one also has

$$\int_{-\infty}^{\infty} f(u)du = 1 \tag{1.33}$$

Furthermore, one obtains the formula

$$P(a < X \leq b) = F(b) - F(a) = \int_{a}^{b} f(u)du \tag{1.34}$$

Hence this probability equals the area under the curve of the density $f(x)$ between $x=a$ and $x=b$, as shown in Figure 1.7.

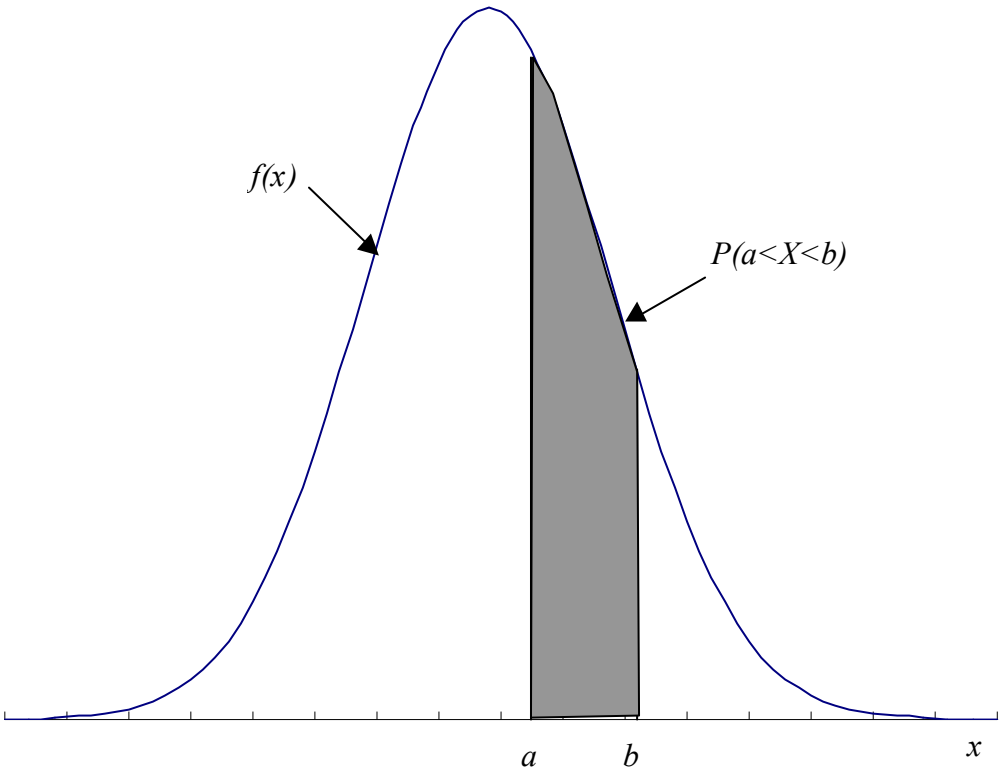

Figure 1.7. Example of probability computation

1.7. Mean and variance of a distribution

The *mean value* or *mean* of a distribution is denoted by μ and is defined by

$$\mu = \sum_{j} x_j f(x_j) \qquad \text{(discrete distribution)} \tag{1.35a}$$

$$\mu = \int_{-\infty}^{\infty} x f(x)\,dx \qquad \text{(continuous distribution)} \qquad (1.35b)$$

where $f(x_j)$ is the probability function of discrete random variable X and $f(x)$ is the density of continuos random variable X. The mean is also known as the *mathematical expectation of X* and is sometimes denoted by $E(X)$.

A distribution is said to be *symmetric* with respect to a number $x = c$ if for every real x,

$$f(c+x) = f(c-x). \qquad (1.36)$$

Theorem 1 – Mean of a symmetric distribution

If a distribution is symmetric with respect to $x = c$ and has a mean μ, then $\mu = c$.

The *variance* of a distribution is denoted by σ^2 and is defined by the formula

$$\sigma^2 = \sum_j (x_j - \mu)^2 f(x_j) \qquad \text{(discrete distribution)} \qquad (1.37a)$$

$$\sigma^2 = \int_{-\infty}^{\infty} (x - \mu)^2 f(x)\,dx \qquad \text{(continuous distribution).} \qquad (1.37b)$$

The positive square root of the variance is called the *standard deviation* and is denoted by σ. Roughly speaking, the variance is a measure of the spread or dispersion of the values which the corresponding random variable X can assume.

The *coefficient of variation of a distribution* is denoted by V and is defined by the formula

$$V = \frac{\sigma}{\mu} \qquad (1.38)$$

Theorem 2 – Linear transformation

If a random variable X has mean μ and variance σ^2, the random variable $X^* = c_1 X + c_2$ has the mean

$$\mu^* = c_1 \mu + c_2 \qquad (1.39)$$

and the variance

$$\sigma^{*2} = c_1^2 \sigma^2 \qquad (1.40)$$

Theorem 3 – Standardized variable

If a random variable X has mean μ and variance σ^2, then the corresponding variable $Z = (X - \mu)/\sigma$ has the mean 0 and the variance 1.

Z is called the *standardized variable* corresponding to X.

If X is any random variable and $g(X)$ is any continuos function defined for all real X, then the number

$$E(g(X)) = \sum_j g(x_j) f(x_j) \quad (X \text{ discrete}) \qquad (1.41a)$$

$$E(g(X)) = \int_{-\infty}^{\infty} g(x) f(x)\,dx \quad (X \text{ continuous}) \qquad (1.41b)$$

is called the *mathematical expectation* of $g(X)$. Here f is the probability function or the density, respectively.

Taking $g(X) = X^k$ ($k = 1, 2, \ldots$), one obtains

$$E(X^k) = \sum_j x_j^k f(x_j) \qquad \text{and} \qquad E(X^k) = \int_{-\infty}^{\infty} x^k f(x)\,dx, \qquad (1.42)$$

respectively. $E(X^k)$ is called the *kth moment* of X. Taking $g(X) = (X-\mu)^k$, one has

$$E((X-\mu)^k) = \sum_j (x_j - \mu)^k f(x_j) \;; E((X-\mu)^k) = \int_{-\infty}^{\infty} (x-\mu)^k f(x)\,dx, \qquad (1.43)$$

respectively. This expression is called the *kth central moment* of X. One can show that

$$E(1) = 1 \tag{1.44}$$
$$\mu = E(X) \tag{1.45}$$
$$\sigma^2 = E((X - \mu)^2). \tag{1.46}$$

Note:
The *mode* of the distribution is the value of the random variable that corresponds to the peak of the distribution (the most likely value).
The *median* of the distribution is the value of the random variable that have 50% chances of smaller values and, respectively 50% chances of larger values.
The *fractile* x_p is defined as the value of the random variable X with p non-exceedance probability ($P(X \leq x_p) = p$).

2. DISTRIBUTIONS OF PROBABILITY

2.1. Binomial and Poisson distributions

One shall now consider special discrete distributions which are particularly important in statistics. One starts with the binomial distribution, which is obtained if one is interested in the number of times an event A occurs in n independent performances of an experiment, assuming that A has probability $P(A) = p$ in a single trial. Then $q = 1 - p$ is the probability that in a single trial the event A does not occur. One assumes that the experiment is performed n times and considers the random variable

X = *number of times A occurs*.

Then X can assume the values 0, 1, .., n, and one wants to determine the corresponding probabilities. For this purpose one considers any of these values, say, $X = x$, which means that in x of the n trials A occurs and in $n - x$ trials it does not occur.

The probability $P(X = x)$ corresponding to $X = x$ equals

$$f(x) = C_n^x p^x q^{n-x} \qquad (x = 0, 1, \ldots, n). \tag{2.1}$$

This is the probability that in n independent trials an event A occurs precisely x times where p is the probability of A in a single trial and $q = 1 - p$. The distribution determined is called the *binomial distribution* or *Bernoulli distribution*. The occurrence of A is called *success*, and the nonoccurrence is called *failure*. p is called the *probability of success in a single trial*. Figure 2.1 shows illustrative examples of *binomial distribution*.

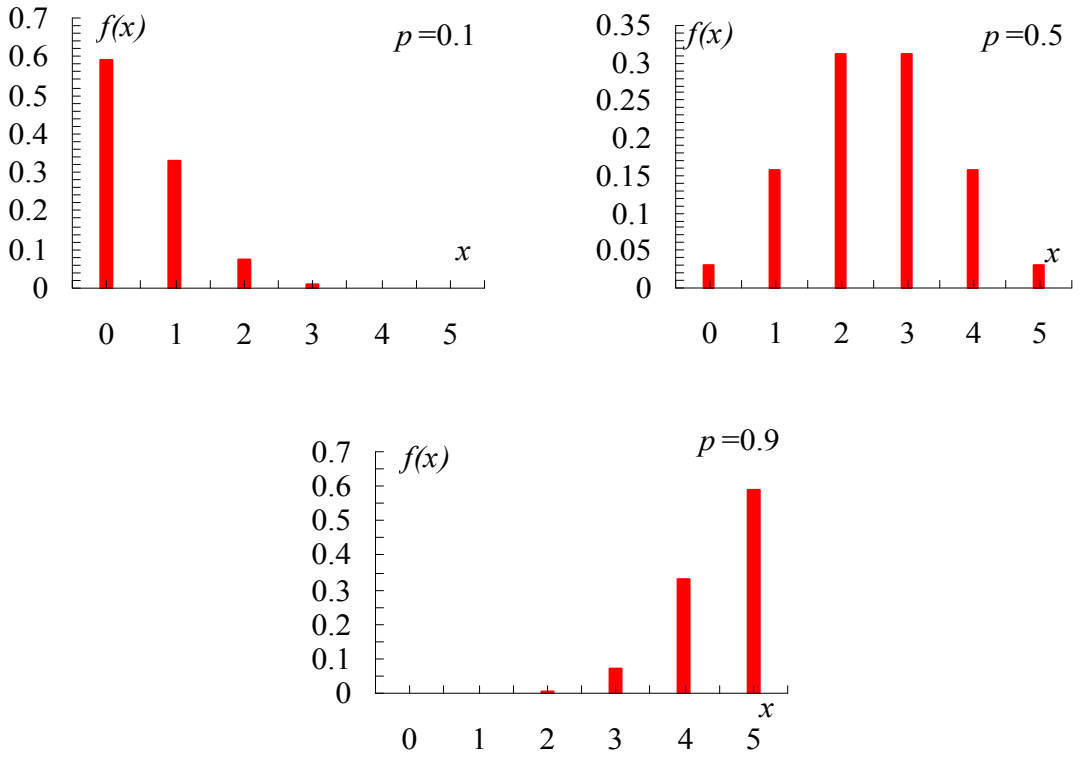

Figure 2.1. Probability function of the binomial distribution for $n = 5$ and various values of p

The binomial distribution has the mean

$$\mu = np \tag{2.2}$$

and the variance

$$\sigma^2 = npq. \qquad (2.3)$$

Note that when $p = 0.5$, the distribution is symmetric with respect to μ.
The distribution with the probability function

$$f(x) = \frac{\mu^x}{x!} e^{-\mu} \qquad (x = 0, 1, \ldots) \qquad (2.4)$$

is called the *Poisson distribution*. Figure 2.2 shows the *Poisson* probability function for some values of μ.

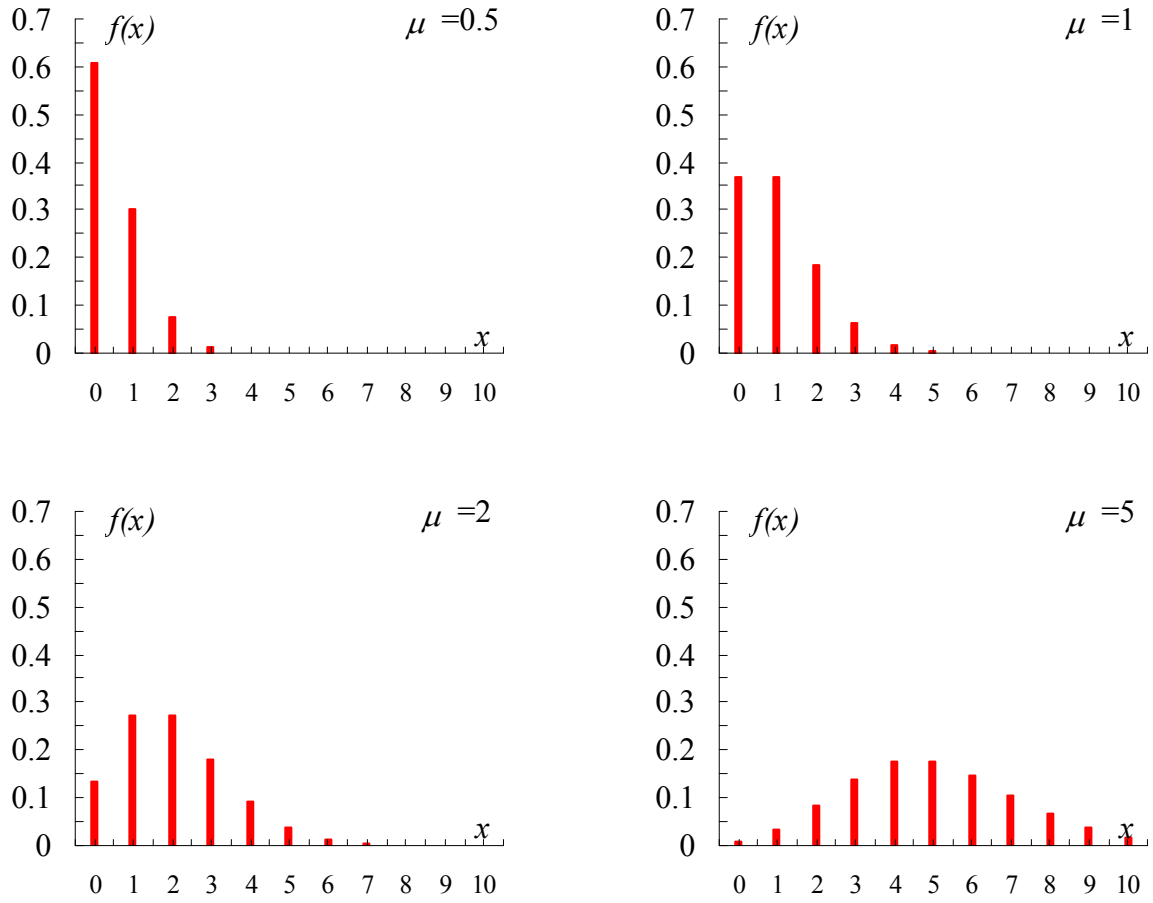

Figure 2.2. Probability function of the *Poisson* distribution for various values of μ

It can be proved that *Poisson* distribution may be obtained as a limiting case of the binomial distribution, if one let $p \to 0$ and $n \to \infty$ so that the mean $\mu = np$ approaches a finite value. The *Poisson* distribution has the mean μ and the variance

$$\sigma^2 = \mu. \qquad (2.5)$$

2.2. Normal distribution

The continuos distribution having the probability density function, *PDF*

$$f(x) = \frac{1}{\sqrt{2\pi}\sigma} e^{-\frac{1}{2}\left(\frac{x-\mu}{\sigma}\right)^2} \qquad (2.6)$$

is called the *normal distribution* or *Gauss distribution*. A random variable having this distribution is said to be *normal* or *normally distributed*. This distribution is very important, because many random variables of practical interest are normal or approximately normal or can be transformed into normal random variables. Furthermore, the normal distribution is a useful approximation of more complicated distributions.

In Equation 2.6, μ is the mean and σ is the standard deviation of the distribution. The curve of *f(x)* is called the *bell-shaped curve*. It is symmetric with respect to μ. Figure 2.3 shows *f(x)* for same μ and various values of σ (and various values of coefficient of variation *V*).

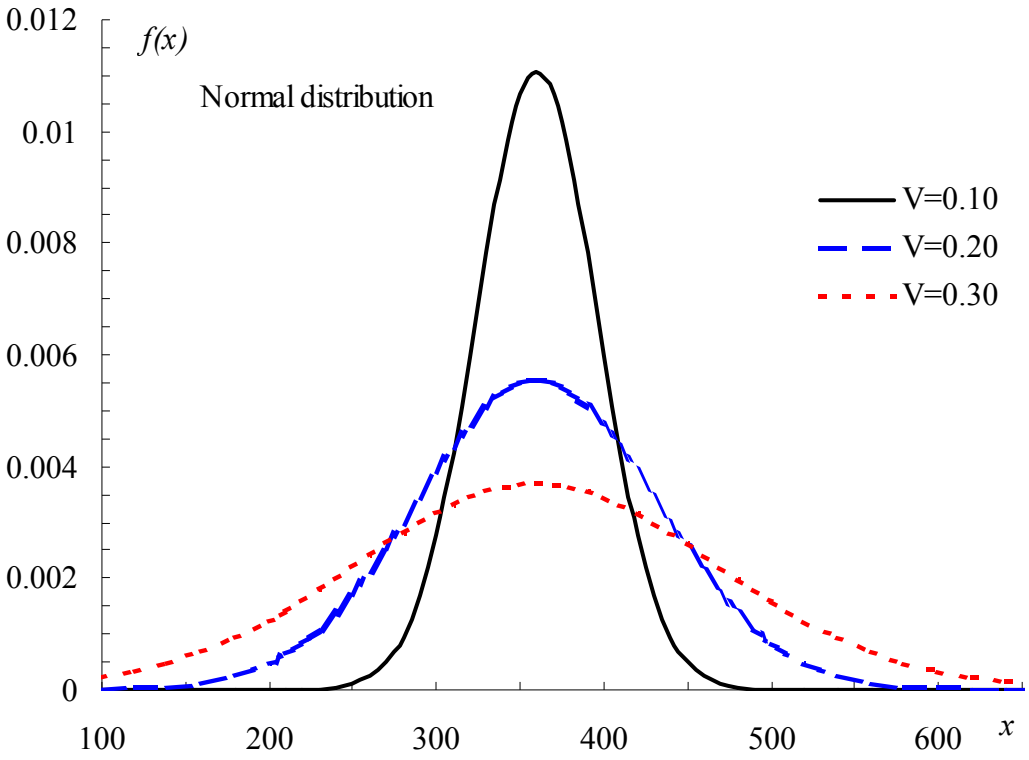

Figure 2.3. Density (2.6) of the normal distribution for various values of *V*

The smaller σ (and *V*) is, the higher is the peak at $x = \mu$ and the steeper are the descents on both sides. This agrees with the meaning of variance.

From (2.6) one notices that the normal distribution has the cumulative distribution function, *CDF*

$$F(x) = \frac{1}{\sqrt{2\pi}\sigma} \int_{-\infty}^{x} e^{-\frac{1}{2}\left(\frac{v-\mu}{\sigma}\right)^2} dv \qquad (2.7)$$

Figure 2.4 shows *F(x)* for same μ and various values of σ (and various values of coefficient of variation *V*).

From (2.7) one obtains

$$P(a < X \le b) = F(b) - F(a) = \frac{1}{\sqrt{2\pi}\sigma} \int_{a}^{b} e^{-\frac{1}{2}\left(\frac{v-\mu}{\sigma}\right)^2} dv \qquad (2.8)$$

The integral in (2.7) cannot be evaluated by elementary methods, but can be represented in terms of the integral

$$\Phi(z) = \frac{1}{\sqrt{2\pi}} \int_{-\infty}^{z} e^{-u^2/2} du \qquad (2.9)$$

which is the distribution function of the normal distribution with mean 0 and variance 1 and has been tabulated. In fact, if one sets $(v - \mu)/\sigma = u$, *then* $du/dv = 1/\sigma$, and one has to integrate from $-\infty$ to $z = (x - \mu)/\sigma$.
The density function and the distribution function of the normal distribution with mean 0 and variance 1 are presented in Figure 2.5.

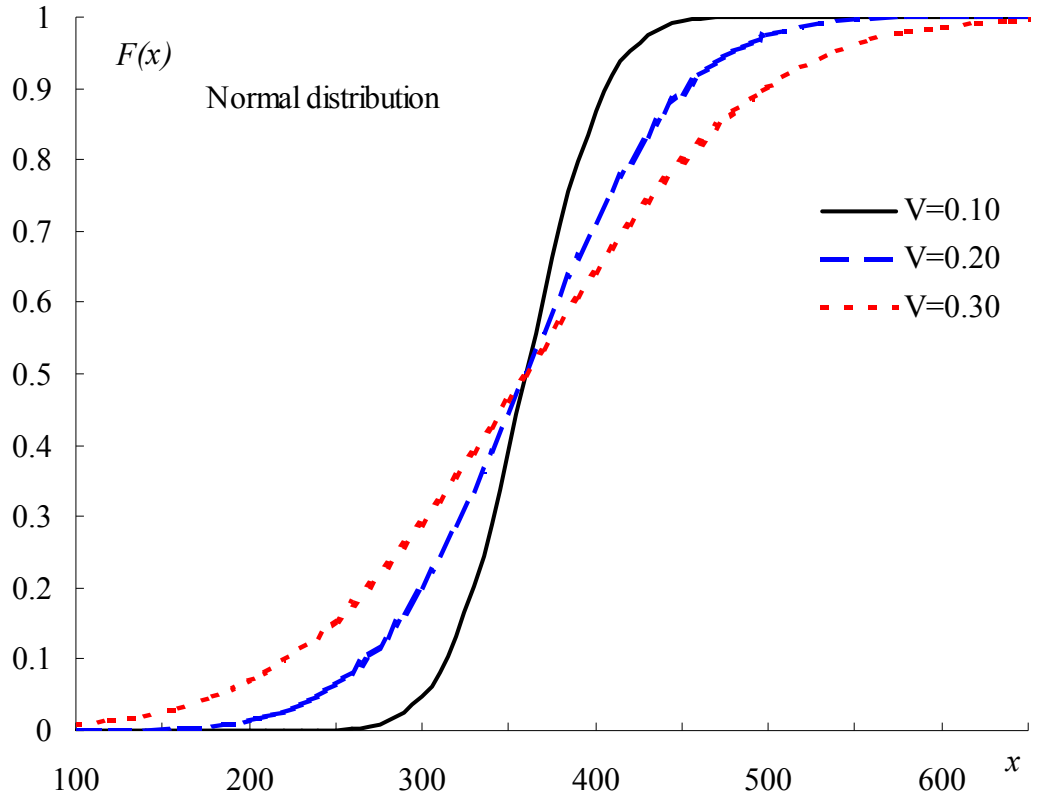

Figure 2.4. Distribution function (2.7) of the normal distribution for various values of V

From (2.7) one obtains

$$F(x) = \frac{1}{\sqrt{2\pi}\sigma} \int_{-\infty}^{(x-\mu)/\sigma} e^{-u^2/2} \sigma du$$

σ drops out, and the expression on the right equals (4) where $z = (x - \mu)/\sigma$, that is,

$$F(x) = \Phi\left(\frac{x-\mu}{\sigma}\right) \tag{2.10}$$

From this important formula and (2.8) one gets

$$P(a < X \le b) = F(b) - F(a) = \Phi\left(\frac{b-\mu}{\sigma}\right) - \Phi\left(\frac{a-\mu}{\sigma}\right) \tag{2.11}$$

In particular, when $a = \mu - \sigma$ and $b = \mu + \sigma$, the right-hand side equals $\Phi(1) - \Phi(-1)$; to $a = \mu - 2\sigma$ and $b = \mu + 2\sigma$ there corresponds the value $\Phi(2) - \Phi(-2)$, etc. Using tabulated values of Φ function one thus finds

$$\begin{aligned} &\text{(a) } P(\mu - \sigma < X \le \mu + \sigma) \cong 68\% \\ &\text{(b) } P(\mu - 2\sigma < X \le \mu + 2\sigma) \cong 95.5\% \\ &\text{(c) } P(\mu - 3\sigma < X \le \mu + 3\sigma) \cong 99.7\% \end{aligned} \tag{2.12}$$

Hence one may expect that a large number of observed values of a normal random variable X will be distributed as follows:

(a) *About 2/3 of the values will lie between* μ-σ and μ+σ
(b) *About 95% of the values will lie between* μ-2σ and μ+2σ
(c) *About 99¾ % of the values will lie between* μ-3σ and μ+3σ.

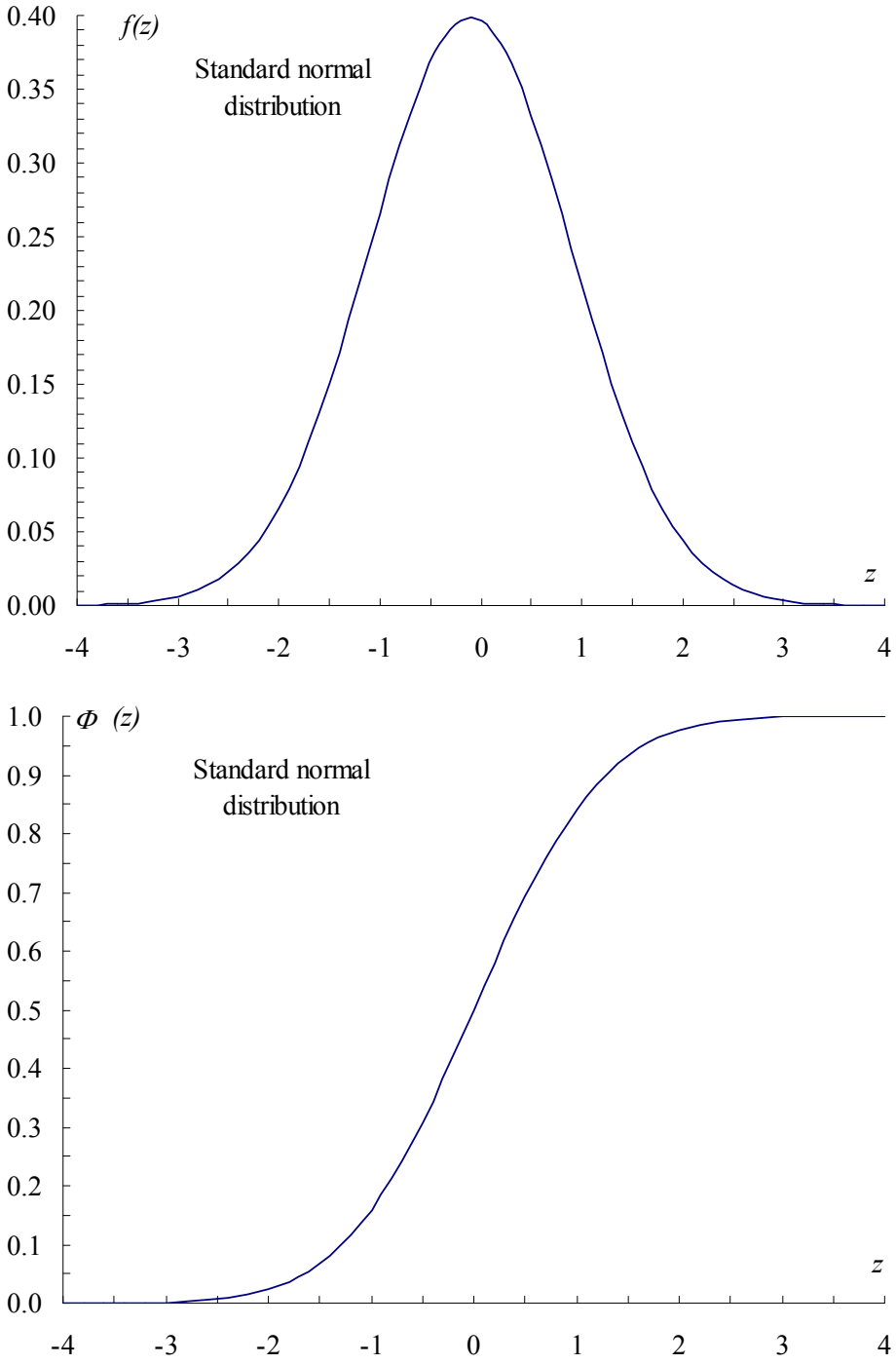

Figure 2.5. Density function and distribution function of the normal distribution with mean 0 and variance 1

This may be expressed as follows.
A value that deviates more than σ from μ will occur about once in 3 trials. A value that deviates more than 2σ or 3σ from μ will occur about once in 20 or 400 trials, respectively. Practically speaking, this means that all the values will lie between μ-3σ and μ+3σ; these two numbers are called *three-sigma limits*.

The fractile x_p that is defined as the value of the random variable X with p non-exceedance probability ($P(X \le x_p) = p$) is computed as follows:

$$x_p = \mu + k_p \cdot \sigma \tag{2.13}$$

The meaning of k_p becomes clear if one refers to the reduced standard variable $z = (x - \mu)/\sigma$. Thus, $x = \mu + z \cdot \sigma$ and k_p represents the value of the reduced standard variable for which $\Phi(z) = p$.
The most common values of k_p are given in Table 2.1.

Table 2.1. Values of k_p for different non-exceedance probabilities p

p	0.01	0.02	0.05	0.95	0.98	0.99
k_p	-2.326	-2.054	-1.645	1.645	2.054	2.326

2.3. Log-normal distribution

The log-normal distribution (Hahn & Shapiro, 1967) is defined by its following property: if the random variable *lnX* is normally distributed with mean μ_{lnX} and standard deviation σ_{lnX}, then the random variable X is log-normally distributed. Thus, the cumulative distribution function *CDF* of random variable *lnX* is of normal type:

$$F(\ln x) = \frac{1}{\sqrt{2\pi}} \cdot \frac{1}{\sigma_{\ln X}} \cdot \int_{-\infty}^{\ln x} e^{-\frac{1}{2}\left(\frac{\ln v - \mu_{\ln X}}{\sigma_{\ln X}}\right)^2} d(\ln v) = \frac{1}{\sqrt{2\pi}} \cdot \frac{1}{\sigma_{\ln X}} \cdot \int_{-\infty}^{x} e^{-\frac{1}{2}\left(\frac{\ln v - \mu_{\ln X}}{\sigma_{\ln X}}\right)^2} \cdot \frac{1}{v} dv \tag{2.14}$$

Since:

$$F(\ln x) = \int_{-\infty}^{x} f(v) dv \tag{2.15}$$

the probability density function *PDF* results from (2.14) and (2.15):

$$f(x) = \frac{1}{\sqrt{2\pi}} \cdot \frac{1}{\sigma_{\ln X}} \cdot \frac{1}{x} \cdot e^{-\frac{1}{2}\left(\frac{\ln x - \mu_{\ln X}}{\sigma_{\ln X}}\right)^2} \tag{2.16}$$

The lognormal distribution is asymmetric with positive asymmetry, i.e. the distribution is shifted to the left. The skewness coefficient for lognormal distribution is:

$$\sqrt{\beta_1} = 3V_X + V_X^3 \tag{2.17}$$

where V_X is the coefficient of variation of random variable X. Higher the variability, higher the shift of the lognormal distribution.
The mean and the standard deviation of the random variable *lnX* are related to the mean and the standard deviation of the random variable X as follows:

$$m_{\ln X} = \ln \frac{m_X}{\sqrt{1 + V_X^2}} \tag{2.18}$$

$$\sigma_{\ln X} = \sqrt{\ln(1 + V_X^2)} \tag{2.19}$$

If V_X is small enough ($V_X \le 0.1$), then:

$$m_{\ln X} \cong \ln m_X \tag{2.20}$$

$$\sigma_{\ln X} \cong V_X \tag{2.21}$$

The *PDF* and the *CDF* of the random variable X are presented in Figure 2.6 for different coefficients of variation.

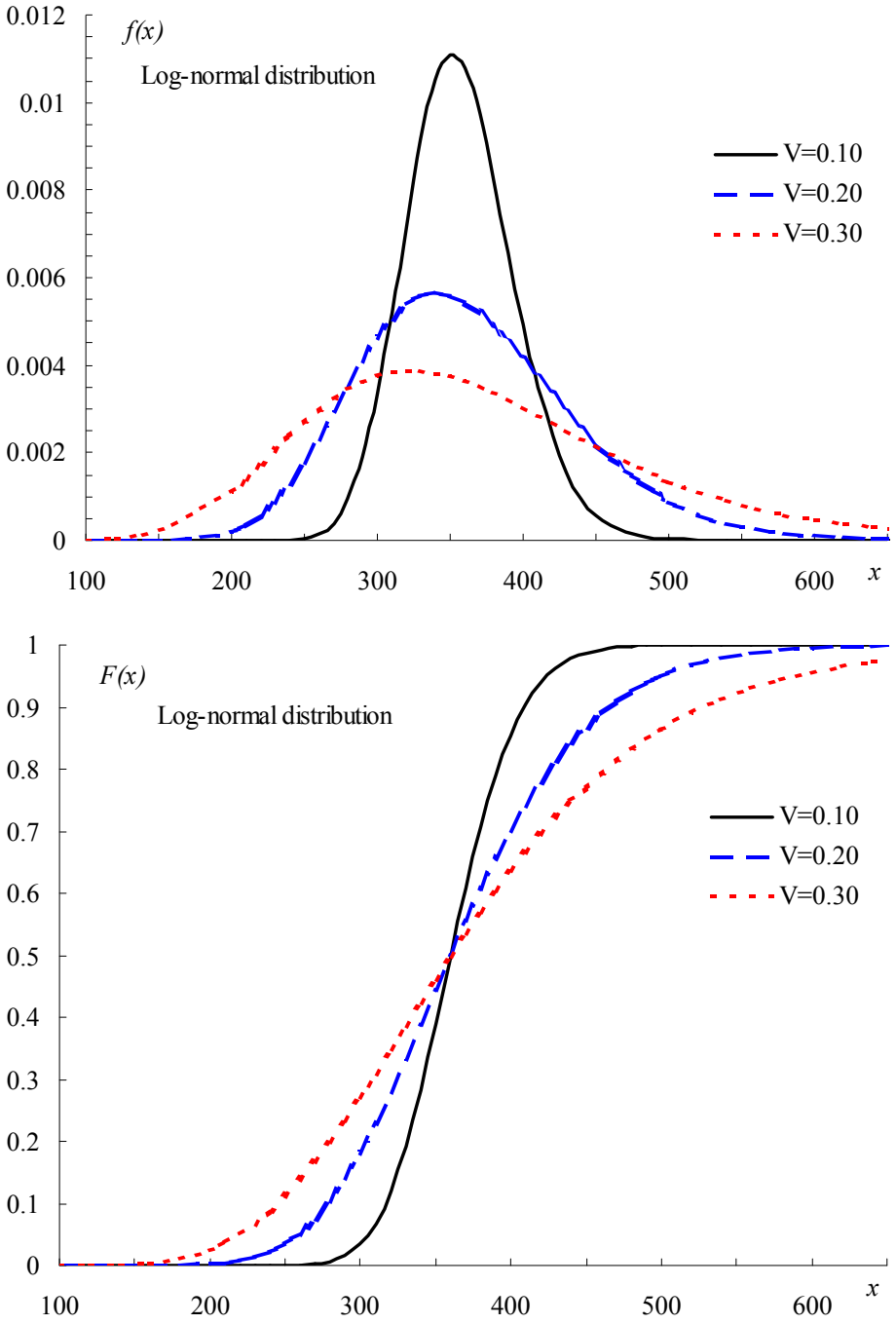

Figure 2.6. Probability density function, $f(x)$ and cumulative distribution function, $F(x)$ of the log-normal distribution for various values of V

If one uses the reduced variable $(lnv - \mu)/\sigma = u$, *then* $du/dv = 1/(v\sigma)$, and one has to integrate from $-\infty$ to $z = (lnx - \mu)/\sigma$. From (2.14) one obtains:

$$\Phi(z) = \frac{1}{\sqrt{2\pi}\sigma} \int_{-\infty}^{(\ln x-\mu)/\sigma} e^{-u^2/2} \cdot \frac{1}{v}\sigma v du = \frac{1}{\sqrt{2\pi}} \int_{-\infty}^{z} e^{-u^2/2} du \qquad (2.22)$$

The fractile x_p that is defined as the value of the random variable X with p non-exceedance probability ($P(X \leq x_p) = p$) is computed as follows, given lnX normally distributed:

$$ln(x_p) = \mu_{lnX} + k_p \cdot \sigma_{lnX} \qquad (2.23)$$

From (2.23) one gets:

$$x_p = e^{\mu_{\ln X} + k_p \cdot \sigma_{\ln X}} \tag{2.24}$$

where k_p represents the value of the reduced standard variable for which $\Phi(z) = p$.

2.4. Distribution of extreme values

The distribution of extreme values was first considered by Emil Gumbel in his famous book "Statistics of extremes" published in 1958 at Columbia University Press. The extreme values distribution is of interest especially when one deals with natural hazards like snow, wind, temperature, floods, etc. In all the previously mentioned cases one is not interested in the distribution of all values but in the distribution of extreme values which might be the minimum or the maximum values. In Figure 2.7 it is represented the distribution of all values of the random variable X as well as the distribution of minima and maxima of X.

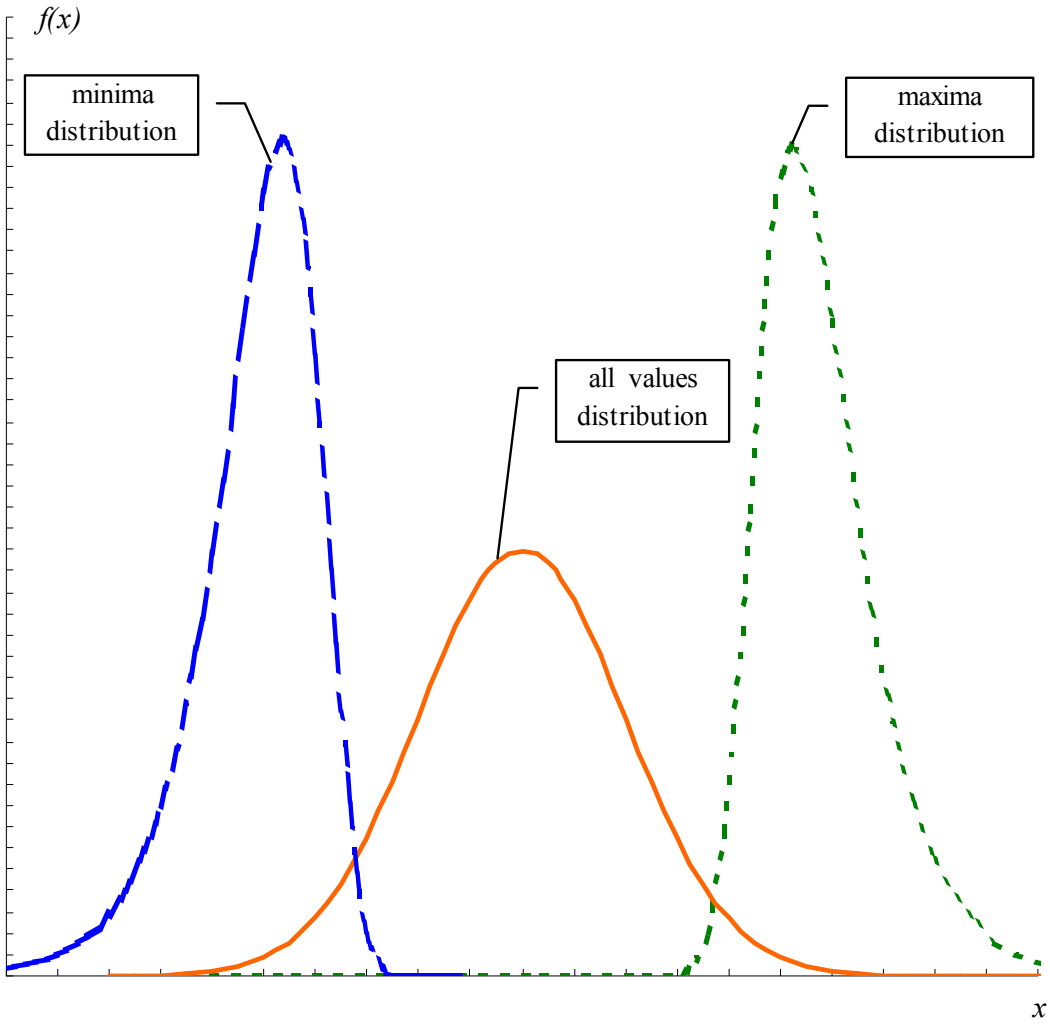

Figure 2.7. Distribution of all values, of minima and of maxima of random variable X

2.4.1. Gumbel distribution for maxima in 1 year

The Gumbel distribution for maxima is defined by its cumulative distribution function, *CDF*:

$$F(x) = e^{-e^{-\alpha(x-u)}} \tag{2.25}$$

where:
$u = \mu_x - 0.45 \cdot \sigma_x$ – mode of the distribution (Figure 2.10)
$\alpha = 1.282 / \sigma_x$ – dispersion coefficient.
The skewness coefficient of Gumbel distribution is positive constant ($\sqrt{\beta_1} = 1.139$), i.e. the distribution is shifted to the left. In Figure 2.8 it is represented the *CDF* of Gumbel distribution for maxima for the random variable X with the same mean μ_x and different coefficients of variation V_x.
The probability distribution function, *PDF* is obtained straightforward from (2.25):

$$f(x) = \frac{dF(x)}{dx} = \alpha \cdot e^{-\alpha(x-u)} \cdot e^{-e^{-\alpha(x-u)}} \tag{2.26}$$

The *PDF* of Gumbel distribution for maxima for the random variable X with the same mean μ_x and different coefficients of variation V_x is represented in Figure 2.9.

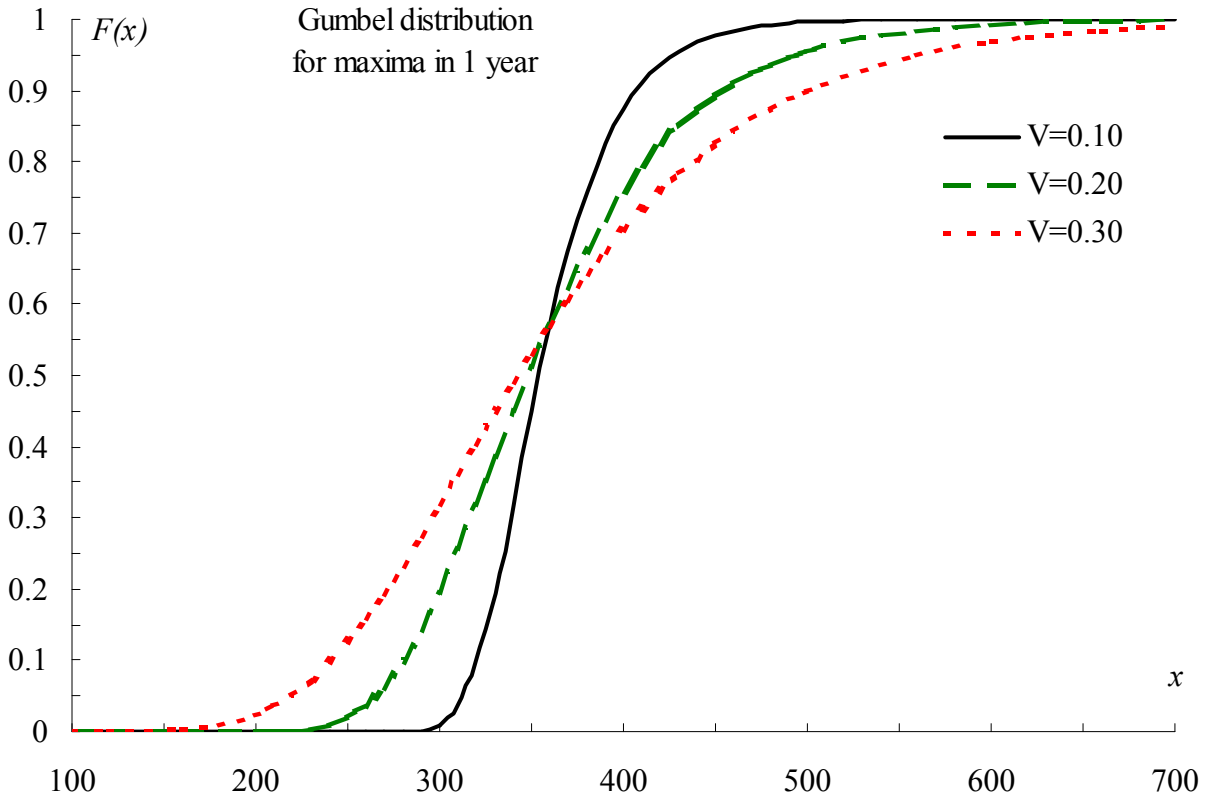

Figure 2.8. *CDF* of Gumbel distribution for maxima for the random variable X with the same mean μ_x and different coefficients of variation V_x.

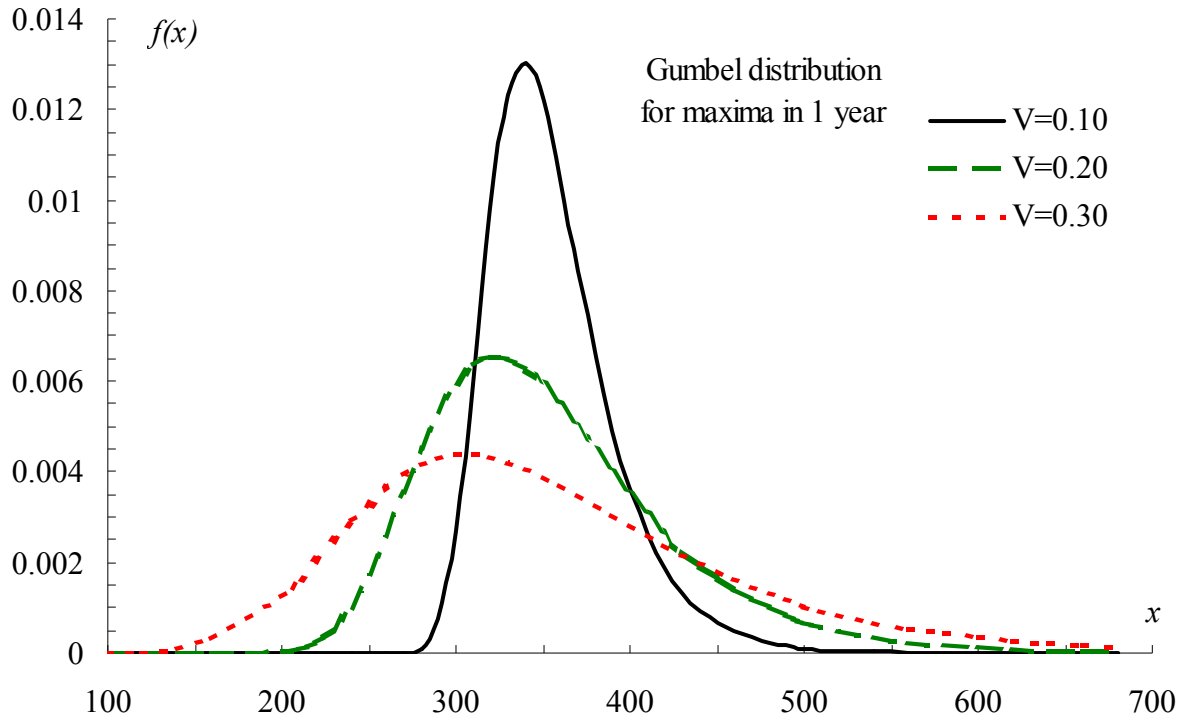

Figure 2.9. *PDF* of Gumbel distribution for maxima for the random variable X with the same mean μ_x and different coefficients of variation V_x.

One can notice in Figure 2.9 that higher the variability of the random variable, higher the shift to the left of the *PDF*.

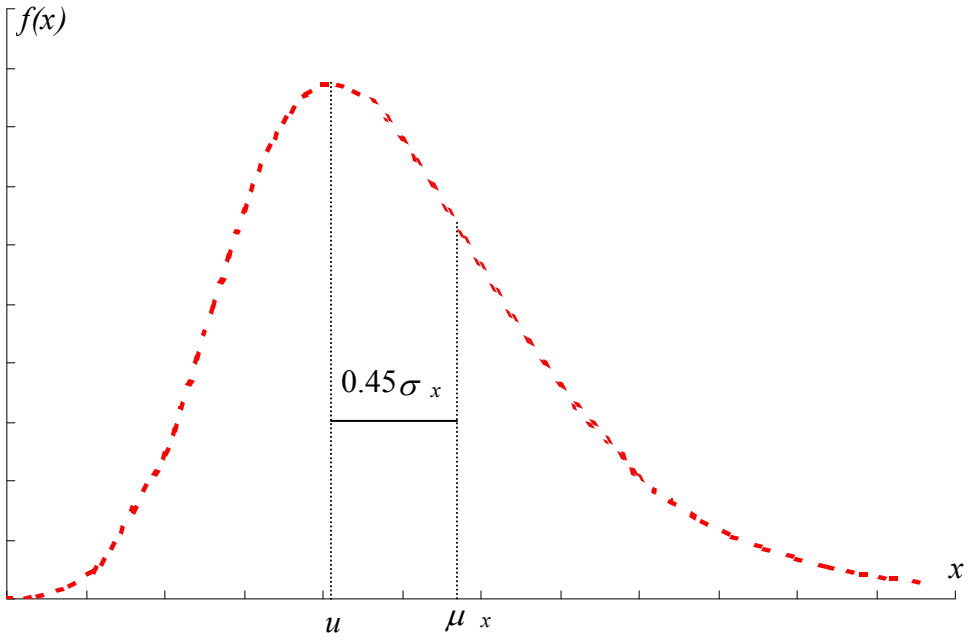

Figure 2.10. Significance of mode parameter u in Gumbel distribution for maxima

The fractile x_p that is defined as the value of the random variable X with p non-exceedance probability ($P(X \leq x_p) = p$) is computed as follows, given X follows Gumbel distribution for maxima:

$$F(x_p) = P(X \le x_p) = p = e^{-e^{-\alpha(x_p - u)}} \tag{2.27}$$

From Equation 2.27 it follows:

$$x_p = u - \frac{1}{\alpha} \cdot ln(-ln\, p) = \mu_x - 0.45\sigma_x - \frac{\sigma_x}{1.282} \cdot ln(-ln\, p) = \mu_x + k_p^G \cdot \sigma_x \tag{2.28}$$

where:

$$k_p^G = -0.45 - 0.78 \cdot ln(-ln\, p) \tag{2.29}$$

The values of $k_p{}^G$ for different non-exceedance probabilities are given in Table 2.2.

Table 2.2. Values of $k_p{}^G$ for different non-exceedance probabilities p

p	0.50	0.90	0.95	0.98
$k_p{}^G$	-0.164	1.305	1.866	2.593

2.4.2. Gumbel distribution for maxima in N years

All the preceding developments are valid for the distribution of maxima in 1 year. If one considers the probability distribution in N ($N>1$) years, the following relation holds true (if one considers that the occurrences of maxima are independent events):

$$F(x)_{N\,years} = P(X \le x) \text{ in } N \text{ years} = [P(X \le x) \text{ in 1 year}]^N = [F(x)_{1\,year}]^N \tag{2.30}$$

where:

$F(x)_{N\,years}$ – *CDF* of random variable X in N years

$F(x)_{1\,year}$ – *CDF* of random variable X in *1* year.

The Gumbel distribution for maxima has a very important property – the reproducibility of Gumbel distribution - i.e., if the annual maxima in 1 year follow a Gumbel distribution for maxima then the annual maxima in N years will also follow a Gumbel distribution for maxima:

$$F(x)_N = \left(F(x)_1\right)^N = \left(e^{-e^{-\alpha_1(x-u_1)}}\right)^N = e^{-Ne^{-\alpha_1(x-u_1)}} =$$

$$= e^{-e^{-\alpha_1(x-u_1)+\ln N}} = e^{-e^{-\alpha_1\left(x-\left(u_1+\frac{\ln N}{\alpha_1}\right)\right)}} = e^{-e^{-\alpha_N(x-u_N)}} \tag{2.31}$$

where:

u_1 – mode of the distribution in 1 year

α_1 – dispersion coefficient in 1 year

$u_N = u_1 + lnN / \alpha_1$ – mode of the distribution in N years

$\alpha_N = \alpha_1$ – dispersion coefficient in N years

The *PDF* of Gumbel distribution for maxima in N years is translated to the right with the amount lnN / α_1 with respect to the *PDF* of Gumbel distribution for maxima in 1 year, Figure 2.11.

Also, the *CDF* of Gumbel distribution for maxima in N years is translated to the right with the amount lnN / α_1 with respect to the *CDF* of Gumbel distribution for maxima in 1 year, Figure 2.12.

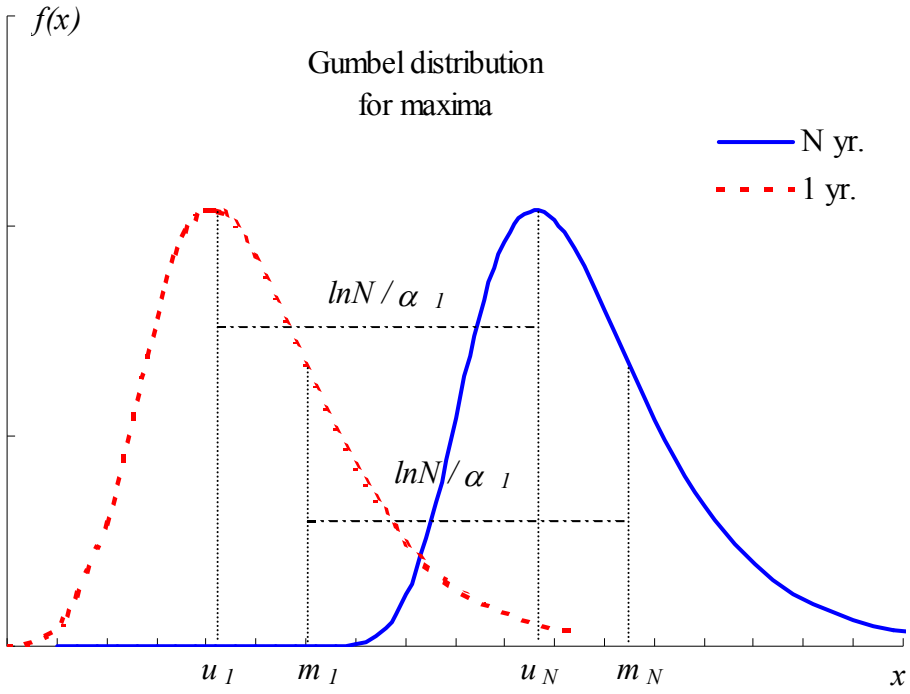

Figure 2.11. *PDF* of Gumbel distribution for maxima in 1 year and in N years

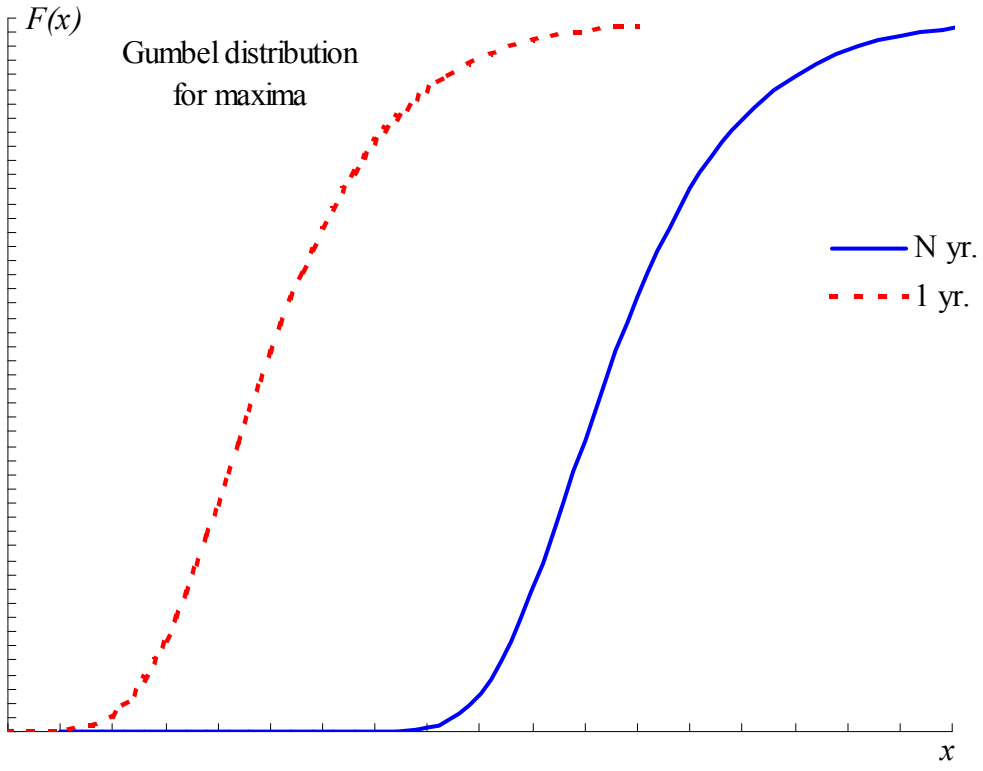

Figure 2.12. *CDF* of Gumbel distribution for maxima in 1 year and in N years

Important notice: The superior fractile x_p ($p >> 0.5$) calculated with Gumbel distribution for maxima in 1 year becomes a frequent value (sometimes even an inferior fractile if N is large, $N \geq 50$) if Gumbel distribution for maxima in N years is employed, Figure 2.13.

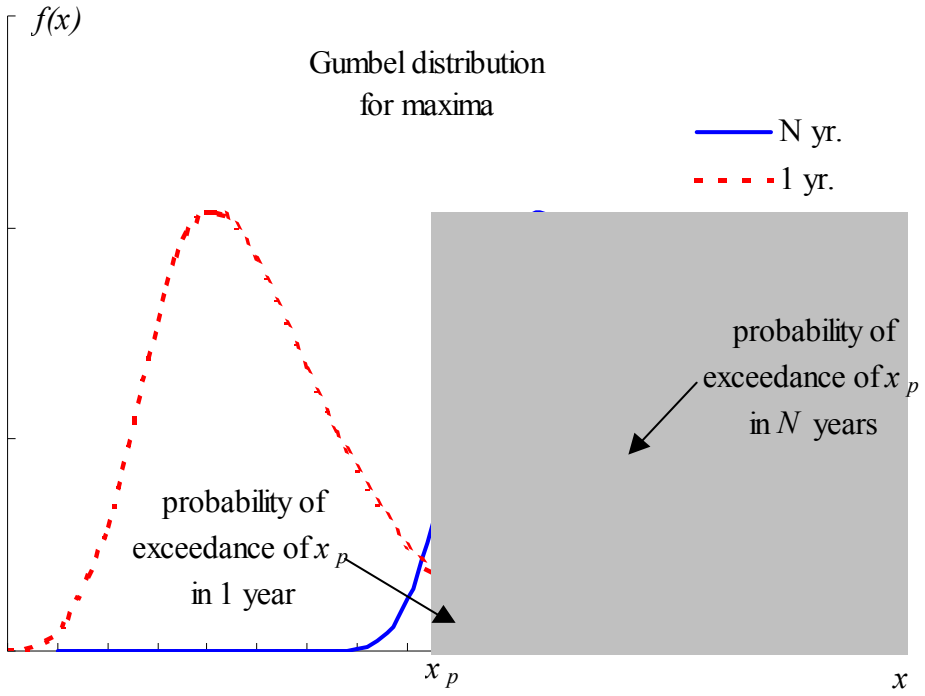

Figure 2.13. Superior fractile x_p in 1 year and its significance in N year

2.5. Mean recurrence interval

The loads due to natural hazards such as earthquakes, winds, waves, floods were recognized as having a randomness in time as well as in space. The randomness in time was considered in terms of the return period or recurrence interval. The recurrence interval also known as a return period is defined as the average (or expected) time between two successive statistically independent events and it is an estimate of the likelihood of events like an earthquake, flood or river discharge flow of a certain intensity or size. It is a statistical measurement denoting the average recurrence interval over an extended period of time, and is usually required for risk analysis (i.e. whether a project should be allowed to go forward in a zone of a certain risk) and also to dimension structures so that they are capable of withstanding an event of a certain return period (with its associated intensity). The actual time T between events is a random variable. In most engineering applications an event denoted the exceedance of a certain threshold associated with loading.

The mean recurrence interval, *MRI* of a value x of the random variable X may be defined as follows:

$$MRI(X > x) = \frac{1}{P_{1year}(X > x)} = \frac{1}{1-p} = \frac{1}{1-F_x(x)} \tag{2.32}$$

where:
p is the annual probability of the event ($X \leq x$)
$F_X(x)$ is the cumulative distribution function of X.

Thus the mean recurrence interval of a value x is equal to the reciprocal of the annual probability of exceedance of the value x. The mean recurrence interval or return period has an inverse relationship with the probability that the event will be exceeded in any one year. For example, a 10-year flood has a 0.1 or 10% chance of being exceeded in any one year and a 50-year flood has a 0.02 (2%) chance of being exceeded in any one year. It is commonly assumed that a 10-year earthquake will occur, on average, once every 10 years and that a 100-year earthquake is so large that we expect it only to occur every 100 years. While this may be statistically true over thousands of years, it is incorrect to think of the return period in this way. The term return period is actually misleading. It does not necessarily mean that the design earthquake of a 10 year return period will return every 10 years. It could, in fact, never occur, or occur twice. It is still a 10 year earthquake, however. This is why the term return period is gradually replaced by the term recurrence interval. The US researchers proposed to use the term return period in relation with the effects and to use the term recurrence interval in relation with the causes.

The mean recurrence interval is often related with the exceedance probability in N years. The relation among MRI, N and the exceedance probability in N years, $P_{exc,N}$ is:

$$P_{exc,N} \cong 1 - e^{-\frac{N}{MRI}} \tag{2.33}$$

Usually the number of years, N is considered equal to the lifetime of ordinary buildings, i.e. 50 years. Table 2.3 shows the results of relation (2.33) for some particular cases considering N=50 years.

Table 2.3 Correspondence amongst MRI, $P_{exc,1\ year}$ and $P_{exc,50\ years}$

Mean recurrence interval, years MRI	Probability of exceedance in 1 year $P_{exc,1\ year}$	Probability of exceedance in 50 years $P_{exc,50\ years}$
10	0.10	0.99
30	0.03	0.81
50	0.02	0.63
100	0.01	0.39
225	0.004	0.20
475	0.002	0.10
975	0.001	0.05
2475	0.0004	0.02

The modern earthquake resistant design codes consider the definition of the seismic hazard level based on the probability of exceedance in 50 years. The seismic hazard due to ground shaking is defined as horizontal peak ground acceleration, elastic acceleration response spectra or acceleration time-histories. The level of seismic hazard is expressed by the mean recurrence interval (mean return period) of the design horizontal peak ground acceleration or, alternatively by the probability of exceedance of the design horizontal peak ground acceleration in 50 years. Four levels of seismic hazard are considered in FEMA 356 – Prestandard and Commentary for the Seismic Rehabilitation of Buildings, as given in Table 2.4. The correspondence between the mean recurrence interval and the probability of exceedance in 50 years, based on Poisson assumption, is also given in Table 2.4.

Table 2.4. Correspondence between mean recurrence interval and probability of exceedance in 50 years of design horizontal peak ground acceleration as in *FEMA 356*

Seismic Hazard Level	Mean recurrence interval (years)	Probability of exceedance
SHL1	72	50% in 50 years
SHL2	225	20 % in 50 years
SHL3	475	10 % in 50 years
SHL4	2475	2 % in 50 years

2.6. Second order moment models

Let us consider a simply supported beam, Figure 2.14:

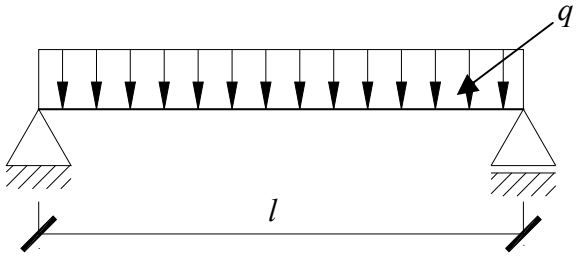

Figure 2.14. Simple supported beam

The design condition (ultimate limit state condition) is:

$$M_{\max} = M_{cap}$$

$$\frac{ql^2}{8} = \sigma_y \cdot W$$

Considering that:

q, σ_y are described probabilistically &

l, W, are described deterministically

and considering

S – sectional effect of load

R – sectional resistance

it follows that:

$$S = \frac{ql^2}{8}; R = \sigma_y \cdot W$$

The following question rises:

If q and σ_y are described probabilistically, how can one describes S and R probabilistically?

To answer the question, two cases are considered in the following:

1. The relation between q and S (σ_y and R) is linear
2. The relation is non linear.

Case 1: Linear relation between random variables, X, Y

$$X \to Y = a \cdot X + b$$

For the random variable X one knows: the probability density function, *PDF*, the cumulative distribution function, *CDF*, the mean, m and the standard deviation, σ. The unknowns are the *PDF*, *CDF*, m and σ for the random variable Y.

If one applies the *equal probability formula*, Figure 2.15:

$$f_X(x)dx = f_Y(y)dy \Leftrightarrow P(x \le X < x+dx) = P(y \le Y < y+dy) \tag{2.34}$$

$$x = \frac{y-a}{b} \quad f_Y(y) = f_X(x)\frac{1}{\frac{dy}{dx}} = \frac{1}{a}f_X(x) = \frac{1}{a}f_X\left(\frac{y-b}{a}\right) \tag{2.35}$$

$\Longrightarrow$ *Distribution of Y ≡ Distribution of X*

Developing further the linear relation it follows that:

$$m_Y = \int_{-\infty}^{+\infty} y f_Y(y)dy = \int_{-\infty}^{+\infty} (a \cdot x + b) \cdot f_X(x)dx = a \cdot \int_{-\infty}^{+\infty} x f_X(x)dx + b \cdot \int_{-\infty}^{+\infty} f_X(x)dx = a \cdot m_X + b$$

$$\sigma_Y^2 = \int_{-\infty}^{+\infty} (y - m_Y)^2 \cdot f_Y(y)dy = \int_{-\infty}^{+\infty} (a \cdot x + b - a \cdot m_X - b)^2 \cdot f_X dx =$$

$$= \int_{-\infty}^{+\infty} a^2 (x - m_X)^2 \cdot f_X(x)dx = a^2 \cdot \sigma_Y^2$$

$$\boxed{\begin{aligned} \sigma_Y &= a \cdot \sigma_X \\ m_Y &= a \cdot m_X + b \end{aligned}} \tag{2.36}$$

$$\boxed{V_Y = \frac{\sigma_Y}{m_Y} = \frac{a \cdot \sigma_X}{a \cdot m_X + b}}$$

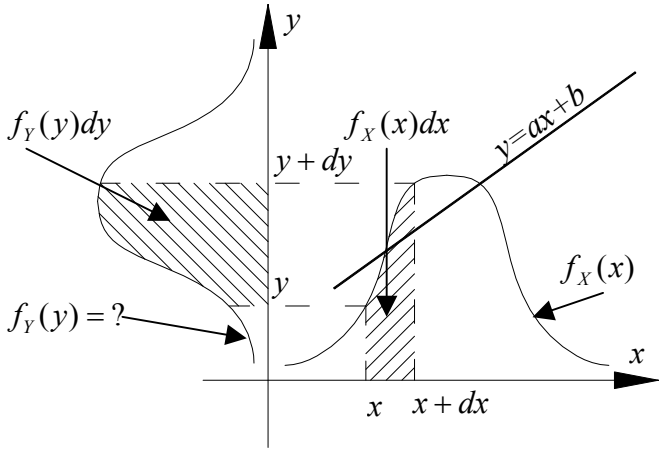

Figure 2.15. Linear relation between random variables *X* and *Y*

Observations:

1. Let the random variable $Y = X_1 + X_2 + X_3 + \ldots + X_n$. If the random variables X_i are normally distributed then *Y* is also normally distributed
2. Let the random variable $Y = X_1 \cdot X_2 \cdot X_3 \cdot \ldots \cdot X$. If the random variables X_i are log-normally distributed then *Y* is also log-normally distributed

Case 2: Non-linear relation between random variables, X, Y

Let the random variables X_i with known means and standard deviations:

$$X_i \begin{cases} m_{X_i} \\ \sigma_{X_i} \end{cases}; i = \overline{1,n}$$

Let the random variable $Y = Y(X_1, X_2, \ldots, X_i, \ldots X_n)$, the relation being non-linear. The mean and the standard deviation of the new random variable *Y*, m_Y, σ_Y can be approximated by:

1. $$m_Y = Y\left(m_{X_1}, m_{X_2}, \ldots, m_{X_n}\right) \tag{2.37}$$

2. $$\sigma_Y^2 \cong \left(\frac{\partial y}{\partial x_1}\right)^2 \cdot \sigma_{X_1}^2 + \left(\frac{\partial y}{\partial x_2}\right)^2 \cdot \sigma_{X_2}^2 + \ldots + \left(\frac{\partial y}{\partial x_n}\right)^2 \cdot \sigma_{X_n}^2 = \sum_{i=1}^{n} \left(\frac{\partial y}{\partial x_i}\right)^2 \cdot \sigma_{X_i}^2 \tag{2.38}$$

Relations 2.37 and 2.38 are the basis for the so-called *First Order Second Moment Models*, *FOSM*.

Few examples of *FOSM* are provided in the following:

- $Y = a \cdot X + b$

1. $m_Y = a \cdot m_X + b$
2. $\sigma_Y^2 = a^2 \cdot \sigma_X^2 \quad \sigma_Y = a \cdot \sigma_X$

- $Y = X_1 \cdot X_2$

1. $m_Y = m_{X_1} \cdot m_{X_2}$
2. $\sigma_Y^2 = (X_2)^2 \cdot \sigma_{X_1}^2 + (X_1)^2 \cdot \sigma_{X_2}^2 = m_{X_2}^2 \cdot \sigma_{X_1}^2 + m_{X_1}^2 \cdot \sigma_{X_2}^2$

$$V_Y = \frac{\sigma_Y}{m_Y} = \frac{\sqrt{m_{X_2}^2 \cdot \sigma_{X_1}^2 + m_{X_1}^2 \cdot \sigma_{X_2}^2}}{m_{X_1} \cdot m_{X_2}} = \sqrt{\frac{\sigma_{X_1}^2}{m_{X_1}^2} + \frac{\sigma_{X_2}^2}{m_{X_2}^2}} = \sqrt{V_{X_1}^2 + V_{X_2}^2}$$

Y	m_Y	σ_Y	V_Y
$X_1 \cdot X_2$	$m_{X_1} \cdot m_{X_2}$		$\sqrt{V_{X_1}^2 + V_{X_2}^2}$
$\frac{X_1}{X_2}$	$\frac{m_{X_1}}{m_{X_2}}$		$\sqrt{V_{X_1}^2 + V_{X_2}^2}$
$\ln X$	$m_{\ln X}$	V_X	

3. STRUCTURAL RELIABILITY ANALYSIS

3.1. The basic reliability problem

The basic structural reliability problem considers only one load effect S resisted by one resistance R. Each is described by a known probability density function, f_S ( ) and f_R( ) respectively. It is important that R and S are expressed in the same units.
For convenience, but without loss of generality, only the safety of a structural element will be considered here and as usual, that structural element will be considered to have failed if its resistance R is less than the stress resultant S acting on it. The probability p_f of failure of the structural element can be stated in any of the following ways, (Melchers, 1999):

$$p_f = P(R \le S) \quad (3.1a)$$
$$= P(R-S \le 0) \quad (3.1b)$$
$$= P(R/S \le 1) \quad (3.1c)$$
$$= P(\ln R - \ln S \le 0) \quad (3.1d)$$

or, in general

$$= P(G(R, S) \le 0) \quad (3.1e)$$

where $G( )$ is termed the *limit state function* and the probability of failure is identical with the probability of limit state violation.
Quite general density functions f_R and f_S for R and S respectively are shown in Figure 3.1 together with the joint (bivariate) density function $f_{RS}(r,s)$. For any infinitesimal element ($\Delta r \Delta s$) the latter represents the probability that R takes on a value between r and $r+\Delta r$ and S a value between s and $s+\Delta s$ as Δr and Δs each approach zero. In Figure 3.1, the Equations (3.1) are represented by the hatched failure domain D, so that the probability of failure becomes:

$$p_f = P(R - S \le 0) = \iint_D f_{RS}(r,s)\,dr\,ds \quad (3.2)$$

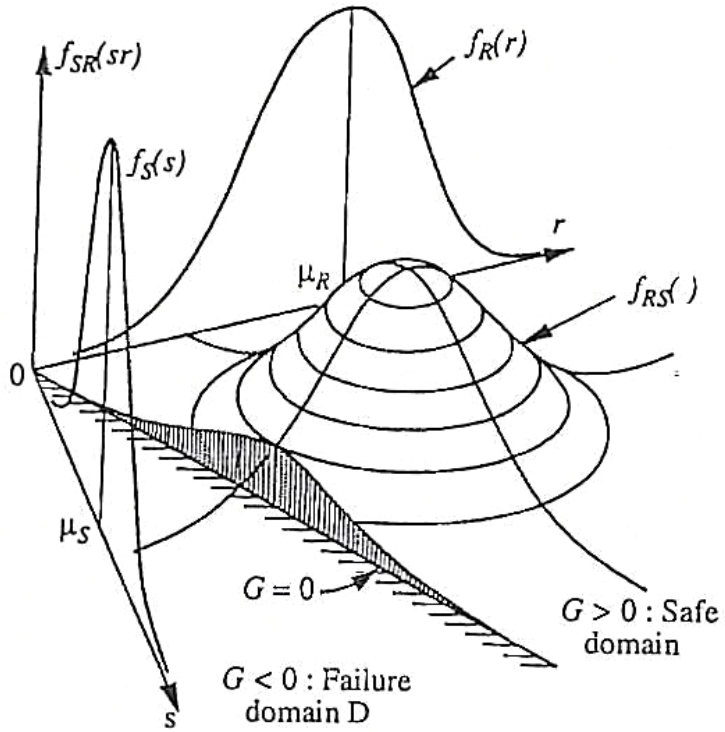

Figure 3.1. Joint density function $f_{RS}(r,s)$, marginal density functions $f_R(r)$ and $f_S(s)$ and failure domain D, (Melchers, 1999)

When R and S are independent, $f_{RS}(r,s)=f_R(r)f_S(s)$ and (3.2) becomes:

$$p_f = P(R-S \le 0) = \int_{-\infty}^{\infty} \int_{-\infty}^{s \ge r} f_R(r) f_S(s) dr\, ds = \int_{-\infty}^{\infty} F_R(x) f_S(x) dx \qquad (3.3)$$

This is also known as a *convolution integral* with meaning easily explained by reference to Figure 3.2. $F_R(x)$ is the probability that $R \le x$ or the probability that the actual resistance R of the member is less than some value x. Let this represent failure. The term $f_s(x)$ represents the probability that the load effect S acting in the member has a value between x and $x+\Delta x$ in the limit as $\Delta x \to 0$. By considering all possible values of x, i.e. by taking the integral over all x, the total probability of failure is obtained. This is also seen in Figure 3.3 where the density functions $f_R(r)$ and $f_S(s)$ have been drawn along the same axis.

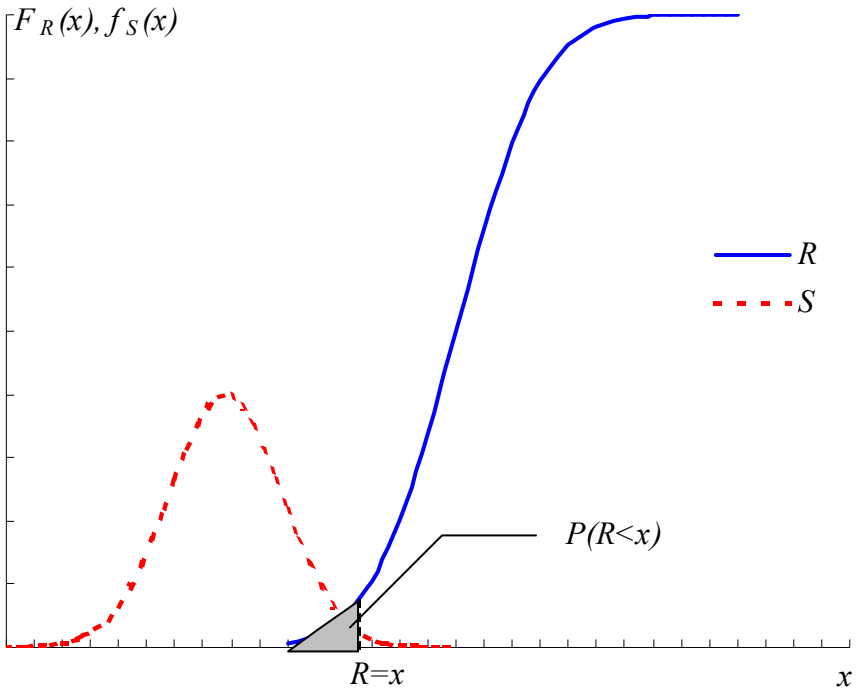

Figure 3.2. Basic R-S problem: $F_R(\,)\,f_S(\,)$ representation

An alternative to expression (3.3) is:

$$p_f = \int_{-\infty}^{\infty} [1 - F_S(x)] f_R(x) dx \qquad (3.4)$$

which is simply the *sum* of the failure probabilities over all cases of resistance for which the load exceeds the resistance.

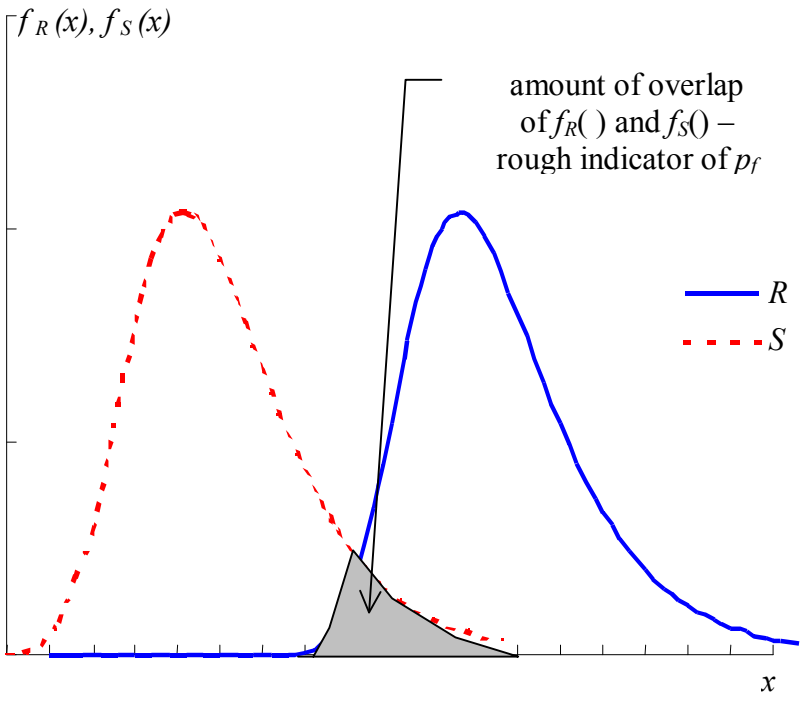

Figure 3.3. Basic *R-S* problem: $f_R(\ ) f_S(\ )$ representation

3.2. Special case: normal random variables

For a few distributions of R and S it is possible to integrate the convolution integral (3.3) analytically. One notable example is when both are normal random variables with means μ_R and μ_S and variances σ_R^2 and σ_S^2 respectively. The safety margin $Z=R-S$ then has a mean and variance given by well-known rules for addition of normal random variables:

$$\mu_Z = \mu_R - \mu_S \tag{3.5a}$$

$$\sigma_Z^2 = \sigma_R^2 + \sigma_S^2 \tag{3.5b}$$

Equation (3.1b) then becomes

$$p_f = P(R - S \le 0) = P(Z \le 0) = \Phi\left(\frac{0 - \mu_Z}{\sigma_Z}\right) \tag{3.6}$$

where $\Phi(\ )$ is the standard normal distribution function (zero mean and unit variance). The random variable $Z = R-S$ is shown in Figure 3.4, in which the failure region $Z \le 0$ is shown shaded. Using (3.5) and (3.6) it follows that (Cornell, 1969)

$$p_f = \Phi\left[\frac{-(\mu_R - \mu_S)}{(\sigma_R^2 + \sigma_S^2)^{1/2}}\right] = \Phi(-\beta) \tag{3.7}$$

where $\beta = \mu_z / \sigma_z$ is defined as *reliability (safety) index*.

If either of the standard deviations σ_R and σ_S or both are increased, the term in square brackets in (3.7) will become smaller and hence p_f will increase. Similarly, if the difference between the mean of the load effect and the mean of the resistance is reduced, p_f increases. These observations may be deduced also from Figure 3.3, taking the amount of overlap of $f_R(\ )$ and $f_S()$ as a rough indicator of p_f.

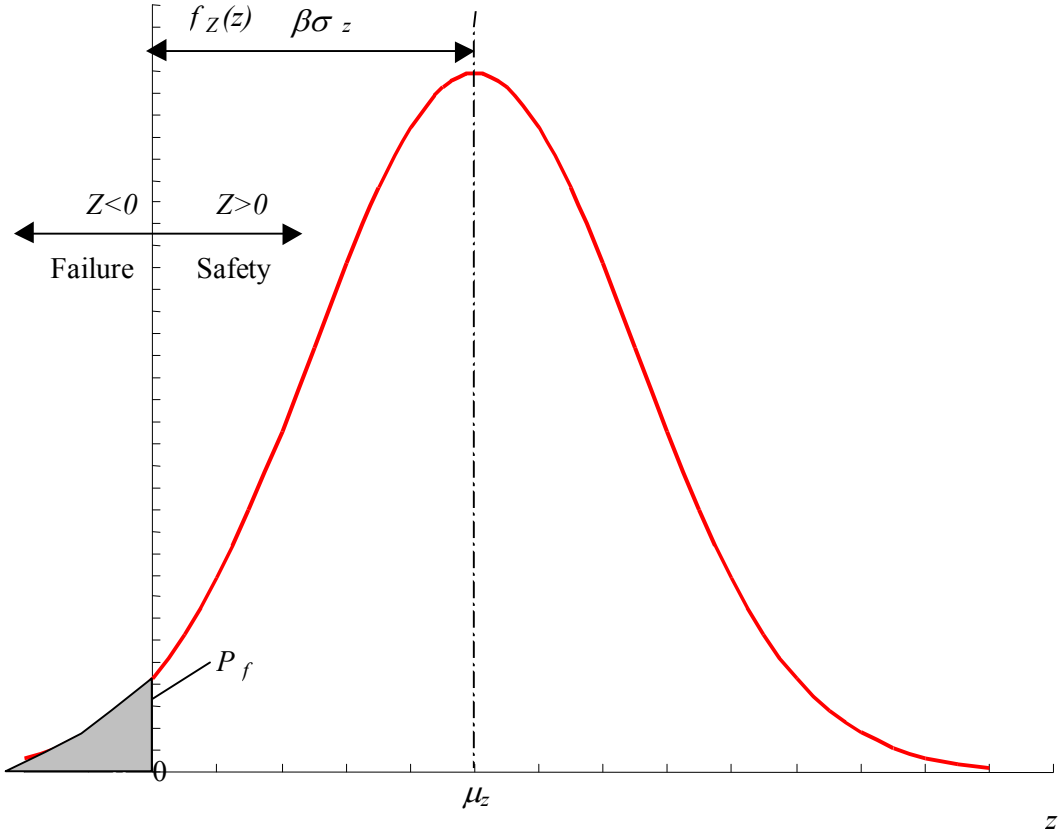

Figure 3.4. Distribution of safety margin $Z = R - S$

3.3. Special case: log-normal random variables

The log-normal model for structural reliability analysis was proposed by Esteva and Rosenblueth in early 70's. Both parameters of the model are considered normal random variables with means μ_R and μ_S and variances σ_R^2 and σ_S^2 respectively. The safety margin $Z = \ln\frac{R}{S}$ then has a mean and a standard deviation given by:

$$\mu_Z = \mu_{\ln\frac{R}{S}} \cong \ln\frac{\mu_R}{\mu_S} \tag{3.8a}$$

$$\sigma_Z = \sigma_{\ln\frac{R}{S}} = V_{\frac{R}{S}} = \sqrt{V_R^2 + V_S^2} \tag{3.8b}$$

Equation (3.1d) then becomes

$$p_f = P\left(\ln\frac{R}{S} \le 0\right) = P(Z \le 0) = \Phi\left(\frac{0 - \mu_Z}{\sigma_Z}\right) \tag{3.9}$$

where $\Phi(\ )$ is the standard normal distribution function (zero mean and unit variance). The random variable $Z = \ln\frac{R}{S}$ is shown in Figure 3.5, in which the failure region $Z \le 0$ is shown shaded. Using (3.8) and (3.9) it follows that

$$p_f = \Phi\left[\frac{0 - \ln\dfrac{\mu_R}{\mu_S}}{\left(V_R^2 + V_S^2\right)^{1/2}}\right] = \Phi(-\beta) \tag{3.10}$$

where $\beta = \mu_z / \sigma_z$ is defined as *reliability (safety) index*,

$$\beta \cong \frac{\ln\dfrac{\mu_R}{\mu_S}}{\sqrt{V_R^2 + V_S^2}}. \tag{3.11}$$

Lindt proposed the following: $\sqrt{V_S^2 + V_R^2} \cong \alpha(V_S + V_R)$ with $\alpha = 0{,}7 \ldots 0{,}75$ for $\frac{1}{3} \le \frac{V_R}{V_S} \le 3$.

Given Lindt's linearization it follows that:

$$\beta = \frac{\ln\dfrac{\mu_R}{\mu_S}}{\alpha(V_R + V_S)} \tag{3.12}$$

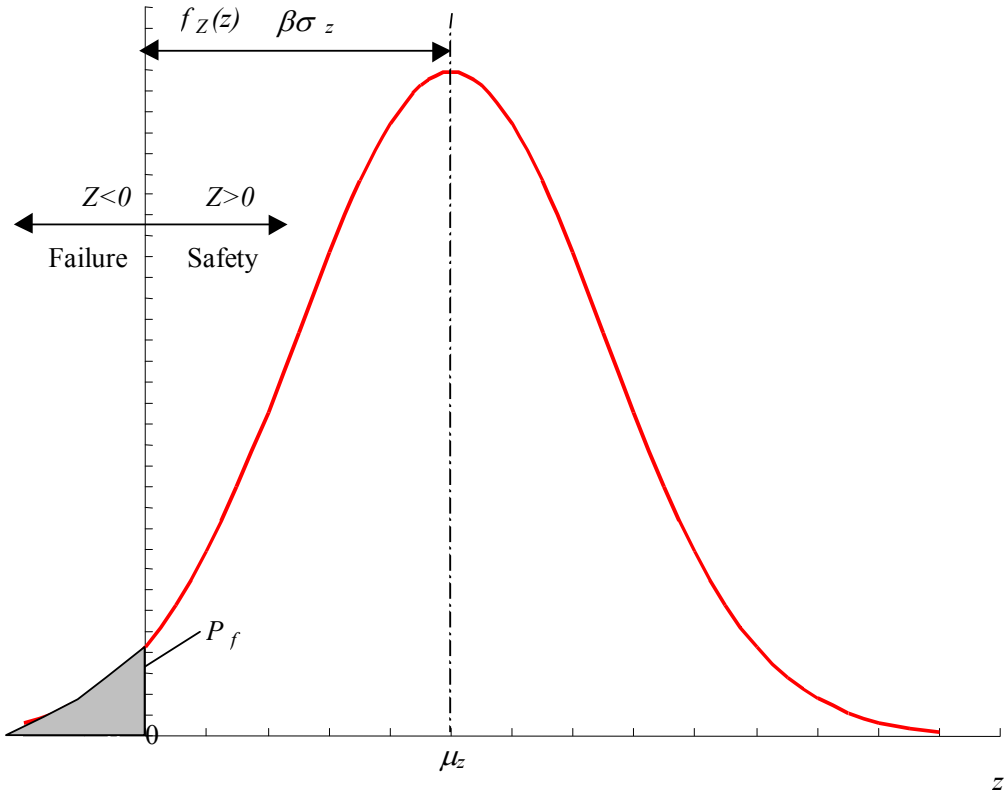

Figure 3.5. Distribution of safety margin $Z = \ln\frac{R}{S}$

3.4. Partial safety coefficients (PSC)

The calibration of partial safety coefficients used in semi-probabilistic design codes is accomplished using the log-normal model using *SOMM*.
From Equation 3.11 one has:

$$\beta = \frac{\ln\frac{m_R}{m_S}}{\alpha\left(V_R + V_S\right)} \Rightarrow \frac{m_R}{m_S} = e^{\alpha\beta\cdot\left(V_R+V_S\right)} \Rightarrow \frac{m_R}{m_S} = e^{\alpha\beta\cdot V_R}\cdot e^{\alpha\beta\cdot V_S} \Rightarrow m_R\cdot e^{-\alpha\beta\cdot V_R} = m_S\cdot e^{\alpha\beta\cdot V_S} \quad (3.13)$$

where $e^{-\alpha\beta\cdot V_R}$ and $e^{\alpha\beta\cdot V_S}$ are called safety coefficients, *SC* with respect to the mean. But one needs the *SC* with respect to the characteristic values of the loads and resistances, the so-called partial safety coefficients, *PSC*. To this aim, one defines the limit state function used in the design process:

$$\underbrace{S_{0.98}\cdot\gamma_{0.98}}_{S_{design}} = \underbrace{R_{0.05}\cdot\phi_{0.05}}_{R_{design}} \quad (3.14)$$

where $\gamma_{0.98}$ and $\phi_{0.05}$ are called partial safety coefficients, *PSC*.
Assuming that *S* and *R* are log-normally distributed, one has:

$$R_{0.05} = e^{m_{\ln R}-1.645\cdot\sigma_{\ln R}} \cong e^{\ln m_R}\cdot e^{-1.645\cdot V_R} = m_R\cdot e^{-1.645\cdot V_R} \quad (3.15)$$

$$S_{0.98} = e^{m_{\ln S}+2.054\cdot\sigma_{\ln S}} \cong e^{\ln m_S}\cdot e^{2.054\cdot V_S} = m_S\cdot e^{2.054\cdot V_S} \quad (3.16)$$

$$\frac{R_{0.05}}{S_{0.98}} = \frac{m_R}{m_S}\cdot\frac{e^{-1.645\cdot V_R}}{e^{2.054\cdot V_S}} = \frac{e^{\alpha\beta\cdot V_R}\cdot e^{\alpha\beta\cdot V_S}\cdot e^{-1.645\cdot V_R}}{e^{2.054\cdot V_S}} \quad (3.17)$$

$$R_{0.05}\cdot\underbrace{e^{(-\alpha\beta+1.645)V_R}}_{\phi_{0.05}} = S_{0.98}\cdot\underbrace{e^{(\alpha\beta-2.054)V_S}}_{\gamma_{0.98}} \quad (3.18)$$

$$\phi_{0.05} = e^{(-\alpha\beta+1.645)V_R} \quad (3.19)$$

$$\gamma_{0.98} = e^{(\alpha\beta-2.054)V_S} \quad (3.20)$$

The partial safety coefficients $\phi_{0.05}$ and $\gamma_{0.98}$ as defined by Equations 3.19 and 3.20 are depend on the reliability index β and the coefficients of variation for resistances and loads, respectively. If the reliability index β is increased, the partial safety coefficient for loads $\gamma_{0.98}$ increases while the partial safety coefficient for resistance $\phi_{0.05}$ decreases. The theory of partial safety coefficients based on lognormal model is incorporated in the Romanian Code *CR0-2005* named „*Cod de proiectare. Bazele proiectarii structurilor in constructii*" (Design Code. Basis of Structural Design).

3.5. Generalized reliability problem

For many problems the simple formulations (3.1a)-(3.1e) are not entirely adequate, since it may not be possible to reduce the structural reliability problem to a simple *R* versus *S*

formulation with R and S independent random variables. A more general formulation is required.

Let the vector $\boldsymbol{X}$ represent all the basic variables involved in the problem. Then the resistance R can be expressed as $R = G_R(\boldsymbol{X})$ and the loading or load effect as $S = G_S(\boldsymbol{X})$. The limit state function $G(R,S)$ in (1e) can be generalized. When the functions $G_R(\boldsymbol{X})$ and $G_S(\boldsymbol{X})$ are used in $G(R,S)$, the resulting limit state function can be written simply as $G(\boldsymbol{X})$, where $\boldsymbol{X}$ is the vector of all relevant basic variables and $G(\ )$ is some function expressing the relationship between the limit state and the basic variables. The limit state equation $G(\boldsymbol{x}) = 0$ now defines the boundary between the *safe* domain $G > 0$ and the *unsafe* domain $G \leq 0$ in n-dimensional basic variable space. Usually, the limit state equation is derived from the physics of the problem. (Note that $\boldsymbol{X}=\boldsymbol{x}$ defines a particular *point* $\boldsymbol{x}$ in the basic variable space).

With the limit state function expressed as $G(\boldsymbol{X})$, the generalization of (3.2) becomes, (Melchers, 1999):

$$p_f = P\left[G(X) \leq 0\right] = \int \ldots \int_{G(X)\leq 0} f_x(x)dx \tag{3.21}$$

Here $f_x(\boldsymbol{x})$ is the joint probability density function for the n-dimensional vector $\boldsymbol{X}$ of the basic variables. If the basic variables themselves are independent, the formulation (3.21) is simplified, as then:

$$f_x(x) = \prod_{i=1}^{n} f_{x_i}(x_i) \tag{3.22}$$

with $f_{xi}(x_i)$ the *marginal* probability density function for the basic variable X_i.

The region of integration $G(\boldsymbol{X}) \leq 0$ in (3.21) denotes the space of limit state violation an is directly analogous to the failure domain D shown in Figure 3.1. Except for some special cases, the integration of (3.21) over the failure domain $G(\boldsymbol{X}) \leq 0$ cannot be performed analytically. However, the solution of (3.21) can be made more tractable by simplification or numerical treatment (or both) of (i) the integration process, (ii) the integrand $f_x(\ )$ and (iii) the definition of the failure domain. Each approach has been explored in the literature. Two dominant approaches have emerged:

(a) using numerical approximations such as simulation to perform the multidimensional integration required in (3.21) – the so-called *Monte Carlo* methods;
(b) sidestepping the integration process completely by transforming $f_x(\boldsymbol{x})$ in (3.21) to a multi-normal probability density function and using some remarkable properties which may then be used to determine, approximately, the probability of failure – the so-called *First Order Second Moment* methods.

3.6. First-Order Second-Moment Reliability Theory

3.6.1. Introduction

In order to perform the integration required in the reliability integral (8), the probability density function $f_x(\ )$ in the integrand can be simplified. The special case of reliability estimation in which each variable is represented only by its first two moments (mean and standard deviation) will be considered hereinafter. This is known as the *second-moment* level of representation. A convenient way in which the second-moment representation might be interpreted is that each random variable is represented by the normal distribution.

Because of their inherent simplicity, the so-called *second-moment* methods have become very popular. Early works by Mayer (1926), Freudenthal (1956), Rzhanitzyn (1957) contained second-moment concepts. Not until the late 1960s, however, was the time ripe for the ideas to gain a measure of acceptance, prompted by the work of Cornell (1969).

3.6.2. Second-moment concepts

It was shown that when the resistance R and load effect S are each normal random variables, the limit state equation is the *safety margin* $Z=R-S$ and the probability of failure p_f is:

$$p_f = \Phi(-\beta) \qquad \beta = \frac{\mu_Z}{\sigma_Z} \tag{3.23}$$

where β is the *reliability index* and $\Phi(\ )$ the standard normal distribution function.
Obviously, equation (3.23) yields the exact probability of failure when both R and S are normally distributed. The same is valid when both R and S are log-normally distributed and the limit state equation is (3.1d). However, p_f defined in this way is only a *nominal* failure probability when R and S have distributions other than normal and log-normal. Conceptually it is probably better in this case not to refer to probabilities at all, but simply to β, the *reliability index*.
As shown in Figure 3.4, β is a measure (in standard deviation σ_Z units) of the distance that the mean, μ_Z is away from the origin Z=0. This point marks the boundary of the *failure* region. Hence β is a direct measure of the safety of the structural element.
For convenience and for clarity in what follows the notation p_{fN} will be used to refer to the nominal probability estimate, i.e. that calculated using second moment approximations.
The above ideas are readily extended in the case where the limit state function is a random function consisting of more than two basic random variables:

$$G(\boldsymbol{X}) = Z(\boldsymbol{X}) = a_0 + a_1X_1 + a_2X_2 + \ldots + a_nX_n \tag{3.24}$$

then $G(\boldsymbol{X}) = Z(\boldsymbol{X})$ is normally distributed and the mean, μ_Z and standard deviation, σ_Z from which β and p_{fN} can be evaluated using (3.23) are:

$$\mu_Z = a_0 + \sum_{i=1}^{n} a_i \mu_{Xi} \tag{3.25a}$$

$$\sigma_Z = \sqrt{\sum_{i=1}^{n} a_i^2 \sigma_{Xi}^2} \tag{3.25b}$$

In general, however, the limit state function $G(\boldsymbol{X})$=0 is not linear. In this case, the most suitable approach is to linearize $G(\boldsymbol{X})$=0 by expanding $G(\boldsymbol{X})$=0 as a first-order Taylor series expansion about some point $\boldsymbol{x}^*$. Approximations which linearize $G(\boldsymbol{X})$=0 will be denoted *first-order* methods.
The first-order Taylor series expansion which linearizes $G(\boldsymbol{X})$=0 at $\boldsymbol{x}^*$ might be denoted $G_L(\boldsymbol{X})$=0 (Figure 3.6). Expansions about the means, μ_X is common in probability theory, but there is no rationale for doing so; it will be shown later that there is indeed a better choice which is the point of maximum likelihood on the limit state function. At this stage, it is sufficient to note that the choice of expansion point directly affects the estimate of β. This is demonstrated in the following example, (Melchers, 1999).

Example 1. The first two moments of Z linearized about $\boldsymbol{x}^*$ rather than μ_X are given by

$$\mu_Z \approx G(\boldsymbol{x}^*) \tag{3.26a}$$

and

$$\sigma_Z^2 \approx \sum \left(\frac{\partial G}{\partial X_i} \right)^2 \Bigg|_{x^*} \cdot \sigma_{Xi}^2 \tag{3.26b}$$

respectively.

Now, if $G(\mathbf{X})=X_1X_2-X_3$ with the random variables X_i being independent and with $\sigma_{X1}=\sigma_{X2}=\sigma_{X3}=\sigma_X$, then $\partial G/\partial X_1=X_2$, $\partial G/\partial X_2=X_1$ and $\partial G/\partial X_3$= -1. Then, (3.26a) and (3.26b) evaluated at the means μ_{Xi} become

$$\mu_Z\big|_{\mu x} = \mu_{X1}\mu_{X2} - \mu_{X3}$$

$$\sigma_Z^2\big|_{\mu x} = \mu_{X2}^2\sigma_{X1}^2 + \mu_{X1}^2\sigma_{X2}^2 + \sigma_{X3}^2 = \sigma_X^2\left(\mu_{X1}^2 + \mu_{X2}^2 + 1\right)$$

However, if the expansion point is taken as $x_1^*=\mu_{X1}/2$, $x_2^*=\mu_{X2}$, $x_3^*=\mu_{X3}$ then the corresponding terms become

$$\mu_Z\big|_{x^*} = \frac{\mu_{X1}}{2}\mu_{X2} - \mu_{X3}$$

$$\sigma_Z^2\big|_{x^*} = \mu_{X2}^2\sigma_{X1}^2 + \left(\frac{\mu_{X1}}{2}\right)^2\sigma_{X2}^2 + \sigma_{X3}^2 = \sigma_X^2\left(\frac{\mu_{X1}^2}{4} + \mu_{X2}^2 + 1\right)$$

It follows readily using (3.23) that:

$$\beta\big|_{\mu x} = \frac{\mu_{X1}\mu_{X2} - \mu_{X3}}{\sigma_X\left(\mu_{X1}^2 + \mu_{X2}^2 + 1\right)}$$

$$\beta\big|_{x^*} = \frac{\frac{1}{2}\mu_{X1}\mu_{X2} - \mu_{X3}}{\sigma_X\left(\frac{1}{4}\mu_{X1}^2 + \mu_{X2}^2 + 1\right)}$$

These are clearly not equivalent, this demonstrating the dependence of β on the selection of the expansion point.

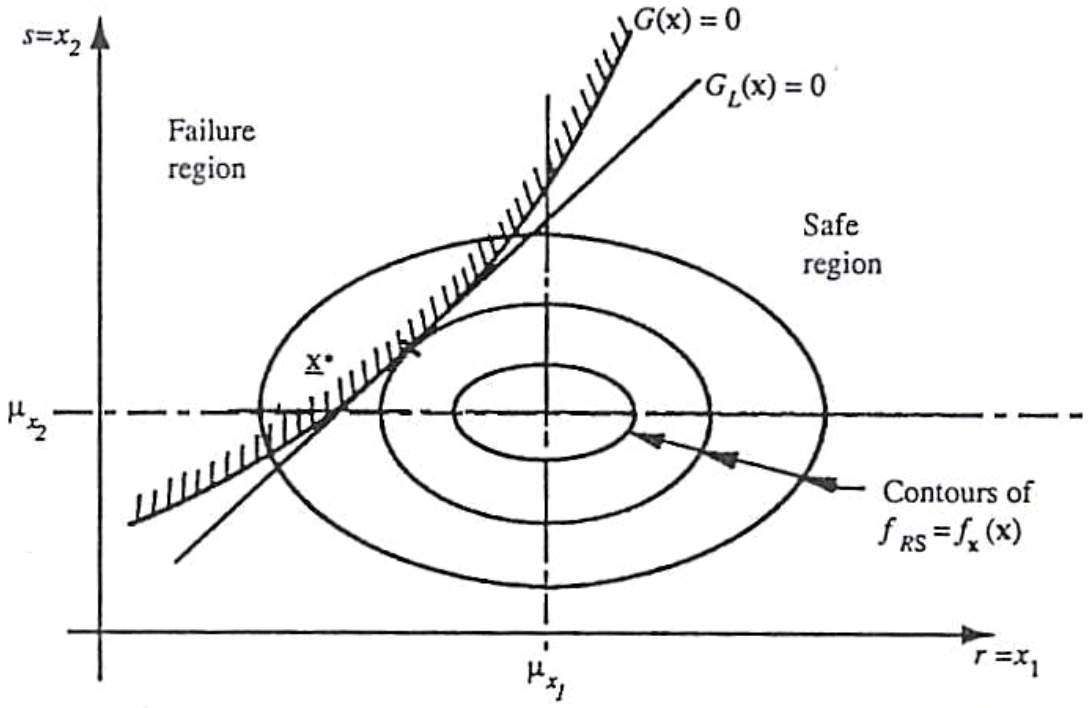

Figure 3.6. Limit state surface $G(\mathbf{x})$ = 0 and its linearized version $G_L(\mathbf{x})$ = 0 in the space of the basic variables, (Melchers, 1999)

3.6.3. The Hasofer-Lind transformation

The first useful (but not essential) step is to transform all variables to their standardized form $N(0, 1)$ (normal distribution with zero mean and unit variance) using well-known transformation:

$$Y_i = \frac{X_i - \mu_{Xi}}{\sigma_{Xi}} \tag{3.27}$$

where Y_i has $\mu_{Yi}=0$ and $\sigma_{Yi}=1$. As a result of applying this transformation to each basic variable X_i, the unit of measurement in any direction in the $\boldsymbol{y}$ space will be $\sigma_{Yi}=1$ in any direction. In this space, the joint probability density function $f_{\boldsymbol{Y}}(\boldsymbol{y})$ is the standardized multivariate normal (Hasofer and Lind, 1974). Of course, the limit state function also must be transformed and is given by $g(\boldsymbol{y})=0$.
The transformation (3.27) can be performed without complication if the normal random variables X_i are all uncorrelated (i.e. linearly independent) random variables. If this is not the case, an intermediate step is required to find a random variable set $\boldsymbol{X'}$ which is uncorrelated, and this new set can be transformed according to (3.27). The procedure for finding the uncorrelated set $\boldsymbol{X'}$ (including means and variances) from the correlated set $\boldsymbol{X}$ is essentially that of finding the eigen-values and eigen-vectors.

3.6.4. Linear limit state function

For simplicity of illustration consider now the important special case in which the limit state function is linear, i.e. $G(\boldsymbol{X}) = X_1-X_2$, shown as $G_L(\boldsymbol{x})=0$ in Figure 3.6. The transformation (3.27) changes the joint probability density function $f_{\boldsymbol{X}}(\boldsymbol{x})$ shown in Figure 3.6 to $f_{\boldsymbol{Y}}(\boldsymbol{y})$ shown in Figure 3.7 in the transformed $\boldsymbol{y}=(y_1, y_2)$ space. The joint probability density function $f_{\boldsymbol{Y}}(\boldsymbol{y})$ is now a bivariate normal distribution $\Phi_2(\boldsymbol{y})$, symmetrical about the origin. The probability of failure is given by the integral of $\Phi_2(\boldsymbol{y})$ over the transformed failure region $g(\boldsymbol{y})<0$, shown part shaded. This can be obtained by integrating in the direction ν ($-\infty<\nu<\infty$) shown in Figure 3.7, to obtain the marginal distribution (Figure 3.8).

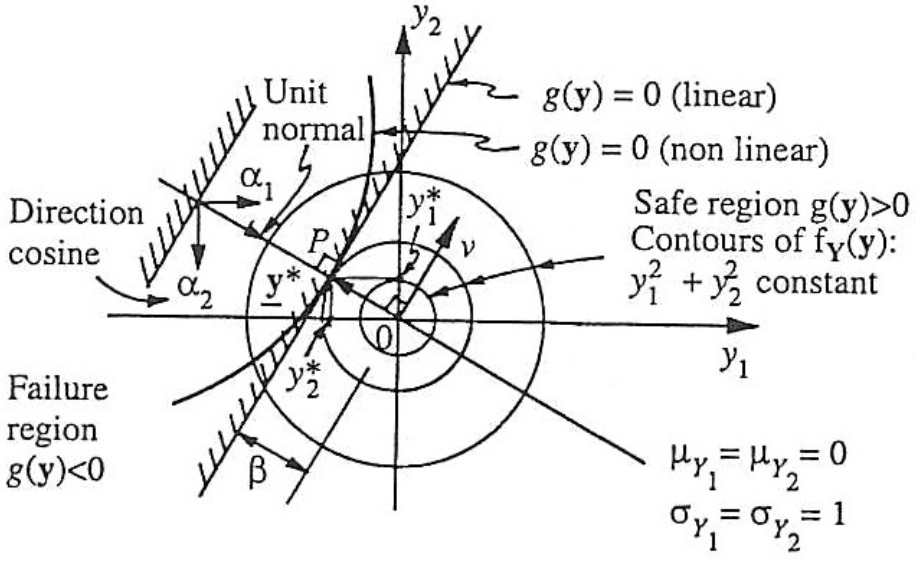

Figure 3.7. Probability density function contours and original (non-linear) and linearized limit state surfaces in the standard normal space, (Melchers, 1999)

By the properties of the bivariate normal distribution the marginal distribution is also normal, and hence the shaded area in Figure 3.8 represents the failure probability $p_f = \Phi(-\beta)$, where β is as shown (note that σ=1 in the β direction since the normalized $\boldsymbol{y}$ space is being used).
The distance β shown in Figure 3.7 is perpendicular to the ν axis and hence is perpendicular to $g(\boldsymbol{y})$=0. It clearly corresponds to the shortest distance from the origin in the $\boldsymbol{y}$ space to the limit state surface $g(\boldsymbol{y})$=0.
More generally, there will be many basic random variables $\boldsymbol{X}=\{X_i, i=1, 2, \ldots n\}$ describing the structural reliability problem. However, the concepts described above carry over directly to an n-dimensional standardized normal space $\boldsymbol{y}$ with a (hyper)plane limit state. In this case the shortest distance and hence the reliability index is given by, (Melchers, 1999):

$$\beta = \min\left(\sum_{i=1}^{n} y_i^2\right)^{1/2} = \min\left(y^T \cdot y\right)^{1/2} \qquad (3.28)$$

subject to $g(\boldsymbol{y}) = 0$, where the y_i represent the coordinates of any point on the limit state surface.

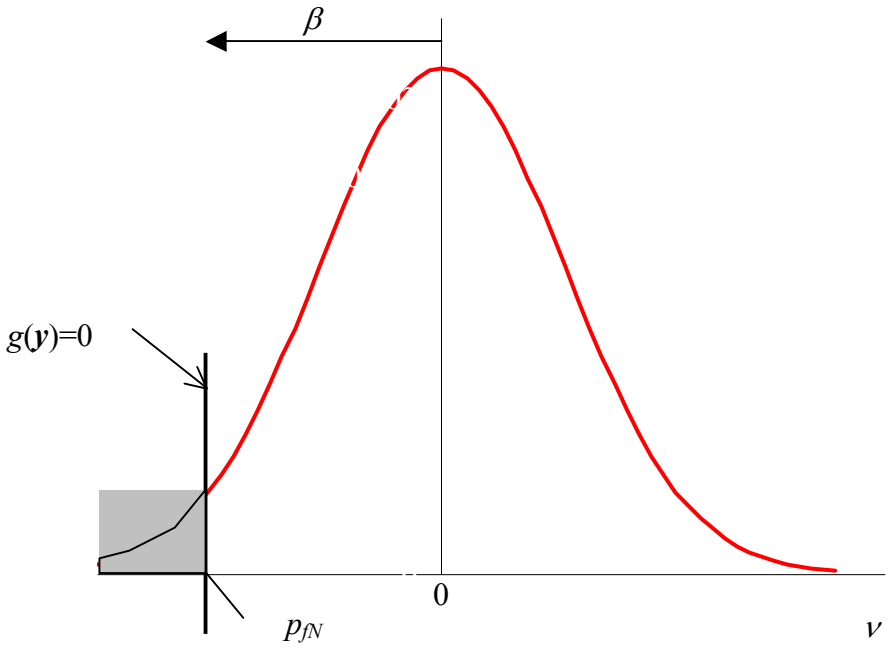

Figure 3.8. Marginal distribution in the space of the standardized normal variables

The particular point for which (3.28) is satisfied, i.e. the point on the limit state surface perpendicular to β, in n-dimensional space, is called the *checking* or *design* point y^*. Obviously, this point is the projection of the origin on the limit state surface. It is obvious from Figures 3.7 and 3.8 that the greatest contribution to the total probability content in the failure region is made by the closest zone to y^*. In fact, y^* represents the point of greatest probability density or the point of *maximum likelihood* for the failure domain.
A direct relationship between the checking point y^* and β can be established as follows. From the geometry of surfaces (e.g. Sokolnikoff and Redheffer, 1958) the outward normal vector to a hyperplane given by $g(\boldsymbol{y})$=0, has the components given by:

$$c_i = \lambda \frac{\partial g}{\partial y_i} \qquad (3.29a)$$

where λ is an arbitrary constant. The total length of the outward normal is

$$l = \left(\sum_i c_i^2 \right)^{1/2} \tag{3.29b}$$

and the direction cosines α_i of the unit outward normal are then

$$\alpha_i = \frac{c_i}{l} \tag{3.29c}$$

With α_i known, it follows that the coordinates of the checking point are

$$y_i^* = y_i = -\alpha_i \beta \tag{3.30}$$

where the negative sign arises because the α_i are components of the outward normal as defined in conventional mathematical notation (i.e. positive with increasing $g(\ )$). Figure 3.7 shows the geometry for the two-dimensional case $\boldsymbol{y} = (y_1, y_2)$.
For a linear limit state function (i.e. a hyperplane in $\boldsymbol{y}$ space) the direction cosines α_i do not change with position along the limit state function, so that it is easy to find a set of coordinates y^* satisfying both Equation (3.28) and equation (3.30).
The equation for the hyperplane $g(\boldsymbol{y}) = 0$ can be written as, (Melchers, 1999)

$$g(y) = \beta + \sum_{i=1}^{n} \alpha_i y_i \tag{3.31}$$

The validity of (3.31) can be verified by applying (3.30).

The linear function in $\boldsymbol{X}$ space corresponding to (3.31) is obtained by applying (3.27)

$$G(x) = \beta - \sum_{i=1}^{n} \frac{\alpha_i}{\sigma_{Xi}} \mu_{Xi} + \sum_{i=1}^{n} \frac{\alpha_i}{\sigma_{Xi}} x_i \tag{3.32a}$$

or

$$G(x) = b_0 + \sum_{i=1}^{n} b_i x_i \tag{3.32b}$$

which is again a linear function.

Also, β can be determined directly from the checking point coordinates y^* using (3.31):

$$\beta = -\sum_{i=1}^{n} y_i^* \alpha_i = -y^{*T} \alpha \tag{3.33}$$

4. SEISMIC HAZARD ANALYSIS

4.1. Deterministic seismic hazard analysis (DSHA)

The deterministic seismic hazard analysis involves the development of a particular seismic *scenario*, i.e. the postulated occurrence of an earthquake of a specified size at a specific location. The *DSHA* is developed in four steps (Reiter, 1990):

1. Identification and characterization of all earthquake sources – geometry and position of the sources and the maximum magnitude for all sources, M;
2. Selection of source-to-site distance parameters, R (epicentral, hypocentral, etc.) for each source zone;
3. Selection of *controlling* earthquake (expected to produce the strongest shaking at the site); use attenuation relations for computing ground motion parameters produced at the site by earthquakes of magnitudes given in step 1 occurring at each source zone;
4. Define the seismic hazard at the site in terms of peak ground acceleration *PGA*, spectral acceleration *SA*, peak ground velocity *PGV*, etc (Y – parameter).

The steps are represented in Figure 4.1.

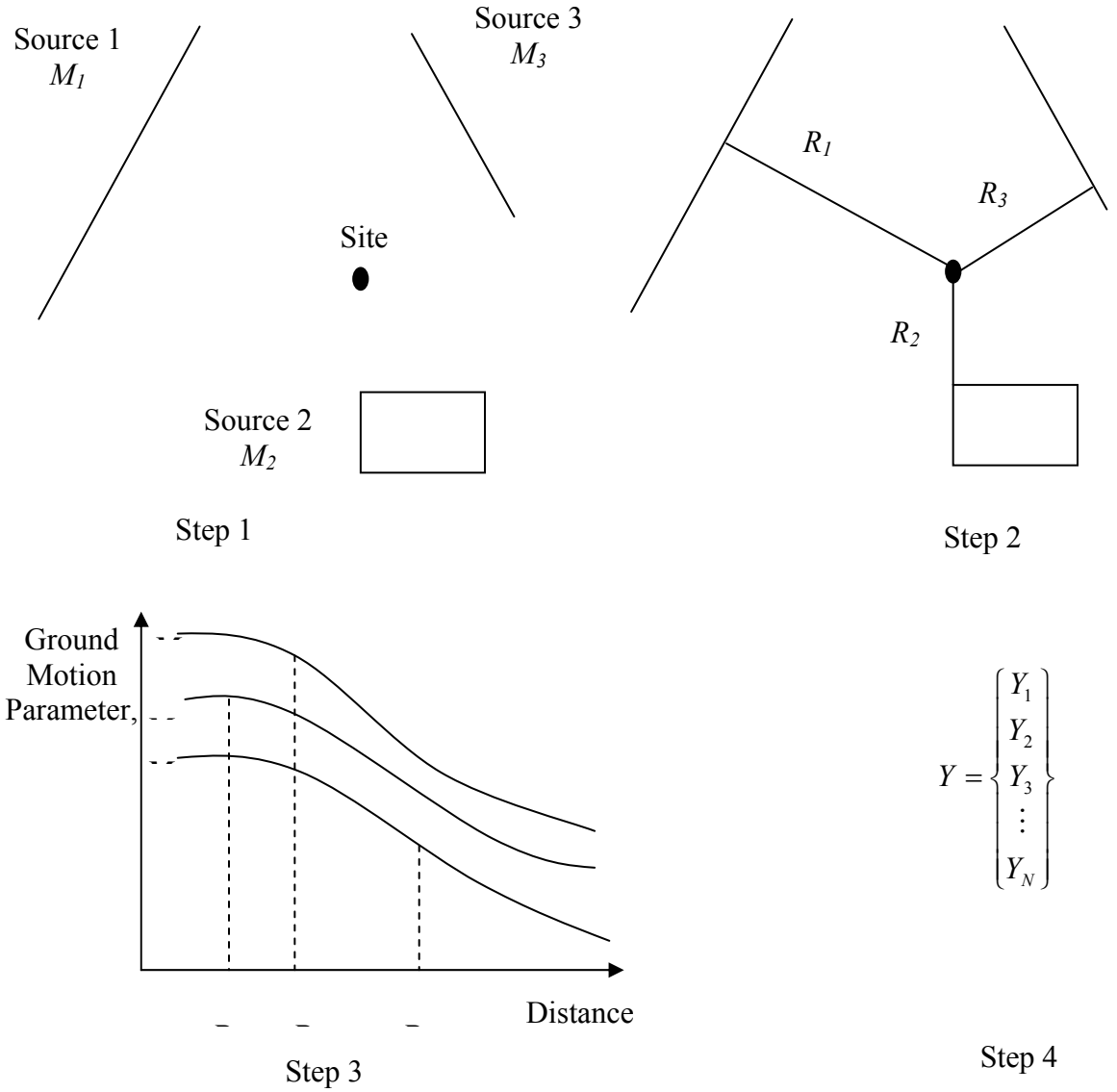

Figure 4.1. Steps in *DSHA*, (Kramer, 1996)

4.2. Probabilistic seismic hazard analysis (PSHA)

The *PSHA* (Cornell, 1968, Algermissen et. al., 1982) is developed in four steps (Reiter, 1990):

1. Identification and characterization of earthquake sources. Besides the information required in step 1 of *DSHA*, it is necessary to obtain the probability distribution of potential rupture location within the source and the probability distribution of source–to-site distance;
2. Definition of seismicity, i.e. the temporal distribution of earthquake recurrence (average rate at which an earthquake of some size will be exceeded);
3. Use predictive (attenuation) relations for computing ground motion parameters produced at the site by earthquakes of any possible size occurring at any possible point in each source zone; uncertainty in attenuation relations is considered in *PSHA*;
4. Uncertainties in earthquake location, size and ground motion prediction are combined and the outcome is the probability that ground motion parameter will be exceeded during a particular time period.

The steps are represented in Figure 4.2.

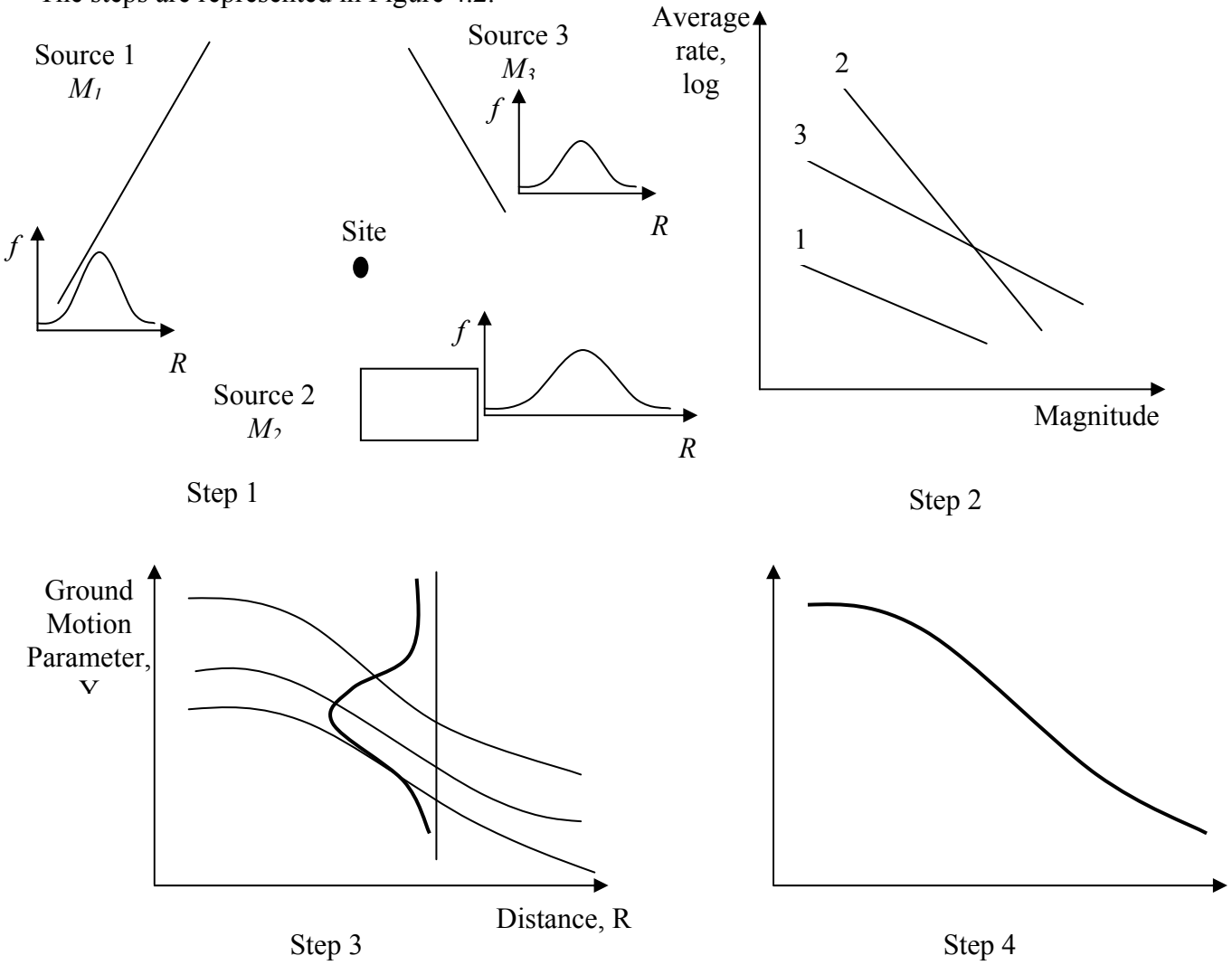

Figure 4.2. Steps in *PSHA*, (Kramer, 1996)

4.3. Earthquake source characterization

The seismic sources can be modeled as:

- point sources
- line sources
- area sources
- volumetric sources.

The spatial uncertainty of earthquake location is taken into account in *PSHA*. The earthquakes are usually assumed to be uniformly distributed within a particular source. The uniform distribution in the source zone does not often translate into a uniform distribution of source-to-site distance.

Another important source of uncertainties is given by the size of the earthquake and by the temporal occurrence of earthquakes. The recurrence law gives the distribution of earthquake sizes in a given period of time. Gutenberg & Richter (1944) organized the seismic data in California according to the number of earthquakes that exceeded different magnitudes during a time period. The key parameter in Gutenberg & Richter's work was the mean annual rate of exceedance, λ_M of an earthquake of magnitude M which is equal to the number of exceedances of magnitude M divided by the length of the period of time. The Gutenberg & Richter law is (Figure 4.3):

$$lg\ \lambda_M = a - b\ M \tag{4.1}$$

where λ_M - mean annual rate of exceedance of an earthquake of magnitude M,

M - magnitude,

a and b – numerical coefficients depending on the data set.

The physical meaning of a and b coefficients can be explained as follows:

10^a – mean yearly number of earthquakes of magnitude greater than or equal to 0.

b – describes the relative likelihood of large to small earthquakes. If b increases the number of larger magnitude earthquakes decreses compared to those of smaller earthquakes (b is the slope of the recurrence plot).

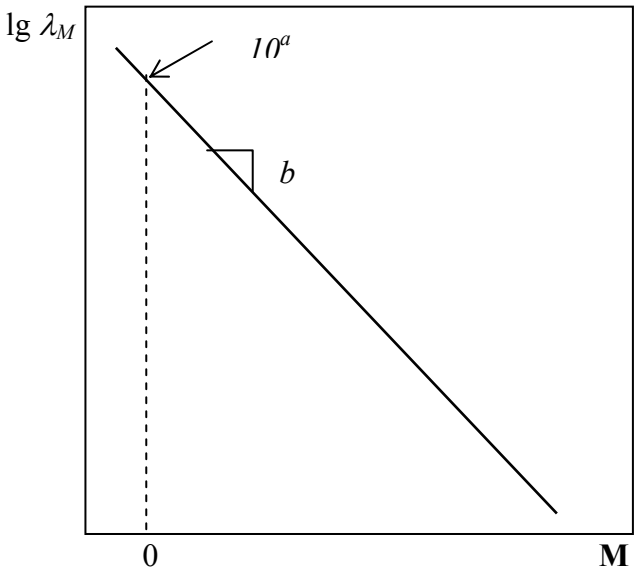

Figure 4.3. The Gutenberg-Richter law

The a and b coefficients are obtained through regression on a database of seismicity form the source zone of interest. Record of seismicity contains dependent events (foreshocks,

aftershocks) that must be removed form the seismicity database because *PSHA* is intended to evaluate the hazard form discrete, independent releases of seismic energy.
The original Gutenberg & Richter law (4.1) is unbounded in magnitude terms. This leads to unreliable results especially at the higher end of the magnitude scale. In order to avoid this inconsistency, the bounded recurrence law is used. The bounded law is obtained and defined hereinafter.
The Gutenberg & Richter law may be reshaped as follows:

$$lg\ \lambda_M = \frac{ln\,\lambda_M}{ln\,10} = a - b\,M \tag{4.2}$$

$$ln\ \lambda_M = a\ ln10 - b\ ln10\ M = \alpha - \beta M \tag{4.3}$$

$$\lambda_M = e^{\alpha - \beta M} \tag{4.4}$$

where $\alpha = a\ ln10 = 2.303\ a$ and $\beta = b\ ln10 = 2.303\ b$.

The form (4.4) of Gutenberg & Richter law shows that the magnitudes follow an exponential distribution.
If the earthquakes smaller than a lower threshold magnitude M_{min} are eliminated, one gets (McGuire and Arabasz, 1990):

$$F_M(M) = P[Mag. \le M \mid M \ge M_{min}] = 1 - P[Mag. > M \mid M \ge M_{min}] =$$

$$= 1 - \frac{\lambda_M}{\lambda_{M_{min}}} = 1 - \frac{e^{\alpha - \beta M}}{e^{\alpha - \beta M_{min}}} = 1 - e^{-\beta(M - M_{min})} \tag{4.5}$$

$$f_M(M) = \frac{dF_M(M)}{dM} = \beta e^{-\beta(M - M\,min)}. \tag{4.6}$$

λ_{Mmin} is the mean annual rate of earthquakes of magnitude M larger or equal than M_{min}.
If both a lower threshold magnitude M_{min} and a higher threshold magnitude M_{max} are taken into account, the probabilistic distribution of magnitudes can be obtained as follows (McGuire and Arabasz, 1990).
The cumulative distribution function must have the unity value for $M = M_{max}$. This yields:

$$F_M(M) = P[Mag. \le M \mid M_{min} \le M \le M_{max}] = \frac{F_M(M)}{F_M(M_{max})} = \frac{1 - e^{-\beta(M - M_{min})}}{1 - e^{-\beta(M_{max} - M_{min})}} \tag{4.7}$$

$$f_M(M) = \frac{dF_M(M)}{dM} = \frac{\beta\, e^{-\beta(M - M_{min})}}{1 - e^{-\beta(M_{max} - M_{min})}}. \tag{4.8}$$

The mean annual rate of exceedance of an earthquake of magnitude M is:

$$\lambda_M = \lambda_{M_{min}}[1 - F_M(M)] = \lambda_{M\,min} \frac{e^{-\beta(M - M_{min})} - e^{-\beta(M_{max} - M_{min})}}{1 - e^{-\beta(M_{max} - M_{min})}} \tag{4.9}$$

where $\lambda_{M_{min}} = e^{\alpha - \beta M_{min}}$ is the mean annual rate of earthquakes of magnitude M larger or equal than M_{min}.
Finally one gets (McGuire and Arabasz, 1990):

$$\lambda_M = e^{\alpha-\beta M_{min}} \frac{e^{-\beta(M-M_{min})} - e^{-\beta(M_{max}-M_{min})}}{1-e^{-\beta(M_{max}-M_{min})}} =$$

$$= e^{\alpha-\beta M_{min}} \frac{e^{-\beta(M-M_{min})}\left[1-e^{-\beta(M_{max}-M)}\right]}{1-e^{-\beta(M_{max}-M_{min})}} =$$

$$= e^{\alpha-\beta M} \frac{1-e^{-\beta(M_{max}-M)}}{1-e^{-\beta(M_{max}-M_{min})}}. \qquad (4.10)$$

4.4. Predictive relationships (attenuation relations)

The predictive relationships usually take the form $Y = f(M, R, P_i)$, where Y is a ground motion parameter, M is the magnitude of the earthquake, R is the source-to-site distance and P_i are other parameters taking into account the earthquake source, wave propagation path and site conditions. The predictive relationships are used to determine the value of a ground motion parameter for a site given the occurrence of an earthquake of certain magnitude at a given distance. The coefficients of the predictive relationships are obtained through multi-variate regression on a particular set of strong motion parameter data for a given seismic source. This is the reason for carefully extrapolating the results of the regression analysis to another seismic source. The uncertainty in evaluation of the ground motion parameters is incorporated in predictive relationships through the standard deviation of the logarithm of the predicted parameter. Finally, one can compute the probability that ground motion parameter Y exceeds a certain value, y^* for an earthquake of magnitude, m at a given distance r (Figure 4.4):

$$P(Y > y^* \mid m, r) = 1 - P(Y \le y^* \mid m, r) = 1 - F_Y(y^*) \qquad (4.11)$$

where F is the CDF of ground motion parameter, usually assumed lognormal.

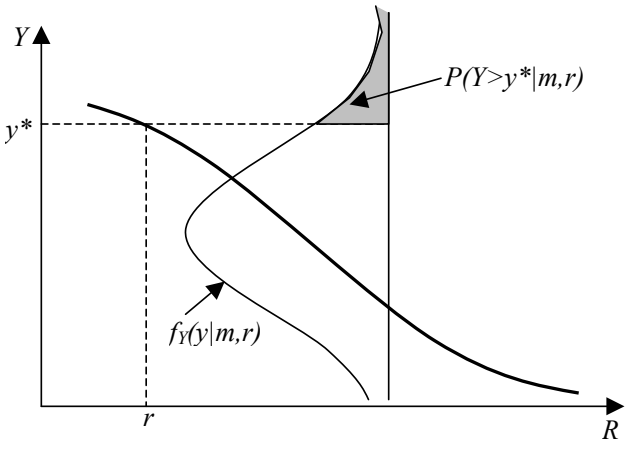

Figure 4.4. Incorporation of uncertainties in the predictive relationships

4.5. Temporal uncertainty

The distribution of earthquake occurrence with respect to time is considered to have a random character. The temporal occurrence of earthquakes is considered to follow, in most cases, a Poisson model, the values of the random variable of interest describing the number of occurrences of a particular event during a given time interval.
The properties of Poisson process are:

1. The number of occurrences in one time interval is independent of the number of occurrences in any other time interval.
2. The probability of occurrence during a very short time interval is proportional to the length of the time interval.
3. The probability of more than one occurrence during a very short time interval is negligible.

If N is the number of occurrences of a particular event during a given time interval, the probability of having n occurrences in that time interval is:

$$P[N = n] = \frac{\mu^n \cdot e^{-\mu}}{n!} \tag{4.12}$$

where μ is the average number of occurrences of the event in that time interval.

4.6. Probability computations

The results of the *PSHA* are given as *seismic hazard curves* quantifying the annual probability of exceedance of different values of selected ground motion parameter.
The probability of exceedance a particular value, y^* of a ground motion parameter Y is calculated for one possible earthquake at one possible source location and then multiplied by the probability that that particular magnitude earthquake would occur at that particular location. The process is then repeated for all possible magnitudes and locations with the probability of each summed, (Kramer, 1996):

$$P(Y > y^*) = P(Y > y^* \mid X) \cdot P(X) = \int P(Y > y^* \mid X) \cdot f_X(x) dx \tag{4.13}$$

where X is a vector of random variables that influence Y (usually magnitude, M and source-to-site distance, R). Assuming M and R independent, for a given earthquake recurrence, the probability of exceeding a particular value, y^*, is calculated using the total probability theorem (Cornell, 1968, Kramer, 1996):

$$P(Y > y^*) = \int\int P(Y > y^* \mid m, r) \cdot f_M(m) \cdot f_R(r) dm dr \tag{4.14}$$

where:
- $P(Y>y^*|m,r)$ – probability of exceedance of y^* given the occurrence of an earthquake of magnitude m at source to site distance r.
- $f_M(m)$ – probability density function for magnitude;
- $f_R(r)$ – probability density function for source to site distance.

4.7. Probabilistic seismic hazard assessment for Bucharest from Vrancea seismic source

The Vrancea region, located when the Carpathians Mountains Arch bents, is the source of subcrustal (60-170km) seismic activity, which affects more than 2/3 of the territory of Romania and an important part of the territories of Republic of Moldova, Bulgaria and Ukraine. According to the 20th century seismicity, the epicentral Vrancea area is confined to a

rectangle of 40x80km^2 having the long axis oriented N45E and being centered at about 45.6^o Lat.N 26.6^o and Long. E.
Two catalogues of earthquakes occurred on the territory of Romania were compiled, more or less independently, by Radu (1974, 1980, 1995) and by Constantinescu and Marza (1980, 1995) Table 4.1. The Radu's catalogues are more complete, even the majority of significant events are also included in the Constantinescu and Marza catalogue. The magnitude in Radu catalogue is the Gutenberg-Richter (1936) magnitude, M_{GR}. The magnitude in Constantinescu & Marza catalogue was the surface magnitude, M_S. Tacitly, that magnitude was later assimilated as Gutenberg-Richter magnitude (Marza, 1995). The Romplus catalogue of *INFP* is a combination of Radu's and Marza's catalogues using moment magnitude, M_w.

Table 4.1. Catalogue of subcrustal Vrancea earthquakes ($M_w \geq 6.3$) occurred during the 20th century

Date		Time (GMT) h:m:s	Lat. N°	Long. E°	RADU Catalogue, 1994				MARZA Catalogue, 1980		www.infp.ro Catalogue, 1998
					h, km	I_0	M_{GR}	M_w	I_0	M_s	M_w
1903	13 Sept	08:02:7	45.7	26.6	>60	7	6.3	-	*6.5*	*5.7*	*6.3*
1904	6 Feb	02:49:00	45.7	26.6	75	6	5.7	-	6	6.3	6.6
1908	6 Oct	21:39:8	45.7	26.5	150	8	6.8	-	*8*	*6.8*	*7.1*
1912	25 May	18:01:7	45.7	27.2	80	7	6.0	-	*7*	*6.4*	*6.7*
1934	29 March	20:06:51	45.8	26.5	90	7	6.3	-	*8*	*6.3*	*6.6*
1939	5 Sept	06:02:00	45.9	26.7	120	6	5.3	-	6	6.1	6.2
1940	22 Oct	06:37:00	45.8	26.4	122	7 / 8	6.5	-	*7*	*6.2*	*6.5*
1940	10 Nov	01:39:07	45.8	26.7	150[1)]	9	7.4	-	*9*	*7.4*	*7.7*
1945	7 Sept	15:48:26	45.9	26.5	75	7 / 8	6.5	-	*7.5*	*6.5*	*6.8*
1945	9 Dec	06:08:45	45.7	26.8	80	7	6.0	-	*7*	*6.2*	*6.5*
1948	29 May	04:48:55	45.8	26.5	130	6 / 7	5.8	-	6.5	6.0	6.3
1977	4 March [2)]	19:22:15	45.34	26.30	109	8 / 9	7.2	7.5	*9*	*7.2*	*7.4*
1986	30 Aug	21:28:37	45.53	26.47	133	8	7.0	7.2	-	-	7.1
1990	30 May	10:40:06	45.82	26.90	91	8	6.7	7.0	-	-	6.9
1990	31 May	00:17:49	45.83	26.89	79	7	6.1	6.4	-	-	6.4

[1)] Demetrescu's original (1941) estimation of 150km is generally accepted today; Radu's initial estimation (1974) was 133 km
[2)] Main shock

As a systematization requirement for seismic hazard assessment, usually it is recommended the use of the moment magnitude, M_w. For Vrancea subcrustal events the relation between two magnitudes can be simply obtained from recent events data given in Table 1, (Lungu et al, 1998):

$$M_w \cong M_{GR} + 0.3 \qquad 6.0 < M_{GR} < 7.7 \tag{4.15}$$

Even the available catalogues of Vrancea events were prepared using the Gutenberg-Richter magnitude M_{GR}, the recurrence-magnitude relationship was herein newly determined using the moment magnitude M_w. The relationship is determined from Radu's 20th century catalogue of subcrustal magnitudes with threshold lower magnitude M_w=6.3.
The average number per year of Vrancea subcrustal earthquakes with magnitude equal to and greater than M_w, as resulting also from Figure 4.5, is (Lungu et al, 1998):

$$\log n(\geq M_w) = 3.76 - 0.73\, M_w \tag{4.16}$$

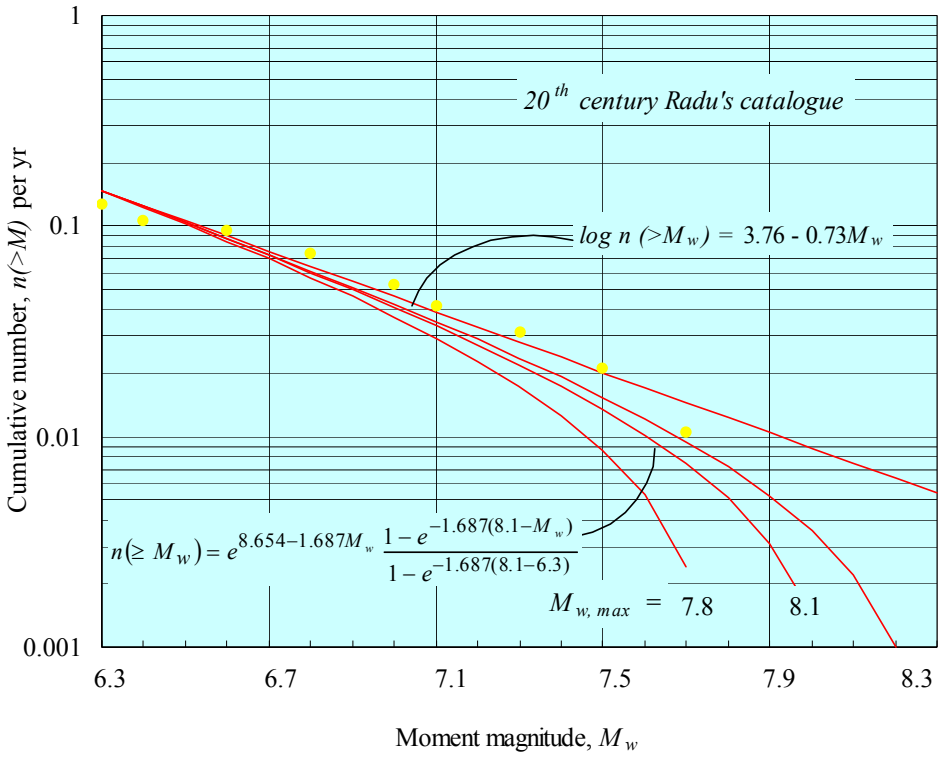

Figure 4.5. Magnitude recurrence relation for the subcrustal Vrancea source ($M_w \geq 6.3$)

The values of surface rupture area (*SRA*) and surface rupture length (*SRL*) from Wells and Coppersmith (1994) equations for "strike slip" rupture were used to estimate maximum credible Vrancea magnitude. According to Romanian geologists Sandulescu & Dinu, in Vrancea subduction zone: $SRL \leq 150 \div 200$ *km*, $SRA < 8000$ *km*^{2}. Based on this estimation, from Table 4.2 one gets:

$$M_{w,max} = 8.1. \tag{4.17}$$

Table 4.2. Application of Wells and Coppersmith equations to the Vrancea source (mean values)

M	M_w	Event	Experienced *SRA*, km^2	Wells & Coppersmith equations	
				$logSRA=-3.42+0.90M_w$	$logSRL=-3.55+0.74M_w$
				SRA, km^2	*SRL*, km
6.7	7.0	May 30,1990	1100[1)]	759	43
7.0	7.2	Aug. 30,1986	1400[1)]	1148	60
7.2	7.5	March 4, 1977	63 x 37=2331[2)]	2138	100
	8.1	Max. credible	-	7413	278

[1)]As cited in Tavera (1991) [2)] Enescu *et al.* (1982)

If the source magnitude is limited by an upper bound magnitude $M_{w,max}$, the recurrence relationship can be modified in order to satisfy the property of a probability distribution, Equation 4.10:

$$n(\geq M_w) = e^{\alpha - \beta M_w} \frac{1 - e^{-\beta(M_{w,\max} - M_w)}}{1 - e^{-\beta(M_{w,\max} - M_{w0})}} \tag{4.18}$$

and, in the case of Vrancea source (Lungu et al., 1999):

$$n(\geq M_w) = e^{8.654 - 1.687 M_w} \frac{1 - e^{-1.687(8.1 - M_w)}}{1 - e^{-1.687(8.1 - 6.3)}} \tag{4.19}$$

In Eq.(4.18), the threshold lower magnitude is $M_{w0}=6.3$, the maximum credible magnitude of the source is $M_{w,max}=8.1$, and $\alpha = 3.76\ ln10 = 8.654$, $\beta = 0.73\ ln10 = 1.687$.
The maximum credible magnitude of the source governs the prediction of source magnitudes in the range of large recurrence intervals, where classical relationship (4.16) does not apply, Table 4.3.

Table 4.3. Mean recurrence interval (MRI) of Vrancea magnitudes, (≥Mw)=1/n(≥Mw)

Date	Gutenberg-Richter magnitude, M_{GR}	Moment magnitude, M_w	*MRI* from Eq. (4.18), years	*MRI* from Eq. (4.16), years
		8.1	-	150
		8.0	*778*	127
		7.9	*475* → *356*	107
		7.8	217	91
10 Nov. 1940	7.4	*7.7*	148	76
		7.6	*100* → *108*	65
4 March 1977	7.2	*7.5*	82	55
		7.4	*63*	46
30 Aug. 1986		*7.3*	*50* → 50	37
	7.0	*7.2*	40	33
30 May 1990	6.7	*7.0*	26	23

The depth of the Vrancea foci has a great influence on the observed seismic intensity. The damage intensity of the Vrancea strong earthquakes is the combined result of both magnitude and location of the focus inside the earth.
The relationship between the magnitude of a destructive Vrancea earthquake *($M_w \geq 6.3$)* and the corresponding focal depth shows that higher the magnitude, deeper the focus (Lungu *et al*., 1999):

$$ln\ h = -0.866 + 2.846\ ln M_w - 0.18\ P \tag{4.20}$$

where P is a binary variable: $P=0$ for the mean relationship and $P=1.0$ for mean minus one standard deviation relationship.
The following model was selected for the analysis of attenuation (Mollas & Yamazaki, 1995):

$$ln\ PGA = c_0 + c_1 M_w + c_2\ lnR + c_3 R + c_4\ h + \varepsilon \tag{4.21}$$

where: *PGA* is peak ground acceleration at the site, M_w- moment magnitude, R - hypocentral distance to the site, h - focal depth, c_0, c_1, c_2, c_3, c_4 - data dependent coefficients and ε - random variable with zero mean and standard deviation $\sigma_\varepsilon = \sigma_{ln\ PGA}$. The values of the coefficients are given in Table 4.4 based on the data from all regions. Details are given elsewhere (Lungu et.al., 1999, Lungu et.al., 2000, Lungu et. al., 2001).

Table 4.4. Regression coefficients inferred for horizontal components of peak ground acceleration during Vrancea subcrustal earthquakes, Equation (4.21)

c_0	c_1	c_2	c_3	c_4	σ_{lnPGA}
3.098	1.053	-1.000	-0.0005	-0.006	0.502

The application of the attenuation relation 4.21 for the Vrancea subcrustal earthquakes of March 4, 1977, August 30, 1986 and May 30, 1990 is represented in Figures 4.6, 4.7 and 4.8.

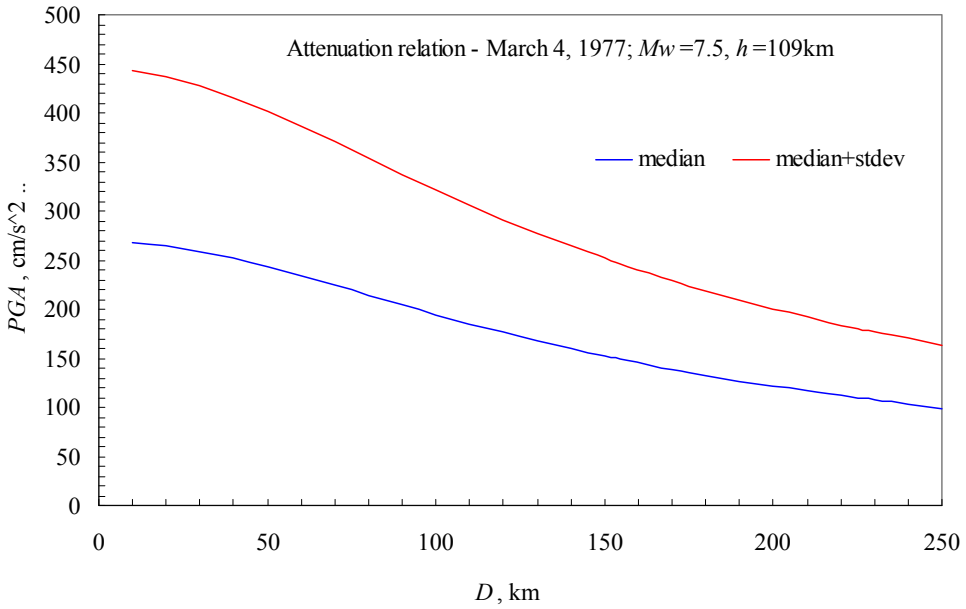

Figure 4.6. Attenuation relation applied for March 4, 1977 Vrancea subcrustal source

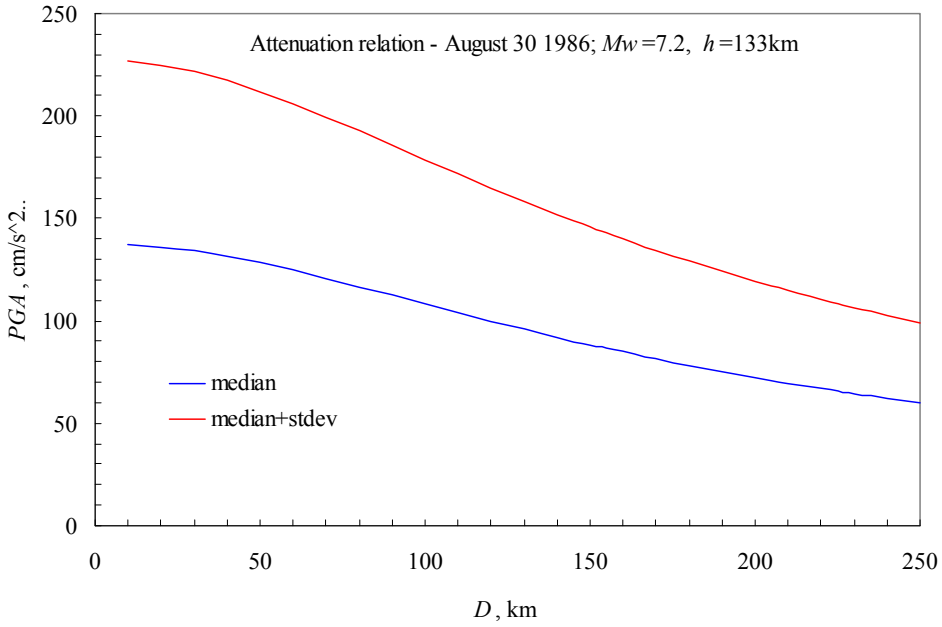

Figure 4.7. Attenuation relation applied for August 30, 1986 Vrancea subcrustal source

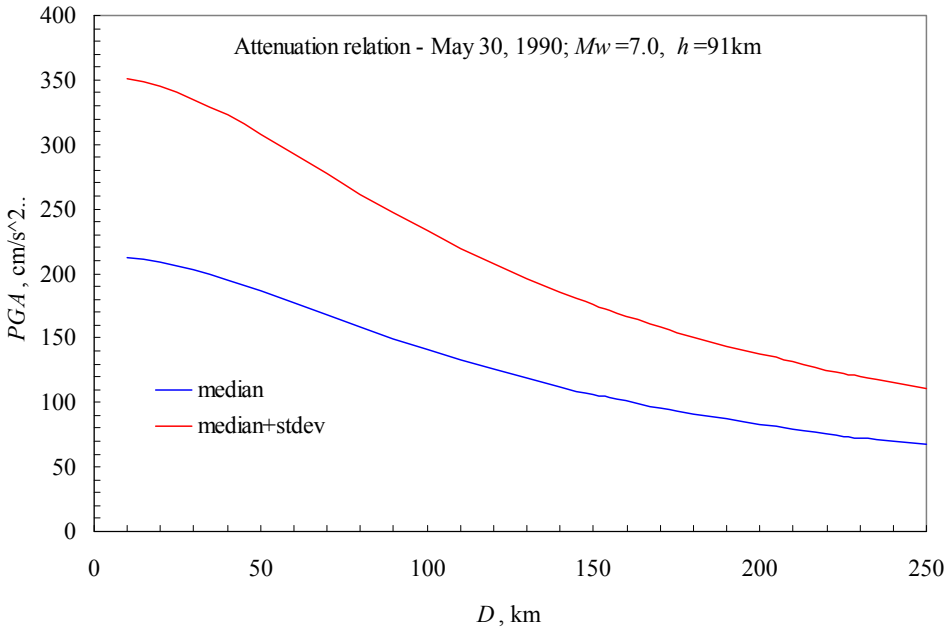

Figure 4.8. Attenuation relation applied for May 30, 1990 Vrancea subcrustal source

For a given earthquake recurrence, the mean annual rate of exceedance of a particular value of peak ground acceleration, *PGA**, is calculated using the total probability theorem (Cornell, 1968, Kramer, 1996):

$$\lambda(PGA > PGA^*) = \lambda_{M\,\min} \iint P(PGA > PGA^* \mid m,r) \cdot f_M(m) \cdot f_R(r) dmdr \qquad (4.22)$$

where:
– $\lambda(PGA>PGA^*)$ – mean annual rate of exceedance of *PGA** ;
- λ_{Mmin} is the mean annual rate of earthquakes of magnitude M larger or equal than M_{min};
- $P(PGA>PGA^*|m,r)$ – probability of exceedance of *PGA** given the occurrence of an earthquake of magnitude m at source to site distance r. This probability is obtained from attenuation relationship (4.21) assuming log-normal distribution for *PGA*;
- $f_M(m)$ – probability density function for magnitude;
- $f_R(r)$ – probability density function for source to site distance.

The probability density function for magnitude is obtained from Eq. (4.8) (Kramer, 1996). The probability density function for source to site distance is considered, for the sake of simplicity, uniform over the rectangle of 40x80km^2 having the long axis oriented N45E and being centered at about 45.6^o Lat.N and 26.6^o Long. E.

The mean annual rate of exceedance of *PGA* – the hazard curve - for Bucharest site and Vrancea seismic source is represented in Figure 4.9. The hazard curve can be approximated by the form $H = k_o \cdot a_g^{-k}$, where a_g is peak ground acceleration, and k_o and k are constants depending on the site (in this case k_o=1.176E-05, k=3.0865).

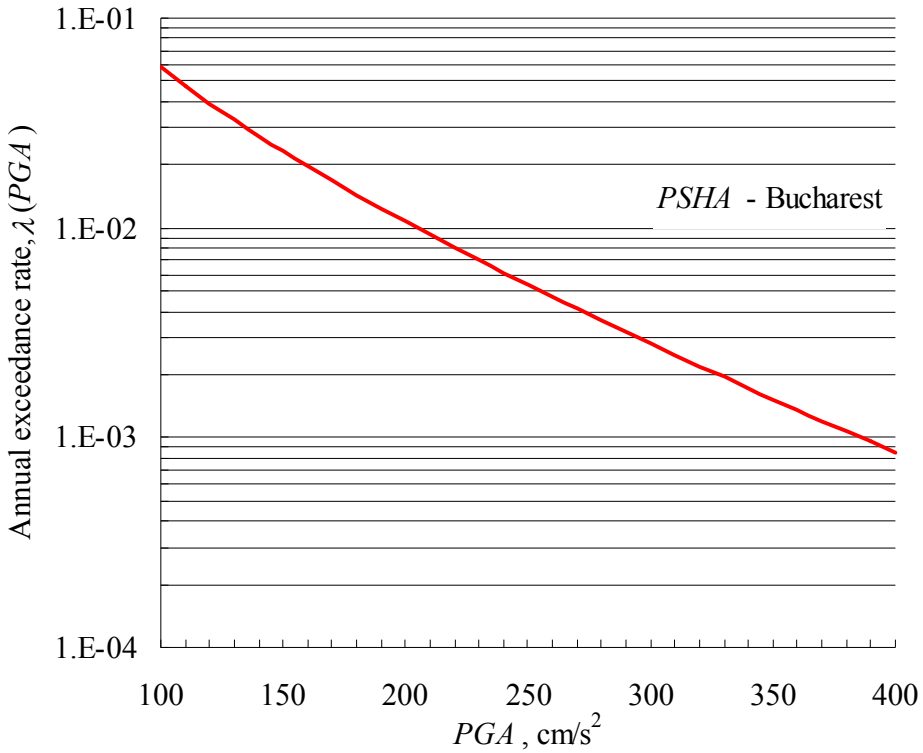

Figure 4.9. Hazard curve for Bucharest from Vrancea seismic source

4.8. Seismic Action in the Romanian Earthquake Resistant Design Code P100-1-2006

The results of the seismic hazard analysis for Romania are incorporated within the new *P100-1-2006* earthquake resistant design code that was enforced from January 1st, 2007. Approved by the Minister of Transport, Constructions and Tourism order no.1711 from 19.09.2006, the code was published in the *Official Gazette of Romani*a No. 803 from 25.09.2006. In the followings excerpts translated in English of the definition of seismic action in the *P100-1-2006* earthquake-resistant design code (seismic action is defined in *P1001-2006*-Chapter 3 and Annex A) are presented.

For the seismic design of buildings, the territory of Romania is divided into seismic hazard zones. The seismic hazard level within each zone is considered to be constant. For important urban centers and for the buildings of special importance it is recommended to evaluate the seismic hazard using instrumental earthquake data and site specific studies. Seismic hazard level indicated in present code is a minimum required level for design. Seismic hazard for design is described by the horizontal peak ground acceleration a_g determined for a reference mean recurrence interval (*MRI*) corresponding to the ultimate limit state. Peak ground acceleration a_g is called in the following "Design Ground Acceleration". The Design Ground Acceleration a_g within each seismic hazard zone, corresponds to a 100 years reference mean recurrence interval. The zonation of the Design Ground Acceleration a_g in Romania is indicated in Figure 4.10 for seismic events having a magnitude mean recurrence interval *MRI* = 100 years, and it is considered for the ultimate limit state design of buildings.

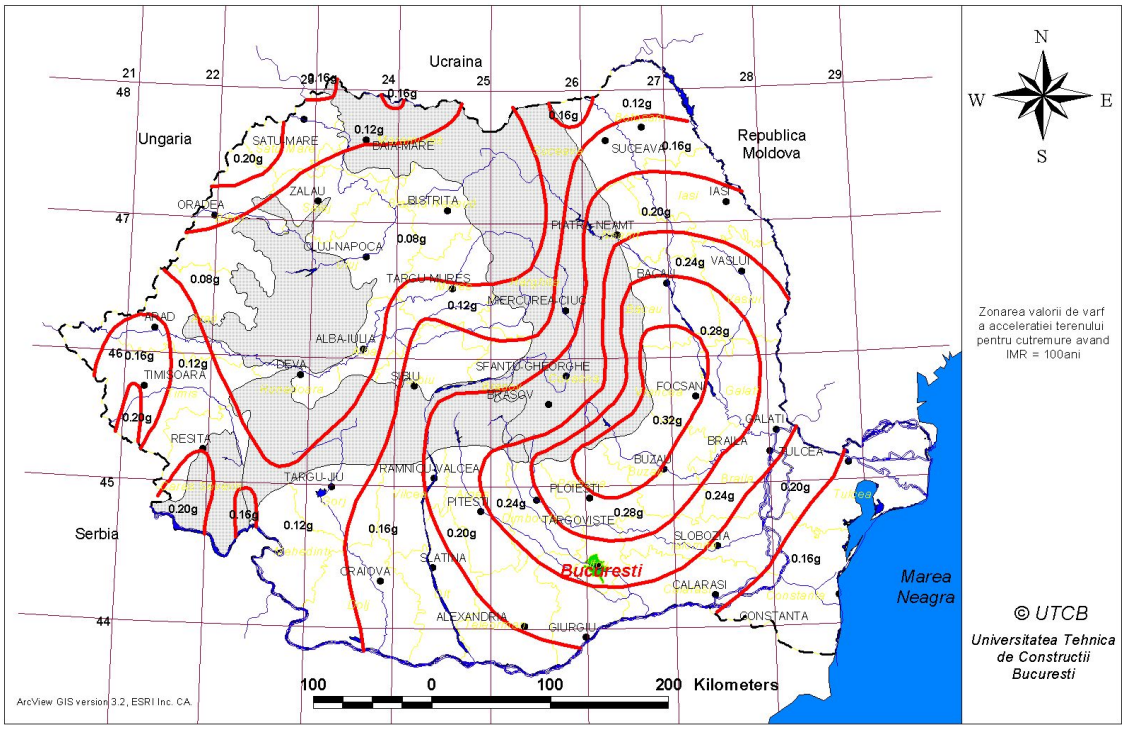

Figure 4.10 P100-1-2006 Zonation map of Romania in terms of design ground acceleration a_g for seismic events with the magnitude mean recurrence interval *MRI* = 100 years

Earthquake ground motion at a free field site is described by the absolute acceleration elastic response spectrum. Earthquake horizontal ground motion is described by two orthogonal

components considered as independent; in design, the elastic absolute acceleration response spectrum is considered to be the same for both horizontal components of ground motion. The normalized acceleration elastic response spectra are obtained by dividing the elastic acceleration response spectra to the design ground acceleration a_g.

The local ground conditions are described by the control (corner) period of the elastic response spectra, T_C, at the considered site. The value of T_C synthetically characterizes the frequency content of earthquake ground motions. The corner period of the elastic response spectra, T_C, represents the limit between the spectrum acceleration sensitive region and the spectrum velocity sensitive region. T_C is measured in seconds. For Romanian seismic and ground conditions and for earthquakes having *MRI* = 100 years, the design zonation map in terms of control (corner) period, T_C, is presented in Figure 4.11. The map was obtained using the existing instrumental data from the horizontal components of earthquake ground motions.

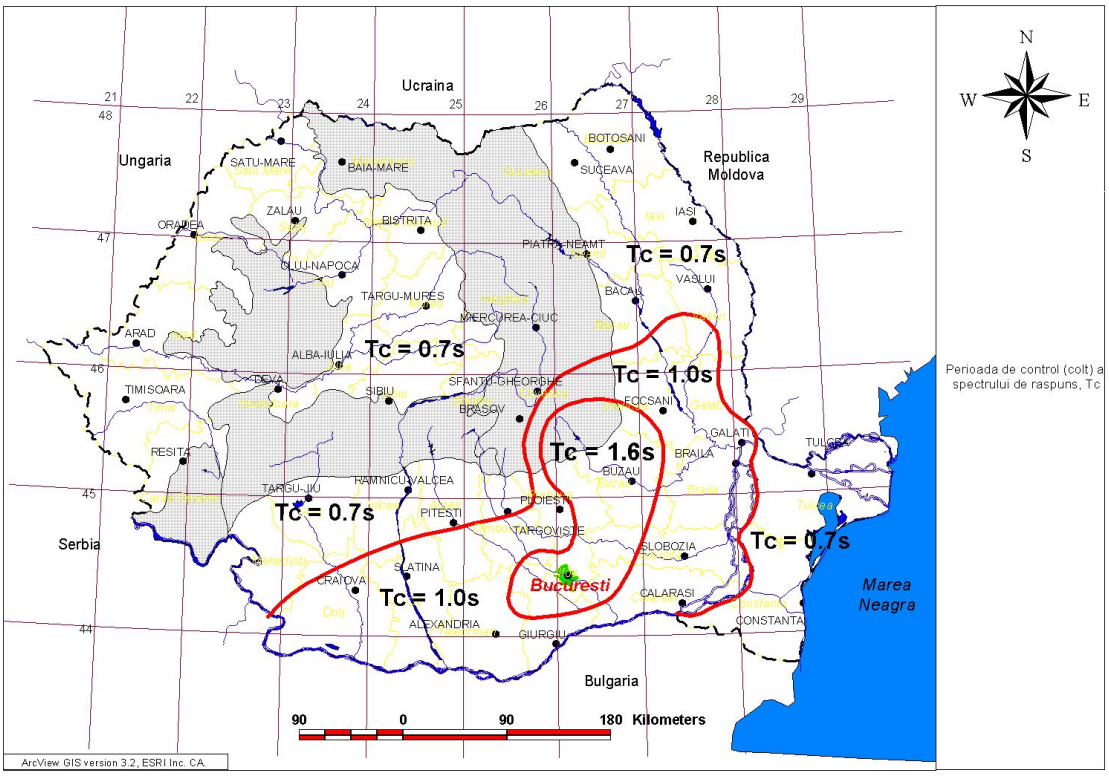

Figure 4.11 P100-1-2006 Zonation map of Romania in terms of the control (corner) period of response spectra, T_C

The shapes of the normalized elastic absolute acceleration response spectra of the horizontal components of ground motion, $\beta(T)$, for a damping ratio $\xi = 0.05$ are given by the following relations, as a function of the control periods T_B, T_C and T_D:

$$0 \le T \le T_B \qquad \beta(\mathrm{T}) = 1 + \frac{(\beta_0 - 1)}{\mathrm{T_B}}\mathrm{T} \qquad (4.23)$$

$$T_B < T \le T_C \qquad \beta(T) = \beta_0 \qquad (4.24)$$

$T_C < T \leq T_D$ $\beta(\mathrm{T}) = \beta_0 \frac{T_C}{T}$ (4.25)

$T > T_D$ $\beta(\mathrm{T}) = \beta_0 \frac{T_C T_D}{T^2}$ (4.26)

where:

$\beta(T)$ represents the normalized elastic acceleration response spectrum
β_0 represents the structure's maximum dynamic amplification factor for the horizontal component of ground motion acceleration
T represents the vibration period of a SDOF elastic structure.

The control (corner) period T_B can be expressed in a simplified manner as a function of T_C: $T_B=0.1T_C$. The control (corner) period T_D of the elastic response spectrum represents the limits between the spectrum constant velocity region and the spectrum constant displacement region. T_B and T_C represent the limits of the periods range for the simplified constant acceleration spectral region. The values of T_B, T_C and T_D are indicated in Table 4.5.

Table 4.5 Response spectrum control periods T_B, T_C, T_D for the horizontal components of earthquake ground motion

Mean recurrence interval of earthquake magnitude	Control Period Values			
MRI = 100 years, for Ultimate Limit State	T_B, s	0,07	0,10	0,16
	T_C, s	0,7	1,0	1,6
	T_D, s	3	3	2

The normalized acceleration elastic response spectra (for $\xi=0.05$) for Romanian seismic and ground conditions are shown in Figure 4.12 as a function of T_B, T_C and T_D (as given in Table 4.5).

For the Banat area for sites characterized by a design ground acceleration $a_g=0.20g$ and $a_g=0.16g$, the normalized acceleration elastic response spectrum presented in Figure 4.13 is considered. For the Banat area sites where a_g=0.12g and a_g=0.08g, the normalized spectrum presented in Figure 4.12 for $T_C \leq 0.7s$ is considered.

The acceleration elastic response spectrum $S_e(T)$ (in m/s^2) is defined as:

$$S_e(T) = a_g \beta(T) \quad (4.27)$$

where a_g is in m/s^2.

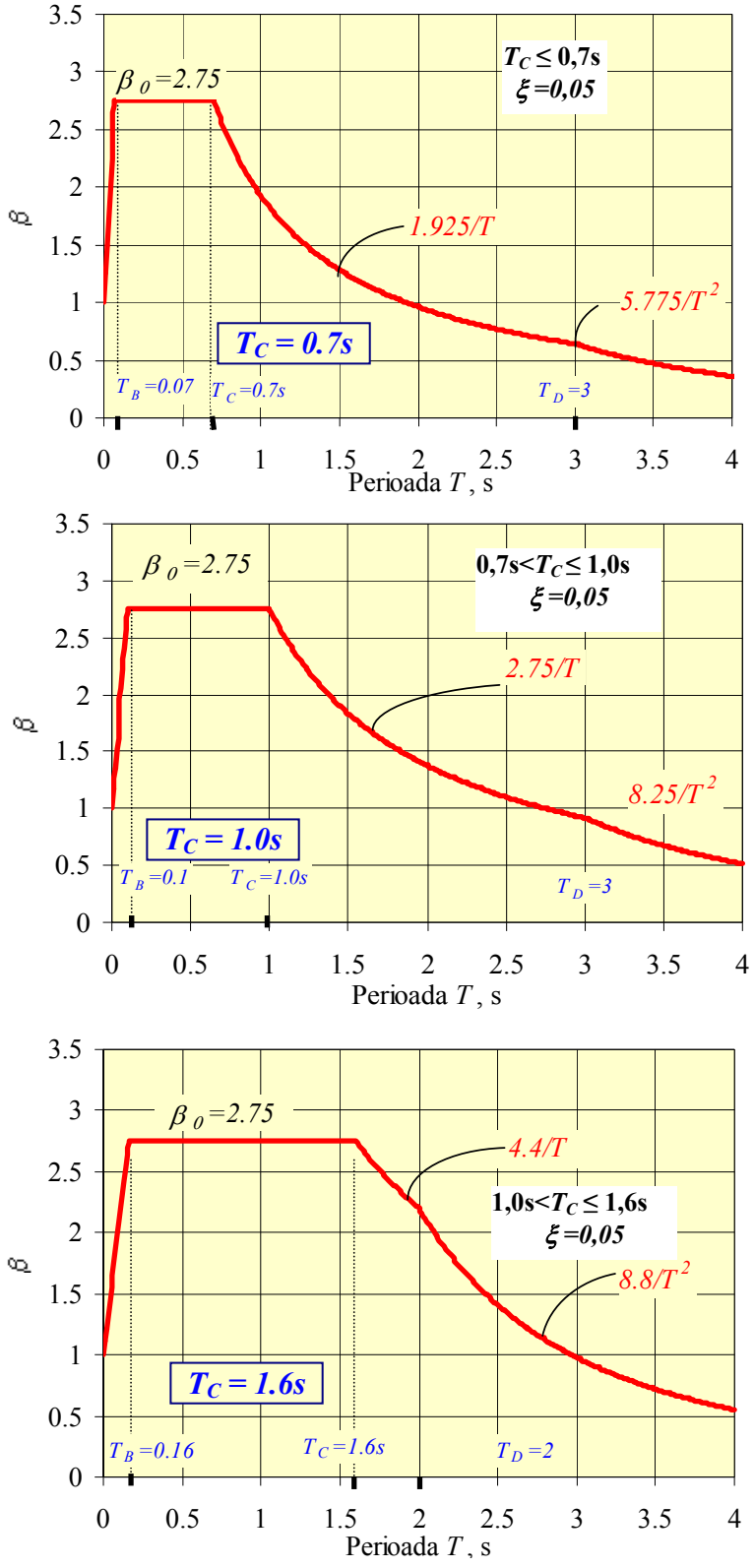

Figure 4.12 P100-1-2006: The normalized acceleration elastic response spectra (for ξ=0.05) for horizontal components of earthquake ground motion, for zones characterized by the control periods: T_C= 0.7, T_C= 1.0 and T_C= 1.6s

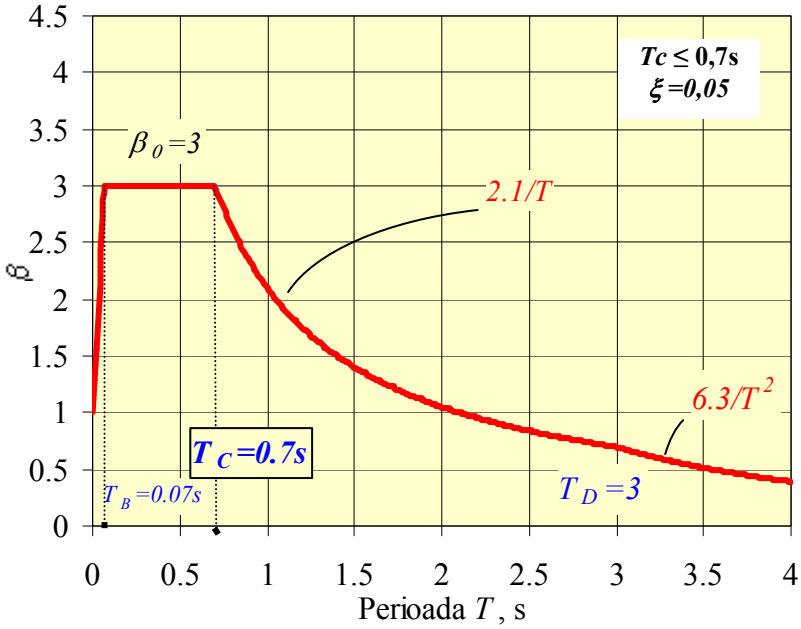

Figure 4.13 P100-1-2006; Crustal seismic sources in Banat area: normalized acceleration elastic response spectra for horizontal components of earthquake ground motion for areas with seismic hazard characterized by $a_g = 0.20g$ and $a_g = 0.16g$

For the Bucharest area, for moderate and large magnitude Vrancea earthquakes (Gutenberg-Richter magnitude $M \geq 7.0$; moment magnitude $M_w \geq 7.2$) exists the clearly instrumented proof of a long predominant period ($T_p = 1.4 \div 1.6s$) of ground vibrations, Figure 4.14.

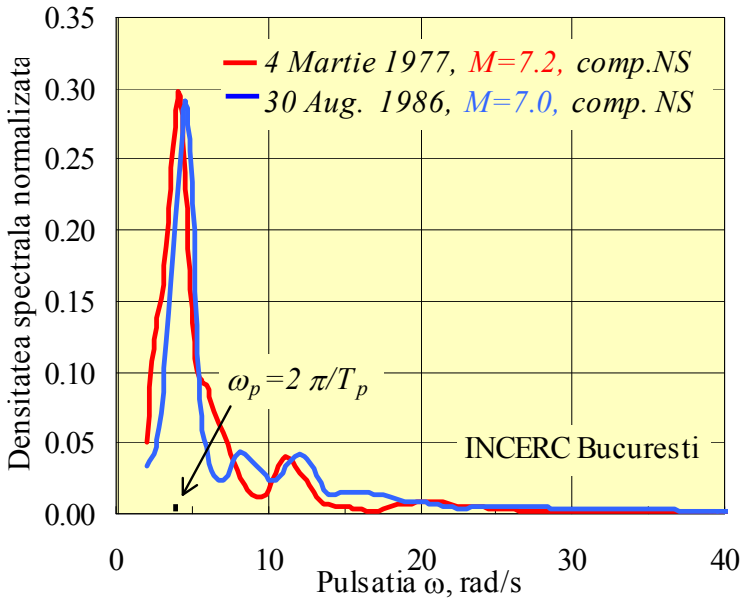

Figure 4.14 Normalised Power Spectral Density for March 4, 1977, NS Comp., and August 30, 1986, NS Comp., recorded at INCERC seismic station in Eastern Bucharest

The displacement elastic response spectrum for horizontal earthquake ground motion components $S_{De}(T)$, expressed in m, is obtained from the acceleration elastic response spectrum $S_e(T)$ using the following relation:

$$S_{De}(T) = S_e(T)\left[\frac{T}{2\pi}\right]^2 \tag{4.28}$$

The vertical component of the seismic action is represented by the acceleration elastic response spectrum for the vertical ground motion component. The shapes of the normalized elastic response spectra of vertical ground motion component $\beta_v(T)$ for a damping ratio $\xi = 0.05$, are described by the following relations as a function of control (corner) periods T_{Bv}, T_{Cv}, T_{Dv} of the vertical component spectra:

$$0 \le T \le T_{Bv} \qquad \beta_v(\mathrm{T}) = 1 + \frac{(\beta_{0v} - 1)}{\mathrm{T_{Bv}}}\mathrm{T} \tag{4.29}$$

$$T_{Bv} < T \le T_{Cv} \qquad \beta_v(T) = \beta_{0v} \tag{4.30}$$

$$T_{Cv} < T \le T_{Dv} \qquad \beta_v(\mathrm{T}) = \beta_{0v}\frac{T_{Cv}}{T} \tag{4.31}$$

$$T > T_{Dv} \qquad \beta_v(\mathrm{T}) = \beta_{0v}\frac{T_{Cv}T_{Dv}}{T^2} \tag{4.32}$$

where $\beta_{ov} = 3.0$ represents the structure's maximum dynamic amplification factor for the vertical ground motion acceleration, considering a damping ratio $\xi = 0.05$.

The corner periods of the normalized elastic response spectra of the vertical earthquake ground motion component, are considered in a simplified manner using the following relations:

$$T_{Bv} = 0{,}1\ T_{Cv} \tag{4.33}$$
$$T_{Cv} = 0{,}45\ T_C \tag{4.34}$$
$$T_{Dv} = T_D. \tag{4.35}$$

The acceleration elastic response spectrum for the vertical component of ground motion, $S_{ve}(T)$, is defined as:

$$S_{ve}(T) = a_{vg}\beta_v(T). \tag{4.36}$$

The design peak ground acceleration value for the vertical component of the earthquake ground motion, a_{vg}, is evaluated as:

$$a_{vg} = 0{,}7\ a_g. \tag{4.37}$$

For design situations in which is necessary an elastic response spectrum computed for a different than the conventional 5% damping ratio, the use the following conversion relation for spectral ordinates is recommended:

$$S_e(T)_{\xi \neq 5\%} = S_e(T)_{\xi_0 = 5\%} \cdot \eta \tag{4.38}$$

where:

$S_e(T)_{\xi_0=5\%}$ - represents the site acceleration elastic response spectrum corresponding to a damping ratio, ξ_0=5%
$S_e(T)_{\xi\neq5\%}$ - represents the site acceleration elastic response spectrum corresponding to another damping ratio, $\xi\neq5\%$
η – the correction factor determined as follows:

$$\eta = \sqrt{\frac{10}{5+\xi}} \geq 0{,}55 \qquad (4.39).$$

The acceleration design spectrum $S_d(T)$, expressed in m/s^2, is an inelastic response spectrum obtained using the following relations:

$$0 < T \leq T_B \qquad S_d(T) = a_g \left[1 + \frac{\frac{\beta_0}{q} - 1}{T_B} T \right] \qquad (4.40)$$

$$T > T_B \qquad S_d(T) = a_g \frac{\beta(T)}{q}. \qquad (4.41)$$

where
q represents the behavior factor (the elastic to inelastic response modification factor), with values depending on the structural system and on the energy dissipation capacity of the structure.
The values of behavior factor q for different types of materials and structural systems are indicated in specific chapters of the P100-1-2006 code.
The design spectrum for the vertical component of the earthquake ground motion is obtained in a similar way. In this case, the behavior factor q value is simply considered equal to 1.5 for all materials and for all structural types with the exception of special cases for which larger values can be justified.

4.9. Seismic Fragility/Vulnerability and Seismic Risk Analysis

4.9.1. Background

Human, economic and ecological costs and losses associated with earthquake disasters are increasing exponentially and these cost and losses pose a systemic risk to society's political and economic bases. It is correspondingly difficult, in some cases impossible, for local, national and global disaster management agencies to cope with the scope, magnitude and complexity of these disasters.

Even utilizing the most advanced technology, it is almost impossible, at the present state of knowledge, to predict exactly when and where an earthquake will occur and how big it will be. An earthquake suddenly hits an area where people are neither prepared nor alerted. Hence, the earthquake often causes huge damage to human society. On the other hand, the other natural disasters like floods and hurricanes are almost predictable, providing some lead time before they hit certain places. People could be alerted with a proper warning system and precautionary measures could be taken to protect lives and properties.

It is therefore urgent and crucial to make the physical environment resistant against earthquakes, strengthening buildings and infrastructure. Action should be taken for seismic risk reductions. Different strategies may be taken to mitigate earthquake disasters, based on appropriate risk assessment.

There is a tendency to think that disaster prevention would cost much more than relief activities. However, the reality is the reverse. Our society has been spending a lot of resources for response activities after disasters; these resources could have been drastically reduced if some had been spent for disaster prevention. There is also a tendency to look at disasters mainly from a humanitarian angle, bringing us into the position of giving priority to the response to disasters. However, relief activities can never save human lives that have already been lost. Response activities can never help immediately resume functions of an urban infrastructure that has already been destroyed. The bottom line is that buildings should not kill people by collapsing and infrastructure should not halt social and economic activities of the city for a long time.

The damage caused by an earthquake could be magnified in areas where:

- People are concentrated;
- Economic and political functions are concentrated;
- Buildings and infrastructure have been built to inadequate standards of design.

The larger an urban area is, the greater the damage would be. As the urban areas are growing rapidly, the seismic risk in the urban areas is also growing rapidly. Even an intermediate earthquake could cause destructive damage to a city.

Fragility/Vulnerability represents the proneness to damage or losses of an exposed built system in relation to a single seismic event. It may be expressed in probabilistic terms (for prediction purposes) or in statistical terms (for purposes of processing the outcome of post-earthquake surveys).
Risk represents the expectancy of damage or losses (expressed in probabilistic terms) in relation to the performance of an exposed built system, as a function of the service duration.

The risk analysis recognizes basically the impossibility of deterministic prediction of events of interest, like future earthquakes, exposure of elements at risk, or chain effects occurring as a consequence of the earthquake-induced damage. Since the expectancy of losses represents the outcome of a more or less explicit and accurate predictive analysis, a prediction must be made somehow in probabilistic terms, by extrapolating or projecting into the future the present experience. A probability-based prediction relies on two major premises:

- the conceptual and methodological framework of the theory of probabilities, of which the law of large number must be explicitly emphasized;
- the assumption that there exists some intrinsic stability and stationarity of objective processes determining the input and outcome of phenomena and events dealt with.

The risk is obtained as the convolution product of hazard, vulnerability and exposure. The general relation for the determination of the total risk can be expressed as (Whitman & Cornell, 1976):

$$P[R_i] = \sum_j P[R_i / S_j] \cdot P[S_j] \tag{4.42}$$

in which $P[\ ]$ signifies the probability of the event indicated within the brackets, R_i denotes the event that the state of system is i, S_j means that the seismic input experienced is level j, and $P[R_i/S_j]$ states the probability that the state of the system will be R_i *given* that the seismic input S_j takes place.

4.9.2. Earthquake Loss Estimation

This chapter describes methods for determining the probability of Slight, Moderate, Extensive and Complete damage to general building stock designed to earthquake resistant seismic codes or not seismically designed, as given in *HAZUS99 Technical Manual – Earthquake Loss Estimation Methodology*. The scope of this chapter includes development of methods for estimation of earthquake damage to buildings given knowledge of the building typology and an estimate of the level of seismic hazard.

The description of the damage states considered (Slight, Moderate, Extensive and Complete) is presented in the following for two main structural typologies and is based on the developments from *HAZUS99 Technical Manual*.

Reinforced Concrete Moment Resisting Frames
Slight Structural Damage: Flexural or shear type hairline cracks in some beams and columns near joints or within joints.
Moderate Structural Damage: Most beams and columns exhibit hairline cracks. In ductile frames some of the frame elements have reached yield capacity indicated by larger flexural cracks and some concrete spalling. Nonductile frames may exhibit larger shear cracks and spalling.
Extensive Structural Damage: Some of the frame elements have reached their ultimate capacity indicated in ductile frames by large flexural cracks, spalled concrete and buckled main reinforcement; nonductile frame elements may have suffered shear failures or bond failures at reinforcement splices, or broken ties or buckled main reinforcement in columns which may result in partial collapse.
Complete Structural Damage: Structure is collapsed or in imminent danger of collapse due to brittle failure of nonductile frame elements or loss of frame stability. Approximately

20%(low-rise), 15%(mid-rise) or 10%(high-rise) of the total area of C1 buildings with Complete damage is expected to be collapsed.

Concrete Shear Walls
Slight Structural Damage: Diagonal hairline cracks on most concrete shear wall surfaces; minor concrete spalling at few locations.
Moderate Structural Damage: Most shear wall surfaces exhibit diagonal cracks; some shear walls have exceeded yield capacity indicated by larger diagonal cracks and concrete spalling at wall ends.
Extensive Structural Damage: Most concrete shear walls have exceeded their yield capacities; some walls have exceeded their ultimate capacities indicated by large, through-the-wall diagonal cracks, extensive spalling around the cracks and visibly buckled wall reinforcement or rotation of narrow walls with inadequate foundations. Partial collapse may occur due to failure of nonductile columns not designed to resist lateral loads.
Complete Structural Damage: Structure has collapsed or is in imminent danger of collapse due to failure of most of the shear walls and failure of some critical beams or columns. Approximately 20%(low-rise), 15%(mid-rise) or 10%(high-rise) of the total area of C2 buildings with Complete damage is expected to be collapsed.

The distribution of the previously mentioned damage probabilities is called the building fragility/vulnerability function (curves). The fragility curves describe the probability of reaching or exceeding different states of damage given peak building response.
The probability of being in or exceeding a given damage state is modeled as a cumulative lognormal distribution. For structural damage, given the spectral displacement, S_d, the probability of being in or exceeding a damage state, ds, is modeled as:

$$P\left[ds \middle| S_d\right] = \Phi\left[\frac{1}{\beta_{ds}} \ln\left(\frac{S_d}{\bar{S}_{d,ds}}\right)\right] \tag{4.43}$$

where: $\bar{S}_{d,ds}$ is the median value of spectral displacement at which the building reaches the threshold of the damage state, ds,
β_{ds} is the standard deviation of the natural logarithm of spectral displacement of damage state, ds, and
Φ is the standard normal cumulative distribution function.

Structural damage fragility curves for buildings are described by median values of drift that define the thresholds of Slight, Moderate, Extensive and Complete damage states. In general, these estimates of drift are different for each building typology (including height) and seismic design level. Structural fragility is characterized in terms of spectral displacement. Median values of structural component fragility are based on building drift ratios that describe the threshold of damage states. Damage-state drift ratios are converted to spectral displacement using Equation (4.44):

$$\bar{S}_{d,Sds} = \delta_{R,Sds} \cdot \alpha_2 \cdot h \tag{4.44}$$

where: $\bar{S}_{d,Sds}$ is the median value of spectral displacement, in cm, of structural components for damage state, *ds*
$\delta_{R,Sds}$ is the drift ratio at the threshold of structural damage state, *ds*

α_2 is the fraction of the building (roof) height at the location of push-over mode displacement

h is the typical roof height, in centimeters, of the building typology of interest.

The total variability of each structural damage state, β_{Sds}, is modeled by the combination of three contributors to structural damage variability, β_C, β_D and $\beta_{M(Sds)}$, as described in Equation (4.45):

$$\beta_{Sds} = \sqrt{\beta_C^{\,2} + \beta_D^{\,2} + \left(\beta_{M(Sds)}\right)^2} \tag{4.45}$$

where:

β_{Sds} is the lognormal standard deviation that describes the total variability for structural damage state, *ds*

β_C is the lognormal standard deviation parameter that describes the variability of the capacity curve

β_D is the lognormal standard deviation parameter that describes the variability of the demand spectrum

$\beta_{M(Sds)}$ is the lognormal standard deviation parameter that describes the uncertainty in the estimate of the median value of the threshold of structural damage state, *ds*.

4.9.3. Case Study on the Expected Seismic Losses of Soft and Weak Groundfloor Buildings

The case study building is located in the city of Bucharest, Figure 4.15. The building was erected in 1960's, it has 11 storeys (B+GF+10S) and its main destination is residential in the upper floors and commercial in the groundfloor, Figure 4.16. The structural system consists of reinforced concrete frames in the groundfloor, Figure 4.17 and RC structural walls in the upper floors, Figure 4.18. The groundfloor is a soft and weak story, with no structural walls. The building consists of 3 parts (A, B and C). In what concerns the case study, part A is under discussion hereinafter. The A building has a rectangular base of 11.42x32.85 m. A staircase connects the buildings "A" and "B". Amongst all 3 buildings there are seismic joints of 3 cm.

Figure 4.15. Satellite view of the building site – 90-96 Mihai Bravu Blvd., Bucharest (from www.earth.google.com)

Figure 4.16. Main façade of the building A

The ground floor height is 4.80m while the height of the rest of the floors is 2.73m.
The soil underneath the building is made of layers of sand with gravel fractions in the medium compacted state, with a 3 daN/cm^2 conventional pressure. The building's footprint area is 380.07 m^2.

The concrete used is B250 (equivalent to C16/20) and the reinforcing steel used is OB37 (equivalent to S235).The RC beams sections vary from 15x55 cm up to 37,5x60 cm. The RC columns sections vary from 40x55 cm to 80x50 cm; there are also two elongated columns of 170x50cm transversally placed in the axes 9 and 10. The structural wall thickness varies from 15 to 20 cm. The slabs are made of reinforced concrete of 8 to 11 cm in thickness. The infrastructure system consists of a rigid box in the basement with continuous foundations under all the structural elements.

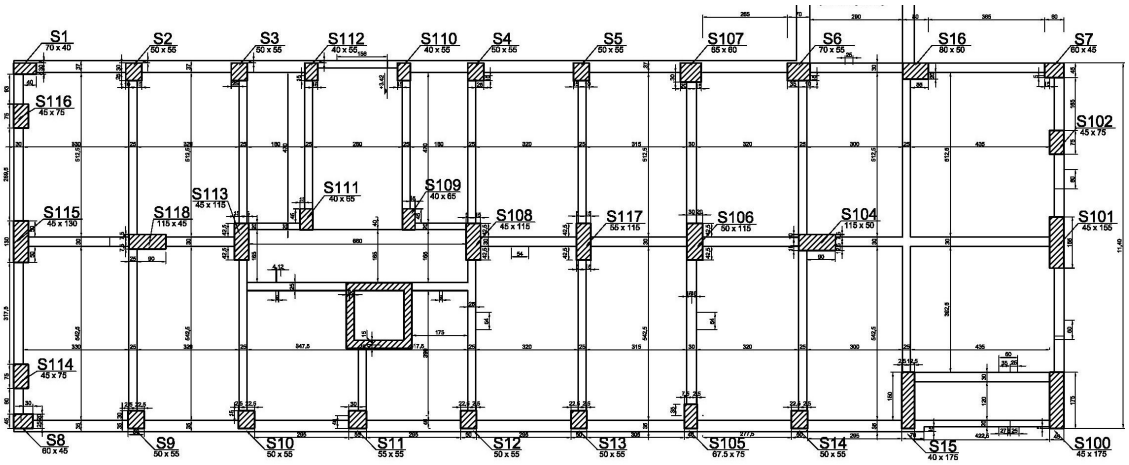

Figure 4.17. Groundfloor plan view

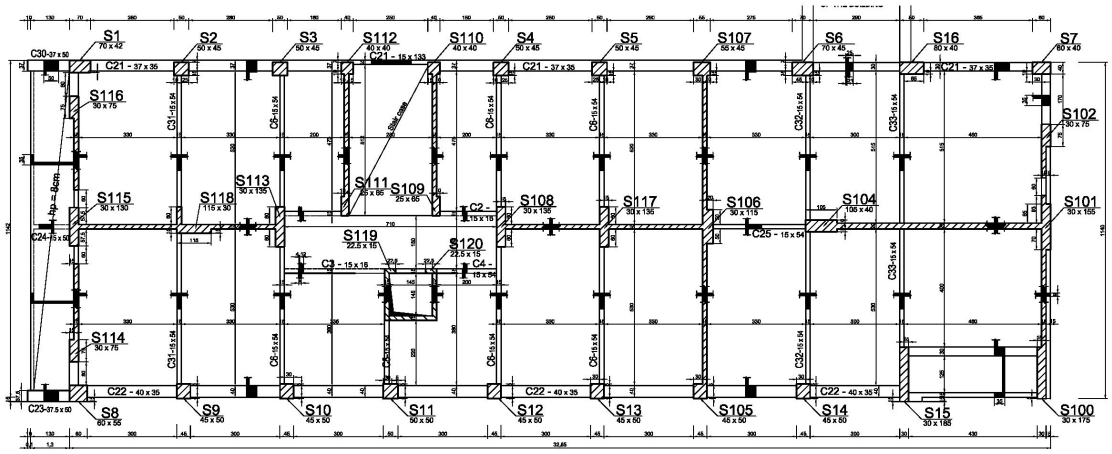

Figure 4.18. Plan view of current floor

The total weight of the building is 5528 t. The building first eigenvalue is 0.68s, the second eigenvalue is 0.56s and the third eigenvalue is 0.45s. The first eigenvector is a translation in the longitudinal direction; the second eigenvector is a translation in transversal direction together with a rigid body rotation around the basement while the third is a rotation around the vertical axis, Figure 4.19.

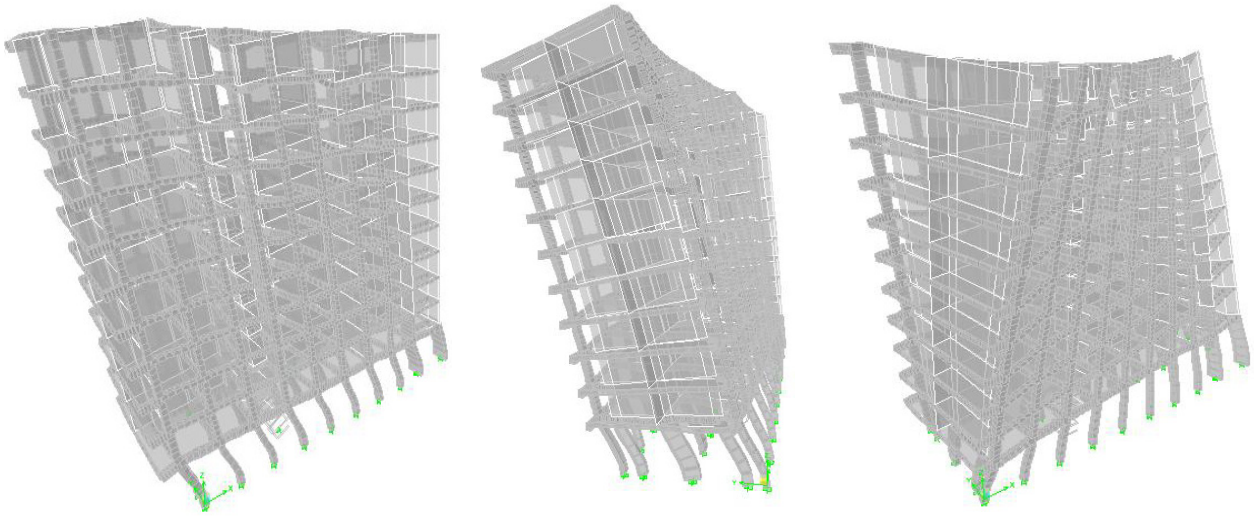

T_1=0.68s T_2=0.56s T_3=0.45s

Figure 4.19. Modal shapes and eigenvalues of the building

The seismic evaluation of the existing building was performed using capacity spectrum method, CSM (ATC40, 1996) with the alternative approach using strength reduction factors proposed by (Chopra&Goel, 1999), as follows:

1. The demand elastic acceleration-displacement response spectrum, *ADRS*, is represented. A demand constant-ductility spectrum is established by reducing the elastic acceleration-displacement spectrum by appropriate ductility-dependent factors that depend on *T*.
2. The capacity curve is plotted on the same graph. A building capacity curve (also known as a push-over curve) is a plot of a building's lateral load resistance as a function of a characteristic lateral displacement (i.e., a force-deflection plot). It is derived from a plot of static-equivalent base shear versus building (e.g., roof) displacement. In order to facilitate direct comparison with earthquake demand (i.e. overlaying the capacity curve with a response spectrum), the force (base shear) axis is converted to spectral acceleration and the displacement axis is converted to spectral displacement.
3. The yielding branch of the capacity curve intersects the demand spectra for several μ values of ductility factor. One of these intersection points, which remains to be determined, will provide the expected spectral displacement. At the one relevant intersection point, the ductility factor calculated from the capacity curve should match the ductility value associated with the intersecting demand spectrum.

Pushover analyses were performed for each direction of the building using ETABS^{TM} computer software. The application of the capacity spectrum method for the existing building is presented hereinafter. The demand elastic acceleration-displacement response spectrum is according to the Romanian Code for Earthquake Resistant Design of Buildings, P100-1/2006, considering two levels of seismic hazard with 80% exceedance probability in 50 years and 40% exceedance probability in 50 years. Nevertheless, for the completeness of the analysis, a third level of seismic hazard with 10% exceedance probability in 50 years was considered. The design peak ground accelerations in Bucharest for the previously mentioned levels of seismic hazard are 0.1*g*, 0.24*g* and 0.35*g*. The corresponding building performance levels are: damage limitation, life safety and collapse prevention, respectively. The results obtained from capacity spectrum method are presented in Figure 4.20 and Table 4.6.

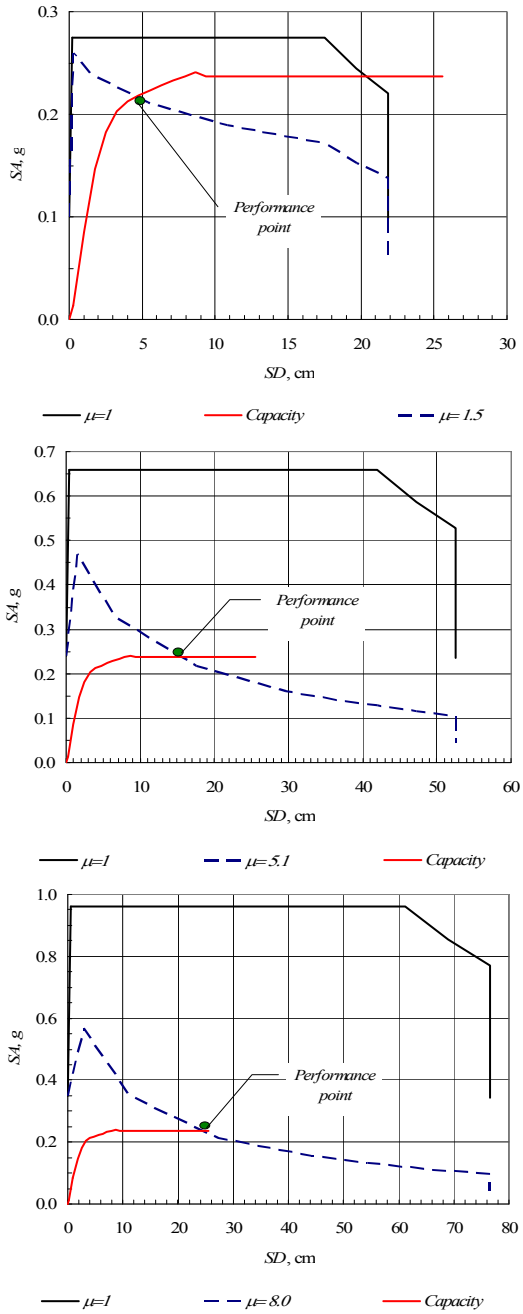

Figure 4.20a. Expected seismic response of existing building for *PGA*=0.1*g* (top), 0.24*g* (middle), 0.35*g* (bottom) – X direction

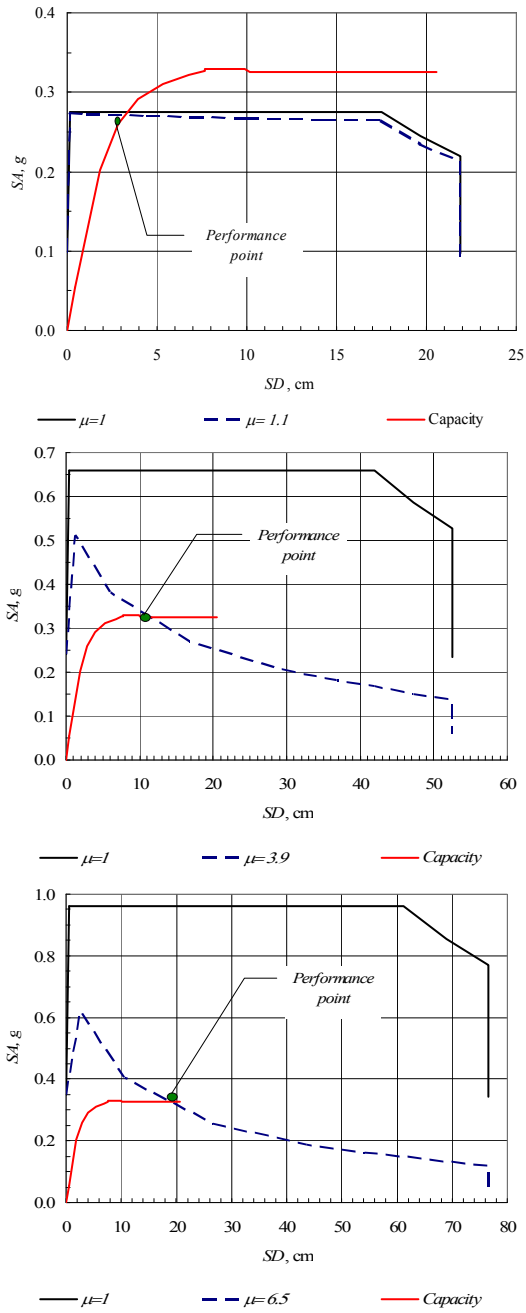

Figure 4.20b. Expected seismic response of existing building for *PGA*=0.1*g* (top), 0.24*g* (middle), 0.35*g* (bottom) – Y direction

Table 4.6. Expected seismic response of existing building

Expected seismic response	X direction			Y direction		
	PGA ['g] =			*PGA* ['g] =		
	0.10	0.24	0.35	0.10	0.24	0.35
SD, cm	4.6	15.5	24.5	3.0	11.3	19.0
SA, 'g	0.22	0.24	0.24	0.26	0.33	0.33
D_{roof}, cm	6.3	21.2	33.5	3.8	14.3	24.1
V, tf	988	1078	1078	994	1224	1224
μ	1.5	5.1	8.0	1.1	3.9	6.5

Note:
X Direction – Longitudinal
Y Direction - Transversal
SD - spectral displacement
SA - spectral acceleration
V - base shear force
W - weight of the building
D_{roof} - lateral displacement at top of building
PGA - peak ground acceleration
μ - displacement ductility

Given the median and standard deviation values of the drift ratios at threshold of damage states given in HAZUS99 for the building typology and the modal participation factor and actual building height, the parameters of the building fragility curves for structural damage states for the case study building are given in Table 4.7:

Table 4.7. Values of building fragility curve parameters for structural damage states

Slight		Moderate		Extensive		Complete	
$\bar{S}_{d,ds}$, cm	β_{ds}	$\bar{S}_{d,ds}$, cm	β_{ds}	$\bar{S}_{d,ds}$, cm	β_{ds}	$\bar{S}_{d,ds}$, cm	β_{ds}
5.1	0.70	8.2	0.81	20.4	0.89	51.1	0.98

The values of the building fragility curve parameters from Table 4.7 are used in relation (4.43) to get the building fragility curves for structural damage states that are presented in Figure 4.21. Given the expected spectral displacements presented in Table 4.6 and the building fragility curves presented in Figure 4.21, the probabilities of being in a given structural damage state are reported in Table 4.8 .

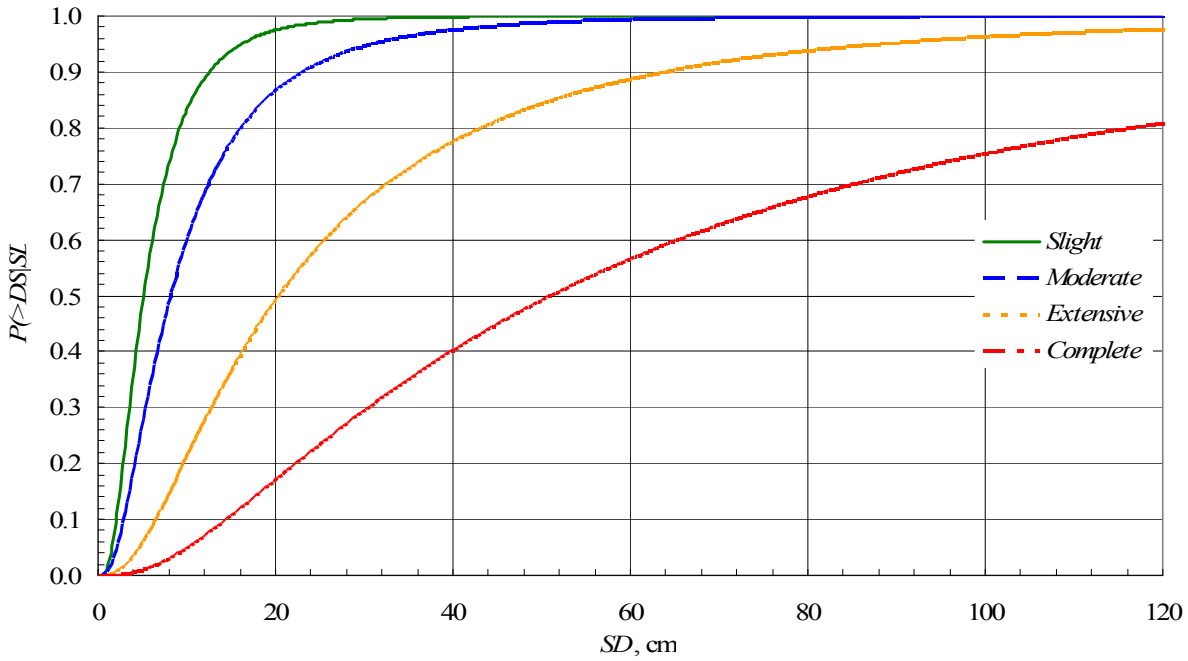

Figure 4.21. Building fragility curves for structural damage states

Table 4.8. Probabilities of being in a given structural damage state

Damage state, d_s	X direction			Y direction		
	PGA ['g] =			*PGA* ['g] =		
	0.10	0.24	0.35	0.10	0.24	0.35
None	5.64E-01	5.66E-02	1.28E-02	8.36E-01	1.58E-01	4.04E-02
Slight	2.00E-01	1.59E-01	7.60E-02	8.71E-02	2.29E-01	1.36E-01
Moderate	1.90E-01	4.07E-01	3.33E-01	6.71E-02	3.92E-01	3.97E-01
Extensive	3.93E-02	2.66E-01	3.53E-01	8.85E-03	1.70E-01	2.92E-01
Complete	6.87E-03	1.12E-01	2.25E-01	1.15E-03	5.12E-02	1.35E-01

The cost of damage is expressed as a percentage of the complete damage state. The assumed relationship between damage states and repair/replacement costs, for both structural and non-structural components, is as follows (HAZUS, 1999):
Slight damage: 2% of complete
Moderate damage: 10% of complete
Extensive damage: 50% of complete
These values are consistent with and in the range of the damage definitions and corresponding damage ratios presented in *ATC-13 Earthquake Damage Evaluation Data for California*.

Given the repair/replacement costs previously mentioned and the distribution of probabilities in Tables 4.8, the expected cost of damage given the incidence of an earthquake can be obtained. The expected costs of damage presented in the following are for structural elements and are expressed as percentage of the replacement cost obtained as weighted averages. The expected costs of damage for the existing building are reported in Table 4.9.

Table 4.9. Expected cost of damage for the existing building (% of replacement cost)

	X direction			Y direction		
	PGA ['g] =			*PGA* ['g] =		
	0.10	0.24	0.35	0.10	0.24	0.35
Structural damage	4.95	28.84	43.64	1.40	17.99	32.34

4.9.4. Full Probabilistic Risk Assessment of Buildings

4.9.4.1. Introduction

The probabilistic risk assessment is not a straightforward matter and involves a high computational effort. The probabilistic risk assessment is aiming at computing the annual probability of exceedance of various damage states for a given structural system. The consistent probabilistic approach is based on the idea of (Cornell & Krawinkler, 2000) using the total probability formula applied in a form that suits the specific needs:

$$P(\geq d_s) = \int_{PGA} \int_{Sd} \Phi(\geq d_s \mid Sd) \cdot f(Sd|PGA) \cdot f(PGA) d(Sd) d(PGA) \qquad (4.46)$$

where:

- $P(\geq d_s)$ – annual probability of exceedance of damage state d_s
– $\Phi(\geq d_s \mid Sd)$ – standard normal cumulative distribution function of damage state d_s conditional upon spectral displacement Sd
- $f(Sd \mid PGA)$ - probability density function of spectral displacement Sd given the occurrence of peak ground acceleration PGA
- $f(PGA)$ – probability density function of peak ground acceleration PGA

One can change Eq. (4.46) to solve for the mean annual rate of exceedance of various damage states for a given structural system:

$$\lambda(\geq d_s) = \sum_{PGA}\sum_{Sd} P(\geq d_s|Sd) \cdot P(Sd|PGA) \cdot \lambda(PGA) \tag{4.47}$$

where:

– $\lambda(\geq d_s)$ – mean annual rate of exceedance of damage state d_s
- $P(\geq d_s \mid Sd)$ – probability of exceedance of damage state d_s conditional upon spectral displacement Sd
- $P(Sd \mid PGA)$ - probability of reaching spectral displacement Sd given the occurrence peak ground acceleration PGA
– $\lambda(PGA)$ – mean annual rate of occurrence of peak ground acceleration PGA.

Consequently, the probabilistic assessment of seismic risk involves the:
1. probabilistic seismic hazard assessment, $\lambda(PGA)$
2. probabilistic assessment of seismic structural response, $P(Sd \mid PGA)$
3. probabilistic assessment of seismic structural vulnerability, $P(\geq d_s \mid Sd)$

Equations (4.46) and (4.47) are disaggregating the seismic risk assessment problem into three probabilistic analysis of: hazard, structural response and vulnerability. Then it aggregates the risk via summation (or integration) over all levels of the variables of interest.

The probabilistic seismic hazard assessment for Bucharest is discussed in Chapter 4.7. The probabilistic assessment of seismic structural response and the probabilistic assessment of seismic structural vulnerability is discussed hereinafter based on a case study for a RC moment resistant frame building located in Bucharest.

4.9.4.2. Probabilistic assessment of seismic structural response

The building analyzed has a reinforced concrete moment resisting frame structure and it was erected in early ‘70’s. It is a thirteen-storey building, the first two storeys being of 3.60 m, all the rest of 2.75 m height. The building has two spans of 6.00 m each in the transversal direction and five spans of 6.00 m each in the longitudinal direction. The concrete is of class Bc 20 and the steel is of quality PC 52. Some details regarding the structural members are given in Table 4.10. Further details can be found elsewhere (Vacareanu, 1998).

The seismic motion intensity is quantified by peak ground acceleration (*PGA*). The seismic motions used in the analyses consist of seven classes of random processes comprising ten samples each. Elastic acceleration spectra are used to simulate samples. The input seismic motions are simulated using a stationary Gaussian model based on elastic acceleration spectra (Shingal & Kiremidjian, 1997). The time histories are generated such as to fit the given response spectrum. The probability distributions of the dynamic amplification factors are used

to obtain an ensemble of response spectra corresponding to a given level of seismic motion (Vacareanu, 2000).
For parametric analysis purpose, the accelerograms are simulated at predefined values of *PGA*, as follows: 0.10g, 0.15g, 0.20g, 0.25g, 0.30g, 0.35g, 0.40g (g – acceleration of gravity).

Table 4.10.Description of the structural members

Storey #	Columns (BxD)	Overall reinfor-cement ratio	Hoop bar diameter	Hoop bar spacing	Beams (BxD)	Bottom reinfor-cement ratio	Top reinfor-cement ratio	Stirrup diameter	Stirrup spacing
	(mm)	(%)	(mm)	(mm)	(mm)	(%)	(%)	(mm)	(mm)
1,2	700 x 900	1.75	8	150	350 x 700	0.30	0.70	6	200
3-5	700 x 750	1.70	8	200	350 x 700	0.32	0.75	6	200
6 – 9	600 x 750	1.40	6	200	300 x 700	0.32	0.60	6	250
10 – 13	600 x 600	1.00	6	200	300 x 600	0.30	0.50	6	250

The structural model in the transversal direction consists of six - two spans - reinforced concrete moment resisting frames acting together due to the action of horizontal diaphragms located at each storey. The computer program *IDARC 2D* (Valles et. al., 1996) is used for performing inelastic dynamic analyses.

To trace the hysteretic response of structural elements, the piece-wise linear three-parameter model that included stiffness degradation, strength deterioration and slip is used to model the response of reinforced concrete structural elements. The trilinear hysteretic model relies on four parameters that scale the main characteristics represented in the model: stiffness deg-radation, strength deterioration and pinching. For analysis purpose, the default values (*HC* = 2.0 ; *HBD* = 0.0; *HBE* = 0.10 ; *HS* = 1.0) are used, these values allowing for nominal stiffness degradation and strength deterioration and no pinching effects.

Nonlinear dynamic analyses are performed for 10 simulated ground motions generated at each value of *PGA*. An integration time step of 0.002s is used in the analyses. The accelerograms last for 20 s and the total duration of the analysis is 21 s. The damping coefficient is 5 % of the critical damping and the structural damping is assumed to be mass proportional.

In damage analysis, the uncertainties associated with seismic demands and structural capacities need to be modeled. The Monte-Carlo technique involves the selection of samples of the random structural parameters and seismic excitations required for nonlinear analyses, the performance of nonlinear analyses and the computation of the structural response. In brief, the Monte-Carlo simulation technique implies the following steps:

- simulation of structural parameters and seismic excitations;
- random permutations of structural parameters and of excitations;

- performing nonlinear analyses using generated samples;
- sample statistics of results of analyses.

The direct Monte-Carlo technique requires a large number of simulation cycles to achieve an acceptable level of confidence in the estimated probabilities. The Latin hypercube technique might be used to reduce the number of simulation cycles. Using the Latin hypercube technique for selecting values of the input variables, the estimators from the simulation are close to the real values of the quantities being estimated. The Latin hypercube technique uses stratified sampling of the input variables, which usually results in a significant decrease in the variance of the estimators (Rubinstein, 1981).

The compressive strength of concrete and the yield strength of steel are the only parameters treated as structural random variables in this case study. Following Galambos et al. (1982), normal probability distribution for concrete strength and lognormal probability distribution for steel strength are used in this research. Concrete strength has a mean of 25 MPa and a coefficient of variation of 15%. Steel strength has a mean of 397 MPa and a coefficient of variation of 7%. For simulation purposes 10 values for concrete and reinforcement strengths are randomly generated and used for each *PGA* value considered within the analysis. Latin hypercube technique is used for randomly combine the generated strength variables and accelerations.

Spectral displacements are calculated using nonlinear dynamic analyses. Data regarding the randomness of the seismic response of the structural system are obtained. The statistic indicators of the spectral displacement obtained at each *PGA* value are used to get the parameters of a lognormal distribution function for that level of intensity of ground motion. The computed mean and standard deviation of the spectral displacements are reported in Table 4.11.

Table 4.11 Mean and standard deviation of spectral displacement conditional upon *PGA*

PGA, 'g	$\mu_{Sd\|PGA}$	$\sigma_{Sd\|PGA}$
0.1	13.1	2.2
0.15	22.8	3.3
0.2	30.0	4.0
0.25	39.5	3.8
0.3	49.8	5.3
0.35	59.0	6.4
0.4	68.7	6.9

Finally, the lognormal probability density function of spectral displacement conditional upon *PGA* is evaluated:

$$f(Sd \mid PGA) = \frac{1}{\sqrt{2\pi}} \cdot \frac{1}{Sd} \cdot \frac{1}{\sigma_{\ln(Sd|PGA)}} \cdot e^{-\frac{1}{2}\left(\frac{\ln(Sd)-\mu_{\ln(Sd|PGA)}}{\sigma_{\ln(Sd|PGA)}}\right)^2} \tag{4.48}$$

Examples of lognormal probability density functions of *Sd* conditional upon *PGA*= 0.1g, 0.2g and 0.3g are presented in Figure 4.22. Using the density functions one obtains probability of

reaching spectral displacement *Sd* given the occurrence of peak ground acceleration, *PGA*, *P(Sd | PGA)*.

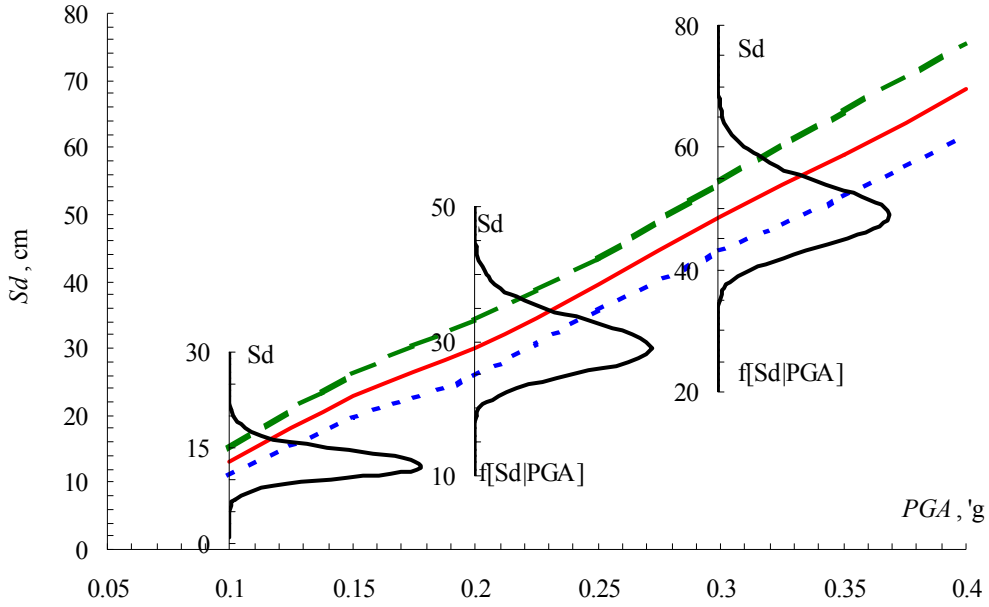

Figure 4.22. Mean and standard deviation of the spectral displacement

4.9.4.3. Probabilistic assessment of seismic structural vulnerability

The probabilistic assessment of seismic structural vulnerability involves the determination of the building vulnerability functions. These functions describe the conditional probability of being in, or exceeding, a particular damage state, d_s, given the spectral displacement, S_d, and is defined as *HAZUS*1999 :

$$P\left[ds|S_d\right] = \Phi\left[\frac{1}{\beta_{ds}} \ln\left(\frac{S_d}{\bar{S}_{d,ds}}\right)\right] \tag{4.49}$$

where:
- $S_{d,ds}$ is the median value of spectral displacement at which the building reaches the threshold of the damage state, *ds*,
- β_{ds} is the standard deviation of the natural logarithm of spectral displacement for damage state *ds*, and
– Φ is the standard normal cumulative distribution function.

For the spectral (maximum) displacement, S_d, expected for the demand earthquake, one determines the structural damage state probabilities using vulnerability functions (Eq. 4.49). *HAZUS*99 includes the vulnerability function parameters, $S_{d,ds}$ and β_{ds} appropriate for each type of building corresponding to USA practice of design and construction. In order to calibrate the vulnerability function parameters appropriate for structural systems which are different from USA practice, the Monte-Carlo simulation technique can be used. For simulation purposes 10 values for concrete and for reinforcement strengths are randomly generated and randomly combined for each push-over analysis.

The outcome of the pushover analyses is a family of capacity curves, which can be described as mean and mean plus/minus one standard deviation capacity curves, Figure 4.23 (Vacareanu et. al., 2001).
For calibration of vulnerability function parameters it is necessary to establish a correlation between Park&Ang (1985) damage index and interstory drift ratio at threshold of damage state. The more recent slightly modified version of Park&Ang index, in which the recoverable deformation is removed from the first term might be used:

$$DI = \frac{Dm - Dy}{Du - Dy} + \beta_e \cdot \frac{\int dE}{F_y \cdot Du} \tag{4.50}$$

where D_m = maximum displacement; D_u = ultimate displacement; D_y = yielding displacement; β_e = strength deterioration parameter; F_y = yielding force and E = dissipated hysteretic energy.

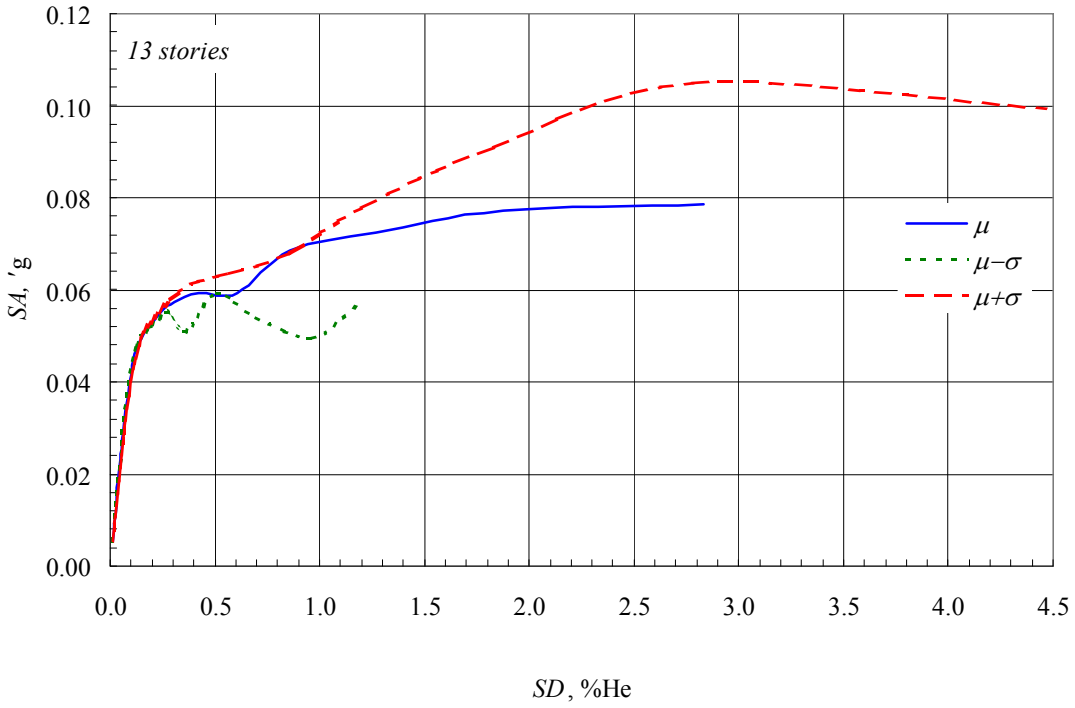

Figure 4.23. Capacity curves from Monte-Carlo simulation

The correlation between Park&Ang damage index and damage state is given in Table 4.12 (Williams & Sexsmith, 1995):

Table 4.12. Relations between damage index and damage state

Range of damage index	Damage state
$DI \leq 0.1$	None
$0.1 < DI \leq 0.25$	Slight
$0.25 < DI \leq 0.40$	Moderate
$0.40 < DI \leq 1.00$	Extensive
$DI > 1.00$	Complete

Using the definition of Park&Ang damage index (Eq. 4.50) and the structural behavior described by the capacity curve, one can determine the correlation between Park&Ang damage index and mean (± 1 standard deviation) interstory drift ratio values, Figure 4.24 (Vacareanu et. al., 2001).

Making vertical sections in Figure 4.24 for the threshold values of Park&Ang damage index given in Table 4.12 one can identify the mean and standard deviation values of interstory drift ratios at threshold of damage state, Table 4.13, Figure 4.25. The median value of spectral displacement at which the building reaches the threshold of the damage state, $S_{d,ds}$ is obtained by multiplying the interstory drift ratio by the height of the building and by the fraction of the building height at the location of push-over mode displacement, Table 4.14. The standard deviation of the natural logarithm of spectral displacement for damage state *ds*, β_{ds} is obtained using the standard deviation of the structural displacement.

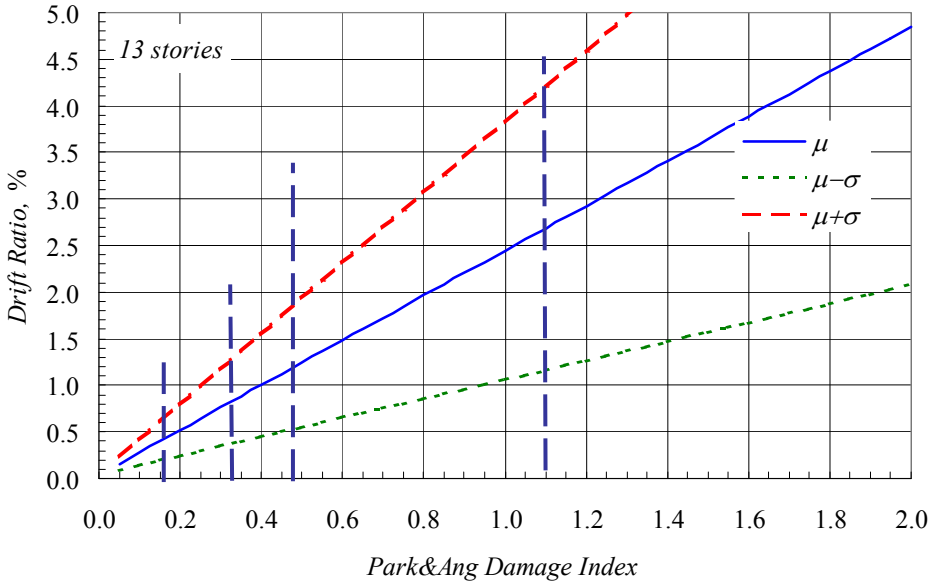

Figure 4.24. Correlation between Park&Ang damage index and interstory drift ratio

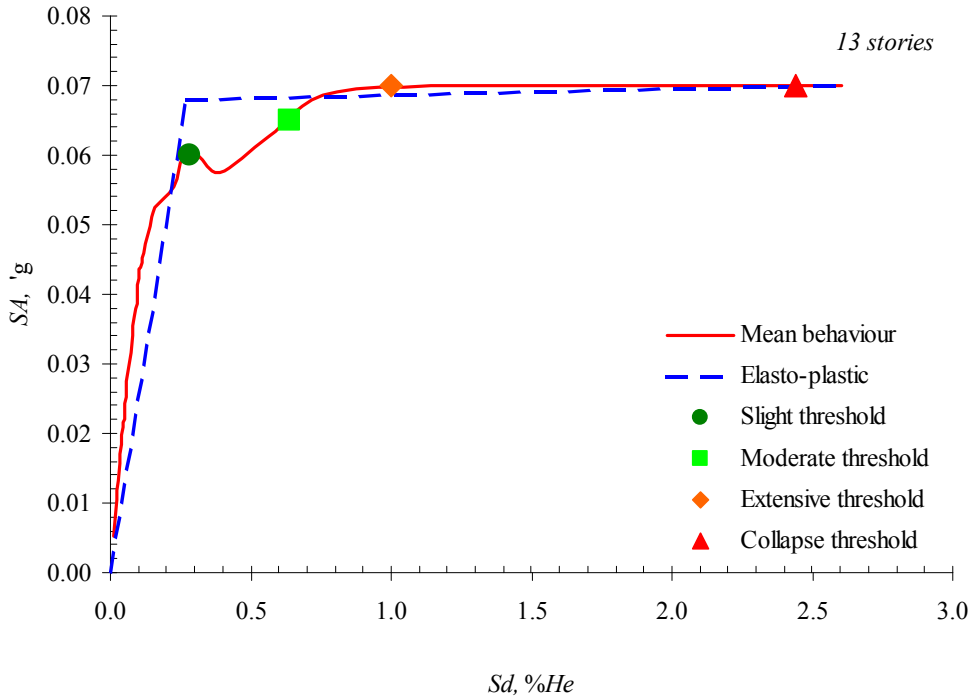

Figure 4.25. Median capacity curve and thresholds of damage states

Table 4.13. Mean interstory drift ratio at threshold of damage state (Monte-Carlo Simulation)

Slight	*Moderate*	*Extensive*	*Complete*
0.0028	0.0064	0.0100	0.0244

Table 4.14. Vulnerability function parameters (Monte-Carlo Simulation)

Slight		*Moderate*		*Extensive*		*Complete*	
$S_{d,ds}$, cm	β_{ds}	$S_{d,ds}$, cm	β_{ds}	$S_{d,ds}$, cm	β_{ds}	$S_{d,ds}$, cm	β_{ds}
7.82	0.66	17.88	0.66	27.94	0.76	68.16	0.91

Once the parameters of vulnerability function $S_{d,ds}$ and β_{ds} are obtained using Eq. 4.49 one can compute and plot the fragility functions, Figure 4.26.

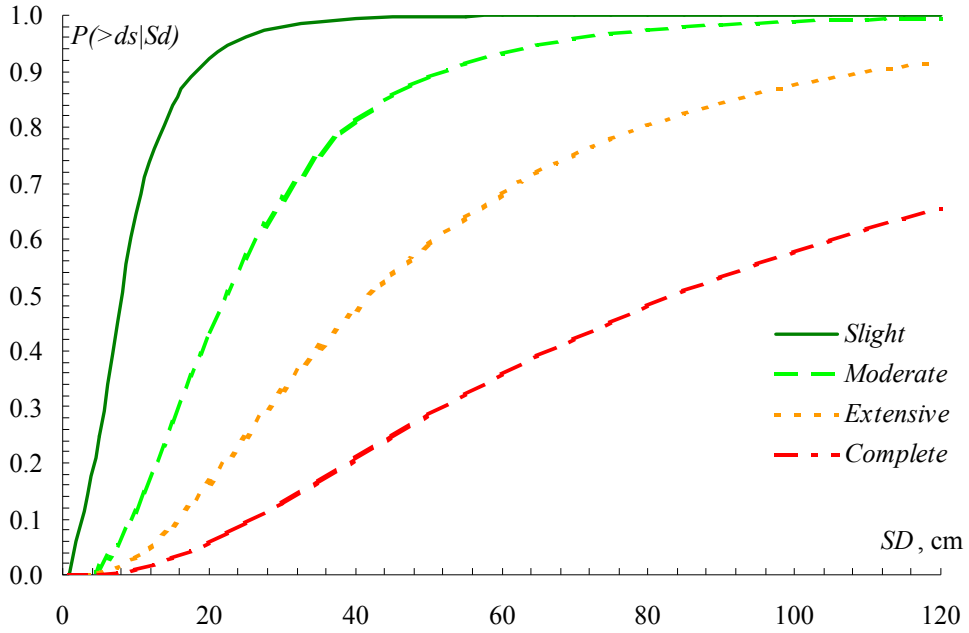

Figure 4.26. Vulnerability functions, Monte-Carlo simulation

4.9.4.4. Risk analysis

Given the results of the probabilistic seismic hazard assessment, $\lambda(PGA)$, the probabilistic assessment of seismic structural response, $P(Sd \mid PGA)$, and the probabilistic assessment of seismic structural vulnerability, $P(\geq d_s \mid Sd)$ one can aggregate the risk via summation (or integration) over all levels of the variables of interest using Equation 4.46. The results on risk are presented as mean annual rate of exceedance of damage state d_s, $\lambda(\geq d_s)$, in Table 4.15. Also, in Table 4.15 is presented the exceedance probability of various damage states in 1 year, 50 years and 100 years assuming that the damage states follows a Poisson distribution:

$$P_{exc}(d_s, T) = 1 - e^{-\lambda(\geq d_s)\cdot T} \tag{4.51}$$

where:

- $P_{exc}(d_s, T)$ - exceedance probability of damage state d_s in time T.

Table 4.15. Results of seismic risk analysis

Damage state - *ds*	Annual exceedance rate, $\lambda(\geq d_s)$	Exceedance prob., $P_{exc}(d_s, T)$ in:		
		T=1 year	T=50 years	T=100 years
Slight	5.1E-02	5.1E-02	9.2E-01	9.9E-01
Moderate	2.6E-02	2.6E-02	7.3E-01	9.3E-01
Extensive	1.2E-02	1.2E-02	4.4E-01	6.9E-01
Complete	4.7E-03	4.7E-03	2.1E-01	3.7E-01

One can notice from Table 4.15 the exceedance probability of complete damage state in 1 year of $4.7 \cdot 10^{-3}$ which is much higher that the commonly accepted probabilities of failure of 10^{-4} to 10^{-5} as in the case of non-seismic loads. The main reason for this high probability comes from the design of the building which was accomplished taking into account an inferior code for earthquake resistant design (*P13-70*) combined with the low level of seismic hazard considered in the design process.

4.9.5. Risk management

The XXth century witnessed a painful history of devastating earthquakes. Economic losses represent an important feature of earthquake-induced phenomena. Sometimes the economic burden and pressure induced by the consequences of an earthquake disaster caused irreparable economic crisis for poor countries. Table 4.16 presents a combination of human and economic losses for major earthquakes in the XXth century (where monetary evaluations were available).

Table 4.16. Human and economic losses produced by earthquakes in XXth century

No.	Date UTC	Location	Deaths	Losses ($bn)	Magnitude
1	1963 July 26	FYROM, Skopje	1,070	0.98	6.2
2	1972 Dec 23	Nicaragua, Managua	5,000	2	6.2
3	1976 Feb 4	Guatemala	23,000	1.1	7.5
4	1976 Jul 27	China, Tangshan	255,000	6	8
5	1977 Mar 4	Romania, Vrancea	1,500	2.0	7.2
6	1979 Apr 15	Montenegro	101	4.5	7
7	1980 Nov 23	Italy, southern Campania	4,680	45	7.2
8	1985 Sep 19	Mexico, Michoacan	9,500	5	8.1
9	1986 Oct 10	El Salvador	1,000	1.5	5.5
10	1988 Dec 7	Turkey-USSR border region Spitak, Armenia	25,000	17	7
11	1989 Oct 17	Loma Prieta	63	8	6.9
12	1990 Jun 21	Western Iran, Gilan	40,000	7.2	7.7
13	1990 Jul 16	Luzon, Philippine Islands	1,621	1.5	7.8
14	1994 Jan 17	Northridge	57	30	6.8
15	1995 Jan 16	Japan, Kobe	5,502	82.4	6.9
16	1999 Jan 25	Colombia	1,185	1.5	6.3
17	1999 Aug 17	Turkey	17,118	20	7.6
18	1999 Sep 20	Taiwan	2,297	0.8	7.6

Human losses in Table 4.16 are represented as a function of magnitude in Figure 4.27. In Figure 4.28 human losses are represented versus economic losses, also based on data in Table 4.16. Based on the data given in Table 4.16, the number of deaths from an earthquake can be related to the magnitude of the earthquake by the following relations:

$$D = 0.002 \cdot e^{1.5M} \quad -lower\ bound\ value$$

$$D = 0.06 \cdot e^{1.5M} \quad -median\ value \tag{4.52}$$

$$D = 0.4 \cdot e^{1.5M} \quad -upper\ bound\ value$$

where
D is the number of deaths, and
M is the magnitude of the earthquake.

The economic losses can be related to the number of deaths from an earthquake by the following relations:

$$\lg L = -0.6 + 0.2 \lg D \quad -lower\ bound\ value$$

$$\lg L = 0.06 + 0.2 \lg D \quad -median\ value \tag{4.53}$$

$$\lg L = 0.9 + 0.2 \lg D \quad -upper\ bound\ value$$

where
L are the economic losses expressed in billion US$, and
D is the number of deaths.

The general characteristics of earthquake-induced disasters as well as the general countermeasures for emergency management are presented in Table 4.17.

Reduction of vulnerability to earthquakes is, clearly, an urgent goal for the coming decades. It is, moreover, one that is realizable as policy makers now have many earthquake mitigation options available. These include insurance, construction codes and standards, strengthening and retrofit, demolition of hazardous structures, relocations, sitting and land-use criteria, training and exercises. The key to success will be to integrate risk assessment and risk management as an ongoing strategy aimed at avoidance of flaws in planning, design, sitting, construction and use which create or increase vulnerability.

The main strategies for mitigation of seismic risk are:

i. Regulating, strengthening, or removing unsafe structures
ii. Enhancing critical utility networks and facilities [e.g., redundancy, backup power]
iii. Improving land use planning

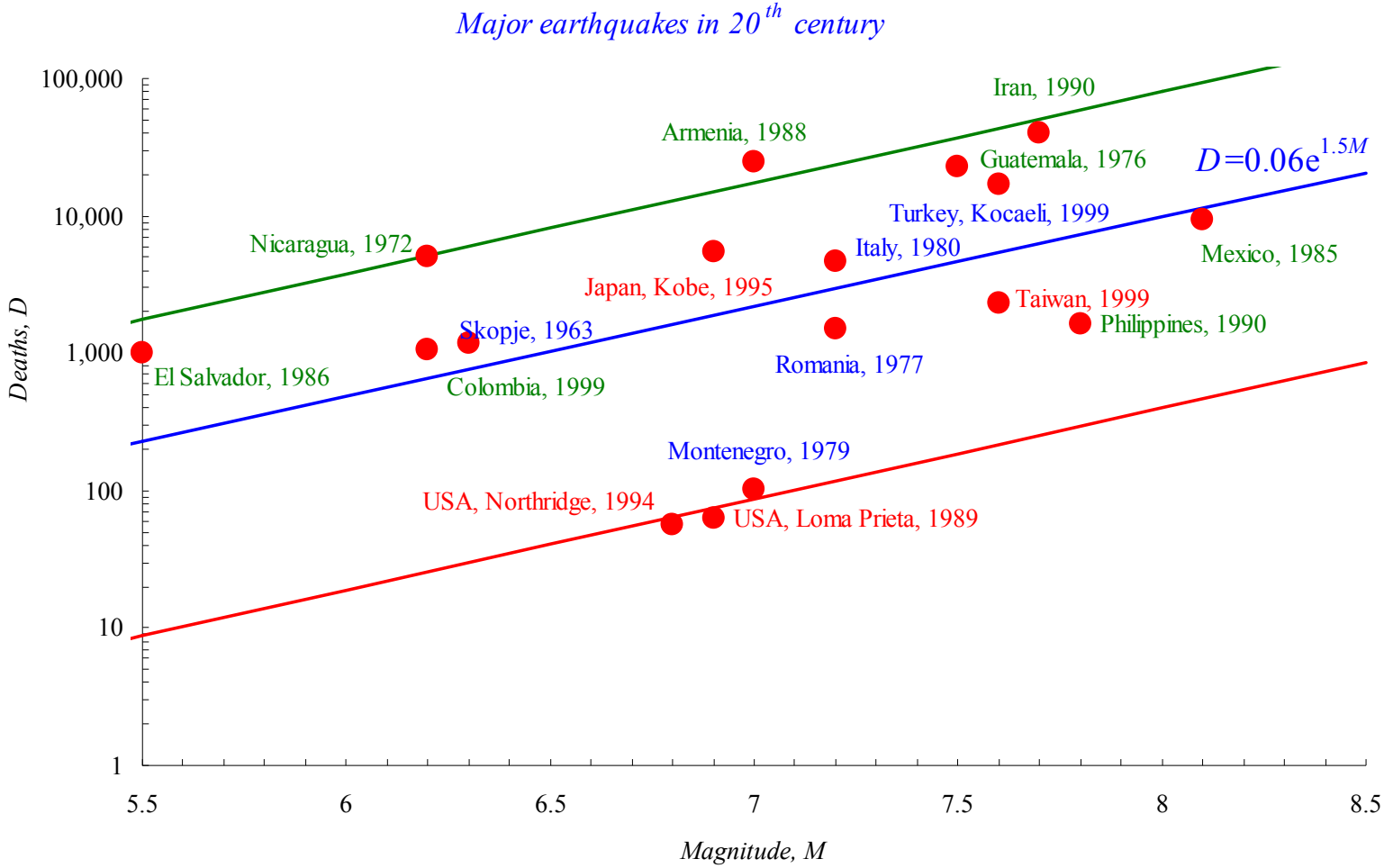

Figure 4.27. Human losses as a function of magnitude

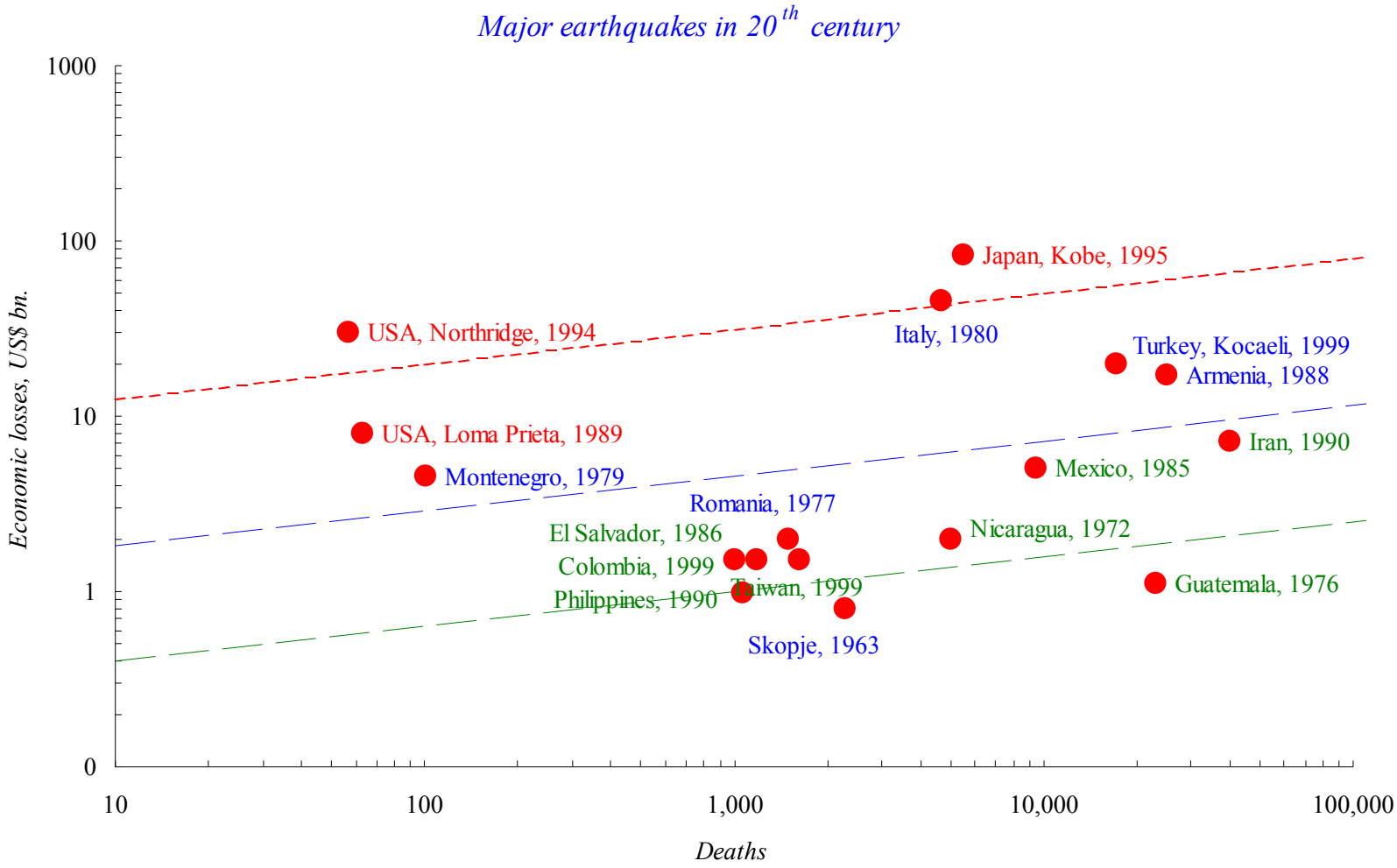

Figure 4.28. Human losses versus economic losses caused by earthquakes

Table 4.17. General characteristics of earthquake disasters, general countermeasures and special problem areas for emergency management

Characteristics	*General counter measures*	*Special problem areas for emergency management*
▪ Usually no warning; following a major earthquake, secondary shocks may give warning of a further earthquake ▪ Onset is sudden ▪ Earthquake-prone areas are generally well identified and well known ▪ Major effects arise mainly from violent ground shacking (vibration), fracture or slippage; especially they include damage (usually very severe) to structures and lifeline systems, plus considerable casualty due to lack of warning.	▪ Development of possible warning indicators ▪ Land-use regulations ▪ Building regulations ▪ Relocation of communities ▪ Public awareness and education programs	▪ Severe and extensive damage, creating the need for urgent counter-measures, especially search and rescue, and medical assistance ▪ Difficulty of access and movement ▪ Widespread loss of or damage to infrastructure, essential services and life support systems ▪ Recovery requirements (e.g. restoration and rebuilding) may be very extensive and costly ▪ Rarity of occurrence in some areas may cause problems for economies of counter-measures and public awareness ▪ Response problems may be severe, extensive and difficult (e.g. rescue from a high occupancy building collapses, or in a circumstances where additionally a chemical or radiation hazard exists, etc.) ▪ Victim identification may often be very difficult

It is the local governments, first of all, that should recognize the risk of disasters within their domain. Decision makers and local government officials have the actual power to make the physical environment resistant against disasters through development policies such as urban

planning, construction of infrastructure, land-use control, and building regulations. If urban infrastructures were to be destroyed by disasters, urban activities would be halted for a long time, severely damaging economic and social activities.

It is the communities and citizens that should recognize the risk of loss of their own houses and lives. They are supposed to build and maintain their houses in good physical condition, while local governments are not able to reinforce a huge number of inappropriately constructed buildings, most of which are owned privately, in developing countries. It is said that earthquakes do not kill people but collapsed buildings and houses do. Unless people take action concerning their existing houses, casualties cannot be reduced by much.

Semi-public companies, which maintain basic urban infrastructures such as the telephone, and water supply, should be prepared for disasters as their disruption could cause serious damage to urban activities. Business leaders and related companies such as building owners, developers, real estate agents, and insurance/reinsurance companies should also understand the seismic risk to their properties, to avoid human loss caused by their collapse and to minimize the damage their businesses.

From experience, it can be said that even if scientists were to lay stress on such seismic risk to local governments, the officials would not take it into account. Only when the government officials can understand the possible damage through their own efforts, are they likely to take the necessary action.

Similarly, although most of the buildings seem highly vulnerable to earthquakes, and although it is obvious that certain houses would be easily destroyed, communities and residents are, in some instances, indifferent to the seismic risk. They will take appropriate action for the reinforcement of their houses only when they understand that they would be killed by their houses or lose their fortunes.

5. INTRODUCTION TO STOCHASTIC PROCESSES

5.1. Background

Physical phenomena of common interest in engineering are usually measured in terms of amplitude versus time function, referred to as a *time history record*. The instantaneous amplitude of the record may represent any physical quantity of interest, for example, displacement, velocity, acceleration, pressure, and so on. There are certain types of physical phenomena where specific time history records of future measurements can be predicted with reasonable accuracy based on one's knowledge of physics and/or prior observations of experimental results, for example, the force generated by an unbalanced rotating wheel, the position of a satellite in orbit about the earth, the response of a structure to a step load. Such phenomena are referred to as *deterministic*, and methods for analyzing their time history records are well known. Many physical phenomena of engineering interest, however, are not deterministic, that is, each experiment produces a unique time history record which is not likely to be repeated and cannot be accurately predicted in detail. Such processes and the physical phenomena they represent are called *random* or *stochastic*. In this case a single record is not as meaningful as a *statistical* description of the totality of possible records.
As just mentioned, a physical phenomenon and the data representing it are considered random hat when a future time history record from an experiment cannot be predicted with reasonable experimental error. In such cases, the resulting time history from a given experiment represents only one physical realization of what might have occurred. To fully understand the data, one should conceptually think in terms of all the time history records that could have occurred, as illustrated in Figure 5.1.

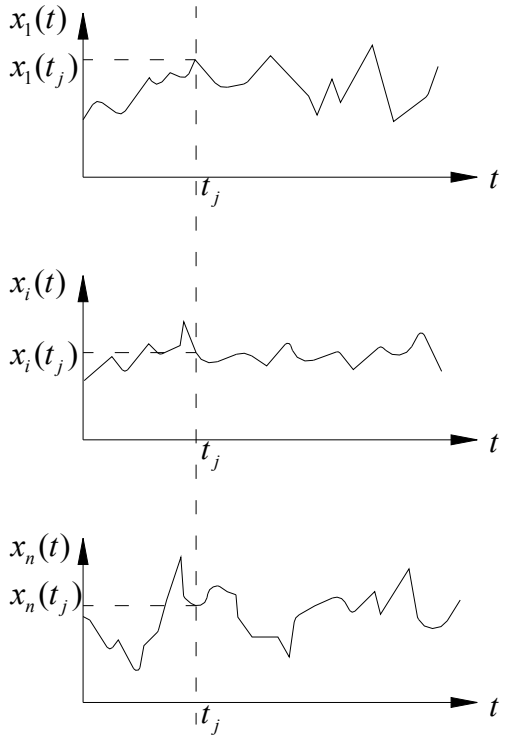

The *ensemble* given by all $x_i(t)$ defines the stochastic process while $x_1(t), x_2(t), ..., x_n(t)$ are the samples.

Figure 5.1. Ensemble of time history records defining a random process

This collection of all time history records $x_i(t)$, i= 1, 2, 3, …, which might have been produced by the experiment, is called the *ensemble* that defines a *random process* $\{x(t)\}$ describing the phenomenon. Any single individual time history belonging to the ensemble is called a *sample* function. Each sample function is sketched as a function of time. The time interval involved is the same for each sample. There is a continuous infinity of different possible sample functions, of which only a few are shown. All of these represent possible outcomes of experiments which the experimenter considers to be performed under identical conditions. Because of variables beyond his control the samples are actually different. Some samples are more probable than others and to describe the random process further it is necessary to give probability information.

5.2. Average properties for describing internal structure of a stochastic process

If one makes a section at t_j one obtains $x_i(t_j)$ that are the values of a *random variable*. Given an ensemble of time history records $\{x(t)\}$ describing a phenomenon of interest, the average properties of the data can be readily computed at any specific time t_j by averaging over the ensemble (theoretically for $n\to\infty$).

The statistical indicators are:

- *the mean*: $m_x(t_j)=\dfrac{\sum_{i=1}^{n} x_i(t_j)}{n}$; (5.1) $m_x(t\ )$ - deterministic function of time
- *the mean square value* $\overline{x^2}(t)$; $\overline{x^2}(t_j)=\dfrac{\sum_{i=1}^{n} x_i^2(t_j)}{n}$ (5.2)
- *the variance* $\sigma_x^2(t_j)$; $\sigma_x^2(t_j)=\dfrac{\sum_{i=1}^{n}\left[x\ (t_j)-m_x(t_j)\right]^2}{n}$ (5.3) $\sigma_x(t_j)=\sqrt{\sigma_x^2(t_j)}$

} time dependent

Considering two different stochastic processes $x(t)$ and $x*(t)$ one may get the same mean and the same variance for both processes (Figure 5.2).

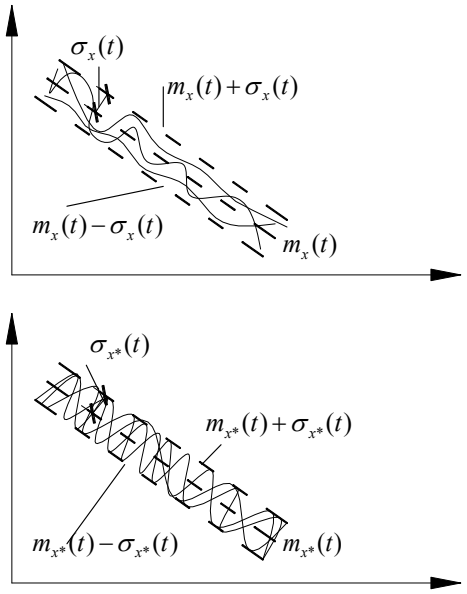

$$\begin{cases} m_x(t)=m_{x^*}(t) \\ \sigma_x(t)=\sigma_{x^*}(t) \end{cases}$$

but $x(t)$ and $x^*(t)$ are different in

Figure 5.2. Two different processes with same mean and same variance

Obviously, the mean and the variance cannot describe completely the internal structure of a stochastic process and additional higher order average values are needed for a complete description.
The average product of the data values at times t_j and t_k called the *correlation function* is given by:

$$\textit{Correlation function: } R_x(t_j,t_k)=\frac{\sum_{i=1}^{n} x_i(t_j)\cdot x_i(t_k)}{n} \tag{5.4}$$

Furthermore, the average product of the data values at times t and $t+\tau$ is called the *autocorrelation* at time delay τ

$$R_x(t,t+\tau)=\frac{\sum_{i=1}^{n} x_i(t)\cdot x_i(t+\tau)}{n} \tag{5.5}$$

$$\text{If } \tau=0 \Rightarrow R_x(t,t)=\overline{x^2}(t). \tag{5.6}$$

The covariance function is defined by:

$$K_x(t_j,t_k)=\frac{\sum_{i=1}^{n}\left[x_i(t_j)-m_x(t_j)\right]\left[x_i(t_k)-m_x(t_k)\right]}{n} \tag{5.7}$$

An important property of the variance function is easily obtained by developing the right hand side member of Equation (5.7):

$$K_x(t_j,t_k)=\frac{\sum_{i=1}^{n}\left[x_i(t_j)\cdot x_i(t_k)\right]}{n}-m_x(t_k)\cdot\frac{\sum_{i=1}^{n}x_i(t_j)}{n}-m_x(t_j)\cdot\frac{\sum_{i=1}^{n}x_i(t_k)}{n}+m_x(t_j)\cdot m_x(t_k)\Rightarrow$$

$$K_x(t_j,t_k)=R_x(t_j,t_k)-m_x(t_j)\cdot m_x(t_k) \tag{5.8}$$

$$\text{If } t_j=t_k=t \Rightarrow \sigma_x^2(t)=\overline{x^2}(t)-m_x^2(t). \tag{5.9}$$

5.3. Main simplifying assumptions

The following assumptions greatly reduce the computational effort and enable the development of analytical solutions in random processes theory.

Stationarity: A random process is said to be *stationary* if its probability distributions are invariant under a shift of the time scale; i.e., the family of probability densities applicable now also applies 10 minutes from now or 3 weeks from now. This implies that all the averages are constants independent of time. Then, the autocorrelation function depends only of the time lag between t_j and t_k.
For stationary data, the average values at all times can be computed from appropriate ensemble averages at a single time t (Figure 5.3).

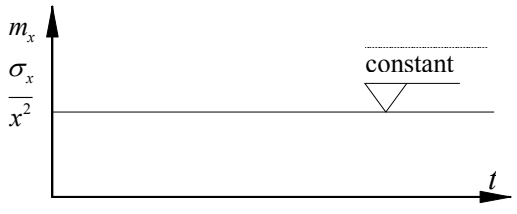

Figure 5.3. Statistical properties of stationary random processes

It is possible to partially verify the stationary assumption experimentally by obtaining a large family of sample functions and then calculating averages such as the mean and autocorrelation for many different times. If the stationary hypothesis is warranted there should be substantial agreement among the results at different times.
For a process to be strictly stationary it can have no beginning and no end. Each sample must extend from $t = -\infty$ to $t = -\infty$. Real processes do in fact start and stop and thus cannot be truly stationary. The nonstationary effects associated with starting and stopping are often neglected in practice if the period of stationary operation is long compared with the starting and stopping intervals. If changes in the statistical properties of a process occur slowly with time, it is sometimes possible to subdivide the process in time into several processes of shorted duration, each of which may be considered as reasonably stationary.

Ergodicity: All the averages discussed so far have been ensemble averages. Given a single sample $x(t)$ of duration T it is, however, possible to obtain averages by averaging with respect time *along the sample*. Such an average is called a *temporal average* in contrast to the ensemble averages described previously.
Within the subclass of *stationary* random processes there exists a further subclass known as *ergodic* processes. An *ergodic* process is one for which ensemble averages are equal to the corresponding temporal averages taken along any representative sample function.
For almost all stationary data, the average values computed over the ensemble at time t will equal the corresponding average values computed over time form a single time history record (theoretically, infinitely long - $T\to\infty$ - practically, long enough). For example, the average values may be computed in most cases by:

$$m_x = \frac{1}{T}\int_0^T x(t)dt \tag{5.10}$$

$$\overline{x^2} = \frac{1}{T}\int_0^T x^2(t)dt \tag{5.11}$$

$$\sigma_x^2 = \frac{1}{T}\int_0^T [x(t)-m_x]^2 dt \Longrightarrow \sigma_x^2 = \frac{1}{T}\int_0^T \left[x^2(t) - 2m_x \cdot x(t) + m_x^2\right]dt \Longrightarrow$$

$$\sigma_x^2 = \underbrace{\frac{1}{T}\int_0^T x^2(t)dt}_{x^2} - \underbrace{2\frac{m_x}{T}\int_0^T x(t)dt}_{2m_x^2} + \underbrace{\frac{m_x^2}{T}\int_0^T dt}_{m_x^2} \Longrightarrow \sigma_x^2 = \overline{x}^2 - m_x^2 \tag{5.12}$$

where $x(t)$ is any arbitrary record from the ensemble $\{x(t)\}$.
The *autocorrelation function* becomes (Figure 5.4):

$$R_x(\tau) = \frac{1}{T}\int_0^T x(t)\cdot x(t+\tau)dt \tag{5.13}$$

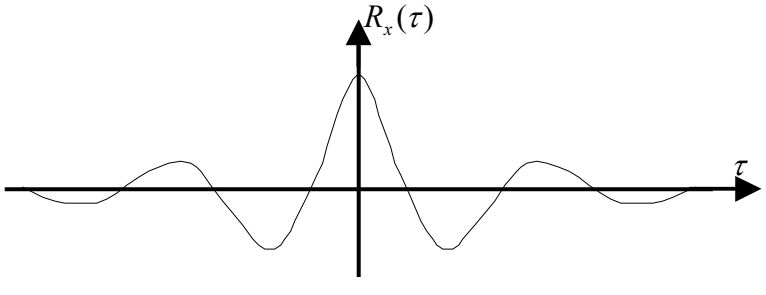

Figure 5.4. Autocorrelation function for a stationary stochastic process

For $\boxed{\tau = 0 \Rightarrow R_x(0) = \overline{x^2}}$ (5.14)

The autocorrelation function is a non-increasing symmetric function with respect to the time origin:

$$\begin{aligned} &R_x(\tau) = R_x(-\tau) \\ &R_x(\tau) \le R_x(0) = \overline{x^2} \end{aligned} \tag{5.15}$$

Sometimes one uses instead of $R_x(\tau)$, $\rho_x(\tau) = \dfrac{R_x(\tau)}{\overline{x^2}}$ (5.16)

that is the *normalized autocorrelation* function ($\rho_x(0) = 1$).

Auto covariance function is defined as:

$$K_x(\tau) = \frac{1}{T}\int_0^T [x(t) - m_x][x(t+\tau) - m_x]dt \tag{5.17}$$

Developing (17) one gets:

$$K_x(\tau) = R_x(\tau) - \frac{m_x}{T}\int_0^T x(t+\tau)dt - \frac{m_x}{T}\int_0^T x(t)dt + \frac{m_x^2}{T}\int_0^T dt \Rightarrow$$

$$\boxed{K_x(\tau) = R_x(\tau) - m_x^2} \tag{5.18}$$

$$\text{If } \tau = 0 \Rightarrow \begin{cases} K_x(0) = \sigma_x^2 \\ \sigma_x^2 = \overline{x^2} - m_x^2 \end{cases} \tag{5.19}$$

The justification for the above results comes from the *ergodic theorem* (Yaglom, 1962, Papoulis, 1977), which states that, for stationary data, the properties computed from time averages over individual records of the ensemble will be the same from one record to the next and will equal the corresponding properties computed from an ensemble average over the records at any time *t* if

$$\frac{1}{T}\int_{-T}^{T} \left| R_{xx}(\tau) - \mu_x^2 \right| d\tau \to 0 \qquad \text{as } T \to \infty. \tag{5.20}$$

In practice, violations of Equation 5.20 are usually associated with the presence of periodic components in the data. Equation 5.20 is a sufficient but not a necessary condition for ergodicity, which means that the time averages are often justified even when periodic components are present or other violations of Equation 5.20 occur; one simply must be more careful in such cases to confirm that the time averaged properties of different records are the same.

In conclusion, for stationary ergodic processes, the ensemble is replaced by one representative function, thus the ensemble averages being replaced by temporal averages, Figure 5.5.

An ergodic process is necessarily stationary since the temporal average is a constant while the ensemble average is generally a function of time at which the ensemble average is performed except in the case of stationary processes. A random process can, however, be stationary without being ergodic. Each sample of an ergodic process must be completely representative for the entire process.

It is possible to verify experimentally whether a particular process is or is not ergodic by processing a large number of samples, but this is a very time-consuming task. On the other hand, a great simplification results if it can be assumed ahead of time that a particular process is ergodic. All statistical information can be obtained from a single sufficiently long sample. In situations where statistical estimates are desired but only one sample of a stationary process

is available, it is common practice to proceed on the *assumption* that the process is ergodic. These initial estimates can then be revised when if further data become available.

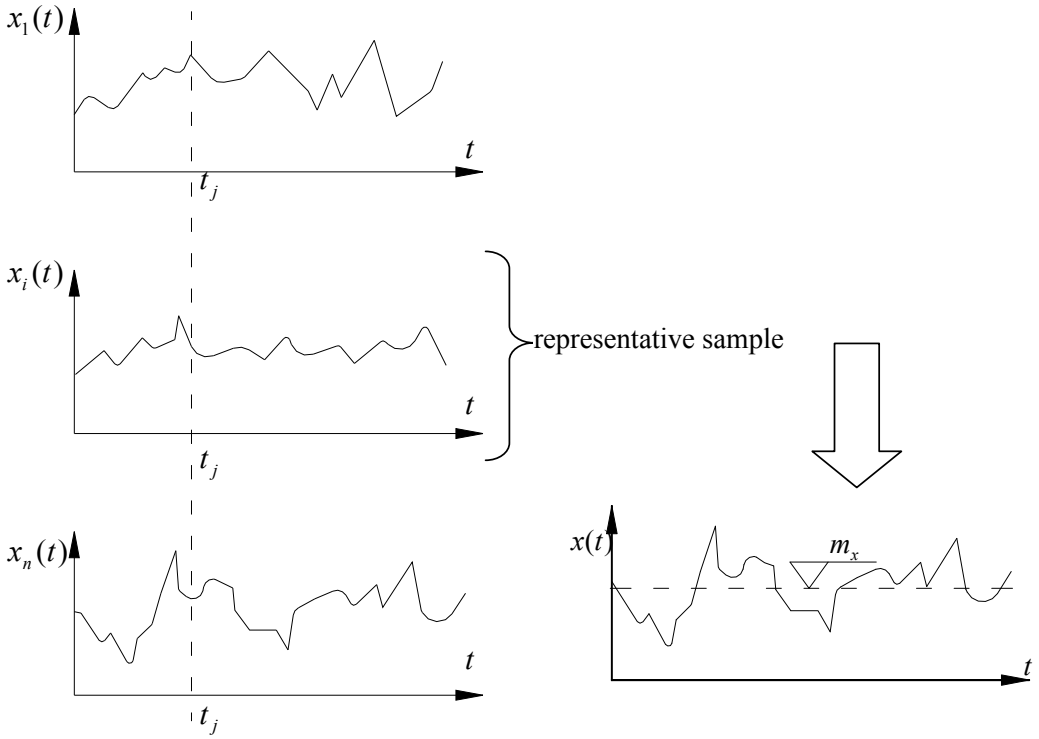

Figure 5.5. Representative sample for a stationary ergodic stochastic process

Zero mean: It is very convenient to perform the computations for *zero mean* stochastic processes. Even if the stationary stochastic process is not *zero mean*, one can perform a translation of the time axis with the magnitude of the mean value of the process (Figure 5.6). In the particular case of *zero mean* stochastic processes, the following relations hold true:

$$R_x(0) = \overline{x^2} = \sigma_x^2 + \underbrace{m_x^2}_{0} = \sigma_x^2 \tag{5.21}$$

$$K_x(\tau) = R_x(\tau) - \underbrace{m_x^2}_{0} = R_x(\tau) \tag{5.22}$$

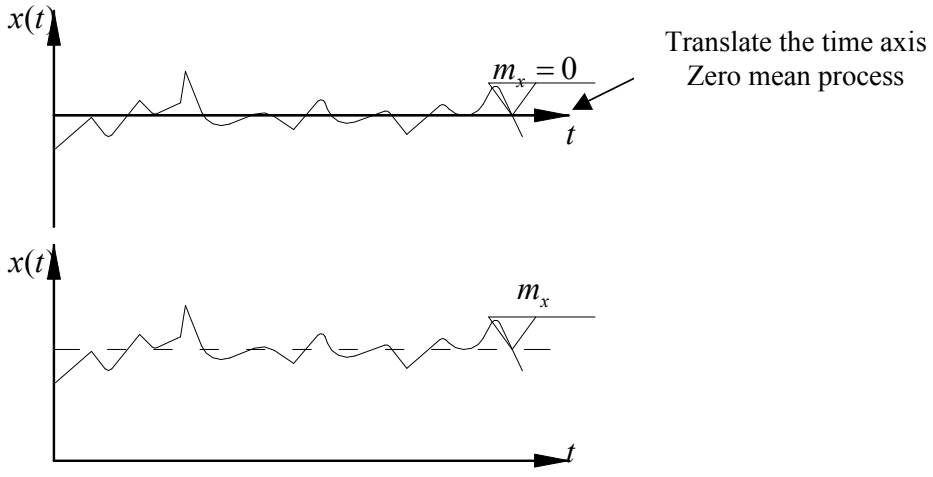

Figure 5.6. *Zero mean stationary ergodic* stochastic process

Normality (*Gaussian*)*:* Before stating the normality assumption, some considerations will be given to probability distribution of stochastic processes.

5.4. Probability distribution

Referring again to the ensemble of measurements, assume there is a special interest in a measured value at some time t_1 that is ξ units or less, that is, $A=x(t_1)\leq \xi$. It follows that the probability of this occurrence is

$$\text{Prob}\left[x(t_1)\leq \xi\right]=\lim_{N\to\infty}\frac{N\left[x(t_1)\leq \xi\right]}{N} \tag{5.23}$$

where $N[x(t_1)\leq \xi]$ is the number of measurements with an amplitude less than or equal to ξ at time t_1. The probability statement in Equation 5.23 can be generalized by letting the amplitude ξ take on arbitrary values, as illustrated in Figure 5.7. The resulting function of ξ is the *probability cumulative distribution function*, *CDF* of the random process $\{x(t)\}$ at time t_1, and is given by

$$F_x(x,t_1)=\text{Prob}\left[x(t_1)\leq \xi\right] \tag{5.24}$$

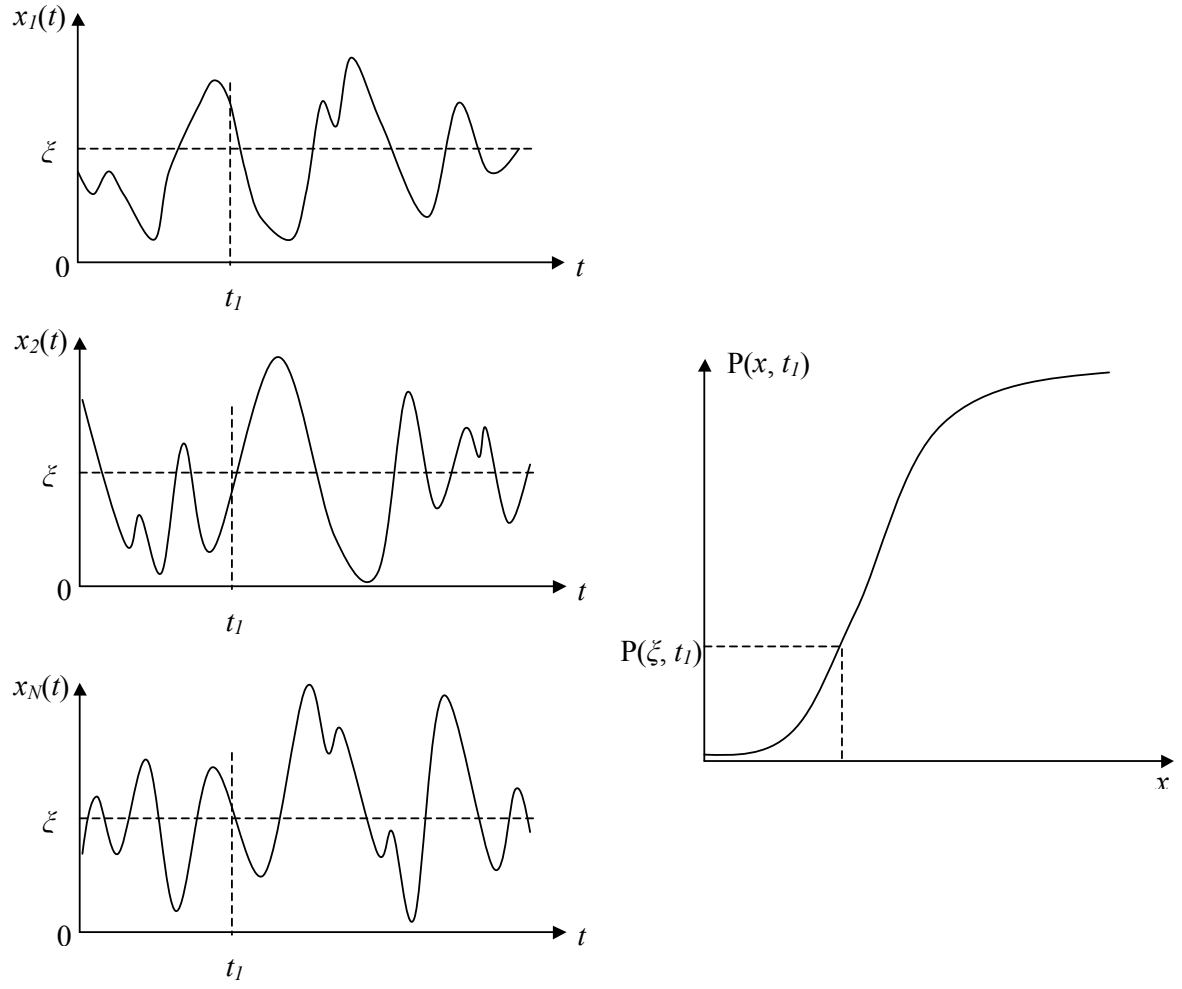

Figure 5.7. General probability distribution function

The probability distribution function then defines the probability that the instantaneous value of $\{x(t)\}$ from a future experiment at time t_1 will be less than or equal to the amplitude ξ of interest. For the general case of nonstationary data, this probability will vary with the time t_1.
For the special case of stationary ergodic data, the probability distribution function will be the same at all times and can be determined from a single measurement $x(t)$ by

$$F_X(x) = \text{Prob}[x(t) \le \xi] = \lim_{T\to\infty} \frac{T[x(t_1) \le \xi]}{T} \tag{5.25}$$

where $T[x(t) \le \xi]$ is the total time that $x(t)$ is less than or equal to the amplitude ξ, as illustrated in Figure 5.8.
In this case, the probability distribution function defines the probability that the instantaneous value of $x(t)$ from a future experiment at an arbitrary time will be less than or equal to any amplitude ξ of interest.

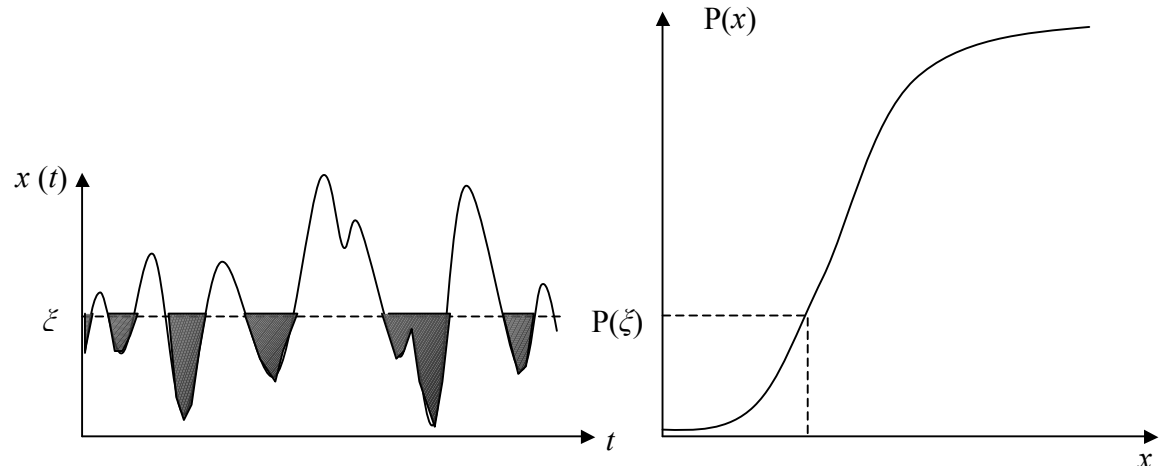

Figure 5.8. Probability distribution function of stationary data

There is a very special theoretical process with a number of remarkable properties one of the most remarkable being that in the stationary case the spectral density (or autocorrelation function) does provide enough information to construct the probability distributions. This special random process is called the *normal random process*. Aside from its analytical advantages the normal process has great importance as a model for real physical processes.

Many random processes in nature which play the role of excitations to vibratory systems are at least approximately normal. This observation is made plausible by the *central limit theorem*. With some restrictions, an interpretation of the central limit theorem is that a random process will be approximately normal if each of its sample functions can be considered to have been generated by the superposition of a large number of independent random sources, none single one of which contributed significantly.

Thus the *normal* (*Gaussian*) assumption implies that the probability distribution of all ordinates of the stochastic process follows a normal (Gaussian) distribution (Figure 5.9).
A very important property of the normal or Gaussian process is its behavior with respect to linear systems. When the excitation of a linear system is a normal process the response will be in general a very different random process but *it will still be normal*.

5.5. Statistical sampling considerations

The number of time history records that might be available for analysis by ensemble averaging procedures, or the length of a given sample record available for analysis by time averaging procedures, will always be finite; that is, the limiting operations $n \to \infty$ and $T \to \infty$ can never be realized in practice. It follows that the average values of the data can only be estimated and never computed exactly. The resulting error in the computation of an average value due to these finite sampling considerations is of major importance to the interpretations and applications of the analyzed data.

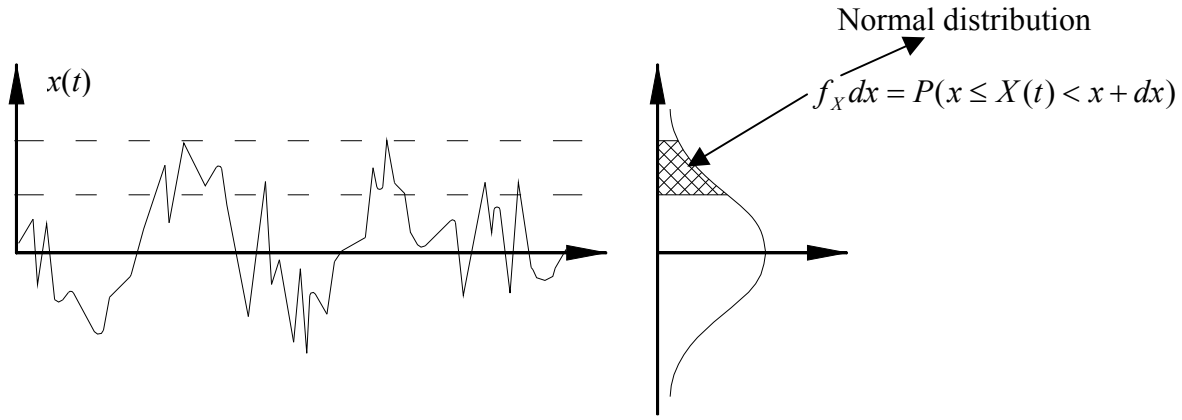

Figure 5.9. *Normal zero mean stationary ergodic* stochastic process

5.6. Other practical considerations

Every effort is usually made in practice to design experiments that will produce stationary data because the necessary analysis procedures for nonstationary data are substantially more difficult. In most laboratory experiments, one can usually force the results of the experiment to be stationary by simply maintaining constant experimental conditions.
In many field experiments as well, there is no difficulty in performing the experiments under constant conditions to obtain stationary data. There are, however, some exceptions. One class of exceptions is when the nature of the experiment requires the mechanisms producing the data of interest to be time dependent. Examples include the vibration of a spacecraft structure during launch. In this case, the experiments can hypothetically be repeated to obtain the ensemble of records that properly represents the nonstationary phenomenon of concern. A second and more difficult class of exceptions is where the basic parameters of the mechanisms producing the data are acts of nature that cannot be controlled by the experimenter. Examples include time history data for seismic ground motions, atmospheric gust velocities and ocean wave heights. In these cases, one cannot even design repeated experiments that would produce a meaningful ensemble. You simply take what you get. The usual approach in analyzing such data is to select from the available records quasistationary segments that are sufficiently long to provide statistically meaningful results for the existing conditions.

6. FOURIER SERIES AND TRANSFORMS

A brief review is given here of some basic Fourier series and Fourier transforms relationships. More detailed discussions are available from the many textbooks on this subject.

6.1. Fourier series

Consider any periodic record $x(t)$ of period T. Then for any value of t

$$x(t) = x(t \pm kT) \qquad k = 1, 2, 3, \ldots \tag{6.1}$$

The fundamental frequency f_1 satisfies

$$f_1 = \frac{1}{T} \tag{6.2}$$

Such periodic data can be expanded in a *Fourier series* according to the following formula:

$$x(t) = \frac{a_0}{2} + \sum_{k=1}^{\infty} \left(a_k \cos 2\pi f_k t + b_k \sin 2\pi f_k t \right) \tag{6.3}$$

where

$$f_k = k f_1 = \frac{k}{T} \qquad k = 1, 2, 3, \ldots \tag{6.4}$$

Thus $x(t)$ is described in terms of sine and cosine waves at discrete frequencies spaced $\Delta f = f_1$ apart. The coefficients $\{a_k\}$ and $\{b_k\}$ are computed by carrying out the following integrations over the period T, say from $(-T/2)$ to $(T/2)$ or from zero to T, that is,

$$a_k = \frac{2}{T} \int_0^T x(t) \cos 2\pi f_k t \, dt \qquad k = 0, 1, 2, \ldots \tag{6.5}$$

$$b_k = \frac{2}{T} \int_0^T x(t) \sin 2\pi f_k t \, dt \qquad k = 1, 2, 3, \ldots \tag{6.6}$$

Note that

$$\frac{a_0}{2} = \frac{1}{T} \int_0^T x(t) dt = \mu_x \tag{6.7}$$

where μ_x is the mean value of $x(t)$. Equations 6.3 to 6.6 are well known and can be put into other equivalent forms using $\omega = 2\pi f$ and $d\omega = 2\pi \, df$ in place of f.

Two alternate Fourier series formulas are also commonly used that follow directly from trigonometric and complex-valued relations. The first such formula is

$$x(t) = X_0 + \sum_{k=1}^{\infty} X_k \cos(2\pi f_k t - \theta_k) \tag{6.8}$$

where

$$X_0 = \frac{a_0}{2} \tag{6.9}$$

$$X_k = \sqrt{a_k^2 + b_k^2} \qquad k = 1, 2, 3, \ldots \tag{6.10}$$

$$\theta_k = \tan^{-1}\left(\frac{b_k}{a_k} \right) \tag{6.11}$$

Here, $x(t)$ is expressed in a polar form rather that a rectangular form using amplitude factors $\{X_k\}$ and phase factors $\{\theta_k\}$ at the discrete frequencies f_k. The second formula is

$$x(t) = \sum_{k=-\infty}^{\infty} A_k e^{i2\pi f_k t} \tag{6.12}$$

where

$$A_0 = \frac{a_0}{2} \tag{6.13}$$

$$A_k = \frac{1}{2}(a_k - ib_k) = \frac{1}{T}\int_0^T x(t) e^{-i2\pi f_k t}\, dt \qquad k = \pm 1, \pm 2, \pm 3, \ldots \tag{6.14}$$

This result is based on *Euler's relation* given by

$$e^{-i\theta} = \cos\theta - i\sin\theta \tag{6.15}$$

Even though $x(t)$ may be real valued, it can be expressed in a theoretical complex-valued form using negative as well as positive frequency components. In particular, the factors $\{A_k\}$ will be complex valued with

$$A_k = |A_k| e^{-i\theta_k} \quad k = \pm 1, \pm 2, \pm 3, \ldots \tag{6.16}$$

where

$$|A_k| = \frac{1}{2}\sqrt{a_k^2 + b_k^2} = \frac{X_k}{2} \tag{6.17}$$

$$\theta_k = \tan^{-1}\left(\frac{b_k}{a_k}\right) \tag{6.18}$$

6.2. Fourier transforms

Suppose the record $x(t)$ is nonperiodic as occurs from stationary random processes or transient processes (deterministic or random). The previous Fourier series representations can be extended by considering what happens as T approaches infinity. This leads to the Fourier integral

$$X(\omega) = \int_{-\infty}^{\infty} x(t) e^{-i\omega t}\, dt \quad -\infty < \omega < \infty \tag{6.19}$$

where $X(\omega)$ will exist if

$$\int_{-\infty}^{\infty} |x(t)|\, dt < \infty \tag{6.20}$$

The quantity $X(\omega)$ defined by Equation 6.19 is called the *direct Fourier transform* (or spectrum) of $x(t)$. Conversely, if $X(\omega)$ is known, then the *inverse Fourier transform* of $X(\omega)$ will give $x(t)$ by the formula

$$x(t) = \frac{1}{2\pi}\int_{-\infty}^{\infty} X(\omega) e^{i\omega t}\, d\omega \qquad -\infty < t < \infty \tag{6.21}$$

The associated $x(t)$ and $X(\omega)$ in Equations 6.19 and 6.21 are said to be *Fourier transform pairs*. Notice that $X(\omega)$ is generally a complex-valued function of both positive and negative frequencies, even when $x(t)$ is real valued. In terms of real and imaginary parts,

$$X(\omega) = X_R(\omega) - iX_I(\omega) \tag{6.22}$$

where

$$X_R(\omega) = |X(\omega)|\cos\theta(\omega) = \int_{-\infty}^{\infty} x(t)\cos\omega t\, dt \tag{6.23}$$

$$X_I(\omega) = |X(\omega)| \sin\theta(\omega) = \int_{-\infty}^{\infty} x(t) \sin \omega t dt \tag{6.24}$$

6.3. Finite Fourier transforms

For a stationary random time history record $x(t)$, which theoretically exists over all time, the integral

$$\int_{-\infty}^{\infty} |x(t)| dt = \infty \tag{6.25}$$

Hence its Fourier transform as given by Equation 6.19 will *not* exist. However, one cannot measure in the field or in the laboratory any $x(t)$ only over some finite time interval T so that $X(\omega)$ is estimated by computing the *finite Fourier transform*

$$X_T(\omega) = X(\omega, T) = \int_0^T x(t) e^{-i\omega t} dt \tag{6.26}$$

Such finite Fourier transforms will *always* exist for finite length records of stationary random processes.

At the discrete frequencies $f_k = (k/T)$, the finite Fourier transform yields

$$X(f_k, T) = TA_k \qquad k = \pm 1, \pm 2, \pm 3, \ldots \tag{6.27}$$

Hence if f is restricted to take on only these discrete frequencies, then the finite Fourier transform calculations will actually produce a Fourier series of period T. For digital processing of data, this is precisely what occurs.

To be specific, one should be aware of digital procedures. When $x(t)$ is sampled at points Δt apart, the record length becomes $T = N\Delta t$, where N is the sample size. This automatically induces a Nyquist cutoff frequency $f_c = (1/2\Delta t)$. Also, the computations treat the data as if they were periodic data of period T. Hence the fundamental frequency is $f_1 = (1/T)$ and results are obtained only at discrete frequencies spaced $\Delta f = f_1$ apart. The continuous record $x(t)$ is replaced by the data sequence $\{x_n\} = \{x(n\Delta t)\}$ for $n = 1, 2, 3, \ldots, N$, and the continuous Fourier transform sequence $X(f)$ is replaced by the discrete Fourier transform sequence $\{X_k\} = \{X(n\Delta f)\}$ for $k = 1, 2, 3, \ldots, N$. Values beyond $k = (N/2)$ can be computed from earlier values since $f_c = (N/2)\Delta f$. The appropriate Fourier transform pair formulas are

$$X_k = X(k\Delta f) = \Delta t \sum_{n=1}^{N} x_n \exp\left(-i2\pi \frac{kn}{N}\right) \qquad k = 1, 2, 3, \ldots, N \tag{6.28}$$

$$x_n = x(n\Delta t) = \Delta f \sum_{k=1}^{N} X_k \exp\left(i2\pi \frac{kn}{N}\right) \qquad n = 1, 2, 3, \ldots, N \tag{6.29}$$

A few consequences of these formulas for real-valued sequences $\{x_n\}$ follow. Let X_k^* be the complex conjugate of X_k. Then

$$\begin{aligned}
&X_{-k} = X_k^* && \text{for all } k \\
&X_{N-k} = X_k^* && \text{for } k = 1, 2, 3, \ldots, N/2 \\
&X_{(N/2)+k} = X_{(N/2)-k}^* && \text{for } k = 1, 2, 3, \ldots, N/2 \\
&X_{k+N} = X_k && \text{for all } k \\
&x_{n+N} = x_n && \text{for all } n
\end{aligned} \tag{6.30}$$

Thus x_n is a repetitive function of n modulo N, and X_k is a repetitive function of k modulo N.

6.4. Delta functions

Consider a rectangular-shaped function $f(t)$ with a magnitude $1/w$ and a width w centered at t=0, as shown in Figure 6.1. The equation of this function is

$$f(t)=\begin{cases}\dfrac{1}{w} & -\dfrac{w}{2}\le t\le\dfrac{w}{2}\\ 0 & |t|>\dfrac{w}{2}\end{cases} \tag{6.31}$$

and the area under the function is given by the integral of $f(t)$ as follows:

$$A=\int_{-\infty}^{\infty} f(t)dt=\int_{-w/2}^{w/2}\frac{dt}{w}=\left(\frac{1}{w}\right)w=1 \tag{6.32}$$

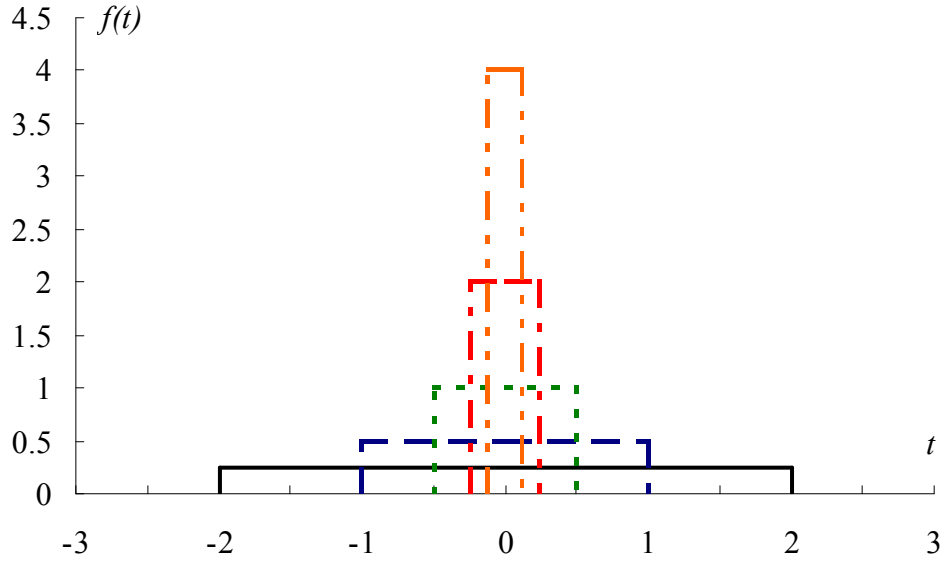

Figure 6.1. Evolution of the delta function

Now let the base of $f(t)$ become increasing small with a corresponding increase in height so as to maintain unity are, as shown in Figure 6.1. In the limit as $w\to 0$, it follows that

$$\delta(t)=\begin{cases}\lim\limits_{w\to 0} f(t)=\infty & t=0\\ 0 & t\neq 0\end{cases} \tag{6.33}$$

but the integral of the function, as given by Equation 6.32, remains unity, that is,

$$\int_{-\varepsilon}^{\varepsilon}\delta(t)dt=\lim_{w\to 0}\left(\frac{w}{w}\right)=1 \tag{6.34}$$

where ε is an arbitrarily small value.

Limiting functions of this type are called *Delta* (*Dirac*) *functions* and are denoted by $\delta(t)$. Delta functions can be positioned at any point t_0 and can have any area A using the notation $A\delta(t\text{-}t_0)$. Specifically,

$$A\delta(t-t_0)=\begin{cases}\infty & t=t_0\\ 0 & t\neq t_0\end{cases} \tag{6.35}$$

$$\int_{t_0-\varepsilon}^{t_0+\varepsilon} A\delta(t-t_0)dt=A \tag{6.36}$$

Furthermore, when any analytic function $x(t)$ is multiplied by a delta function $\delta(t-t_0)$ and integrated, the result is the value of $x(t)$ at $t=t_0$, that is

$$\int_{-\infty}^{\infty} x(t)\delta(t-t_0)dt = x(t_0) \tag{6.37}$$

Thus the delta function can help pick out particular values of $x(t)$ at $t=t_0$.
The direct Fourier transform $X(f)$ associated with a delta function $\delta(t)$ is given by

$$X(f) = \int_{-\infty}^{\infty} \delta(t)e^{-i2\pi ft}dt = 1 \qquad \text{for all } f \tag{6.38}$$

The inverse Fourier transform relation gives

$$x(t) = \int_{-\infty}^{\infty} X(f)e^{i2\pi ft}df = \int_{-\infty}^{\infty} e^{i2\pi ft}df = \delta(t) \tag{6.39}$$

Table 6.1. Special Fourier transform pairs

$x(t)$	$X(f)$
1	$\delta(f)$
$e^{i2\pi fot}$	$\delta(f-f_0)$
$x(t-t_0)$	$X(f)\ e^{-i2\pi fto}$

7. POWER SPECTRAL DENSITY (PSD) FUNCTION OF A STATIONARY ERGODIC RANDOM FUNCTION

7.1. Background and definitions

Returning to random processes one recalls that for stationary processes the autocorrelation function $R(\tau)$ was a function of the interval $\tau = t_2 - t_1$. A frequency decomposition of $R(\tau)$ can be made in the following way

$$R_x(\tau) = \int_{-\infty}^{+\infty} S_x(\omega) \cdot e^{i\omega r} d\omega \tag{7.1}$$

where $S_x(\omega)$ is essentially (except for the factor 2π) the Fourier transform of $R(\tau)$

$$S_x(\omega) = \frac{1}{2\pi} \int_{-\infty}^{+\infty} R_x(\tau) \cdot e^{-i\omega\tau} d\tau \tag{7.2}$$

$S_x(\omega)$ is a *non-negative*, *even* function of ω.
A physical meaning can be given to $S_x(\omega)$ by considering the limiting case of Equation 7.1 in which $\tau = 0$

$$R_x(0) = \overline{x^2} = \int_{-\infty}^{+\infty} S_x(\omega) d\omega \tag{7.3}$$

The *mean square* of the process equals the sum over all frequencies of $S_x(\omega)d\omega$ so that $S_x(\omega)$ can be interpreted as *mean square spectral density* (or *power spectral density*, *PSD*). If the process has *zero mean*, the *mean square* of the process is equal to the *variance* of the process

$$R_x(0) = \int_{-\infty}^{+\infty} S_x(\omega) d\omega = \overline{x^2} = \sigma_x^2 + \underbrace{m_x^2}_{0} = \sigma_x^2 \tag{7.4}$$

The Equations 7.1 and 7.2 used to define the spectral density are usually called the *Wiener – Khintchine* relations and point out that $R_x(\tau), S_x(\omega)$ are a pair of Fourier transforms.

Note that the dimensions of $S_x(\omega)$ are mean square per unit of circular frequency. Note also that according to Equation 7.3 both negative and positive frequencies are counted.
It is like a *random process* is decomposed in a sum of harmonic oscillations of random amplitudes at different frequencies and the variance of random amplitudes is plotted against frequencies. Thus the *power spectral density* **(***PSD***)** is obtained (Figure 7.1). The *power spectral density* function gives the image of the *frequency content* of the stochastic process.

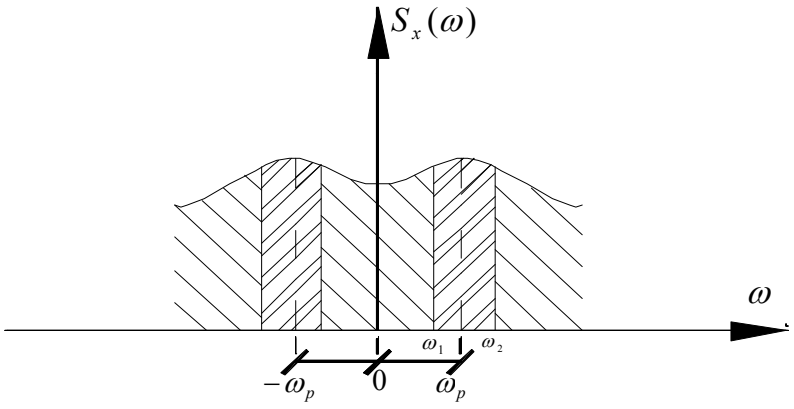

Figure 7.1 Power spectral density function

As one can notice from Equation 7.3 and from Figure 7.1, the area enclosed by the *PSD* function in the range $[\omega_1, \omega_2]$ represents the variance of the amplitudes of the process in that particular range. The predominant frequency of the process, ω_p, indicates the frequency around whom most of the power of the process is concentrated.

The *PSD* so defined is convenient in analytical investigations. In experimental work a different unit of spectral density is widely used. The differences arise owing to the use of *cycles per unit time* in place of radians per unit time and owing to counting *only positive frequencies*. The *experimental spectral density* will be denoted by $G_x(f)$ where f is frequency in *Hz*. The relation between $S_x(\omega)$ and $G_x(f)$ is simply

$$G_x(f) = 4\pi S_x(\omega) \tag{7.5}$$

The factor 4π is made up of a factor of 2π accounting for the change in frequency units and a factor of 2 accounting for the consideration of positive frequencies only, instead of both positive and negative frequencies for an even function of frequency. In place of Equation 7.3 one has

$$R(0) = \sigma_x^2 = \int_{-\infty}^{+\infty} S_x(\omega)d\omega = \int_0^{+\infty} G_x(\omega)d\omega = 2\int_0^{+\infty} S_x(\omega)d\omega = 2\int_0^{+\infty} S_x(\omega)2\pi df = \int_0^{+\infty} G_x(f)df \tag{7.6}$$

for the relation between the variance of the zero-mean process and the experimental *PSD*.

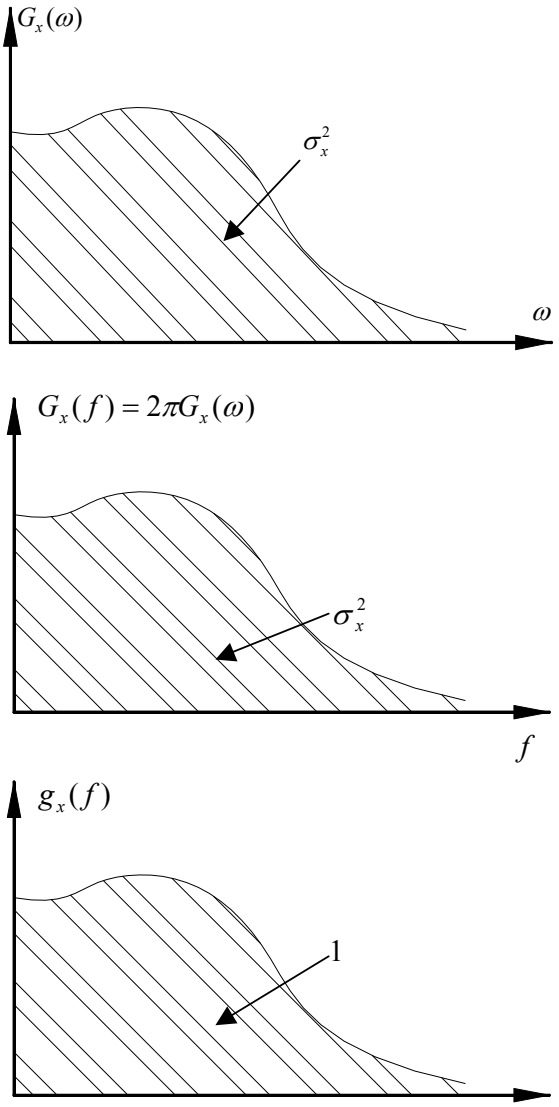

$S_x(\omega)$ - bilateral *PSD*

$G_x(\omega)$ - unilateral *PSD*

$\omega = 2\pi f$

$g_x(f)$ =normalized unilateral *PSD*

$$g_x(f) = \frac{G_x(f)}{\sigma_x^2}$$

Figure 7.2. Various representations of *PSD*

The *PSD* is the Fourier transform of a temporal average (the autocorrelation function) and thus the spectral density of a random process is itself a kind of temporal average and plays the role of a density distribution of the variance along the frequency axis.
It can be shown that for *real* processes the autocorrelation function is an *even* function of τ and that it assumes its peak value at the origin. If the process contains no periodic components then the autocorrelation function approaches zero as $\tau \to \infty$. If the process has a sinusoidal component of frequency ω_0 then the autocorrelation function will have a sinusoidal component of the same frequency as $\tau \to \infty$.
If the process contains no periodic components then *PSD* is finite everywhere. If, however, the process has a sinusoidal component of frequency ω_0 then the sinusoid contributes a finite amount to the total mean square and the *PSD* must be infinite at $\omega=\omega_0$; i.e., the spectrum has an infinitely high peak of zero width enclosing a finite area at ω_0. In particular, if the process does not have zero mean then there is a finite zero frequency component and the spectrum will have a spike at $\omega=0$.
For practical computations, Equations 7.1 and 7.2 become:

$$R_x(\tau) = \int_{-\infty}^{+\infty} S_x(\omega) \cos \omega\tau d\omega \tag{7.7}$$

$$S_x(\omega) = \frac{1}{2\pi} \int_{-\infty}^{+\infty} R_x(\tau) \cos \omega\tau d\tau \tag{7.8}$$

if one uses

$$e^{\pm i\omega t} = \cos \omega t \pm \sin \omega t$$

and keeps just the real parts of the integrands in Equations 7.1 and 7.2.

7.2. Properties of first and second time derivatives

Given a stationary random process $x(t)$, then the random processes $\dot{x}(t) = \frac{d}{dt}[x(t)]$, each of whose sample functions is the temporal derivative of the corresponding sample $x(t)$, and $\ddot{x}(t) = \frac{d^2}{dt^2}[x(t)]$, each of whose sample functions is the temporal second derivative of the corresponding sample $x(t)$, are also stationary random processes. Furthermore, the following relations hold true:

$$R_{\dot{x}}(\tau) = -R_x''(\tau) = -\frac{d^2}{d\tau^2}[R_x(\tau)] \tag{7.9}$$

$$R_{\ddot{x}}(\tau) = R_{\dot{x}}''(\tau) = \frac{d^4}{d\tau^4}[R_x(\tau)] \tag{7.10}$$

Using Equation 7.3 in 7.9 and 7.10, for a zero mean process is follows:

$$\begin{cases} \sigma_{\dot{x}}^2 = \int_{-\infty}^{+\infty} S_{\dot{x}}(\omega) d\omega = \int_{-\infty}^{+\infty} \omega^2 S_x(\omega) d\omega = -R''(0) \\ \sigma_{\ddot{x}}^2 = \int_{-\infty}^{+\infty} S_{\ddot{x}}(\omega) d\omega = \int_{-\infty}^{+\infty} \omega^4 S_x(\omega) d\omega = R''''(0) \end{cases} \tag{7.11}$$

7.3. Frequency content indicators

The frequency content of ground motion is the crucial concept for the understanding of the mechanism of ground motion to damage structures. The maximum values of structure response are when the structure frequency and the major part of the frequency content of ground motion fall in the same frequency band.
The frequency content can be described:
1. Directly, by the power spectral density function (PSD), obtained from stochastic modeling of the acceleration process;
2. Indirectly, by the response spectra obtained from numerical integration of the motion equation for the SDOF structure.
The stochastic measures of frequency content are related to the power spectral density function of stationary segment of the ground motion. They are:
(i) The dimensionless indicator ε (Cartwright & Longuet - Higgins);
(ii) The Kennedy – Shinozuka indicators f_{10}, f_{50} and f_{90} which are fractile frequencies below which 10%, 50% and 90% of the total cumulative power of PSD occur and the frequencies f_1, f_2 and f_3 corresponding to the highest 1,2,3 peaks of the PSD.
To define the frequency content indicators, one has to introduce first the *spectral moment of order "i"*:

$$\lambda_i = \int_{-\infty}^{+\infty} \omega^i S_x(\omega) d\omega \tag{7.12}$$

It follows from Equations 6.4, 7.11 and 7.12 that:

$$\lambda_0 = \int_{-\infty}^{+\infty} S_x(\omega) d\omega = \sigma_x^2 \tag{7.13}$$

$$\lambda_2 = \int_{-\infty}^{+\infty} \omega^2 S_x(\omega) d\omega = \sigma_{\dot{x}}^2 \tag{7.14}$$

$$\lambda_4 = \int_{-\infty}^{+\infty} \omega^4 S_x(\omega) d\omega = \sigma_{\ddot{x}}^2 \tag{7.15}$$

The Cartwright & Longuet-Higgins indicator is:

$$\varepsilon = \sqrt{1 - \frac{\lambda_2^2}{\lambda_0 \cdot \lambda_4}} \tag{7.16}$$

Wide frequency band processes have ε values close to 2/3 and smaller than 0.85. Narrow frequency band seismic-processes of long predominant period (i.e. superposition of a single harmonic process at a short predominant frequency, f_p and a wide band process) are characterized by ε values greater than 0.95.
The *RMS* value of the ground acceleration process is the square root of two-order spectral moment $\lambda_0^{1/2}$ and is very sensitive to the strong motion duration definition.
Cumulative power of the PSD is defined by:

$$\text{Cum } G(\omega_1) = \int_0^{\omega_{cut-off}} \mathrm{G}(\omega)\mathrm{d}\omega \tag{7.17}$$

where the cut-off frequency is the reverse of the double of time interval used in process digitization.

The duration for computing *PSD* of the stationary segment of the acceleration process should be selected as $D = T_{0.9} - T_{0.1}$, where $T_{0.9}$ and $T_{0.1}$ are the times at which 90% and 10% of the total cumulative energy of the accelerogram are reached. Alternative duration definitions are: $D = T_{0.95} - T_{0.05}$ or $D = T_{0.75} - T_{0.05}$.
The Kennedy-Shinozuka indicators are f_{10}, f_{50}, f_{90} and can be defined as:

$$\int_0^{f_{10}} g_x(f)df = 0.1 \tag{7.18}$$

$$\int_0^{f_{50}} g_x(f)df = 0.5 \tag{7.19}$$

$$\int_0^{f_{90}} g_x(f)df = 0.9 \tag{7.20}$$

The physical meaning of the above indicators is that for f_{10} - the area enclosed by the normalized spectral density situated to the left of f_{10} is equal to 10% of the total area.

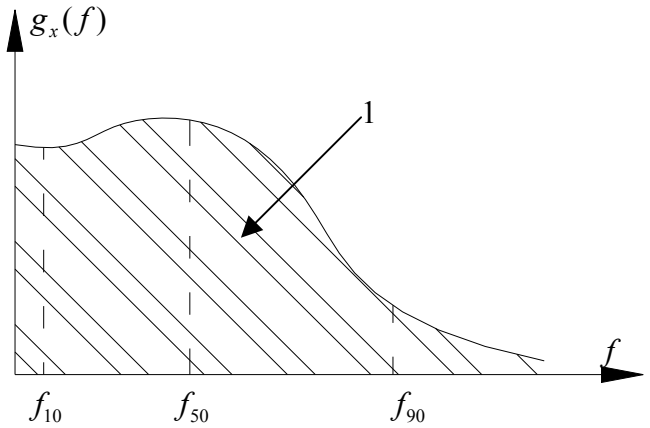

Figure 7.3. Kennedy – Shinozuka indicators

The difference $f_{90} - f_{10}$ gives an indication on the bandwidth of the process.

7.4. Wide-band and narrow-band random process

The *PSD* of a stationary random process is usually an incomplete description of the process but it does constitute a partial description. Here this description is examined for two extreme cases: a wide-band spectrum and a narrow-band spectrum.

7.4.1. Wide-band processes. White noise

A *wide-band* process is a stationary random process whose *PSD* has significant values over a band or range of frequencies which is of roughly the same order of magnitude as the center frequency of the band. A wide range of frequencies appears in representative sample functions of such a process. An example of a wide-band spectrum is displayed in Figure 7.4.

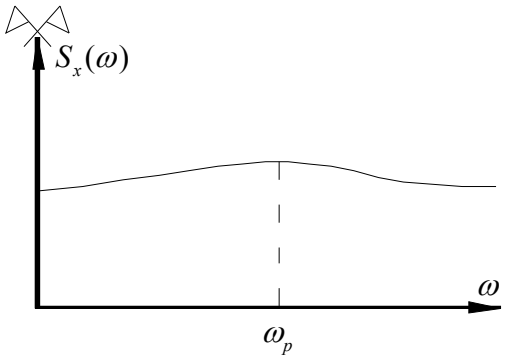

wide band process

Figure 7.4. Example of wide band spectrum

In analytical investigations a common idealization for the spectrum of a wide-band process is the assumption of a *uniform PSD*, S_0 as shown in Figure 7.5. A process with such a spectrum is called *white noise* in analogy with white light which spans the visible spectrum more or less uniformly. *Ideal* white noise is supposed to have a uniform density over *all* frequencies. This is a physically unrealizable concept since the mean square value (equal to the variance for zero-mean processes) of such a process would be *infinite* because there is an infinite area under the spectrum. Nevertheless, the ideal white noise model can sometimes be used to provide physically meaningful results in a simple manner.

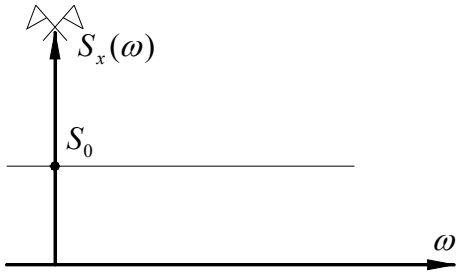

Figure 7.5. Theoretical white noise ($-\infty < \omega < +\infty$) and $\sigma_x^2 \to \infty$

The *band-limited* white noise spectrum shown in Figure 7.6 is a close approximation of many physically realizable random processes.

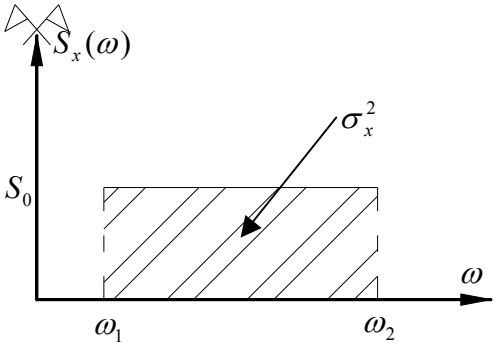

Figure 7.6. Band-limited white noise, $\sigma_x^2 = 2 \cdot S_0(\omega_2 - \omega_1)$

For band-limited white noise the autocorrelation function is, Figure 7.7:

$$R_x(\tau) = \int_{-\infty}^{+\infty} S_x(\omega) \cdot e^{i\omega\tau} d\omega = 2\int_{0}^{+\infty} S_x(\omega) \cdot \cos(\omega\tau) d\omega = 2S_0 \int_{\omega_1}^{\omega_2} \cos(w\tau) d\tau =$$

$$= 2\frac{S_0}{\tau} \sin \omega\tau \Big|_{\omega_1}^{\omega_2} = 2\frac{S_0}{\tau} \left[\sin \omega_2\tau - \sin \omega_1\tau\right] \qquad (7.21)$$

For a wide band process the autocorrelation function is vanishing quickly (~2cycles). Here is a finite variance $\sigma_x^2 = 2 \cdot S_0(\omega_2 - \omega_1)$ and nonzero correlation with the past and the future, at least for short intervals.

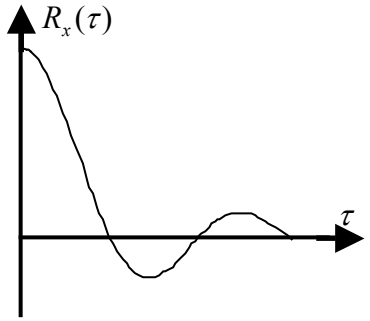

Figure 7.7. Autocorrelation function corresponding to the band-limited white noise spectra

7.4.2. Narrow band processes

A narrow-band process is a stationary random process whose *PSD* has significant values only in a band or range of frequencies whose width is small compared with the magnitude of the center frequency of the band, Figure 7.8. Only a narrow range of frequencies appears in the representative samples of such a process. Narrow-band processes are typically encountered as response variables in strongly resonant vibratory systems when the excitation variables are wide-band processes.
If it can be assumed that the process is *normal* then it is possible to compute the average or expected frequency of the cycles.

7.4.2.1. Expected frequency of narrow-band process

When a stationary normal random process with zero mean has a narrow-band spectrum, the statistical average frequency or expected frequency is ω_0 where:

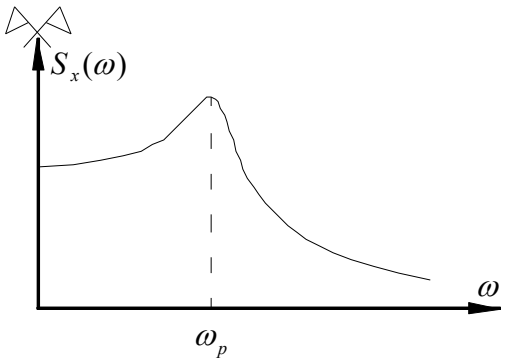

narrow band process

Figure 7.8. Narrow band spectrum

$$\omega_0^2 = \frac{\int_{-\infty}^{\infty} \omega^2 S_x(\omega) d\omega}{\int_{-\infty}^{\infty} S_x(\omega) d\omega} = -\frac{R''(0)}{R(0)} = \frac{\sigma_{\dot{x}}^2}{\sigma_x^2} \tag{7.22}$$

This result is simply stated and has a simple interpretation; i.e., ω_0^2 is simply a weighted average of ω^2 in which the *PSD* is the weighting function. The establishment of this result, by S. O. Rice represented a major advance in the theory of the random processes. Following is a brief outline of the procedure.

Let $x(t)$ be a stationary process and let v_a^+ be the expected frequency of crossing the level $x=a$ with positive slope. It will be seen that for a narrow-band process v_0^+ is just the expected frequency of cycles so that $\omega_0 = 2\pi\, v_0^+$. It is no more difficult to consider a general value of a at this point and set $a = 0$ at the end.

We next consider the geometry involved in a sample function crossing the level $x=a$ during a particular small time interval dt. The situation is sketched in Figure 7.9. All sample functions cross the line $t=t$ but only a small fraction of these cross the line $x=a$ with positive slope $\dot{x}>0$ during the interval dt. Two such samples are indicated in the Figure 7.9. We suppose that dt is so small that the samples can be treated as straight lines in the interval. If a sample crosses $t = t$ with an x value less than a then it will also cross $x=a$ with positive slope during the time dt if its slope $\dot{x}$ at $t = t$ has any value from ∞ down to the limiting value $(a-x)/dt$. Using this statement we can examine each sample at $t = t$ and decide whether or not its combination of x and $\dot{x}$ values will yield a crossing of $x = a$.

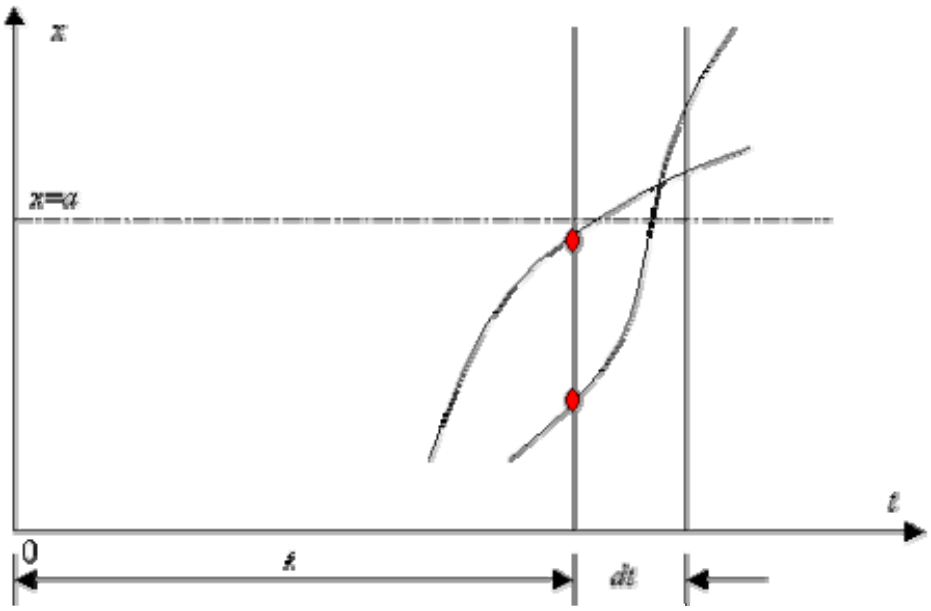

Figure 7.9. Sample functions which cross $x = a$ during the interval dt

If one assumes that $x(t)$ is a stationary normal zero-mean process, one finds the expected number of crossing the level $x=a$ with positive slope:

$$v_a^+ = \frac{1}{2\pi}\frac{\sigma_{\dot{x}}}{\sigma_x}\exp\left(-\frac{a^2}{2\sigma_x^2}\right) \tag{7.23}$$

The standard deviations in Equation 7.23 are obtained from Equations 7.6 and 7.11. Returning to our original problem, we set $a = 0$ in Equation 7.23 to obtain the expected frequency, in crossings per unit time, of zero crossings with positive slope. Finally if the process narrow-band, the probability is very high that each such crossing implies a complete "cycle" and thus the expected frequency, in cycles per unit time, is ν_0^+. It should be emphasized that this result is restricted to normal processes with zero mean.

7.4.2.2. Autocorrelation function of narrow-band processes

For band-limited white noise, Figure 7.10, the autocorrelation function is:

$$R_x(\tau) = \int_{-\infty}^{+\infty} S_x(\omega) \cdot e^{i\omega\tau} d\omega = 2\int_{0}^{+\infty} S_x(\omega) \cdot \cos(\omega\tau) d\omega = 2S_0 \int_{\omega_1}^{\omega_1+\Delta\omega} \cos(w\tau) d\tau =$$

$$= 2\frac{S_0}{\tau} \sin\omega\tau \Big|_{\omega_1}^{\omega_1+\Delta\omega} = 2\frac{S_0}{\tau}\left[\sin(\omega_1+\Delta\omega)\tau - \sin\omega_1\tau\right] \qquad (7.24)$$

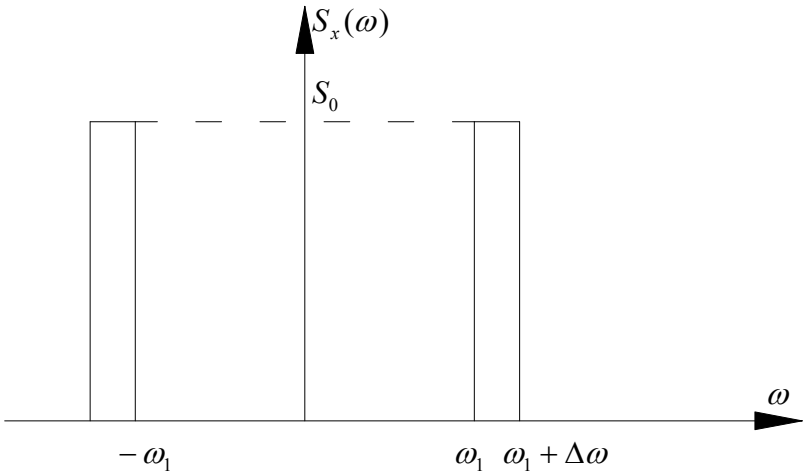

Figure 7.10. Band-limited white noise, $\sigma_x^2 = 2S_0\Delta\omega$

For narrow-band processes, the autocorrelation function is periodically and is vanishing slowly, Figure 7.11.

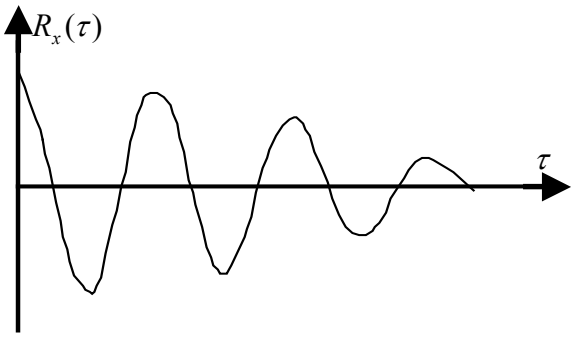

Figure 7.11. Autocorrelation function of narrow-band processes

8. DYNAMIC RESPONSE OF SDOF SYSTEMS TO STOCHASTIC PROCESSES

When attention is focused on the response of structural systems to random vibration it is generally possible to identify an *excitation* or input and a *response* or output. The excitation may be a motion (i.e., acceleration, velocity, or displacement), or a force history. The response may be a desired motion history or a desired stress history. When the excitation is a random process, the response quantity will also be a random process. The central problem of this chapter is the determination of information regarding the response random process from corresponding information regarding the excitation process.
A general solution to this problem for stationary processes is described in the case where the vibratory structure is a linear time-invariant system and explicit solutions are obtained for systems with one degree of freedom.
A vibratory system is said to be linear and time-invariant if its equations of motions take the form of *linear* differential equations with *constant coefficients*. A system with a single degree of freedom can be described by a *single* second-order ordinary differential equation.
The general problem is shown schematically in Figure 8.1. The excitation history is $x(t)$ and the response history is $y(t)$. At present, these are still generalized quantities. In preparation for the case where input and output are both random vibrations we review the case where they are individual particular functions.

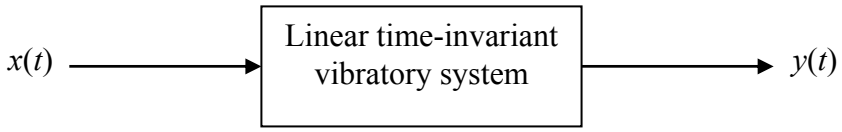

Figure 8.1. Block diagram of excitation-response problem

If $x(t)$ is a specified deterministic time history then it is possible to obtain a specific answer for $y(t)$ by integrating the differential equations of motion, subject to initial conditions.

8.1. Complex frequency response

It is a property of linear time-invariant systems that when the excitation is steady state simple harmonic motion (without beginning or end) then the response is also steady state simple harmonic motion at the same frequency. The amplitude and phase of the response generally depend on the frequency. A concise method of describing the frequency dependence of the amplitude and phase is to give the *complex frequency response* or *transfer function* $H(\omega)$. This has the property that when the excitation is the real part of $e^{i\omega t}$ then the response is the real part of $H(\omega)\ e^{i\omega t}$. The complex transfer function $H(\omega)$ is obtained analytically by substituting

$$x = e^{i\omega t} \tag{8.1}$$

$$y = H(\omega)e^{i\omega t} \tag{8.2}$$

in the equations of motion, canceling the $e^{i\omega t}$ terms, and solving *algebraically* for $H(\omega)$.
Since $H(\omega)$ is essentially an output measure for unit input its dimensions will have the dimensions of the quotient y/x. In complex structures where more than one response is of interest it will be necessary to use subscripts to suitably identify which complex transfer function is being considered.
Knowledge of a transfer function $H(\omega)$ for all frequencies contains all the information necessary to obtain the response $y(t)$ to an arbitrary known excitation $x(t)$. The basis for this remark is the *principle of superposition*, which applies to *linear systems*. The superposition

here is performed *in the frequency domain* using Fourier's method. When $x(t)$ has a period then it can be decomposed into sinusoids forming a Fourier series. The response to each sinusoid, separately, is provided by $H(\omega)$ and these responses form a new Fourier series representing the response $y(t)$. When $x(t)$ is not periodic but has a *Fourier transform*

$$X(\omega) = \int_{-\infty}^{\infty} x(t) e^{-i\omega t} dt \tag{8.3}$$

then an analogous superposition is valid. For each frequency component separately Equations 8.1 and 8.2 yield:

$$Y(\omega) = H(\omega) X(\omega) \tag{8.4}$$

as the Fourier transform of the response $y(t)$. The response itself is given by the *inverse Fourier transform* representation

$$y(t) = \frac{1}{2\pi} \int_{-\infty}^{\infty} Y(\omega) e^{i\omega t} d\omega \tag{8.5}$$

Telescoping Equations 8.3, 8.4 and 8.5 provides a very general input-output relation for a wide class of inputs $x(t)$

$$y(t) = \frac{1}{2\pi} \int_{-\infty}^{\infty} H(\omega) e^{i\omega t} d\omega \int_{-\infty}^{\infty} x(\tau) e^{-i\omega\tau} d\tau \tag{8.6}$$

In principle, knowledge of $H(\omega)$ permits evaluation of Equation 8.6 to give the explicit response $y(t)$ for an arbitrary excitation $x(t)$.

8.2. Impulse response

A general solution for the response of a linear time-invariant system may also be obtained by superposing unit solutions *in the time domain*. If $x(t)$ is the *unit impulse* and has the form

$$x(t) = \delta(t - \tau) \tag{8.7}$$

where $\delta(t\text{-}\tau)$ is the *Dirac* delta function which is zero except at $t=\tau$ where the ordinate is infinite and it encloses *unit* area. In case $x(t)$ represents an *acceleration* history then $\delta(t\text{-}\tau)$ represents the acceleration that accompanies an instantaneous *unit change in velocity*. When $x(t)$ represents a *force* history then $\delta(t\text{-}\tau)$ represents a blow with unit *impulse* in the sense of classical mechanics.

Let the response $y(t)$, of the system in Figure 8.1, to the excitation $\delta(t\text{-}\tau)$ be called the *impulse-response function* $h(t\text{-}\tau)$. It is assumed that $y(t)$ is zero prior to $t=\tau$ so that $h(t\text{-}\tau)$ is obtained by solving the differential equations of motions with $\delta(t\text{-}\tau)$ as the excitation and with zero initial conditions for $t<\tau$. Essentially, $h(t\text{-}\tau)$ is response per unit of *excitation multiplied by time*.

The impulse-response function $h(t\text{-}\tau)$, once obtained, contains all the information necessary to find the response $y(t)$ to an arbitrary known excitation $x(t)$. The basis for this remark is once more the *principle of superposition*. The superposition now is accomplished *in the time domain*. This is illustrated in Figure 8.2 where an arbitrary excitation $x(t)$ is shown divided into differential elements. A typical area element at $t=\tau$ has width $d\tau$ and height $x(\tau)$. This area can be approximated by an impulse of magnitude $x(\tau)d\tau$ applied at $t=\tau$. The response at $t=t$ to this impulse would be

$$[x(\tau) d\tau] h(t - \tau)$$

Then, because of the linearity, the response $y(t)$ due to all such elements in the past of $x(t)$ is given by the following *superposition* or *convolution* integral

$$y(t) = \int_{-\infty}^{t} x(\tau)h(t-\tau)d\tau \tag{8.8}$$

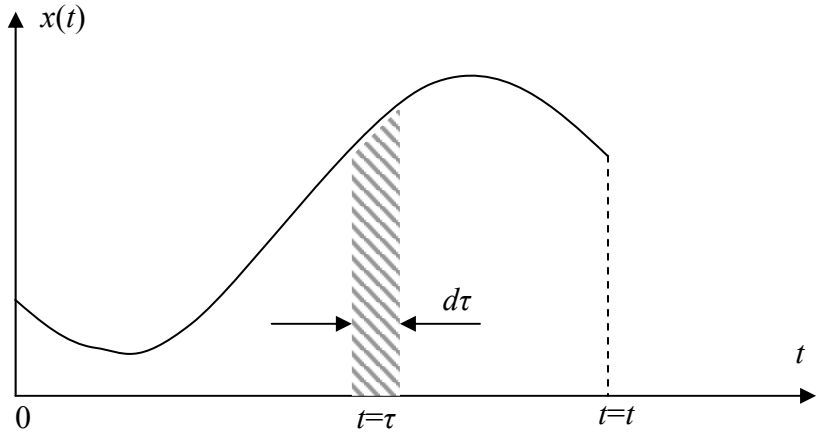

Figure 8.2. Arbitrary excitation $x(t)$ is represented by a sum of infinitesimal impulses of magnitudes $x(\tau)d\tau$ applied at times τ

Furthermore, of one remembers that $h(t-\tau)$ vanishes when $\tau>t$ (i.e., when the response is considered *before* the impulse is applied) then one can replace the upper limit in Equation 8.8 by ∞ without changing the value of the integral

$$y(t) = \int_{-\infty}^{\infty} x(\tau)h(t-\tau)d\tau \tag{8.9}$$

An alternative form of Equation 8.9 may be obtained by changing the integration variable from τ to $\theta = t-\tau$

$$y(t) = \int_{-\infty}^{\infty} x(t-\theta)h(\theta)d\theta \tag{8.10}$$

Either Equation 8.9 or 8.10 provides a general input-output relation giving the explicit response $y(t)$ to an arbitrary known excitation $x(t)$. Thus these superposition integrals accomplish the same purpose as the Fourier integral representation, Equation 8.6.
It is pointed out that $H(\omega)$ is in fact just the Fourier transform of $h(t)$. A simple way to show this is to insert a unit impulse $\delta(\tau)$ for $x(\tau)$ in Equation 8.6. Evaluating the integral one finds

$$h(t) = \frac{1}{2\pi}\int_{-\infty}^{\infty} H(\omega)e^{i\omega t}d\omega \tag{8.11}$$

since in the second integral of Equation 8.6 $x(\tau)$ is zero everywhere except at $\tau = 0$ where it has unit area and since $e^{-i\omega t}$ is also unity at $\tau = 0$ the complete second integral is unity.
Thus, $H(\omega)$ is in fact just the Fourier transform of $h(t)$

$$H(\omega) = \int_{-\infty}^{\infty} h(t)e^{-i\omega t}dt \tag{8.12}$$

8.3. Single degree of freedom (SDOF) systems

To illustrate the preceding ideas one considers now the system shown in Figure 8.3 where a single mass is attached to a moving support by means of a linear rod in parallel with a linear dashpot. One suppose that the motion of the support is known in terms of its acceleration $a(t)$ and that one is interested in the relative displacement $y(t)$ between the mass and the support.

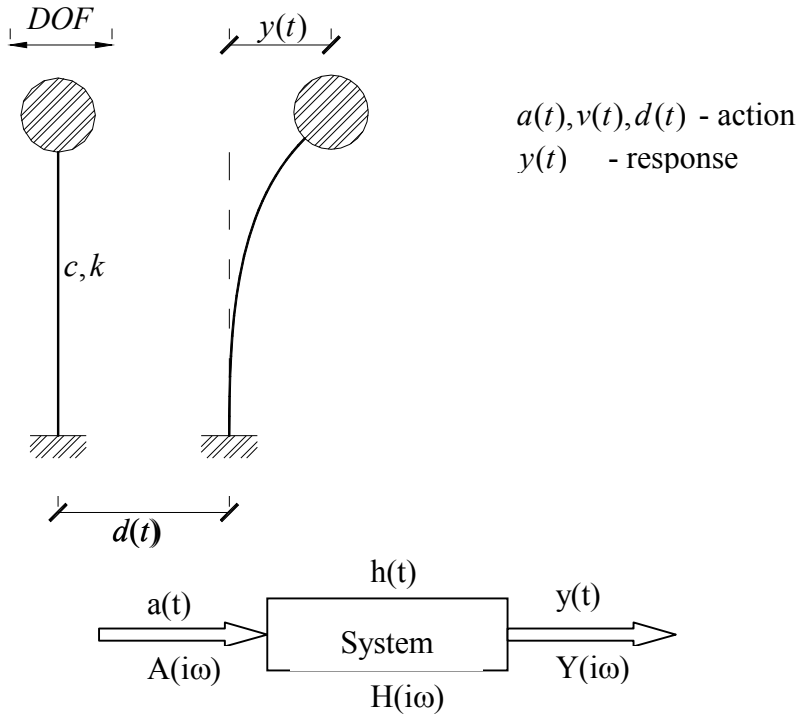

Figure 8.3. *SDOF* system and excitation-response diagram associated with this system

Newton's law of motion in terms of relative displacement provides the following differential equation

$$F^{inertia}(t) + F^{damping}(t) + F^{restoring}(t) = 0 \tag{8.13}$$

which simplifies to

$$\ddot{y}(t) + 2\xi\omega_0 \cdot \dot{y}(t) + \omega_0^2 \cdot y(t) = -a(t) \tag{8.14}$$

where:
ξ – damping ratio
ω_0 – natural circular frequency of the *SDOF* system.
Equation 8.14 can be solved in the time domain or in the frequency domain.

8.3.1. Time domain
One uses the solution of Equation 8.14 given by Duhamel's integral

$$y(t) = \int_0^t a(\tau) \cdot h(t-\tau) d\tau \tag{8.15}$$

where:

$$h(t) = -\frac{1}{\omega_d} e^{-\xi\omega_0 t} \cdot \sin \omega_d t \tag{8.16}$$

is the impulse-response function to unit and the damped circular frequency is

$$\omega_d = \omega_0 \sqrt{1-\xi^2} \tag{8.17}$$

8.3.2. Frequency domain

The solution of the problem in the frequency domain is given by adapting the Equation 8.4

$$Y(\omega) = H(\omega) \cdot A(\omega) \tag{8.18}$$

where:

$A(\omega)$ – Fourier transform of the excitation (input acceleration) given by

$$A(\omega) = \int_{-\infty}^{+\infty} a(t) \cdot e^{-i\omega t} dt \tag{8.19}$$

$H(\omega)$ - transfer function of the system

$Y(\omega)$ – Fourier transform of the response (relative displacement).

If the excitation is the real part of the complex function $e^{i\omega t}$, then, the response is the real part of the complex function $H(\omega)e^{i\omega t}$. Consequently, the transfer function $H(\omega)$ is obtained by making the substitution $a(t) = e^{i\omega t}$ and $y(t) = H(\omega)e^{i\omega t}$ in equation 8.14, canceling the $e^{i\omega t}$ terms, and solving *algebraically* for $H(\omega)$:

$$H(\omega)e^{i\omega t} \cdot (i\omega)^2 + 2\xi\omega_0 \cdot H(\omega)e^{i\omega t} \cdot (i\omega) + \omega_0^2 \cdot H(\omega)e^{i\omega t} = -e^{i\omega t}$$

$$-\omega^2 \cdot H(\omega) + i\omega \cdot 2\xi\omega_0 \cdot H(\omega) + \omega_0^2 \cdot H(\omega) = -1$$

$$H(\omega)\left[-\omega^2 + \omega_0^2 + i \cdot 2\xi\omega_0 \cdot \omega\right] = -1$$

$$H(\omega) = \frac{-1}{\omega_0^2\left[1 - \left(\frac{\omega}{\omega_0}\right)^2 + i \cdot 2\xi \cdot \frac{\omega}{\omega_0}\right]} \tag{8.20}$$

Note that here $H(\omega)$ has the dimensions of displacement per unit acceleration.

The square of the modulus of the complex transfer function is given by

$$\left|H(\omega)\right|^2 = \frac{1}{\omega_0^4\left\{\left[1 - \left(\frac{\omega}{\omega_0}\right)^2\right]^2 + 4\xi^2 \cdot \left(\frac{\omega}{\omega_0}\right)^2\right\}} \tag{8.21}$$

The maximum response of the system is, Figure 8.4

$$\left|y_{\max}(t)\right| = \left|H(\omega)\right| \tag{8.22}$$

and the employment of Equations 8.21 and 8.22 gives the maximum response of the system as:

$$|y_{\max}(t)| = \frac{1}{\omega_0^2 \cdot \sqrt{\left[1-\left(\frac{\omega}{\omega_0}\right)^2\right]^2 + 4\xi^2 \cdot \left(\frac{\omega}{\omega_0}\right)^2}} \tag{8.23}$$

The modulus of the non-dimensional complex transfer function is given by, Figure 8.4

$$|H_0(\omega)| = \frac{1}{\sqrt{\left[1-\left(\frac{\omega}{\omega_0}\right)^2\right]^2 + 4\xi^2 \cdot \left(\frac{\omega}{\omega_0}\right)^2}} \tag{8.24}$$

which is related to the modulus of the complex transfer function by

$$|H(i\omega)| = \frac{1}{\omega_0^2} \cdot |H_0(i\omega)| \tag{8.25}$$

The maximum value of the maximum response is reached for $\omega = \omega_0$ and is given by, Figure 8.4

$$\max|y_{\max}(t)| = \frac{1}{\omega_0^2} \cdot \frac{1}{2\xi} = \frac{m}{k} \cdot \frac{1}{2\xi} \tag{8.26}$$

where m is the mass of the *SDOF* system and k is the stiffness of the *SDOF* system ($k = m\omega_0^2$).

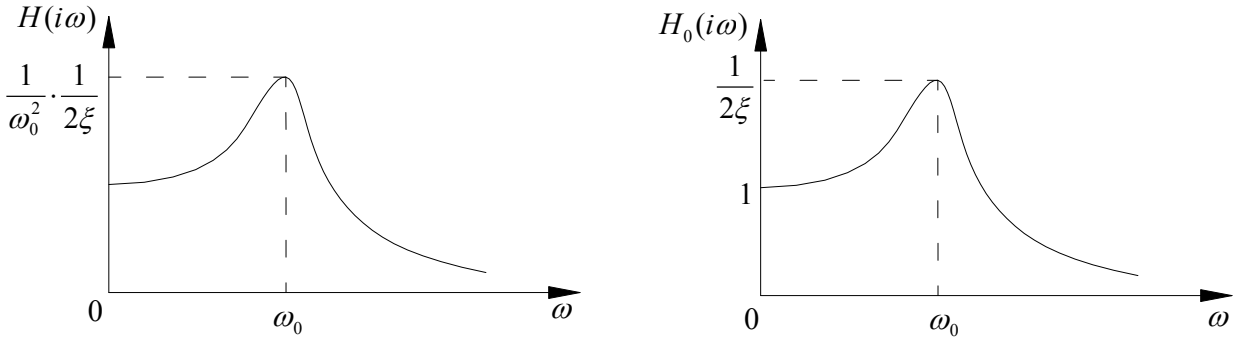

Figure 8.4. Modulus of the complex transfer function and of the non-dimensional transfer function

Once the solution of Equation 8.18 is computed, one can go back in time domain by using the inverse Fourier transform

$$y(t) = \frac{1}{2\pi} \int_{-\infty}^{+\infty} Y(i\omega) e^{i\omega t} d\omega \tag{8.27}.$$

8.4. Excitation-response relations for stationary random processes

The main assumptions used in the following are, Figure 8.5:

- *SDOF*
- action
  - Stationary
  - Ergodic
  - Zero-mean
  - Normal
- structure with elastic behavior

→ response

- Stationary
- Ergodic
- Zero-mean
- Normal

The previous section has dealt with the excitation-response or input-output problem for linear time-invariant systems in terms of particular responses to particular excitations. In this section the theory is extended to the case where the excitation is no longer an individual time history but is an ensemble of possible time histories; i.e., a random process. When the excitation is a stationary random process then the response is also a stationary random process. One shows how the more important statistical properties of the response process can be deduced from knowledge of the system and of the statistical properties of the excitation.

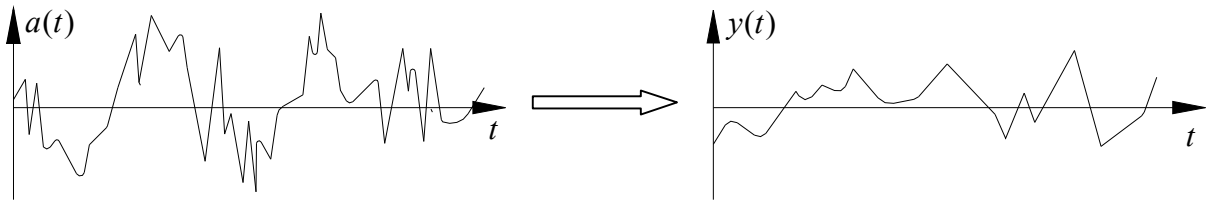

Figure 8.5. Excitation-response processes

8.4.1. Mean value of the response

It is desired to obtain the *mean*, $m_{y(t)}$ or expected value, $E[y(t)]$ of the response process. For any individual sample excitation and response one has the relation 94:

$$y(t) = \int_{-\infty}^{\infty} x(t-\theta)h(\theta)d\theta$$

Using $E[\ ]$ to denote ensemble average (which for ergodic processes is equal to the temporal average) one imagines Equation 8.10 to be written for x, y pair and then one averages:

$$E[y(t)] = E\left[\int_{-\infty}^{\infty} x(t-\theta)h(\theta)d\theta\right] \tag{8.28}$$

Since integration and averaging are both linear operations their interchange is permissible

$$E[y(t)] = \int_{-\infty}^{\infty} E[x(t-\theta)]h(\theta)d\theta \tag{8.29}$$

Now $E[x(\tau)]$ is a constant independent of τ when x is a *stationary* random process so that finally

$$E[y(t)] = E[x(t)]\int_{-\infty}^{\infty} h(\theta)d\theta \tag{8.30}$$

which gives the mean of the output process in terms of the mean of the input process. The integral in Equation 8.30 is a system constant which can be given alternatively by setting ω=0 in Equation 8.12 to obtain

$$H(0) = \int_{-\infty}^{\infty} h(\theta)d\theta \tag{8.31}$$

Finally, using Equations 8.30 and 8.31 one gets the relation between the means of the input and output random processes as

$$E[y(t)] = E[x(t)]H(0) \tag{8.32}$$

Note that $E[y(t)]$ is actually independent of t.
In particular, if the input has zero mean value than so does the output. If the input is an acceleration zero-mean process:

$$m_a(t) = E[a(t)] = const = 0$$

the response process is also zero-mean process:

$$m_y(t) = E[y(t)] = |H(0)| \cdot m_a(t) = \frac{1}{\omega_0^2} \cdot m_a(t) = 0 .$$

8.4.2. Input-output relation for spectral densities
The relation between the *PSD* of the excitation $x(t)$ and the spectral density of the response $y(t)$ is simply

$$S_y(\omega) = H(-\omega) \cdot H(\omega) S_x(\omega) \tag{8.33}$$

A slightly more compact form is achieved by noting that the product of $H(\omega)$ and its complex conjugate may be written as the square of the modulus of $H(\omega)$; i.e.,

$$S_y(\omega) = |H(\omega)|^2 \cdot S_x(\omega) \tag{8.34}.$$

The power spectral density of the response is equal to the square of modulus of the transfer function multiplied with the power spectral density of the excitation. Note that this is an *algebraic* relation and only the *modulus* of the complex transfer function $H(\omega)$ is needed.
8.4.3. Mean square response
The mean square $E[y^2]$ of the stationary response process $y(t)$ can be obtained when the spectral density $S_y(\omega)$ of the response is known according to Equation 7.3. These may be restated in terms of the input process $x(t)$ by using the result 8.34 just obtained.
Thus if the input *PSD* $S_x(\omega)$ is known

$$E[y^2] = \int_{-\infty}^{+\infty} S_y(\omega) d\omega = \int_{-\infty}^{+\infty} |H(\omega)|^2 \cdot S_x(\omega) d\omega = \frac{1}{\omega_0^4} \cdot \int_{-\infty}^{+\infty} |H_0(\omega)|^2 \cdot S_x(\omega) d\omega \tag{8.35}$$

In particular, if the output has zero mean value, the mean square is equal to the variance of the stationary response process $y(t)$ and equation 8.35 turns to:

$$\sigma_y^2 = \int_{-\infty}^{+\infty} S_y(\omega) d\omega = \int_{-\infty}^{+\infty} |H(\omega)|^2 \cdot S_x(\omega) d\omega \tag{8.36}$$

The procedure involved in Equation 8.36 is depicted in Figure 8.6 for stationary ergodic zero-mean acceleration input process.

8.5. Response of a SDOF system to stationary random excitation

As an application of the general results of the preceding section one studies the simply vibratory system illustrated in Figure 8.3. The excitation for this system is the acceleration $a(t)$ of the foundation and the response $y(t)$ is the relative displacement between the foundation and the suspended mass. One shall consider two cases: first when the excitation is white noise; and, second, when the vibratory system is low damped.

8.5.1. Response to band limited white noise

The excitation $a(t)$ is taken to be a stationary random process with band limited white spectrum with uniform spectral density S_0. The response $y(t)$ will also be a random process. Because the excitation is stationary the response process will also be *stationary*. If, in addition, the input is known to be *ergodic* then so also will be the output. Similarly, if it is known that the input is a *normal* or Gaussian process then one knows that the output will also be a normal process. Aside from these general considerations the results of the previous sections permit us to make quantitative predictions of output statistical averages (which are independent of the ergodic or Gaussian nature of the processes).

Thus, let us suppose that the excitation has zero mean. Then according to Equation 8.32 the response also has *zero mean*.

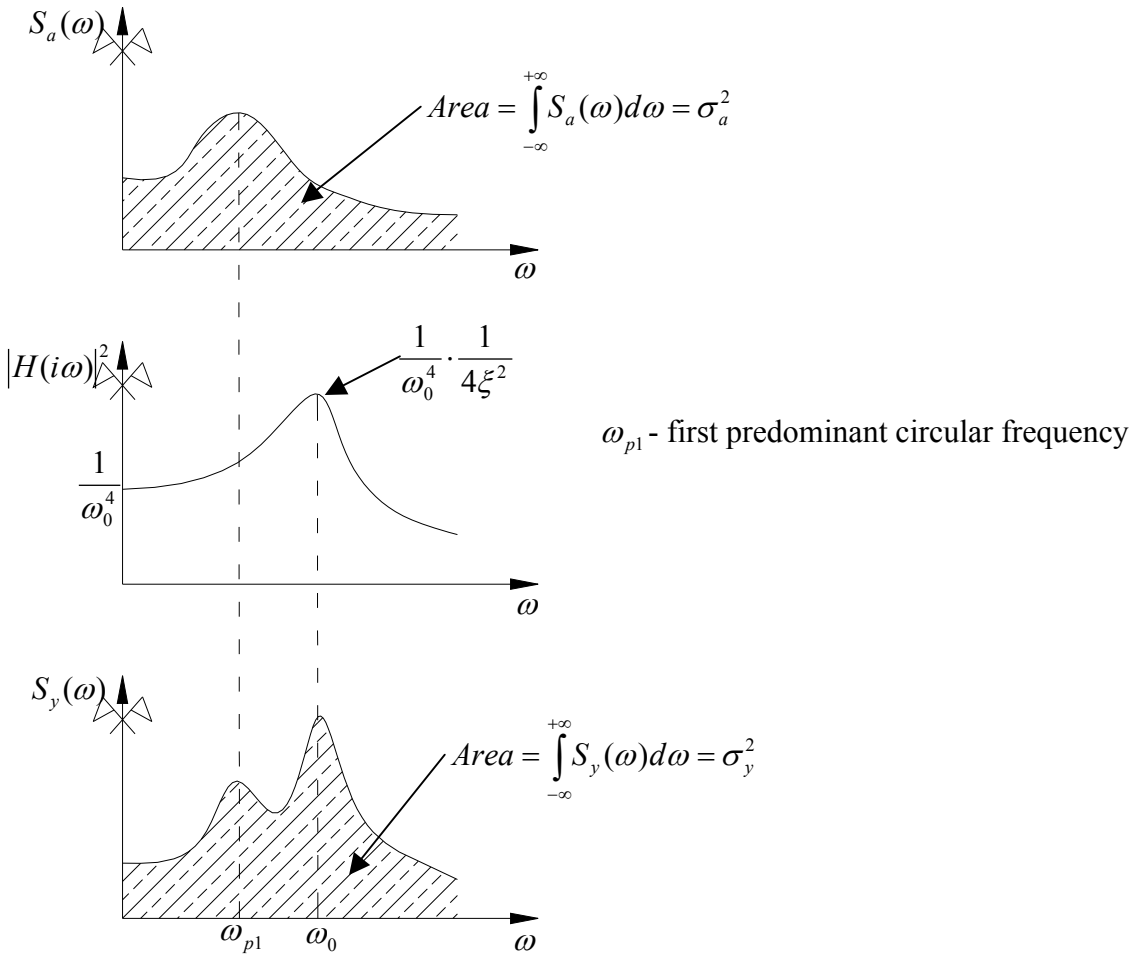

ω_{p1} - first predominant circular frequency

Figure 8.6. Variance of output process from the *PSD* of the input process

The corresponding analysis in the frequency domain involves simple calculations. The spectrum of the input is simply the constant S_0. The spectrum of the output follows from Equation 8.34, Figure 8.7:

$$S_y(\omega) = |H(\omega)|^2 \cdot S_0 = \frac{1}{\omega_0^4 \left\{ \left[1 - \left(\frac{\omega}{\omega_0} \right)^2 \right]^2 + 4\xi^2 \cdot \left(\frac{\omega}{\omega_0} \right)^2 \right\}} \cdot S_0 \qquad (8.37)$$

The mean square of the response (equal to the variance of the process in case of zero-mean processes) can be deduced from the spectral density of the response using

$$\sigma_y^2 = \frac{1}{\omega_0^4}\int_{-\infty}^{+\infty}\left|H_0(i\omega)\right|^2 \cdot S_a(\omega)d\omega =$$
$$= \frac{S_0}{\omega_0^4}\cdot \underbrace{\int_{-\omega_L}^{+\omega_L}\left|H_0(i\omega)\right|^2 d\omega}_{\cong \frac{\pi\omega_0}{2\xi}} \cong \frac{S_0}{\omega_0^4}\cdot\frac{\pi\omega_0}{2\xi} = \frac{\pi}{2}\cdot\frac{S_0}{\xi\omega_0^3} \qquad (8.38)$$

In case the process is *normal* or Gaussian it is completely described statistically by its spectral density. The first-order probability distribution is characterized by the variance alone in this case where the mean is zero.

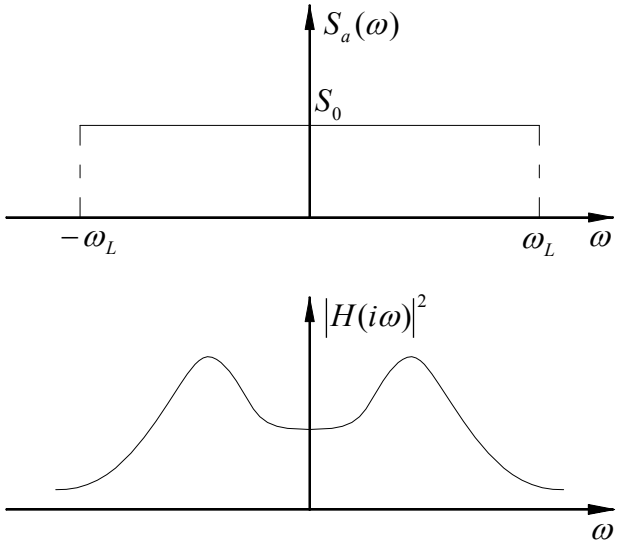

Figure 8.7. Band limited white noise and transfer function of the system

8.5.2. SDOF systems with low damping

For the systems with low damping ($\xi < 0.1$), the transfer function of the system has a very sharp spike at $\omega = \omega_0$ and the amplitudes of the function decreases rapidly as moving away from ω_0. At a distance of $\pm\xi\omega_0$ from ω_0 the amplitude of the transfer function is half the maximum amplitude. Because of this particular aspect of the transfer function of SDOF systems with low damping, the product under the integral in Equation 8.36 will raise significant values only in the interval $\omega_0 \pm \xi\omega_0$ and one can assume that the *PSD* of the input excitation is constant in this interval and equal to $S_a(\omega_0)$, Figure 8.8. Thus, Equation 8.38 valid for band-limited white noise is also applicable and the variance of the response process is equal to $\sigma_y^2 \cong \frac{\pi \cdot S_a(\omega_0)}{2\xi\omega_0^3}$.

Note: If the mean and the variance of the displacement response process are known, the mean and the variance of the velocity and the acceleration response processes can be found using the relations:

$$\dot{y} = \omega_0 \cdot y$$
$$\ddot{y} = \omega_0^2 \cdot y$$
$$m_{\dot{y}} = \omega_0 \cdot m_y = 0$$
$$m_{\ddot{y}} = \omega_0^2 \cdot m_y = 0$$
$$\sigma_{\dot{y}}^2 = \omega_0^2 \cdot \sigma_y^2 = \frac{\pi S_a(\omega_0)}{2\xi\omega_0}$$
$$\sigma_{\ddot{y}}^2 = \omega_0^4 \cdot \sigma_y^2 = \frac{\pi\omega_0 S_a(\omega_0)}{2\xi}.$$

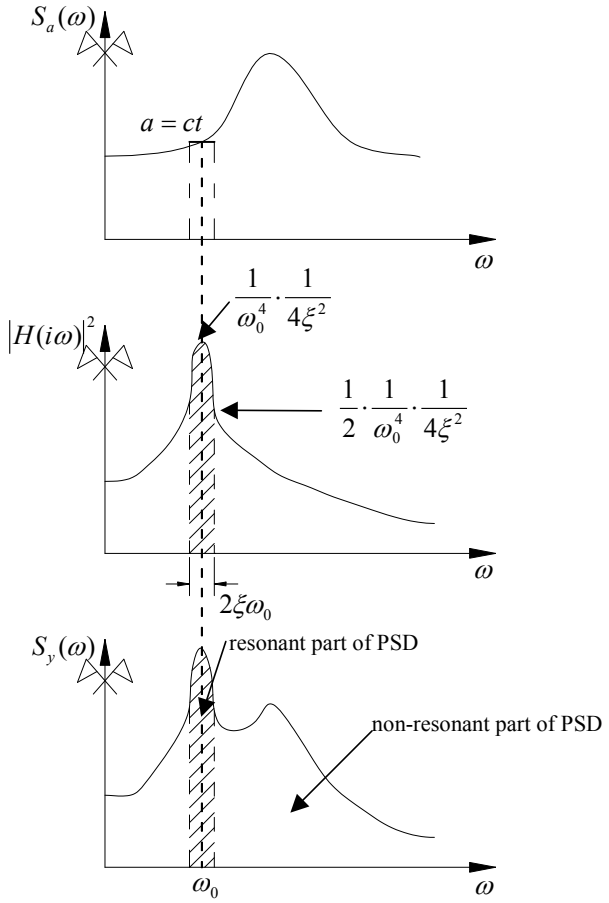

$$\sigma_y^2 = \sigma_{REZONANCE}^2 + \underbrace{\sigma_{NON-REZ}^2}_{neglected} \cong \sigma_{REZONANCE}^2$$

Figure 8.8. Computation of response process variance for *SDOF* systems with low damping

8.5.3. Distribution of the maximum (peak) response values

Let $y(t)$ be a stationary ergodic normal process, Figure 8.9. The distribution of all values of the process is known to follow a Gaussian distribution type. One is interested in the distribution of the maximum response values.

Let ν_b^+ be the expected frequency of crossing the level $x=b$ (b is called barrier or threshold value) with positive slope. Basically, one counts how many times the process intersects the barrier in unit time with positive slope, $\begin{matrix} y(t) > b \\ \dot{y}(t) > 0 \end{matrix}$.

The question to be answered here is what is the number of crossings over threshold „b" with positive slope in unit time, ($\nu_{(b)}^+$)? The problem was already analyzed:

$$\nu_{(b)}^+ = \frac{1}{2\pi} \cdot \frac{\sigma_{\dot{y}}}{\sigma_y} \cdot \exp\left(-\frac{b^2}{2\sigma_y^2}\right) = \frac{1}{2\pi} \cdot \sqrt{\frac{\int_{-\infty}^{+\infty} \omega^2 S_y(\omega) d\omega}{\int_{-\infty}^{+\infty} S_y(\omega) d\omega}} \cdot \exp\left(-\frac{b^2}{2\sigma_y^2}\right) \tag{8.39}$$

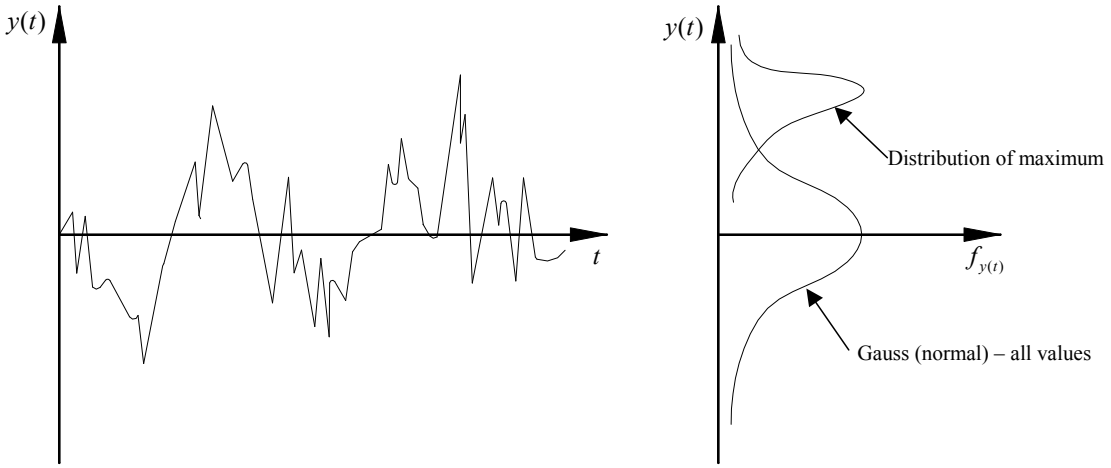

Figure 8.9. Distribution of all values and of the maximum values of the stationary ergodic normal response process $y(t)$

If one uses the spectral moments $\lambda_i = \int_{-\infty}^{+\infty} \omega^i S_y(\omega) d\omega$, the variance of the response is equal to the spectral moment of order zero, $\lambda_0 = \sigma_y^2$ and the variance of the first derivative of the response is equal to the spectral moment of second order, $\lambda_2 = \sigma_{\dot{y}}^2$ and Equation 8.39 becomes:

$$\nu_{(b)}^+ = \frac{1}{2\pi} \cdot \sqrt{\frac{\lambda_2}{\lambda_0}} \cdot \exp\left(-\frac{b^2}{2\sigma_y^2}\right) \tag{8.40}$$

The expected frequency, in crossings per unit time, of zero crossings with positive slope (the average number of zero crossings with positive slope in unit time) is obtained setting b=0 in Equation 8.40:

$$\nu_0 = \frac{1}{2\pi} \cdot \sqrt{\frac{\lambda_2}{\lambda_0}} \tag{8.41}$$

Finally, combining Equations 8.40 and 8.41, one gets the expected number of crossing the level $x=a$ with positive slope:

$$\nu^{+}_{(b)} = \nu_0 \cdot \exp\left(-\frac{b^2}{2\sigma_y^2}\right) \tag{8.42}$$

For getting the distribution of the peak values of the response process one uses the Davenport's approach. The maximum (peak) response is normalized as:

$$\eta = \frac{y_{\max}}{\sigma_y} \tag{8.43}$$

The normalized response process as well as the distribution of the peak values of the response are represented in Figure 8.10.
Considering the new random variable, η one can proof that its probability distribution is of exponential type:

$$\text{CDF: } F_\eta = \exp(-\nu^{+}(y_{\max}) \cdot t) \tag{8.44}$$

where t is the time interval under consideration.

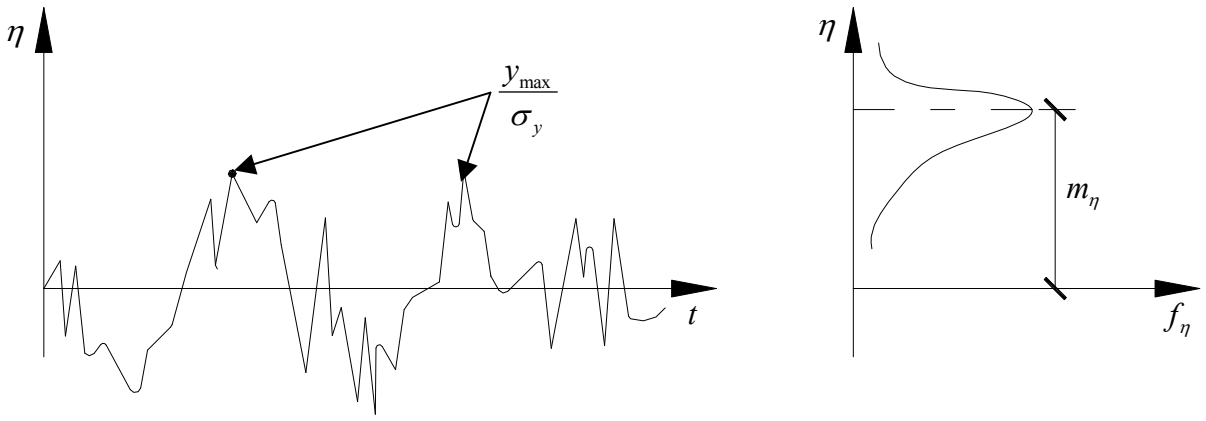

Figure 8.10. Normalized response and distribution of peak values

Combining Equation 8.44 with Equations 8.42 and 8.43 one gets the cumulative distribution function, *CDF*:

$$F_\eta = \exp\left(-\nu_0 \exp\left(-\frac{\eta^2\sigma_y^2}{2\sigma_y^2}\right) \cdot t\right) = \exp\left(-\nu_0 t \exp\left(-\frac{\eta^2}{2}\right)\right) = e^{-\nu_0 t \cdot e^{-\frac{\eta^2}{2}}} \tag{8.45}$$

The probability distribution function, *PDF* is obtained by:

$$\text{PDF: } f_\eta = \frac{dF_\eta}{d\eta} \tag{8.46}$$

The probability density function and the cumulative distribution function of the normalized peak response, η are represented in Figure 8.11 and Figure 8.12, respectively.

The mean value of the distribution, m_η (mean of the maximum (peak) response values) is

$$m_\eta = \sqrt{2\ln(\nu_0 t)} + \frac{0.577}{\sqrt{2\ln(\nu_0 t)}} \tag{8.47}$$

while the standard deviation of the maximum response values is

$$\sigma_\eta = \frac{\pi}{6} \cdot \frac{1}{\sqrt{2\ln(\nu_0 t)}} \tag{8.48}$$

Combining Equations 8.38, 8.43 and 8.47, one gets the mean of maximum response values:

$$m_{y_{\max}} = m_\eta \cdot \sigma_y = \left(\sqrt{2\ln(\nu_0 t)} + \frac{0.577}{\sqrt{2\ln(\nu_0 t)}} \right) \cdot \sqrt{\frac{\pi \cdot S_a(\omega_0)}{2\xi\omega_0^3}} \tag{8.49}$$

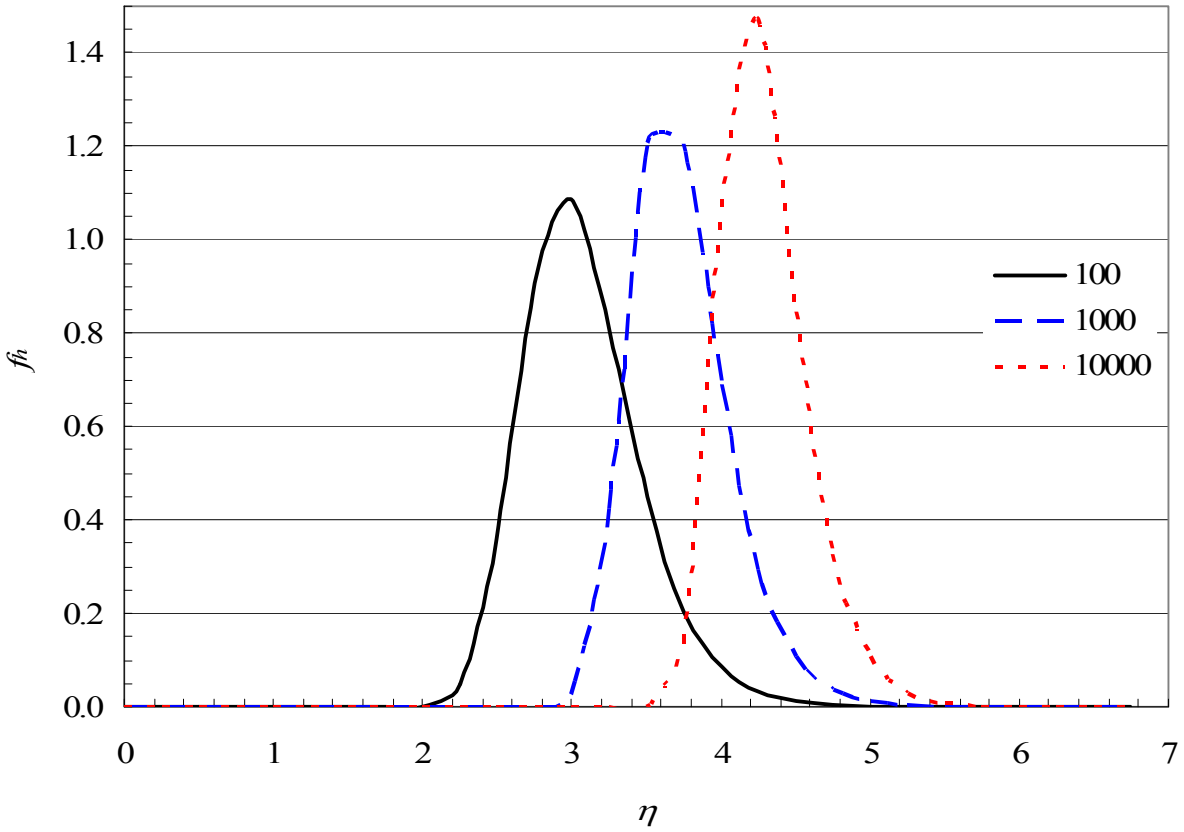

Figure 8.11 Probability density function of the normalized peak response η for various $\nu_0 T$ values

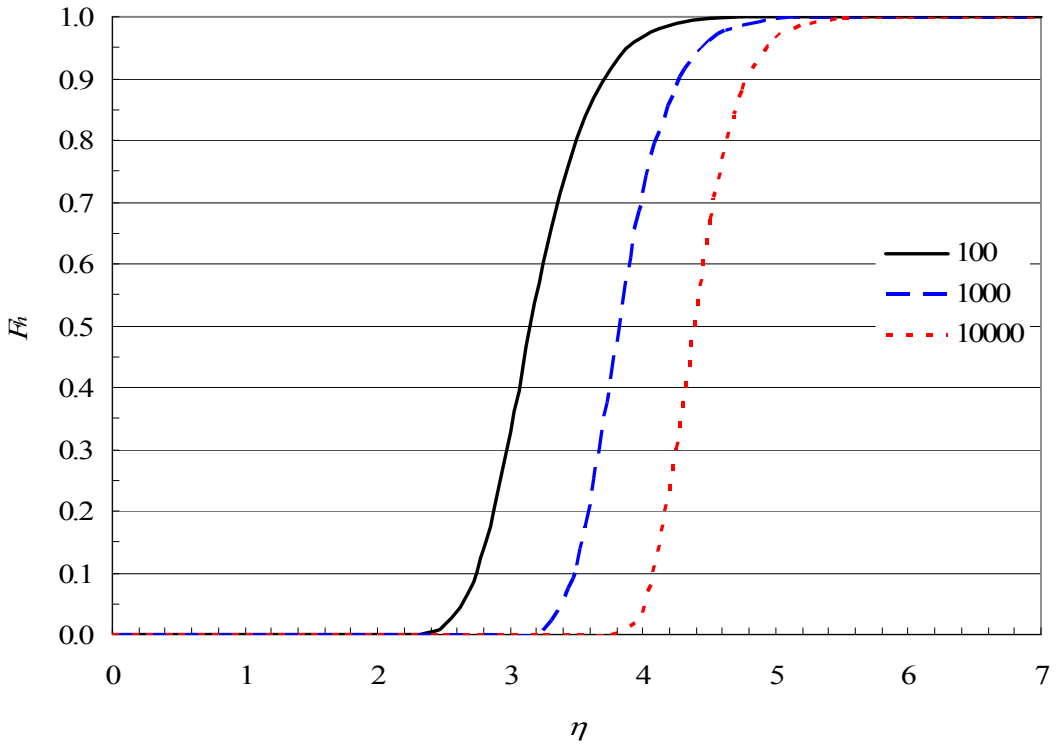

Figure 8.12 Cumulative distribution function of the normalized peak response η for various $\nu_0 T$ values

Finally, one has to answer the following question, Figure 8.13: What is the maximum response with p non-exceedance probability in the time interval T?
The maximum response with p non-exceedance probability in the time interval T is given by:

$$y_{\max}(p,T) = \eta_{p,T} \cdot \sigma_y \tag{8.50}$$

Returning to Equation 8.45, the *CDF* gives the non-exceedance probability p of $\eta_{p,T}$:

$$F(\eta_{p,T}) = p = e^{-\nu_0 T \cdot e^{-\frac{\eta_{p,T}^2}{2}}} \tag{8.51}$$

It follows from Equation 8.51 that:

$$\ln(p) = -\nu_0 T \cdot e^{-\frac{\eta_{p,T}^2}{2}}$$

$$\ln(-\ln(p)) = \ln\left(\nu_0 T \cdot e^{-\frac{\eta_{p,T}^2}{2}}\right) = \ln(\nu_0 T) - \frac{\eta_{p,T}^2}{2}$$

$$\eta_{p,T}^2 = 2\ln(\nu_0 T) - 2\ln(-\ln(p))$$

$$\eta_{p,T} = \sqrt{2\ln(\nu_0 T) - 2\ln(-\ln(p))} \tag{8.52}$$

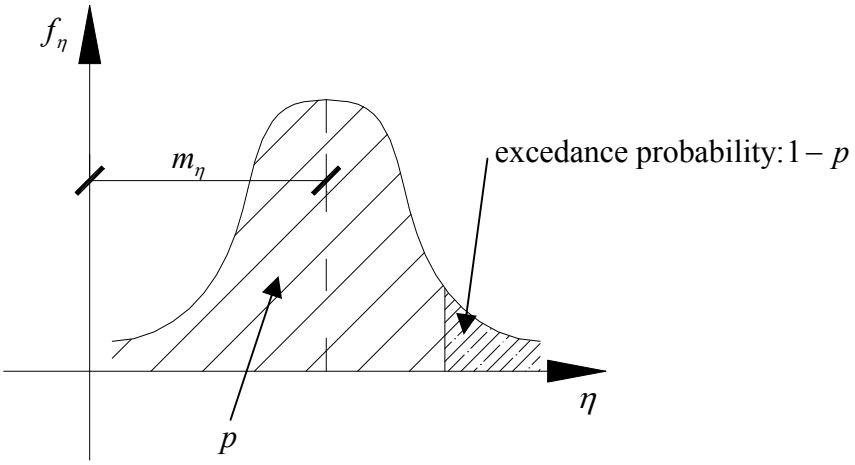

Figure 8.13. Distribution of normalized peak values of the response

The normalized maximum response with p non-exceedance probability in the time interval T, $\eta_{p,T}$ is represented in Figure 8.14.

The maximum response with p non-exceedance probability in the time interval T is:

$$y_{\max}(p,T) = \sqrt{2\ln(\nu_0 T) - 2\ln(-\ln(p))} \cdot \sqrt{\frac{\pi \cdot S_a(\omega_0)}{2\xi\omega_0^3}} \tag{8.53}$$

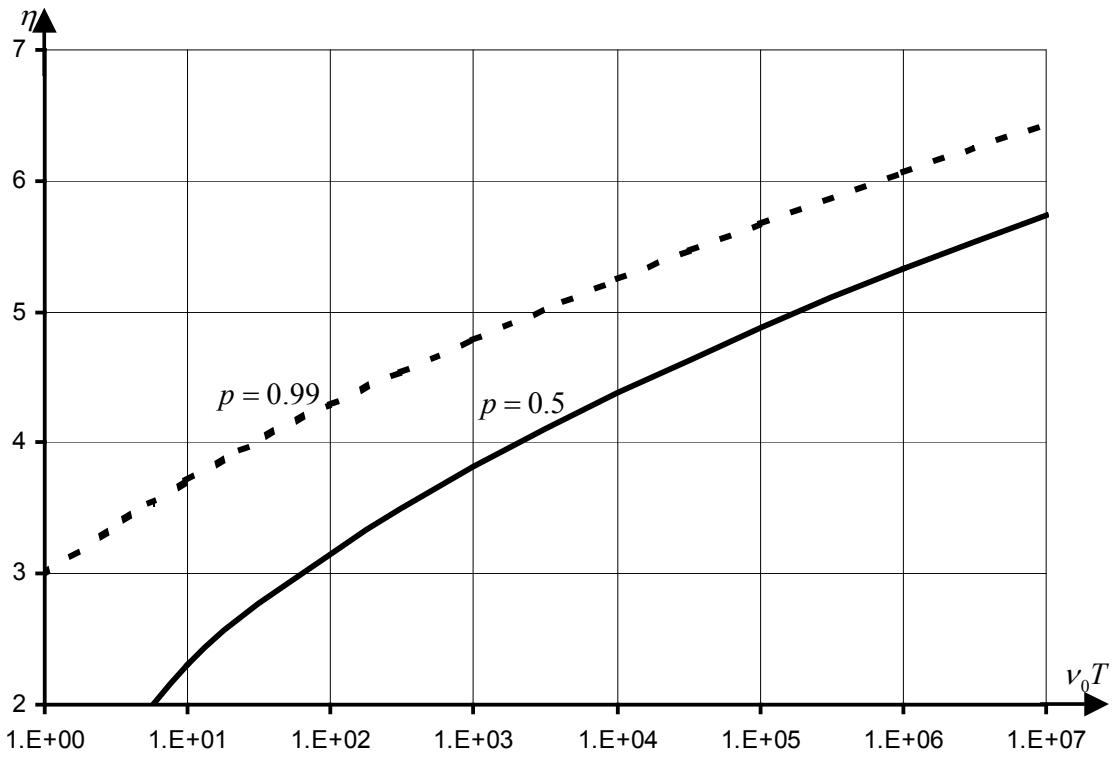

Figure 8.14. Normalized maximum response with p non-exceedance probability in the time interval T

9. ALONG-WIND DYNAMIC RESPONSE OF BUILDINGS AND STRUCTURES

The along-wind dynamic response of buildings and structures is presented according to the Romanian technical regulation *NP 082-04* „Cod de proiectare privind bazele proiectarii si actiuni asupra constructiilor. Actiunea vantului" Deisgn Code. Basis of Design and Loads on Buildings and Structures. Wind Loads, that is in line with and compatible to *EUROCODE* 1: Actions on structures — Part 1-4: General actions — Wind actions.

9.1. General

Wind effects on buildings and structures depend on the exposure of buildings, structures and their elements to the natural wind, the dynamic properties, the shape and dimensions of the building (structure.

The random field of natural wind velocity is decomposed into a mean wind in the direction of air flow (x-direction) averaged over a specified time interval and a fluctuating and turbulent part with zero mean and components in the longitudinal (x-) direction, the transversal (y-) direction and the vertical (z-) direction.

The sequence of maximum annual mean wind velocities can be assumed to be a Gumbel distributed sequence with possibly direction dependent parameters. The turbulent velocity fluctuations can be modeled by a zero mean stationary and ergodic Gaussian process.

The wind force acting per unit area of structure is determined with the relations:

(i) For rigid structures of smaller dimensions:

$$w = c_a\left(c_g c_r\right)\cdot Q_{ref} = c_a c_e Q_{ref} \tag{9.1}$$

(ii) For structures sensitive to dynamic effects (natural frequency < 1Hz) and for large rigid structures:

$$w = c_d c_a c_e Q_{ref} \tag{9.2}$$

where:

Q_{ref} is the reference (mean) velocity pressure
c_r - roughness factor
c_g - gust factor
c_e - exposure factor
c_a - aerodynamic shape factor
c_d -dynamic factor.

9.2 Reference wind velocity and reference velocity pressure

The reference wind velocity, $U_{ref}^{10\,min}$ is the wind at 10m above ground, in open and horizontal terrain exposure, averaged on 10 min time interval (*EUROCODE 1* and *NP 082-04*). For other than 10 min averaging intervals, in open terrain exposure, the following relationships may be used:

$$1.05U_{ref}^{1h} = U_{ref}^{10min} = 0.83U_{ref}^{1min} = 0.67U_{ref}^{3s}. \tag{9.3}$$

The distribution of maximum annual mean wind velocity fits a Gumbel distribution for maxima:

$$F_{\overline{U}}(x) = exp\{-exp[-\alpha_1(x-u_1)]\} \tag{9.4}$$

The mode u and the parameter α_1 of the distribution are determined from the mean m_1 and the standard deviation σ_1 of the set of maximum annual velocities:

$$u = m_1 - \frac{0.577}{\alpha_1}, \qquad \alpha_1 = \frac{1.282}{\sigma_1}. \tag{9.5}$$

The coefficient of variation of maximum annual wind velocity, $V_1 = \sigma_1 / m_1$ depends on the climate and is normally between 0.10 and 0.40; the mean of the maximum annual wind velocities is usually between 10 m/s to 50 m/s.

The lifetime (N years) maxima of wind velocity are also Gumbel distributed. The mean and the standard deviation of lifetime maxima are functions of the mean and of the standard deviation of annual maxima:

$$F_{\overline{U}}^{N}(x) = exp\{-exp[-\alpha_N(x-u_N)]\} \tag{9.6}$$

$$m_N = m_1 + \frac{\ln N}{1.282}\sigma_1, \qquad \sigma_N = \sigma_1. \tag{9.7}$$

The reference wind velocity having the probability of non-exceedance during one year, p = 0.98, is so called "characteristic" velocity, $U_{0.98}$. The mean recurrence interval (MRI) of the characteristic velocity is T= 50 yr. For any probability of non-exceedance p, the fractile U_p of Gumbel distributed random variable can be computed as follows:

$$U_p = m_1 + \left[-0.45 - \frac{1}{1.282}\ln(-\ln p)\right]\sigma_1 \tag{9.8}$$

The characteristic velocity can be determined as follows:

$$U_{T=50yr} = U_{0.98} = m_1 + 2.593 \cdot \sigma_1 \tag{9.9}$$

Generally, it is not possible to infer the maxima over dozens of years from observations covering only few years. For reliable results, the number of the years of available records must be of the same order of magnitude like the required mean recurrence interval.

The wind velocity pressure can be determined from wind velocity (standard air density ρ=1.25kg/m^3) as follows:

$$Q_{ref}[Pa] = \frac{1}{2}\cdot\rho\cdot U_{ref}^2 = 0.612\cdot U_{ref}^2\,[m/s] \tag{9.10}$$

The conversion of velocity pressure averaged on 10 min into velocity pressure averaged on other time interval can be computed from Eq. (9.3):

$$1.1Q_{ref}^{1h} = Q_{ref}^{10min} = 0.7Q_{ref}^{1min} = 0.44Q_{ref}^{3s}. \tag{9.11}$$

9.3 Probabilistic assessment of wind hazard for buildings and structures

The meteorological existing database comprises the maximum annual wind velocity (at 10 m, averaged on 1 min) at more than 120 National Institute of Meteorology and Hydrology (INMH) locations in Romania, at which wind measurements are made. The period of records for those locations is between 20 to 60 years, up through 1991, when the meteorological datasets were provided by INMH, Bucharest-Baneasa, to the civil engineers via Building Research Institute (INCERC), Bucharest.

The extreme value distribution used for the estimation of the characteristic wind velocity is the Gumbel distribution for maxima, Table 9.1. The distribution is recommended by American Standard for Minimum Design Loads for Buildings, *ASCE 7-98, 2000* and fits very well the available Romanian data.

The coefficient of variation of the maximum annual wind velocity is in the range V_U = 0.15÷0.3 with mean 0.23 and standard deviation 0.06. The V_U values have the same order of magnitude like American values (quoted in LRFD studies) and are greater than those proposed by the CIB report (1991). The coefficient of variation of the velocity pressure (square of the velocity) is approximately double the coefficient of variation of the velocity:

$$V_Q = 2\,V_U. \tag{9.12}$$

The Romanian climate is softer in the intra-Carpathians area, in Transylvania than in Moldavia and central Walachia. The Northeastern part of Moldova has the highest, in Romania, reference wind velocity. Locally, in the mountain areas of the Southwestern part of Romania, there are very high velocities, too.

Table 9.1. Reference wind velocity and velocity pressure having MRI=50 yr. (0.02 annual probability of exceedance)

Zone	$U_{ref}^{1\,min}$	Q_{ref}^{1}	$U_{ref}^{10\,min}$	Q_{ref}^{10min}
	m/s	kPa	m/s	kPa
1	31	0.60	25.8	0.4
2	35	0.75	28.9	0.5
3	41	0.90	34.0	0.7

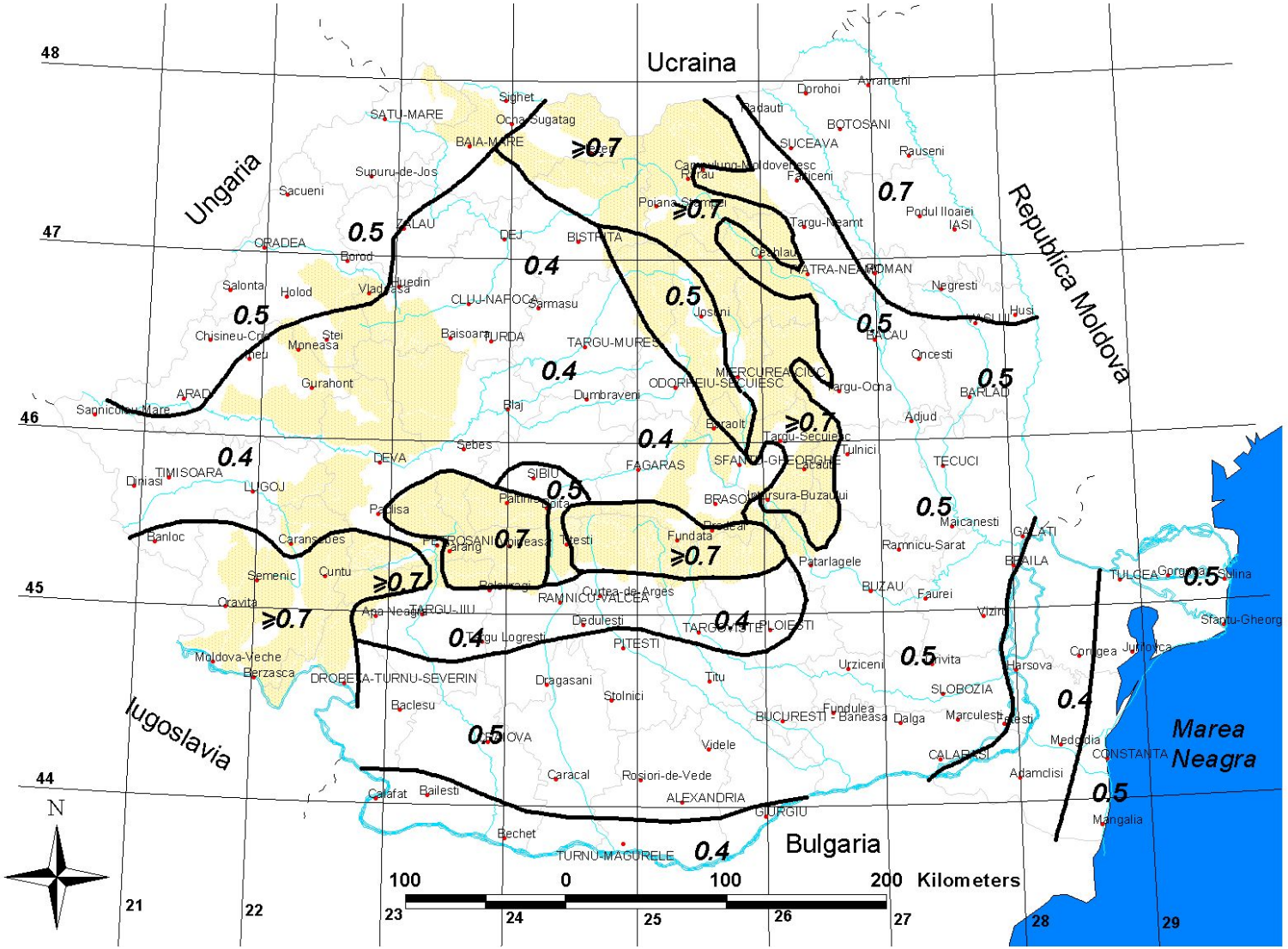

Figure 9.1. The characteristic wind velocity pressure, kPa with mean recurrence interval MRI=50 yr. – wind velocity averaged on 10 min. at 10 m above ground

9.4 Terrain roughness and Variation of the mean wind with height

The roughness of the ground surface is aerodynamically described by the roughness length, z_o, (in meters), which is a measure of the size and spacing of obstacles on the ground, Table 9.2. Alternatively, the terrain roughness can be described by the surface drag coefficient, κ, corresponding to the roughness length, z_o:

$$\kappa = \left(\frac{k}{ln \frac{z_{ref}}{z_0}} \right)^2 = \left(\frac{1}{2.5 ln \frac{10}{z_0}} \right)^2 \tag{9.13}$$

where $k \cong 0.4$ is von Karman´s constant and $z_{ref} = 10$ m.

Various terrain categories are classified in Table 9.2 according to their approximate roughness lengths. The distribution of the surface roughness with wind direction must be considered.

Table 9.2. Roughness length z_o, in meters, for various terrain categories [1) 2)]

Terrain category	Terrain description	Range of z_o, in m	Code value
A. Open sea. Smooth flat country	Areas exposed to the wind coming from large bodies of water; snow surface; Smooth flat terrain with cut grass and rare obstacles.	0.001 ↓ 0.005	0.003
B. Open country	High grass (60 cm) hedges and farmland with isolated trees; Terrain with occasional obstructions having heights less than 10 m (some trees and some buildings)	0.01 ↓ 0.1	0.05
C. Sparsely built-up urban areas. Wooded areas	Sparsely built-up areas, suburbs, fairly wooded areas (many trees)	0.1 ↓ 0.7	0.3
D. Densely built-up urban areas. Forests	Dense forests in which the mean height of trees is about 15m; Densely built-up urban areas; towns in which at least 15% of the surface is covered with buildings having heights over 15m	0.7 ↓ 1.2	1.0
E. Centers of Very large cities	Numerous large high closely spaced obstructions: more than 50% of the buildings have a height over 20m	≥ 2.0	2.0

[1)] Smaller values of z_o provoke higher mean velocities of the wind

[2)] For the full development of the roughness category, the terrains of types A to D must prevail in the up wind direction for a distance of at least of 500m to 1000m, respectively. For category E this distance is more than 1 km.

The variation of the mean wind velocity with height over horizontal terrain of homogenous roughness can be described by the logarithmic law:

$$U(z) = \frac{1}{k} u_*(z_0) \ln \frac{z}{z_0} \qquad \text{for } z > d_o >> z_o \tag{9.14}$$

where:

$U(z)$ - the mean velocity of the wind at height z above ground, m/s

z_o - the roughness length, m

k - von Karman's constant ($k \cong 0.4$)

d_o - the lowest height of validity of Eq. (9.14)

$u_*(z_0)$ - friction velocity defined as function of surface frictional shear stress, and measured as:

$$u_*(z_0) = \frac{U(z)}{2.5 \ln \frac{z}{z_0}} . \tag{9.15}$$

The logarithmic profile is valid for moderate and strong winds (mean hourly velocity > 10 m/s) in neutral atmosphere (where the vertical thermal convection of the air may be neglected). Even the Eq. (9.14) holds through the whole atmospheric boundary layer, its use is recommended only in the lowest 200m, or 0.1δ, where δ is the depth of the boundary layer. The lowest height of validity for the Eq.(9.14), d_o is close to the average height of dominant roughness elements : i.e. from less than 1 m, for smooth flat country to more than 15 m, for centers of cities. On account of this, Eq.(9.14) is more precisely valid as:

$$U(z) = \frac{1}{k} u^*(z_0) \ln \frac{z - d_0}{z_0} ; z \geq d_o. \tag{9.16}$$

In engineering practice, Eq.(9.16) is very conservatively used with $d_o = 0$.

With respect to the reference height, z_{ref}=10m and reference (open terrain) exposure, $z_{o,ref}$, the relation between wind velocities in two different roughness categories at two different heights can be written approximately as:

$$\frac{U(z)}{U_{ref}} = \frac{\frac{1}{k} u^*(z_0)}{\frac{1}{k} u^*(z_{0,ref})} \frac{\ln \frac{z}{z_0}}{\ln \frac{z}{z_{0,ref}}} = \left(\frac{z_0}{z_{0,ref}} \right)^{0.07} \frac{\ln \frac{z}{z_0}}{\ln \frac{z_{ref}}{z_{0,ref}}} . \tag{9.17}$$

The mean wind velocity pressure at height z is defined by:

$$Q(z) = \frac{1}{2} \rho U^2(z) \tag{9.18}$$

where ρ is the air density (ρ=1.25 kg/m^3 for standard air).

The roughness factor (*EUROCODE 1* and *NP 082-04*) describes the variation of the mean velocity pressure with height above ground and terrain roughness as function of the reference velocity pressure. From Eq. (9.17) and (9.18) one gets:

$$c_r(z) = \frac{Q(z)}{Q_{ref}} = \frac{U(z)^2}{U_{ref}^2} = \left[\frac{\left(\frac{z_0}{z_{0,ref}} \right)^{0.07}}{\ln \frac{z_{ref}}{z_{0,ref}}} \right]^2 \left(\ln \frac{z}{z_0} \right)^2 = k_r^2(z_0) \cdot \left(\ln \frac{z}{z_0} \right)^2 . \text{for } z > z_{min} \tag{9.19a}$$

$$c_r(z) = c_r(z = z_{min}) \qquad \text{for } z \le z_{min} \qquad (9.19b)$$

The roughness factor in *EUROCODE 1* notation is called exposure factor in the American Code *ASCE 7-98*, 2000. The roughness factor is represented in Figure 9.2.

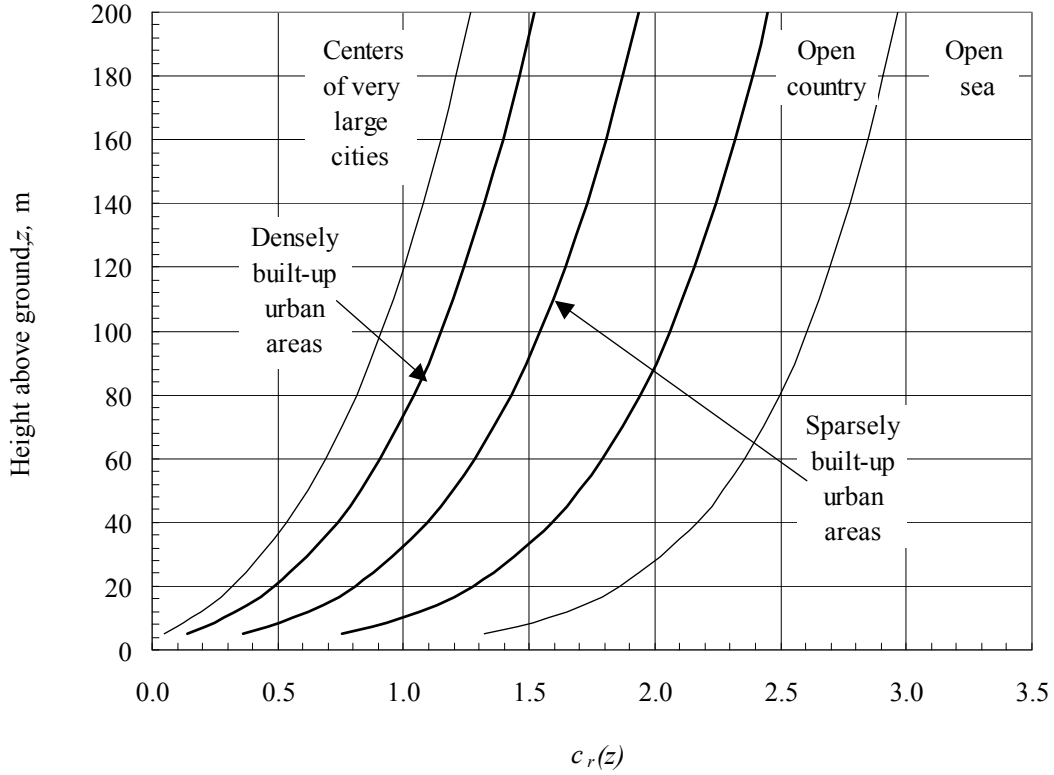

Figure 9.2. Roughness factor, $c_r(z) = k_r^2(z_0) \cdot \left(ln \frac{z}{z_0} \right)^2$

9.5. Stochastic modelling of wind turbulence

9.5.1 Intensity of turbulence

The wind turbulence has a spatial character. In the neutral atmospheric surface layer, for $z << \delta$, the root mean square value of the three-dimensional velocity fluctuations in the airflow deviating from the longitudinal mean velocity can be assumed independent of the height above ground (u_* - friction velocity):

$$\sigma_u = \beta_u u_* \qquad \text{Longitudinal} \qquad (9.20)$$

$$\sigma_v = \beta_v u_* \qquad \text{Transversal} \qquad (9.21)$$

$$\sigma_w = \beta_w u_* \qquad \text{Vertical.} \qquad (9.22)$$

For $z < 0.1h$, the ratios σ_v/σ_u and σ_w/σ_u near the ground are constant irrespective the roughness of the terrain (*ESDU*, 1993):

$$\frac{\sigma_v}{\sigma_u} \cong 0.78 \qquad (9.23)$$

$$\frac{\sigma_w}{\sigma_u} \cong 0.55 \,. \tag{9.24}$$

The variance of the longitudinal velocity fluctuations can be expressed from non-linear regression of measurement data, as function of terrain roughness (Solari, 1987):

$$4.5 \le \beta_u^2 = 4.5 - 0.856 \ln z_0 \le 7.5 \tag{9.25}$$

The stochastic model for along-wind turbulence is represented in Figure 9.3.

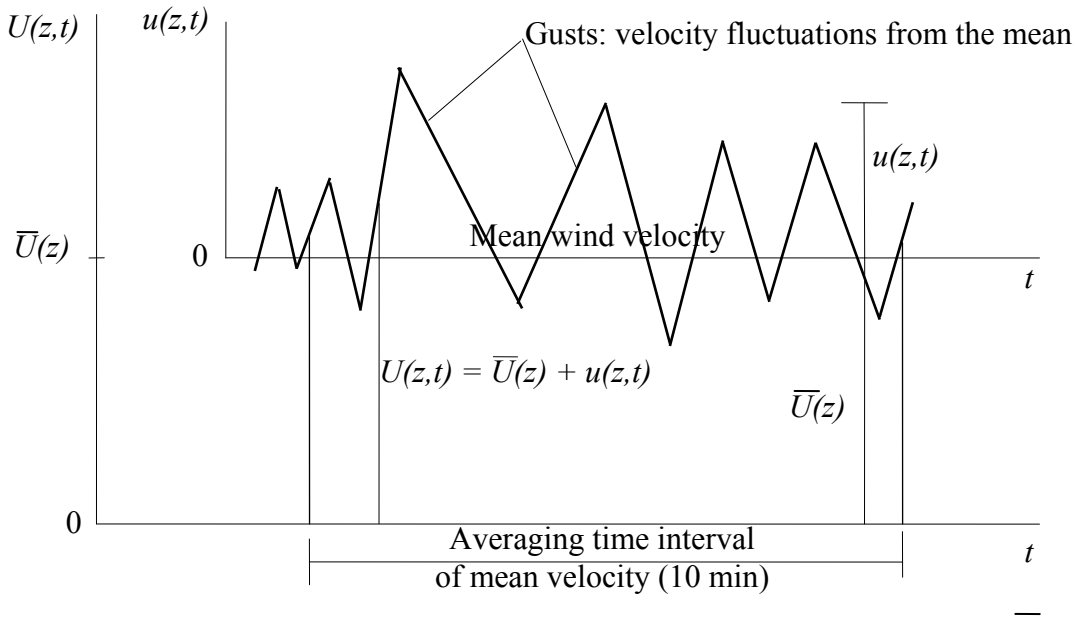

Figure 9.3. Stochastic process of the wind velocity at height z above ground: $U(z,t) = U(z) + u(z,t)$

The standard deviation of the longitudinal velocity fluctuations, β_u, is plotted in Figure 9.4.

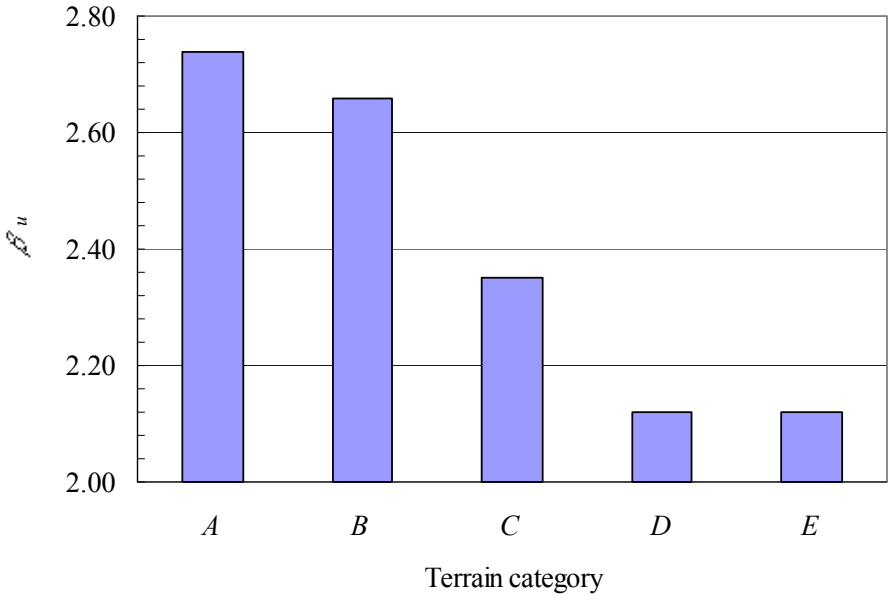

Figure 9.4. Standard deviation of the longitudinal velocity fluctuations, β_u

The intensity of longitudinal turbulence is the ratio of the root mean squared value of the longitudinal velocity fluctuations to the mean wind velocity at height z (i.e. the coefficient of variation of the velocity fluctuations at height z):

$$\mathrm{I_u(z)} = \frac{\sqrt{\mathrm{u(z,t)^2}}}{\mathrm{U(z)}} = \frac{\sigma_u}{U(z)} \tag{9.26}$$

The longitudinal turbulence intensity at height z can be written in the form:

$$\mathrm{I_u(z)} = \frac{\beta_u \cdot u_*}{u_* \cdot 2.5 \ln \frac{z}{z_0}} = \frac{\beta_u}{2.5 \ln \frac{\mathrm{z}}{\mathrm{z_0}}} \qquad \text{for } z > z_{min} \tag{9.27a}$$

$$I_u(z) = I(z = z_{\min}) \qquad \text{for } z \leq z_{min} \tag{9.27b}$$

In open terrain it may approximately be assumed as: $1/[\ln(z/z_0)]$.

The transversal and the vertical intensity of turbulence can be determined by multiplication of the longitudinal intensity $I_u(z)$ by the ratios σ_v/σ_u and σ_w/σ_u. Representative values for intensity of turbulence are represented in Figure 9.5.

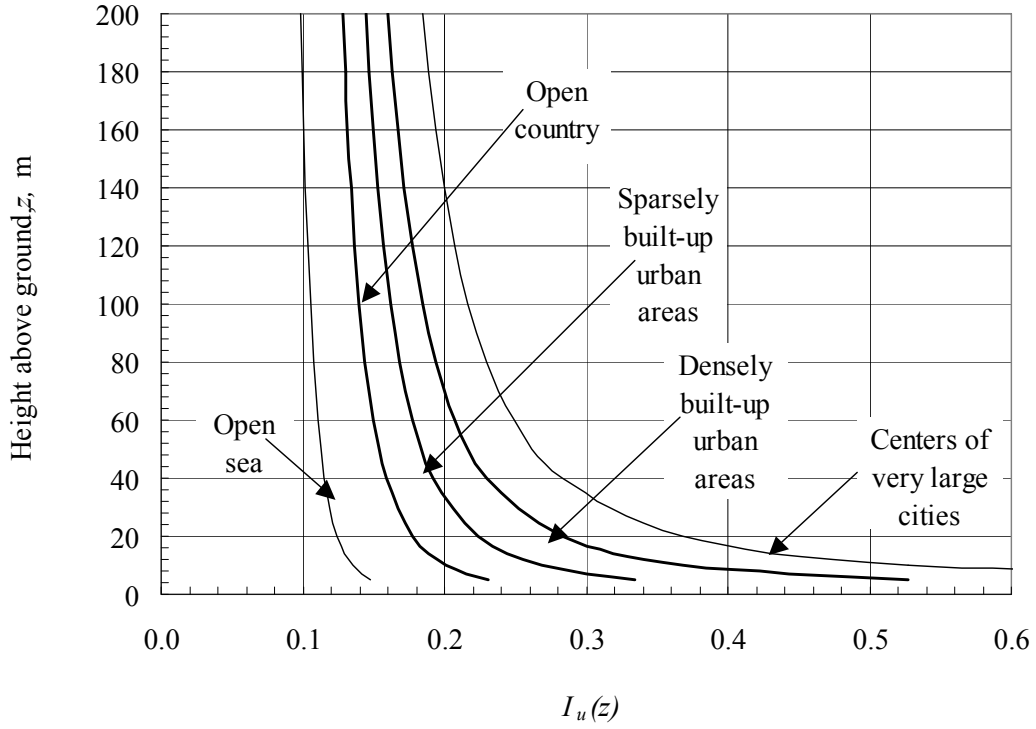

Figure 9.5. Intensity of longitudinal turbulence, $\mathrm{I_u(z)} = \frac{\beta}{2.5 \ln \frac{\mathrm{z}}{\mathrm{z_0}}}$

9.5.2 Power spectral density for along-wind gustiness

From numerous proposals for the spectral density of along-wind gustiness: Karman (1948), Panovski (1964), Davenport (1967), Harris (1968), Flicht (1970), Kaimal (1972), Simiu

(1974,1975), ESDU (1976, 1985), Naito (1978, 1983), Kareem (1985), Solari (1987,1993) those of Davenport, Solari and von Karman were selected. The power spectra are given as normalized (i.e. unit area) and unilateral (i.e. half sided) spectral densities. The normalizing parameter of spectra is the variance σ_u^2 of the wind velocity process. The spectra are represented in terms of frequency, n, in Hz, on a logarithmic scale i.e. $n \cdot G_u(n)$ is plotted on a linear scale versus lg$n$.

A comparative study of these spectral densities is presented. In characterizing wind turbulence, the length scale of turbulence, $L_u(z)$, plays an important role. The length scale of turbulence is a comparative measure of the average size of gusts in appropriate directions and is an important scaling factor in determining how rapidly gust properties vary in space. The integral length scale of turbulence from Couniham, used by Solari for *EC1* (denoted by L_u), was also selected in NP 082-04. The formulas of the 3 spectral densities and the length scale of turbulence are summarized in Table 9.3 and compared in Figure 9.6.

Table 9.3. Normalized (unit area) half sided power spectra of the along-wind gust velocity

Solari in *Eurocode 1*	Davenport in *NBC* of Canada	von Karman in *JCSS* and *CIB* codes
$\frac{nG_u(n)}{\sigma_u^2} = \frac{6.868x}{(1+10.32x)^{\frac{5}{3}}}$ $x=L_u\, n / U(z)$, where: $L_u=300(z/300)^{0.46+0.074\ln z_0}$	$\frac{nG_u(n)}{\sigma_u^2} = \frac{\frac{2}{3}x^2}{(1+x^2)^{\frac{4}{3}}}$ where: $x=1200\, n / U(z)$ Mean spectrum for $10<z<150$m	$\frac{nG_u(n)}{\sigma_u^2} = \frac{4x}{(1+70.8\,x^2)^{\frac{5}{6}}}$ $x=L_u\, n / U(z)$, where: $L_u=300(z/300)^{0.46+0.074\ln z_0}$

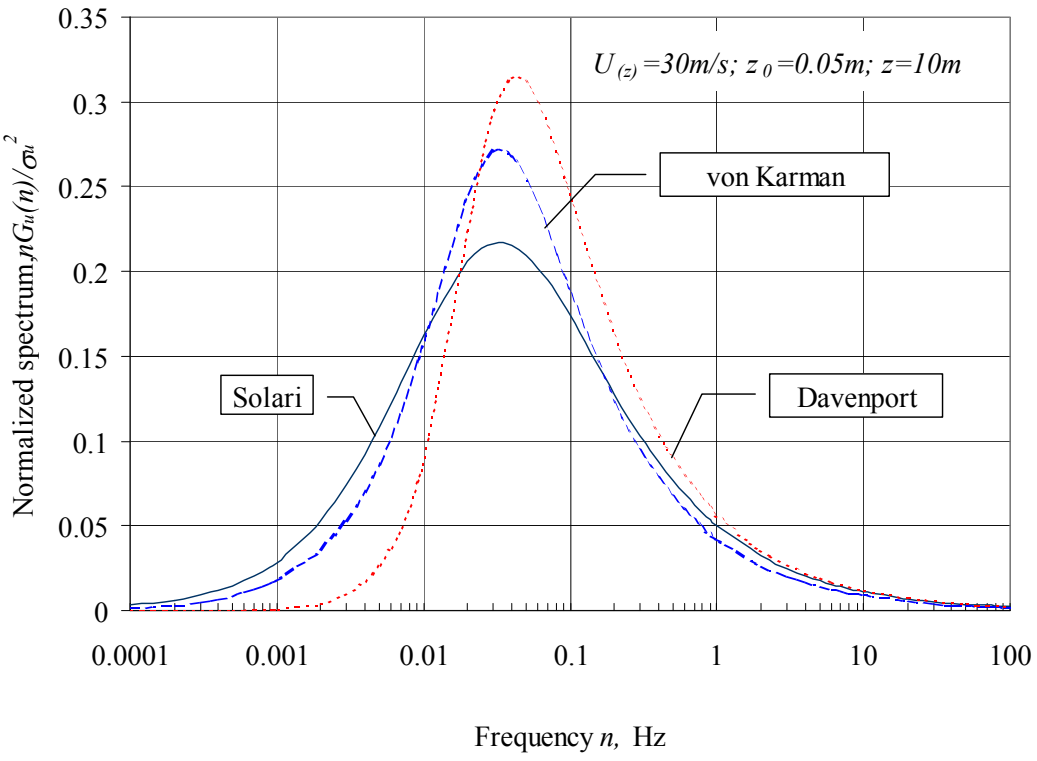

Figure 9.6. Comparison of Solari, von Karman and Davenport normalized (unit area)

half sided power spectra for along-wind gustiness (z=10m)

9.6 Gust factor for velocity pressure

The gust factor for velocity pressure is the ratio of the peak velocity pressure to the mean wind velocity pressure:

$$c_g(z) = \frac{q_{peak}(z)}{Q(z)} = \frac{Q(z) + g \cdot \sigma_q}{Q(z)} = 1 + g \cdot V_q = 1 + g\left[2 \cdot I_u(z)\right] \qquad (9.28)$$

where:

$Q(z)$ is the mean velocity pressure of the wind

$\sigma_q = \overline{q(z,t)^2}^{1/2}$ - root mean square value of the longitudinal velocity pressure fluctuations from the mean

V_Q - coefficient of variation of the velocity pressure fluctuations (approximately equal to the double of the coefficient of variation of the velocity fluctuations):

$$V_Q \cong 2\, I(z) \qquad (9.29)$$

g - the peak factor for velocity pressure (equal to 3.5 in *EC1*).

The gust factor for velocity pressure is represented in Figure 9.7.

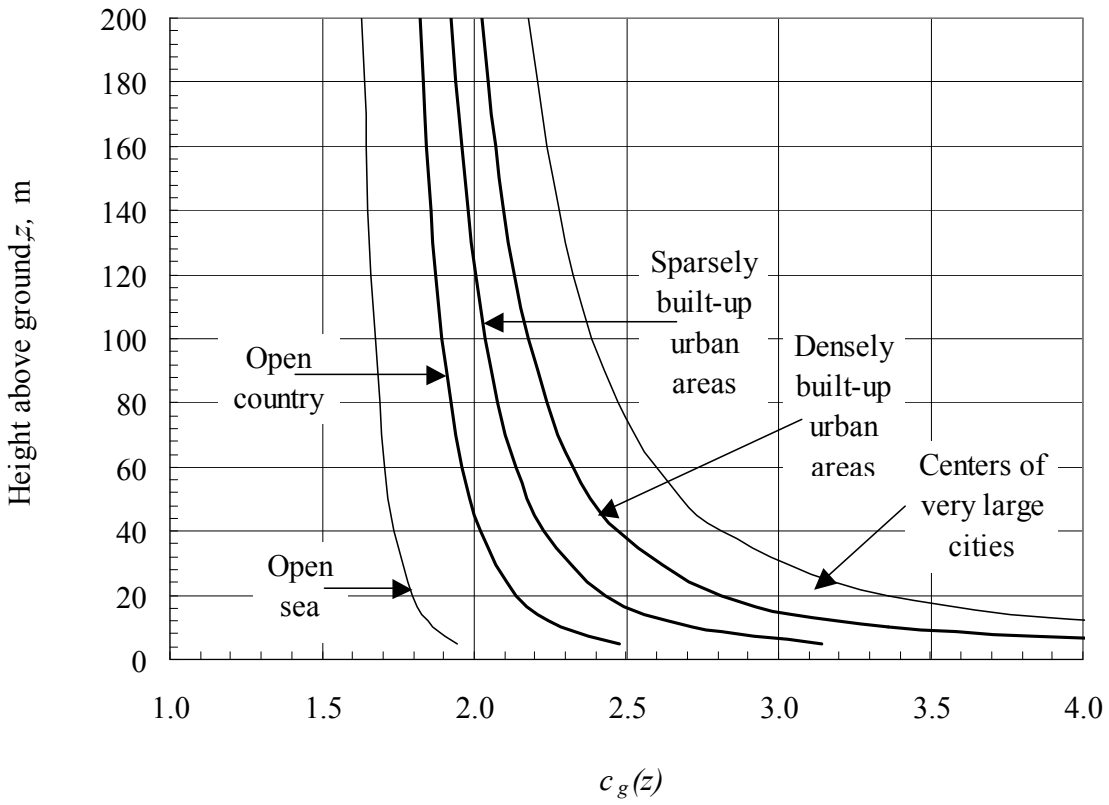

Figure 9.7. Gust factor for velocity pressure, $c_g(z) = 1 + g\left[2 \cdot I_u(z)\right]$

9.7 Exposure factor for peak velocity pressure

The peak velocity pressure at the height z above ground is the product of the gust factor, the roughness factor and the reference velocity pressure:

$$Q_g(z) = c_g(z)\, c_r(z)\, Q_{ref} \tag{9.30}$$

The exposure factor is defined as the product of the gust and roughness factors:

$$c_e(z) = c_g(z)\, c_r(z). \tag{9.31}$$

The exposure factor is plotted in Figure 9.8.

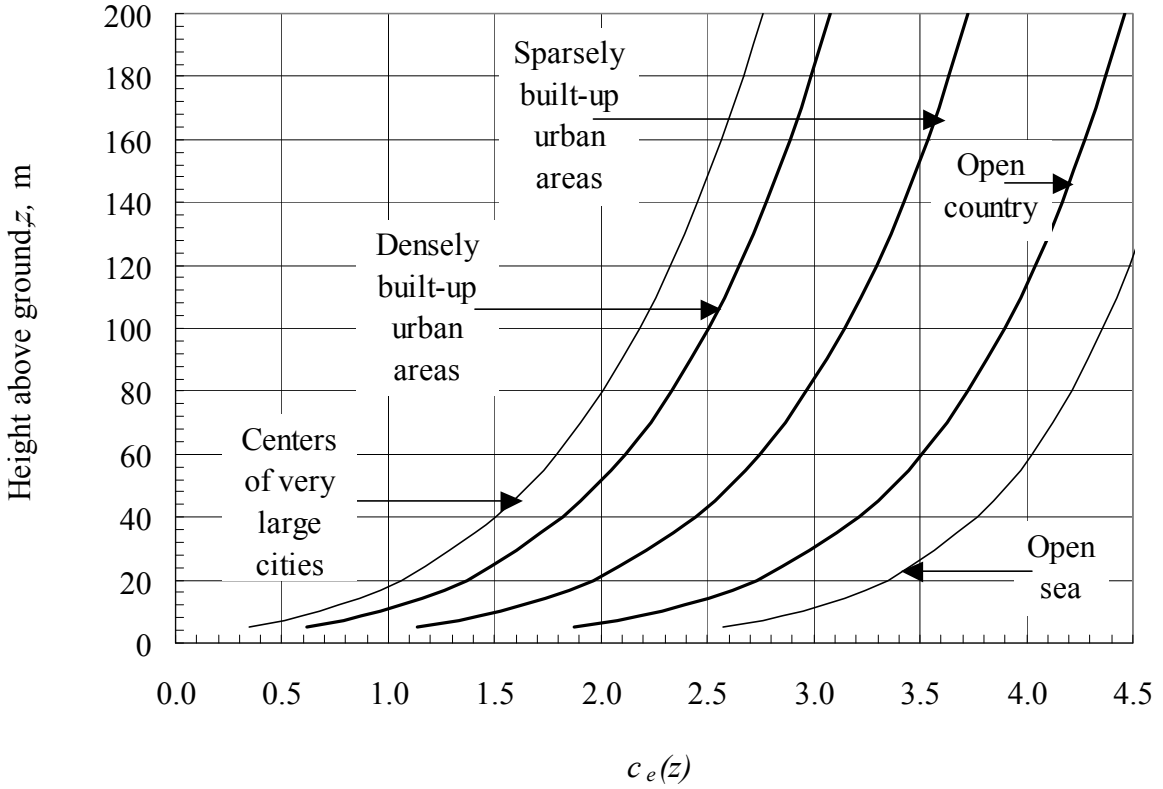

Figure 9.8. Exposure factor, $c_e(z) = c_g(z)\, c_r(z)$

The exposure factor (*Eurocode 1*) is called the combined factor in American wind literature.

9.8. Dynamic response factor

According to *EUROCODE 1* and *NP 082-04* format, the dynamic factor is defined by:

$$C_d = \frac{1 + 2gI_v(z_{eq})\sqrt{Q_0^2 + R_x^2}}{1 + 7I_v(z_{eq})} \tag{9.32}$$

where:

g – the peak factor for computing the peak response of the structure with respect to the mean response averaged on $t = 10$ *min.* $= 600$ *s*

$I_v(z_{eq})$ – intensity of turbulence at height $z = z_{eq}$

Q_0^2 - the background response part

R_x^2 - the resonant response part.

The intensity of turbulence at height $z = z_{eq}$ is defined by:

$$I_v(z_{eq}) = \frac{1}{c_t \ln \frac{z_{eq}}{z_0}} \tag{9.33}$$

where $c_t = 1.0$ - topographic factor and $z_0 = 0.05$ is the roughness length for reference terrain category.

The background response part, Q_0^2, is given by, Figure 9.9:

$$Q_0^2 = \frac{1}{1 + 0.9\left[\frac{b_{med} + h}{L_i(z_{eq})}\right]^{0.63}} \tag{9.34}$$

where:

b_{med} is the width of the structure
h – height of the structure
z_{eq} – equivalent height of the structure
$L_i(z_{eq})$ – integral length scale of the turbulence in terrain category

$$L_i(z_{eq}) = 300\left(\frac{z_{eq}}{300}\right)^{0.46 + 0.074 \ln z_0} . \tag{9.35}$$

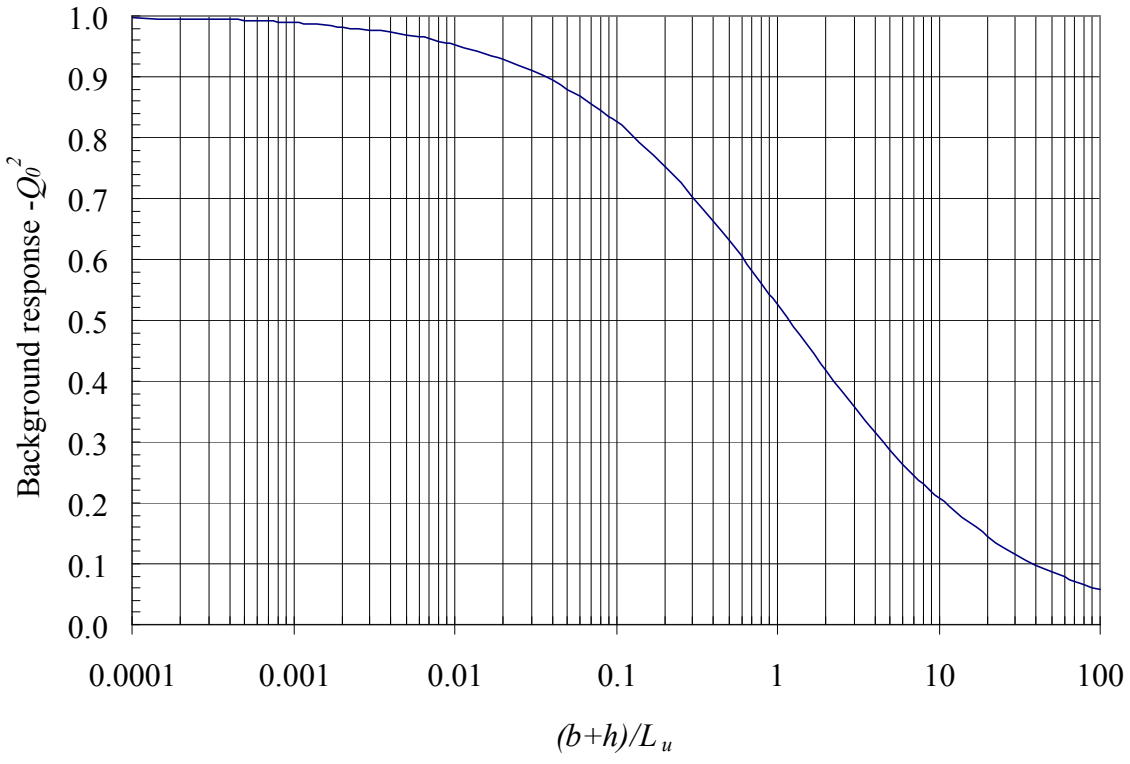

Figure 9.9. Background response $Q_0^2 = \frac{1}{1 + 0.9\left[\frac{b_{med} + h}{L_i(z_{eq})}\right]^{0.63}}$

The resonant response part R_x^2 is given by:

$$R_x^2 = \frac{\pi^2}{2\delta_s} R_N R_{\eta_h} R_{\eta_b} \tag{9.36}$$

where:

R_N – the resonant nondimensional power spectral density function for $n = n_{1,x}$

R_η - the aerodynamic admittance functions for uniform lateral displacement (fundamental mode shape without node point)

δ_s – logarithmic damping decrement of along wind vibration.

The resonant nondimensional power spectral density function R_N is defined by, Figure 9.10:

$$R_N = \frac{6.8 N_x}{\left(1 + 10.2 N_x\right)^{5/3}} \tag{9.37}$$

where:

N_x – nondimensional frequency of the structure

$$N_x = \frac{n_{1,x} \cdot L_i(z_{eq})}{V_m(z_{eq})} \tag{9.38}$$

and

$n_{1,x}$ – fundamental frequency of along wind vibration of structures

$V_m(z_{eq})$ – mean wind velocity for the height $z = z_{eq}$.

The aerodynamic admittance functions for uniform lateral displacement R_η is given by, Figure 9.11:

$$R_\eta = \frac{1}{\eta} - \frac{1}{2\eta^2}\left(1 - e^{-2\eta}\right) \tag{9.39}$$

where η is, respectively, η_h and η_b

and

η - normalized frequency, given by:

$$\eta_h = \frac{4.6 n_{1,x} \cdot h}{L_i(z_{eq})} \qquad \text{and} \qquad \eta_b = \frac{4.6 n_{1,x} \cdot b_{med}}{L_i(z_{eq})}. \tag{9.40}$$

The peak factor for computing the peak response of the structure with respect to the mean response averaged on $t = 10$ *min.* $= 600$ *s*, g, is given by:

$$g = \sqrt{2 \ln \nu t} + \frac{0.6}{\sqrt{2 \ln \nu t}} \tag{9.41}$$

where:

ν - the expected frequency of the structure under wind gusts excitation, in Hz

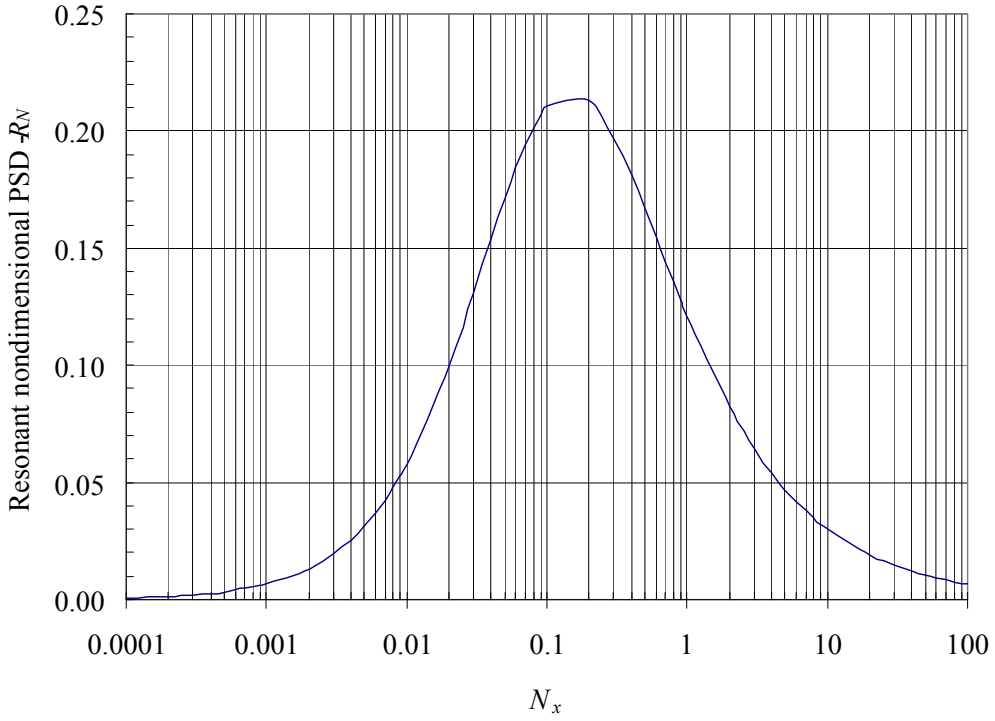

Figure 9.10. Resonant nondimensional power spectral density function $R_N = \dfrac{6.8N_x}{(1+10.2N_x)^{5/3}}$

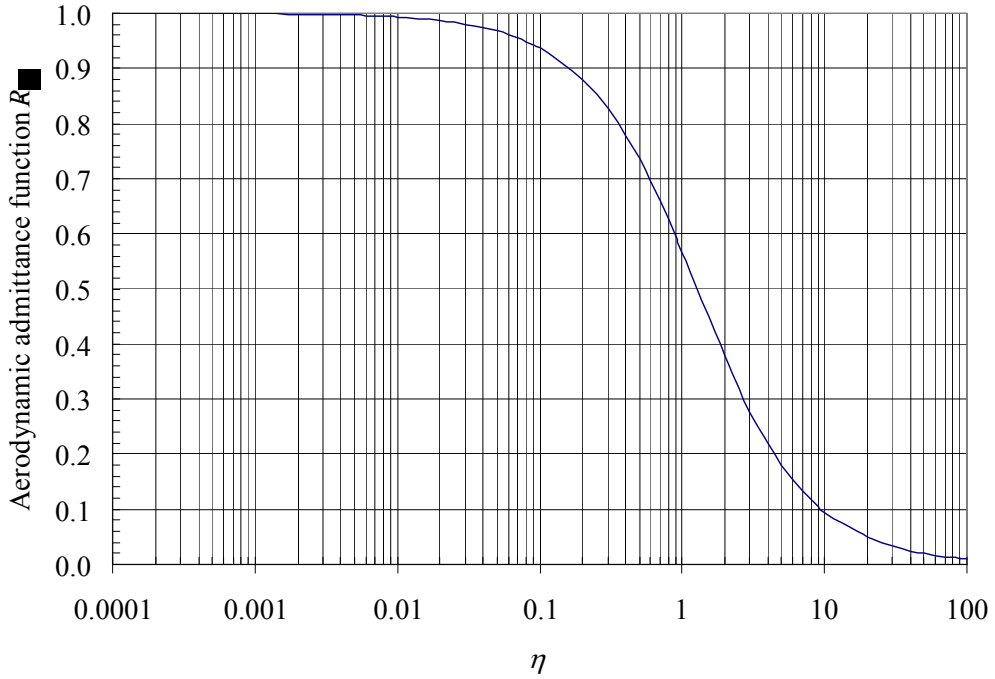

Figure 9.11. Aerodynamic admittance functions for uniform lateral displacement

$$R_\eta = \frac{1}{\eta} - \frac{1}{2\eta^2}\left(1 - e^{-2\eta}\right)$$

$$\nu = \left[\frac{\nu_0^2 Q_0^2 + n_{1,x}^2 R_x^2}{Q_0^2 + R_x^2} \right]^{1/2} \tag{9.42}$$

ν_0 – the expected frequency of gust loading on rigid structures, in Hz

$$\nu_0 = \frac{V_m(z_{eq})}{L_i(z_{eq})} \frac{1}{1.11 \cdot S^{0.615}} \tag{9.43}$$

S - factor for computing the expected frequency of gusts

$$S = 0.46 \left(\frac{b+h}{L_i(z_{eq})} \right) + 10.58 \frac{\sqrt{b \cdot h}}{L_i(z_{eq})}. \tag{9.44}$$

Typical values of the critical damping ratio (or logarithmic damping decrement) should be selected from appropriate national or international documents.

Acknowledgements

The authors deeply acknowledge the Technical University of Civil Engineering of Bucharest, the Faculty of Civil, Industrial and Agricultural Buildings and the Faculty of Engineering in Foreign Languages for understanding the necessity and importance of *Structural Reliability and Risk Analysis Course* and for supporting it.

The authors express their gratitude to Dr. Cristian Arion for constructing the GIS maps of Figure 9.1. Also, the authors deeply acknowledge the contribution of Eng. Alexandru Basarab Chesca in typewriting parts of Chapters 5, 7 and 8 and in performing the structural analysis of case study building of Chapter 4.9.3.

Last, but not least, the authors convey their thanks to the Reinforced Concrete Department for welcoming and supporting the activity of *Structural Reliability and Risk Analysis Group* over past nearly 20 years.

References

- Aldea, A., *Evaluarea hazardului seismic din sursa Vrancea in conditiile de teren specifice teritoriului Romaniei*. Teza de doctorat, Universitatea Tehnica de Constructii Bucuresti, 2002, 256 p.
- Aldea, A., Arion, C., Ciutina, A., Cornea, T., Dinu, F., Fulop, L., Grecea, D., Stratan, A., Vacareanu, R., 2004. *Constructii amplasate in zone cu miscari seismice puternice*, coordonatori Dubina, D., Lungu, D., Ed. Orizonturi Universitare, Timisoara 2003, , ISBN 973-8391-90-3, 479 p.
- Aldea, A., Lungu, D., Arion, A., 2003. "GIS microzonation of site effects in Bucharest based on existing seismic and geophysical evidence", *6ème Colloque National Association Française du Génie Parasismique* 2003, Palaiseau, France, 8p., CD-ROM
- Benjamin, J R, & Cornell, C A, Prob*ability, statistics and decisions for civil engineers*, John Wiley, New York, 1970
- Ditlevsen, O. & Madsen, H.O., *Structural Reliability Methods. Monograph*, (First edition published by John Wiley & Sons Ltd, Chichester, 1996, ISBN 0 471 96086 1), Internet edition 2.2.5 http://www.mek.dtu.dk/staff/od/books.htm, 2005
- EN 1991-1-4, *Eurocode 1: Actions on Structures – Part 1-4 : General Actions – Wind Actions*, CEN, 2005
- *FEMA 356*, *Prestandard and Commentary for the Seismic Rehabilitation of Buildings*, FEMA & ASCE, 2000
- Ferry Borges, J.& Castanheta, M., *Siguranta structurilor* – traducere din limba engleza, Editura Tehnica, 1974
- FEMA, *HAZUS – Technical Manual* 1999. Earthquake Loss Estimation Methodology, 3 Vol.
- Kreyszig, E., *Advanced Engineering Mathematics* – fourth edition, John Wiley & Sons, 1979
- Kramer, L. S., *Geotechnical Earthquake Engineering*, Prentice Hall, 1996
- Lungu, D., Arion, C., Aldea, A., Demetriu, S., 1999, "*Assessment of seismic hazard in Romania based on 25 years of strong ground motion instrumentation",* NATO ARW Conference on strong motion instrumentation for civil engineering structures, Istanbul, Turkey, June 2-5, 1999.
- Lungu, D., Aldea, A., Arion, C., Cornea, T., 1998. *"Seismic hazard zonation in Eastern Europe",* Second International Conference on Earthquake Hazard and Seismic Risk Reduction, September 15-21, Yerevan, Armenia by Kluwer Academic Publisher, 1999.
- Lungu D., Aldea A., Zaicenco A., Cornea T., 1998. *PSHA and GIS technology - tools for seismic hazard macrozonation in Eastern Europe.* XIth European Conference on Earthquake Engineering, Paris, France, 6-11 September, Proceedings, p.99
- Lungu D., Cornea T., Nedelcu C., 1998. *Probabilistic hazard assessment and site-dependent response for Vrancea earthquakes.* In Vrancea Earthquakes. Tectonics, Hazard and Risk Mitigation, Kluwer Academic publishers b.v., Wenzel F., Lungu D., editors, p.251-268
- Lungu D., Aldea A., Demetriu S., Cornea C., Craifaleanu I., 1995. *Uniform hazard response spectra in soft soil condition and EUROCODE 8.* 7th International Conference on Application of Statistics and Probability in Civil Engineering, Reliability and Risk Analysis, ICASP-7, Paris, July 10-13, Proceedings Vol.1, p.619-626, A.A. Balkema, Rotterdam

- Lungu, D. & Ghiocel, D., *Metode probabilistice in calculul constructiilor*, Editura Tehnica, 1982
- Lungu, D., Văcăreanu, R., Aldea, A., Arion, C., *Advanced Structural Analysis*, Conspress, 2000
- Madsen, H. O., Krenk, S., Lind, N. C., *Methods of Structural Safety*, Prentice-Hall, 1986
- Melchers, R. E., *Structural Reliability Analysis and Prediction*, John Wiley & Sons, 2nd Edition, 1999
- MTCT, P100-1/2006 *Cod de proiectare seismică - Partea I - Prevederi de proiectare pentru clădiri*, 2007
- MTCT, CR0-2005 *Cod de proiectare. Bazele proiectarii structurilor in constructii*, 2005
- MTCT, NP 082-04 *Cod de proiectare. Bazele proiectării şi acţiuni asupra construcţiilor. Acţiunea vântului*, 2005
- Park, Y.-J & Ang, A. H.-S.. *Mechanistic seismic damage model for reinforced concrete*. Journal of Structural Engineering. ASCE vol. 111 (4): 722-739, 1985
- Rubinstein, R. Y., *Simulation and the Monte Carlo method*. John Wiley & Sons, New York, 1981
- Văcăreanu, R., Chesca, A. B., Georgescu, B., Seki, M. – "*Case study on the expected seismic losses of soft and weak groundfloor buildings*" - Proceedings of the International Symposium on Strong Vrancea Earthquakes and Risk Mitigation, Bucharest, 2007, p. 388-401
- Văcăreanu, R., Lungu, D., Aldea, A., Arion, C. May 2005. *WP7 Handbook – Seismic Risk Scenarios*, Bulletin of the Technical University of Civil Engineering Bucharest, 2/2003, p. 97-117
- Vacareanu, R., Aldea, A., Arion, C., 2003. "*Probabilistic risk assessment of current buildings*" VIe Colloque National AFPS, Genie Parasismique-Aspects Dynamiques et Vibratoires en Genie Civil, vol III, p.153-160.,
- Văcăreanu, R., *Monte Carlo Simulation Technique for Vulnerability Analysis of RC Frames – An Example*. - Bulletin on Technical University of Civil Engineering of Bucharest, 1/2000, pg. 9-18